Characterization of novel pharmacological Caspase-6 inhibitors provides insight on developing treatments against Alzheimer disease

by

Prateep Pakavathkumar

Department of the Integrated Program in Neuroscience,
McGill University, Montreal

June 2017

A thesis submitted to McGill University in partial fulfillment of the requirements of the degree of Doctor of Philosophy

"If I have seen further than others,
it is by standing upon the shoulders of Giants"

- ***Sir Isaac Newton***

Table of contents

Table of contents i

Abstract vii

Résumé viii

Preface x

First-authored manuscripts x

Author contributions xi

Collaborative manuscripts xii

Acknowledgements xiii

Abbreviations list xiv

List of Tables xix

List of Figures xx

Introduction 1

1. Literature Review 4

1.1 Apoptosis 4

1.1.1 The discovery of apoptosis 4

1.2 Discovering caspases and link to cell death proteases 4

1.2.1 The evolution of caspases 4

1.2.2 The first mammalian caspase 5

1.2.3 Apoptosis in Caenorhabditis elegans 5

1.2.4 The mammalian caspases 6

1.3 Caspases are classified based on sequence similarities, substrate preferences, or function 13

1.3.1 Phylogenetic classification of human caspases 14

1.3.2 Substrate preference-based classification of human caspases 14

1.3.3 Functional classification of human caspases 15
1.4 Molecular platforms for apoptotic and inflammatory pathways 16
1.4.1 The death-inducing signaling complex and the extrinsic pathway 17
1.4.2 The apoptosome and the intrinsic apoptotic pathway 19
1.4.3 The inflammasomes and pyroptosis 20
1.4.4 The PIDDosome and mitotic catastrophe 21
1.4.5 The Ripoptosome at the crossroads between apoptosis and necroptosis 22
1.5 Caspase functions in apoptosis and beyond 22
1.5.1 Caspase functions in systematic dismantling of dying cells 23
1.5.2 Non-apoptotic caspase functions in immune cells 24
1.5.3 Non-apoptotic caspase functions in the nervous system 25
1.5.4 Other non-apoptotic functions 27
1.6 Caspase-6 transcriptional control, alternative splicing, and tissue expression 29
1.6.1 Little is known about *CASP6* gene transcriptional regulation 29
1.6.2 The alternatively spliced Caspase-6 isoform 31
1.6.3 Caspase-6 is expressed at low levels in the healthy brain 32
1.7 Caspase-6 enzyme structural analysis 33
1.7.1 The 3D structure of Caspase-6 and its active site 33
1.7.2 Unprocessed inactive Caspase-6 34
1.7.3 Caspase-6 processing by inter- and intramolecular cleavage 34
1.7.4 Changes in the Caspase-6 active site upon substrate binding and pH 35
1.8 Caspase-6 post-translation modifications (PTMs) 36
1.8.1 Caspase-6 phosphorylation at serine 257 37
1.8.2 Caspase-6 palmitoylation at cysteine residues 37
1.9 Caspase-6 activation follows canonical activation cascades and can self-activate .. 38
1.9.1 Caspase-6 is activated both downstream and upstream of other caspases 39
1.9.2 Caspase-6 self-activates in mammalian cells 40
1.10 Caspase-6 substrates and protein interaction analysis 40
1.10.1 Caspase-6 cleaves many cytoskeletal proteins in human neurons 40
1.10.2 Caspase-6 signalling pathways in human T lymphocytes 41
1.10.3 Caspase-6 protein-protein interaction network 42

1.11 Caspase-6 mediates axonal degeneration 43
1.11.1 Caspase-6 is activated in peripheral neurons leading to axonal degeneration 44
1.11.2 Caspase-6-mediated axonal degeneration in the CNS 45
1.12 Caspase-6 is activated early in Alzheimer disease 47
1.12.1 Caspase-6 is activated in sporadic and familial AD brains 48
1.12.2 Caspase-6 is activated early during AD pathogenesis 48
1.12.3 Caspase-6 activity can increase Aβ production, disrupt the cytoskeleton, and impair the ubiquitin-proteasome system 49
1.12.4 Caspase-6 is part of a pro-inflammatory cycle in AD brains 50
1.13 Caspase-6 activation in other neurodegenerative diseases 51
1.13.1 Caspase-6 cleaves mutant huntingtin protein in mouse models 51
1.13.2 Caspase-6 cleaves DJ-1 in PD 52
1.13.3 Caspase-6 is activated following ischemic stroke 53
1.14 Caspase-6 inhibitors: proteins, peptides, and small molecules 55
1.14.1 Endogenous protein Caspase-6 inhibitors 56
1.14.2 Zinc-mediated Caspase-6 inhibition 58
1.14.3 Pharmacological Caspase-6 inhibitors 58
1.15 Hypothesis and Thesis objectives 61
1.16 Figures and legends 62
1.17 Tables 72
2. Methylene blue inhibits caspases by oxidation of the catalytic cysteine 77
2.1 Preface 77
2.2 Abstract 77
2.3 Introduction 78
2.4 Results 80
2.4.1 Methylene blue and its derivatives inhibit the activity of caspases in vitro 80
2.4.2 Competitive mode of inhibition for phenothiazines on Caspase-6 81
2.4.3 Methylene blue and its derivatives inhibit the activity of caspases in cell lines and primary cultures of human neurons 81
2.4.4 Methylene Blue and its derivatives inhibit the activity of Casp3 in vivo 83

2.4.5 Methylene blue inhibits Casp6 by oxidation of catalytic cysteine Cys163 84
2.5 Discussion..... 85
2.6 Materials and methods 87
2.7 Acknowledgements 92
2.8 Figures and legends..... 93
2.9 Supplemental material..... 103
2.9.1 Materials and methods 103
2.9.2 Figures and legends..... 105
3. Caspase vinyl sulfone small molecule inhibitors prevent axonal degeneration in human neurons and reverse cognitive impairment in Caspase-6-overexpressing mice 108
3.1 Preface..... 108
3.2 Abstract..... 108
3.3 Introduction..... 109
3.4 Results 112
3.4.1 NWL-117 and −154 are potent peptide-based vinyl methyl sulfone inhibitors of recombinant active Casp6 112
3.4.2 NWL inhibitors inhibit recombinant initiator caspases and Casp6 at sub-micromolar concentrations 112
3.4.3 NWL-117 and −154 are non-toxic and potent inhibitors of Casp6 activity in Casp6-transfected HCT116 cells..... 113
3.4.4 NWL inhibitors block Casp6 activity within minutes in Casp6-transfected HCT116 cells 113
3.4.5 NWL inhibitors are non-toxic and prevent Casp6dependent neuritic degeneration in APP^{WT}-transfected human CNS neurons..... 114
3.4.6 NWL-117 penetrates the blood-brain barrier and reaches high nanomolar concentrations in mouse brains..... 115
3.4.7 Treatment of human Casp6 knock-in mice with NWL-117 improves their performance in the novel object recognition (NOR) task..... 115

3.4.8 Casp6 substrates, synaptic proteins, and glial inflammation markers are unchanged in mice hippocampi following NWL-117 treatment 116
3.5 Discussion 116
3.6 Materials and methods 122
3.7 Acknowledgements 131
3.8 Figures and legends 132
3.9 Tables 143
3.10 Supplementary information 145
3.10.1 Figures and legends 145
4. Discussion 149
4.1 Assessing whether Caspase-6 inhibition will produce adverse effects 149
4.1.1 Information from genetic Caspase-6 ablation models 149
4.1.2 Caspase-6 inhibitors show few signs of toxicity in mice or humans 150
4.2 Other mechanisms to achieve specific Caspase-6 inhibition 151
4.2.1 CRISPR-Cas9-mediated transcriptional blockade 151
4.2.2 Antisense oligonucleotides to destabilize RNA or promote splicing into Mch2β. 152
4.2.3 Sequestering Caspase-6 away from its substrates or facilitating its degradation .. 153
4.3 Difficulties in CNS drug development for AD 154
4.3.1 AD animal models do not possess sufficient predictive value and clinical trials have been poorly designed 155
4.3.2 AD neuropsychiatric symptoms are not a focus of animal models or clinical trials 156
4.3.3 Caspase-6-overexpressing mice serve as a model for age-dependent cognitive impairment 157
4.4 Caspase-6 inhibition may combat cognitive decline in AD, but cannot treat all the underlying pathologies 157
4.4.1 There are several risk factors for AD that may or may not lead to Caspase-6 activation 158
4.4.2 Several other caspases are linked to AD 158
4.5 Conclusion 160

References i

Appendix I..i

Abstract

Caspase-6 is a cysteinyl aspartic-specific protease that is activated during pre-clinical stages of Alzheimer disease (AD) and correlates negatively with cognitive performance. We propose that Caspase-6 inhibition may combat the age-dependent cognitive decline in AD. Several Caspase-6 inhibitors have been developed, yet none have proven to be strong enough candidates to pursue clinical trials. To address this, two novel Caspase-6 inhibitors were studied.

Methylene blue is a Tau aggregation inhibitor that has been tested in phase III clinical trials against AD. Mass spectrometric analysis demonstrates that methylene blue oxidizes Caspase-6's catalytic cysteine, which represents a novel inhibitory post-translational modification. Moreover, methylene blue and its derivatives, azure A and azure B, inhibit Caspase-1, -3, or -6 activity *in vitro*, in human colorectal carcinoma cells, in human neurons, or in mice at non-toxic concentrations. Methylene blue's half-maximal inhibitory concentration (IC_{50}) against Caspase-3 and -6 is comparable to concentrations required to achieve Tau aggregation inhibition. These results suggest that methylene blue has therapeutic neuroprotective and anti-inflammatory properties through Caspase-6 and -1 inhibition, respectively, while Caspase-3 inhibition could disrupt tissue homeostasis.

The therapeutic potential of small molecule vinyl sulfone Caspase-6 inhibitors developed by New World Laboratories' (NWL) is presented. NWL compounds have IC_{50} values in the sub-μM range and inhibit Caspase-6 *in vitro*, in human colorectal carcinoma cells, and in human neurons at non-toxic concentrations. Moreover, Caspase-6 inhibition prevents axonal degeneration in human neurons transfected with amyloid precursor protein. In mice overexpressing human Caspase-6, mass spectrometry reveals that NWL-117 can penetrate the blood-brain barrier. Interestingly, NWL-117 treatment restores novel object recognition in Caspase-6 mice, although changes in synaptic proteins, glial inflammation markers, or Caspase-6 substrates are not evident. These experiments suggest that Caspase-6-mediated damage is reversible strengthening the rationale for continued Caspase-6 inhibitor development.

The studies presented here demonstrate that 1) oxidation and 2) vinyl methyl sulfones can effectively inhibit Caspase-6 in biological settings. These results may help future Caspase-6 inhibitor development to allow clinical assessment of the Caspase-6 hypothesis in AD.

Keywords : Caspase-6, Alzheimer disease, vinyl sulfones, human neurons, methylene blue

Résumé

La Caspase-6, une enzyme à cystéine coupant spécifiquement après une aspartate, est activée pendant les stades précoces de la maladie Alzheimer (MA), et corrèle négativement avec la performance cognitive. Nous proposons que la Caspase-6 est une cible thérapeutique intéressante pour combattre le déclin cognitif lié à l'âge dans la MA. Plusieurs inhibiteurs de la Caspase-6 ont été développés, mais, aucun de ces inhibiteurs n'est un bon candidat pour poursuivre des essais cliniques. Pour cette raison, deux nouveaux inhibiteurs de la Caspase-6 ont été étudiés.

Le bleu de méthylène est un inhibiteur de l'agrégation de la protéine Tau qui a été testé en troisième phase d'étude clinique contre la MA. L'analyse par spectrométrie de masse a démontré que le bleu de méthylène peut oxyder la cystéine catalytique de la Caspase-6 ce qui représente un nouveau mécanisme d'inhibition par modification post-traductionnel. De plus, le bleu de méthylène et ses dérivés, azure A et azure B, inhibent l'activité de la Caspase-1, -3, ou -6 *in vitro*, dans des cellules de carcinome colorectal humaines, dans des neurones primaires humains, ou dans des souris à des concentrations non-toxiques. La concentration du bleu de méthylène nécessaire pour inhiber à 50% (IC_{50}) la Caspase-3 et -6 est comparable aux concentrations nécessaires pour inhiber l'agrégation de Tau. Ces résultats suggèrent que le bleu de méthylène est neuroprotecteur et anti-inflammatoire à cause de l'inhibition de la Caspase-6 et -1, respectivement. Tandis que l'inhibition de la Caspase-3 pourrait perturber l'homéostasie des tissus.

Le potentiel thérapeutique des petites molécules vinyles sulfoniques développé par New World Laboratories (NWL) comme inhibiteur de Caspase-6 est aussi présenté. Les composés de NWL ont des $IC_{50} < 1$ μM et inhibent la Caspase-6 *in vitro*, dans des cellules de carcinome colorectal humaines, dans des neurones primaires humains à des concentrations non-toxiques. L'inhibition de la Caspase-6 empêche la dégénérescence axonale dans des neurones humains transfectés avec la protéine précurseur de l'amyloide. Dans des souris qui surexpriment la Caspase-6, l'analyse par spectrométrie de masse dévoile la capacité de NWL-117 à traverser la barrière hématoencéphalique. Notamment, des traitements avec NWL-117 rétablis la mémoire épisodique (reconnaissance d'objets nouveaux) dans les souris Caspase-6, même si la présence de protéines synaptiques, marqueurs gliaux d'inflammation, ou de substrats de Caspase-6

n’avaient pas changé. Ces expériences suggèrent que les dommages liés à l’activité Caspase-6 peuvent être réversés ce qui renforce le rationnel derrière le développement des inhibiteurs.

Les études présentées démontrent que 1) l’oxydation et 2) les vinyles sulfones inhibent la Caspase-6 dans des contextes biologiques. Ces résultats pourraient aider le futur développement d’inhibiteurs de la Caspase-6 pour permettre d’évaluer cliniquement l’hypothèse de la Caspase-6 dans la MA.

Mots-clés : Caspase-6, Maladie Alzheimer, vinyle sulfoniques, neurones humains, bleu méthylène

Preface

First-authored manuscripts

As an original contribution to knowledge, this thesis describes two types of caspase inhibitors as a framework for the development of therapies targeting Caspase-6 in the context of neurodegenerative diseases, chiefly, Alzheimer disease. I exercise my right to write a manuscript-based thesis containing open access published works for Chapter 2 and 3. Methylene blue (Chapter 2), a Tau aggregation inhibitor that has been tested in phase III clinical trials against Alzheimer disease, was found to inhibit caspase function through oxidation of critical cysteine residues. Similarly, small molecule irreversible active site-directed vinyl sulfone inhibitors developed by New World Laboratories Inc. (Chapter 3) demonstrated the ability to prevent or reverse Caspase-6-mediated phenotypes in human neurons and in mice, respectively. This thesis includes work that has been performed in collaboration with my peers. The author contributions are clearly stated on the next page. This thesis is presented in four chapters: the introduction and the literature review, research data that was published in *Scientific Reports* on methylene blue-mediated inhibition of caspases, research data that that was published in *Molecular Neurodegeneration* on caspase vinyl sulfone small molecule inhibitors, finishing with a general discussion and conclusion.

This thesis contains the following manuscripts:

Chapter 2

Pakavathkumar, P., Sharma, G., Kaushal, V., Foveau, B., and LeBlanc, A.C. (2015). Methylene blue inhibits caspases by oxidation of the catalytic cysteine. Sci Rep 5, 13730-13743

Chapter 3

Pakavathkumar, P., Noel, A., Lecrux, C., Tubeleviciute-Aydin, A., Hamel, E., Ahlfors, J.E., and LeBlanc, A.C. (2017). Caspase vinyl sulfone small molecule inhibitors prevent axonal degeneration in human neurons and reverse cognitive impairment in Caspase-6-overexpressing mice. Mol Neurodegener 12, 22.

Author contributions

Chapter 2

PP generated data for figures 2.1d-f, 2.3, 2.4a-c, 2.4e-f, 2.5 and wrote the manuscript. GS generated figures 2.1b-c, 2.1g, 2.2, 2.6 and wrote the manuscript. VK generated figure 2.4d. BF helped with the figure 2.5 experimental design. ALB contributed to the experimental design, wrote some of the manuscript and oversaw the writing of the paper. All authors saw and approved the final version of the manuscript. PP and GS are co-first authors.

Chapter 3

PP designed, performed experiments, analysed data for figures 3.1a, 3.1c, 3.2-3.4, 3.6, and wrote the majority of the manuscript. CLL performed the intra-carotid injections necessary for table 3.2 and EH helped write the manuscript. ATA designed, performed experiments, analyzed data for IC_{50} determination against Caspase-6 for figure 3.1b, and helped write the manuscript. AN designed, performed experiments, analyzed data for behavioural assessment of mice for figure 3.5, and helped write the manuscript. JEA provided data for IC_{50} values against different caspases for table 3.1, analyzed data, and helped write the manuscript. ALB designed experiments, analyzed data, and helped write the manuscript. All authors read and approved the final manuscript.

Collaborative manuscripts

During my training in Dr. LeBlanc's laboratory I was given the opportunity to participate in research activities outside my thesis objectives. A great deal of time and energy was spent on two collaborative projects although the contributions present in the final manuscript are slight. These collaborations are listed below with a description of my contribution.

1) LeBlanc, A.C., Ramcharitar, J., Afonso, V., Hamel, E., Bennett, D.A., Pakavathkumar, P., and Albrecht, S. (2014). Caspase-6 activity in the CA1 region of the hippocampus induces age-dependent memory impairment. Cell Death Differ 21, 696-706.

   Contribution : I performed western blot analysis for figure 2h, isolation and homogenization of cortical and hippocampal tissue from several different cohorts of mice, and Caspase-6 activity assays.

2) Kaushal, V., Dye, R., Pakavathkumar, P., Foveau, B., Flores, J., Hyman, B., Ghetti, B., Koller, B.H., and LeBlanc, A.C. (2015). Neuronal NLRP1 inflammasome activation of Caspase-1 coordinately regulates inflammatory interleukin-1-beta production and axonal degeneration-associated Caspase-6 activation. Cell Death Differ 22, 1676-1686.

   Contribution : I performed western blot analysis for figure 4b, 4e, 4i, and 5c-e. I performed additional experiments not included in the manuscript including troubleshooting immunoprecipitation protocols for NLRP1 interaction with other inflammasome components in human neurons and transfected cells and I helped write the manuscript.

Acknowledgements

The work presented in this thesis would not have been possible without the knowledgeable mentorship provided by *Dr. Andrea C. LeBlanc*. From beginning to end, I received a tremendous amount of guidance and support from her and it shaped me into the scientist I am today. Thank you for sharing your passion and resolve for science.

I would like to thank the two members of my advisory committee, *Dr. Giuseppina Ursini-Siegel* and *Dr. Chantal Autexier* for monitoring my research progress and suggesting improvements throughout the last seven years.

This thesis was made possible by past and present lab members. Without them, my graduate studies would not have been the treasure trove of casual and scientific conversations, close friendships, productive workdays and weekends, and fun nights it was. Know that you are all ingrained in my memories forever.

Special mentions to a few colleagues that welcomed me into the lab 7 years ago. *Vik*, I loved seeing your practical approach to science, I learned a lot about the politics of science from you. *Olivier*, I wish I could have learned more from you, our time together was too short. *Andrea*, thank you for teaching me the ropes without asking anything in return. *Jasmine and Sarah*, your combined energy could fuel the Sun, I hope to maintain our friendships for the rest of my life. *Marcus*, I always respected your insight on scientific and real world issues, I know you'll be successful in the future. *Benedicte*, j'aurais jamais imaginé avoir eu une amie pendant tout mon doc avec qui je m'entendrai aussi bien, quel plaisir d'avoir partagé tous mes histoires avec toi! The list can go on forever, but thank you all sincerely for making every day memorable.

The biggest chunk of this thesis is dedicated to the five pillars of my life: *Appa*, *Amma, Anna*, *Arny,* and, my wife, *Lama*. Family is often taken for granted because of their unconditional love. The nurturing, caring, and loving members of my family gave and keep giving me the strength necessary to overcome all of life's obstacles with ease. I am eternally indebted to you. Thank you taking part in my life's journey.

Abbreviations list

Aβ	Amyloid β
Ac-nLPnLD-AMC	Acetylated-norleucine-Pro-norleucine-Asp-AMC
Ac-VEID-AFC	Acetylated-Val-Glu-Iso-Asp-AFC
AD	Alzheimer disease
ADP	Adenosine diphosphate
AFC	7-amino-4-trifluoromethylcoumarin
AMC	7-amino-4-metyhylcoumarin
AMPA	α-amino-3-hydroxy-5-methyl-4-isoxazolepropionic
ANOVA	Analysis of variance
Apaf-1	Apoptotic protease-activating factor-1
APP	Amyloid precursor protein
ARK5	Adenosine monophosphate kinase-related kinase 5
ASC	Apoptosis-associated speck-like protein containing a CARD
ASO	Antisense oligonucleotide
ATP	Adenosine triphosphate
BACE	β-site APP cleaving-enzyme
Bcl-2	B-cell lymphoma-2
BIR	Baculoviral IAP repeat
BSA	Bovine serum albumin
C. elegans	*Caenorhabditis elegans*
CAG	Cytomegalovirus early enhancer/chicken β-actin fusion promoter
CAMKIIa	Calmodulin kinase II alpha
CARD	Caspase recruitment domain
Casp6	Caspase-6
Casp6p20	p20 subunit of active Caspase-6
Casp6p20p10	Self-activating form of Caspase-6 lacking the pro-domain
Ced	*Caenorhabditis elegans* cell death gene
cFLIP	Cellular FLICE-like inhibitory protein
cFLIP$_L$	cFLIP long
cFLIP$_S$	cFLIP short
CHAPS	3-[(3-cholamidopropyl)-dimethylammonio]2-hydroxy-1-propanesulfonic acid
CHO	Aldehyde
cIAP	Cellular inhibitors of apoptosis protein
CIF	Caspase inhibitory factor

CLB	Cell lysis buffer
CNS	Central nervous system
COS	African green monkey kidney cells in origin with simian virus 40
CRISPR	Clustered regularly interspaced palindromic repeats
CrmA	Cowpox response modifier A
CSF	Cerebrospinal fluid
CYLD	Cylindromatosis
CytC	Cytochrome C
dATP	Deoxyadenosine triphosphate
DD	Death domain
DED	Death effector domain
DEVD-AMC	Aspartate-glutamate-valine-aspartate-7-amino-4-methylcoumarin
DISC	Death-inducing signaling complex
DMSO	Dimethyl sulfoxide
DNA	Deoxyribonucleic acid
DNAse	Deoxyribonuclease
DR3	Death receptor 3
DTT	Dithiothreitol
Δp97	p97-cleaved by Caspase-6
ΔproCaspase-6	Prodomain removed Caspase-6
EDTA	Ethylenediaminetetraacetic acid
EGFP	Enhanced green fluorescent protein
ELISA	Enzyme-linked immunosorbent assay
ERC	Entorhinal cortex
ERICE	Evolutionarily related ICE
EST	Expressed sequence tag
FADD	Fas-associating death domain-containing protein
FasL	Fas ligand
FLICA	Fluorochrome-labelled inhibitors of caspases
FLICE	FADD-like ICE
FMK	Fluoromethyl ketones
GABA	γ-aminobutyric acid
GALN	Galactosamine
GFAP	Glial fibrillary acidic protein
GSWFI	Glycine-serine-tryptophan-phenylalanine-isoleucine

HCT116	Human colorectal carcinoma cell line
HD	Huntington's disease
HEK293T	Human embryonic kidney
HIV	Human immunodeficiency virus
HtrA2	High temperature requirement protein A2
Htt	Huntingtin
IAP	Inhibitors of apoptosis protein
Iba1	Ionized calcium binding adapter molecule 1
IBM	IAP-binding motif
IC_{50}	Half-maximal inhibitory concentration
ICE	Interleukin-1β(IL-1β)-converting enzyme
ICE-LAP	ICE-like apoptotic protease
ICE_{rel}-II	ICE-related-II
Ich	Ice and Ced-3 homolog
Ich-1_L	Ice and Ced-3 homolog 1 long
Ich-1_S	Ice and Ced-3 homolog 1 short
IMA	Isatin Michael acceptors
IPTG	Isopropyl β-D-1-thiogalactopyranoside
K562	Chronic myelogenous leukemia
K_i	Inhibitory constant representing concentration at 50% inhibition
KI	Knock-in
K_m	Michaelis constant representing concentration at 50% V_{max}
LC/MS/MS	Liquid chromatography and tandem mass spectrometry
LDH	Lactate dehydrogenase
LPS	Lipopolysaccharide
LRR	Leucine-rich repeat
MCAo	Middle cerebral artery occlusion
Mch	Mammalian Ced-3 homologues
MCI	Mild cognitively impaired
Mhtt	Mutant Huntingtin protein
MOMP	Mitochondrial outer membrane permeabilization
MTT	3-(4,5-dimethylthiazol-2-yl)2,5-diphenyltetrazolium bromide
NAD+	Nicotinamide dinucleotide
NAIP	Neuronal apoptosis inhibitory protein

NCI	Non-cognitively impaired
Nedd	Neural precursor cell-expressed developmentally downregulated gene
NFκB	Nuclear factor κ B
NFTs	Neurofibrillary tangles
NGF	Nerve growth factor
NLR	NOD-like receptors
NLRC	NLR with a caspase recruitment domain
NLRP	NLR with a pyrin domain
NMAT	Nicotinamide mononucleotide adenylyltransferase
NOD	Nucleotide-binding oligomerization domain
NOR	Novel object recognition
Nt	Non-treated
NWL	New World Laboratories Inc.
p10	Small Caspase-6 subunit
p20	Large Capase-6 subunit
p97ΔCasp6	p97 cleaved by Caspase-6
PARP	Poly(ADP-ribose) polymerase
PBS	Phosphate-buffered saline
PCR	Polymerase chain reaction
PD	Parkinson's disease
PEG	Polyethylene glycol
PI3K	Phosphatidylinositol-4,5-bisphosphate 3-kinase
PIDD	p53-induced protein with a DD
PIPES	Piperazine-N, N-bis (2-ethanesulfonic acid)
PKCζ	Protein kinase C zeta
pNA	*p*-nitroaniline
PS1	Presenilin 1
PS2	Presenilin 2
PSD95	Post-synaptic density protein 95
PTM	Post-translational modification
PTN	Pleiotrophin
PYD	Pyrin domain
QACRG	Glutamine-alanine-cysteine-arginine-glycine
qPCR	Quantitative PCR
R110	Rhodamine
RAIDD	RIP-associated Ich-1/CED homologous protein with a DD
Raptor	Regulatory-associated protein of mTOR

RGC	Retinal ganglion cell
RIP1	Serine/threonine poly-ubiquitinated receptor interacting protein kinase 1
RT-PCR	Reverse-transcriptase polymerase chain reaction
S1-S4	Subsites 1-4
SB	Stennicke's buffer
SDS	Sodium dodecyl sulfate
siRNA	Small interfering RNAs
SMAC/DIABLO	Second mitochondria-derived activator of caspase
SNP	Single nucleotide polymorphism
Sox	Sex determining region Y-box
STAT	Signal transducer and activator of transcription
TAT	HIV's transactivation of transcription
TauΔCasp6	Tau cleaved by Caspase-6
tBid	Truncated Bcl-2 homology domain 3-interacting domain death agonist
TLCK	N-α-Tosyl-L-LysinylChloromethylketone
TNFα	Tumor necrosis factor α
TNFR	TNFα receptor
TPCK	N-Tosyl-LPhenylalaninyl-Chloromethylketone
TRADD	TNFR1-associated death domain protein
TRAF2	TNFR2-associated factor 2
TRAIL-R	TNF-related-apoptosis-inducing ligand receptor
TSS	Transcription start site
TubΔCasp6	Tubulin cleaved by Caspase-6
UPR	Unfolded protein response
VCP/p97	Valosin-containing protein/p97
$\mathbf{V_{max}}$	Maximum velocity of the reaction (M/s)
WT	Wild-type
XIAP	X-linked inhibitor of apoptosis protein
Y2H	Yeast-two hybrid
Z-VAD-FMK	Benzyloxycarbonyl-valine-alanine-aspartate-fluoromethyl ketone
Z-VEID-FMK	Benzyloxycarbonyl-valine-glutamate-isoleucine-aspartate-fluoromethyl ketone

List of Tables

Table 1.1 Clan CD proteases. 72
Table 1.2 Caspase-6 deficient models and their phenotypes. 73
Table 1.3 Caspase-6 leads to axonal degeneration in several different models. 74
Table 1.4 Different types, targets, and mechanisms developed for Caspase-6 inhibition. 75
Table 1.5 Baculoviral and inhibitors of apoptosis proteins and their caspase targets. 76
Table 3.1 Half-maximal inhibitory concentrations (IC50) of NWL-117 and NWL-154 against recombinant Caspase-1 to -10* 143
Table 3.2 Hippocampal and plasma concentrations of NWL-117 following injections through the internal carotid artery of mice* 144

List of Figures

Figure 1.1 General caspase structure. 62
Figure 1.2 Preferred substrate cleavage sequences for different caspase groups. 63
Figure 1.3 Phylogenetic relationship between caspases. 64
Figure 1.4 Classically-defined roles for caspases in apoptosis and inflammation. 65
Figure 1.5 Schematic of extrinsic and intrinsic apoptotic signaling cascades. 66
Figure 1.6 Schematic of predicted transcription factor binding sites on the CASP6 gene. 67
Figure 1.7 Caspase-6 transcription can be upregulated by p53 with two splice variants. 68
Figure 1.8 Caspase-6 crystal structures. 69
Figure 1.9 Caspase-6 substrates in human neuronal extracts. 70
Figure 1.10 Neoepitope antibodies distinguish between full length and cleaved substrates. ... 71
Figure 2.1 Inhibition of caspases in vitro by phenothiazines. 93
Figure 2.2 Michaelis-Menten kinetic analyses of phenothiazines on RCasp6. 94
Figure 2.3 Toxicity of methylene blue, azure A, and azure B in HCT116 cells and human primary neurons. 95
Figure 2.4 Methylene blue, azure A, and azure B inhibit active Casp6 in HCT116 cells and human primary neurons. 97
Figure 2.5 Methylene Blue inhibits Casp3 activity in liver of mice treated with LPS/GALN. 99
Figure 2.6 Methylene blue and azure B oxidizes the catalytic Cys163 of active Casp6. 101
Supplemental Figure S2.1 Recombinant Caspases are highly active and functional. 105
Supplemental Figure S2.2 Phenothiazines inhibit fluorescence in a dose-dependent manner. 106
Supplemental Figure S2.3 Proteasome inhibitors do not inhibit DEVDase activity in mice liver extracts. 107
Fig. 3.1 NWL inhibitors are irreversible peptide vinyl sulfone inhibitors of Casp6. 132
Fig. 3.2 Non-toxic concentrations of NWL-117 and −154 inhibit Casp6 activity in HCT116 cells. 133
Fig. 3.3 NWL-117 and -154 rapidly inhibit Casp6 activity in HCT116 cells. 135
Fig. 3.4 Non-toxic concentrations of NWL-117 and -154 inhibit Casp6 activity in primary human neurons. 138

Fig. 3.5 Acute NWL-117 administration reverses novel object recognition deficits in Casp6-overexpressing KI/Cre mice. 139
Fig. 3.6 Hippocampal levels of synaptic and glial markers are unchanged with NWL-117 treatment. 141
Supplemental Figure S3.2 NWL inhibitors do not alter mitochondrial activity after 48 hours of treatment and serum-deprivation increases TubΔCasp6 immunoreactivity. 146
Supplemental Figure S3.3 Time-lapse imaging in EGFP-Veh and APP^{WT}-NWL-117-treated primary human neurons. 147
Supplemental figure S3.4 PSD95 levels are unchanged in hippocampi from NWL-117 treated mice. 148

Introduction

The first caspase was discovered as the enzyme responsible for interleukin-1β maturation (Cerretti et al., 1992; Thornberry et al., 1992), but the interest in caspases exploded following the cloning of cell death defective genes in *Caenorhabditis elegans* (Yuan et al., 1993). The link between apoptotic programmed cell death and cysteinyl proteases started the relentless search for and discovery of 10 additional human caspases involved in inflammation and initiation or execution of apoptosis (Thornberry, 1997). Researchers identified multi-protein complexes involved in caspase activation during apoptosis and inflammation such as the death-inducing signalling complex, the apoptosome, and the inflammasome (Kischkel et al., 1995; Li et al., 1997; Zou et al., 1997; Martinon et al., 2002). Caspase activation cascades were also elucidated during apoptotic signaling identifying some caspases as upstream activators of other caspases (Slee et al., 1999; Inoue et al., 2009). However, caspases were found to be more than just harbingers of death since these enzymes are involved in several physiological functions in immune, nervous, and other tissues.

Caspase-6, historically identified as an effector caspase, has non-apoptotic functions important for axonal degeneration and cognitive decline. Caspase-6 can render human cell lines and neurons vulnerable to additional insults, but cannot cause apoptosis on its own (LeBlanc et al., 1999; Klaiman et al., 2009; Gray et al., 2010; Sivananthan et al., 2010b). In contrast, Caspase-6 is activated in several models of trophic factor deprivation in peripheral mouse neurons (Nikolaev et al., 2009; Vohra et al., 2010; Cusack et al., 2013; Ozturk et al., 2013) and is important for degeneration of central nervous system human and mouse neurons (Park et al., 2010; Sivananthan et al., 2010b; Monnier et al., 2011; Uribe et al., 2012). Caspase-6 cleaves several cytoskeletal proteins in primary human neurons that may compromise axon and synapse integrity (Klaiman et al., 2008). In Alzheimer disease (AD), a neurodegenerative disease that is the leading cause of dementia in the elderly, there is a significant increase in active Caspase-6 and Caspase-6-cleaved targets in neuritic plaques, neuropil threads, and neurofibrillary tangles compared to healthy age-matched controls (Guo et al., 2004; Klaiman et al., 2008; Albrecht et al., 2009; Halawani et al., 2010). A correlation also exists in cognitively normal individuals where high Caspase-6 activity results in lower cognitive performance (Albrecht et al., 2007). In

fact, active Caspase-6 is found in the human entorhinal cortex (Ramcharitar et al., 2013a; LeBlanc et al., 2014), the first area affected in AD (Braak and Braak, 1997), and correlates negatively with episodic memory scores (Ramcharitar et al., 2013a), the first type of memory affected in AD. Moreover, Caspase-6 overexpression in the CA1 region of the mouse hippocampus results in early inflammation and age-dependent episodic and spatial memory deficits (LeBlanc et al., 2014). Thus, Caspase-6 is an important effector of axonal degeneration and cognitive decline.

Caspase-6 has become an important therapeutic target in neurodegenerative diseases, but inhibitors have yet to reach clinical trials. Although some viral and endogenous proteins inhibit Caspase-6 activation or activity (Zhou et al., 1998; Zhang et al., 2001; Lee et al., 2010; Waldron-Roby et al., 2015), their clinical use is limited. Similarly, peptide-based and small molecule inhibitors lack specificity for Caspase-6 and have not been tested extensively in biological systems (Nyormoi et al., 2003; James et al., 2004; Ekici et al., 2006; Henzing et al., 2006; McStay et al., 2008; Pereira and Song, 2008; Chu et al., 2009; Leyva et al., 2010; Aharony et al., 2015). Some interesting Caspase-6 inhibitors targeting the enzyme-substrate complex or the inactive Caspase-6 zymogen have been developed (Heise et al., 2012; Stanger et al., 2012; Murray et al., 2014), but additional experiments are required to test their biological efficacy. Hence, Caspase-6 inhibitors are still far from clinical testing.

For that reason, this thesis aims to aid Caspase-6 inhibitor development by characterizing two novel caspase inhibitors. Methylene blue was a compound in phase III clinical trials for Alzheimer disease and other frontotemporal dementias involving microtubule associated protein Tau aggregation (Wischik et al., 2014). Methylene blue inhibits Tau aggregation by oxidizing key cysteine residues (Akoury et al., 2013; Crowe et al., 2013). Considering that caspases require reduced cysteines for catalytic activity (Stennicke and Salvesen, 1997), this thesis presents data on the potential of methylene blue and its derivatives, azure A and azure B, to inhibit caspase activity *in vitro*, in cells, and *in vivo*. In addition, New World Laboratories Inc. developed membrane permeable and non-toxic small molecule vinyl sulfone caspase inhibitors. This thesis also shows the potential beneficial effects of Caspase-6 inhibition in axonal degeneration models in human primary neurons and memory deficits in Caspase-6-overexpressing mice. One project highlights a novel mechanism for Caspase-6 inhibition via

oxidation of the catalytic cysteine and the other provides evidence in biologically relevant models that Caspase-6 inhibition can be neuroprotective. These studies urge continued Caspase-6 inhibitor development to achieve increased potency, tolerability, selectivity, and blood-brain barrier permeability for human clinical trials against age-related cognitive decline and AD.

1. Literature Review

1.1 Apoptosis

1.1.1 The discovery of apoptosis

Programmed cell death had been observed in silkmoths and worms in the 1960's by several different scientists. It was understood that cell death was a mechanism that eliminated unwanted cells. This was first described in the study of larval silkmoth maturation where cells or tissues that were no longer beneficial for the adult were lost (Lockshin and Williams, 1964). The term apoptosis (APE oh tosis), from Greek roots meaning falling off or dropping off of leaves from a tree, was employed by Kerr and colleagues from the University of Aberdeen to describe the sequential steps of programmed cell death (Kerr et al., 1972). The process of apoptosis has since then been characterized meticulously to include features of cell retraction, rounding, membrane blebbing, nuclear envelope breakdown, chromatin condensation, deoxyribonucleic acid (DNA) fragmentation, apoptotic body formation, and phagocytosis by neighbouring cells (Taylor et al., 2008). Compared to necrosis, which results in cell membrane rupture and the release of cytotoxic and inflammatory cytoplasmic contents, apoptosis proceeds serenely by sequestering cellular components within intact membranes. Thus, apoptosis allows the systematic removal of undesired cells while avoiding an immune response.

1.2 Discovering caspases and link to cell death proteases

1.2.1 The evolution of caspases

The ancestral origin of caspases was identified by comparative genomic analysis, a technique that searches for structure and sequence similarities across species and organisms. Using this approach, it was discovered that caspase-like genes are found in α-protobacteria, a close relative to mitochondria (Aravind and Koonin, 2002). It is believed that eukaryotic cells inherited protocaspases from the endosymbionts that are mitochondria and that these protocaspases evolved into metacaspases, paracaspases, and caspases throughout the different kingdoms of life. In fact, even phytoplankton, photosynthetic microorganisms that played a

fundamental role in shaping the marine ecosystems and Earth's climate, lived at the mercy of caspase-like proteins 2.2 billions years before our time (Bidle, 2016). These genetically encoded proteins have been perfected through billions of years of evolution and their discovery traces back to the late 20th century.

1.2.2 The first mammalian caspase

In the early 90's, pro-inflammatory cytokine interleukin-1β(IL-1β)-converting enzyme (ICE) was cloned from a human acute monocytic leukemia cell line (Cerretti et al., 1992; Thornberry et al., 1992). ICE was initially characterized as an oligomeric cysteinyl protease expressed in the cytoplasm of peripheral blood cells that could cleave many substrates including IL-1β. Since ICE's primary amino acid sequence did not match to other known proteases, ICE became the first member of the newly created Family C14 of Clan CD proteases (**Table 1.1**). ICE's amino acid sequence has a prodomain, large subunit, and small subunit that can be separated by autoprocessing upon overexpression (**Fig. 1.1**) (Miller et al., 1993). Unique to Family C14 proteases is the requirement for an aspartic acid residue at position P^1 of the peptide substrate (**Fig. 1.2**) based on the Schechter and Berger notation (Schechter and Berger, 1967; Kostura et al., 1989; Sleath et al., 1990; Howard et al., 1991). This gives its members the name caspase for cysteine-dependent aspartic-directed proteases. The importance of ICE/Caspase-1 in inflammatory processes was just starting to be unveiled, while groups around the world dashed to search for other members of the newly founded caspase family.

1.2.3 Apoptosis in *Caenorhabditis elegans*

Meanwhile, researchers Ellis H.M. and Horvitz H.R. had already spent a few years dissecting out the programmed cell death that occurred in 131 cells of the nematode *Caenorhabditis Elegans* (*C. elegans*). The death of these 131 cells is pre-determined as it is genetically encoded and occurs predictably during development. Using ethyl methylsulfonate as a mutagen, researchers created lineages of *C. elegans* that had defects in apoptosis and mapped the mutations to the *C. elegans* death (ced) genes ced-3 and ced-4 (Ellis and Horvitz, 1986). By combining mutations in ced-3 and ced-4 with *C. elegans* which had the egg-laying mutation, a mutation that showed premature death of hermaphrodite-specific neurons or ced-1

and ced-2 mutations that had impairments in engulfment of dead cells, scientists outlined a pathway for programmed cell death. CED-3 and CED-4 proteins were hypothesized to respond to death cues and initiate apoptosis within the cell (Yuan and Horvitz, 1990). Hints as to how these proteins initiated programmed cell death only came after the ced-3 gene was cloned. What researchers discovered was that CED-3 and ICE/Caspase-1 were orthologous proteins (Yuan et al., 1993). This indicated for the first time that cysteinyl proteases were crucial components of the cell death machinery. Since then, only 24 years have passed, yet over 85 000 research articles have been published on caspases.

1.2.4 The mammalian caspases

Currently, 18 mammalian caspases have been identified with 12 found in humans. Caspases are unique proteases because they require an aspartic acid in the P^1 position of their substrates and are generated as a single polypeptide which needs to be processed at specific aspartic acid residues to separate the prodomain, large subunit, and small subunit (**Fig. 1.1**). The craze to discover new caspases led several independent groups to use multiple inconsistent names when cloning the enzymes. To harmonize the nomenclature, scientists who cloned and characterized different caspases formed a committee to develop guidelines (Alnemri et al., 1996). Guidelines for referring to the unprocessed form (e.g. pro-caspase-1), the different subunits (large and small), and the gene name of caspases (*CASP*) was explicitly described. In addition, it was decided that the numbering of each caspase should represent the order in which they were discovered. For this section of the literature review, the cloning, tissue expression, and initial roles of caspases will be presented in chronological order. The cloning of ICE/Caspase-1 has already been discussed (**Section 1.2.2**).

Caspase-2 was originally identified by Dr. Noda's group from RIKEN in Tokyo that was interested in studying the genes responsible for the development and differentiation of neural precursor cells isolated from the mouse embryonic neural tube. The genes that were differentially expressed were termed neural precursor cell-expressed developmentally downregulated gene (Nedd) which included *CASP2* (Nedd2) (Kumar et al., 1992). When the importance of ICE/CED-3 in cell death emerged in 1993, Dr. Yuan's research group from Harvard Medical School cloned *CASP2* from a human fetal brain cDNA library that encoded

two alternatively spliced mRNA of ICE and Ced-3 homolog (Ich-1) which were called long (Ich-1_L) and short (Ich-1_S) (Wang et al., 1994). Both isoforms were detected by reverse-transcriptase polymerase chain reaction (RT-PCR) in different adult mouse tissues. Ich-1_L overexpression resulted in apoptosis of rat fibroblast, human cervical adenocarcinoma, and mouse/rat neuroblastoma/glioma cells, whereas Ich-1_S overexpression prevented rat fibroblast cell death after serum withdrawal. It was hypothesized that Ich-1_S had an inhibitory effect on Ich-1_L in cells. Surprisingly, the group from RIKEN dismissed the short isoform of Nedd2 as it was not easily detected in adult mouse tissues by northern blot analysis (Kumar et al., 1994). In any case, Nedd2/Ich-1/Caspase-2 was primarily assigned a pro-apoptotic role.

Caspase-3 is by far the most studied caspase as it is referred to in nearly 50 000 articles. It was cloned by researchers working in Dr. Alnemri's laboratory based on an expressed sequence tag (EST), a reverse complement sequence of mRNA, that was available in GenBank, a genetic sequence database. The EST had significant homology to Ced-3, so oligonucleotide primers were used to amplify this new gene from human Jurkat T-lymphocytes (Fernandes-Alnemri et al., 1994). Caspase-3 also went by several names such as Apopain, CPP32, Yama, and sterol regulatory element-binding protein cleavage activity 1. Caspase-3 shares higher identity with CED-3 than Caspase-1 or Caspase-2 and retains the highly conserved pentapeptide glutamine-alanine-cysteine-arginine-glycine (QACRG) sequence containing the catalytic cysteine. Caspase-3 expression was seen in different cancer cell lines but most notably in cells derived from the hematopoietic lineage which lacked Caspase-1 expression. Finally, Caspase-3 overexpression by infection of Sf9 insect cells induced apoptosis and led to the processing of Caspase-3 into large and small subunits. Taken together, Caspase-3 was another *bona fide* pro-apoptotic enzyme.

The cloning of Caspase-4 was published by three independent laboratories within a 2 month period in 1995 (Faucheu et al., 1995; Kamens et al., 1995; Munday et al., 1995). The first to publish was Dr. Lalanne's group from France. Using primers based on Southern blot data on exon 6 of ICE, RT-PCR on human neutrophils and placental RNA led to the amplification of a cDNA encoding a protein with 64% amino acid identity to Caspase-1. This new protein called Tx was the first member of the caspase family to show such a high level of similarity with Caspase-1. Tx was not able to cleave IL-1β, but did process inactive Caspase-1 and Tx mutants

into large and small subunits when co-transfected in African green monkey kidney cells in origin with simian virus 40 (COS). Tx was also found to induce rounding of the cell body and DNA condensation when overexpressed in COS cells suggesting a pro-apoptotic function. Unlike the group from France, researchers led by Dr. Kamens at the BASF Bioresearch Corporation cloned Caspase-4 from a thymus cDNA library using the entire ICE sequence as a probe. They found that Ich-2/Caspase-4 could cleave IL-1β, with a preference for cleavage at D^{27} (Kamens et al., 1995). The difference in their findings could be explained by experimental conditions, as purified proteins are more likely to interact together compared to proteins present in a cellular milieu. Finally, Dr. Nicholson's laboratory from the Merck Frosst Center for Therapeutic Research in Montreal Quebec cloned Caspase-4 from a human acute monocytic leukemia cell line cDNA library which they named ICE-related-II (ICE_{rel}-II) (Munday et al., 1995). Their findings and conclusions were similar to the two earlier publications, except that ICE_{rel}-II did not process IL-1β or itself upon overexpression in sf9 cells. Only overexpression of a truncated ICE_{rel}-II caused apoptotic morphology in fibroblasts. All in all, Caspase-4 was the first of the caspases to show high sequence identity to Caspase-1 and showed apoptosis-inducing capabilities.

Dr. Nicholson's group at Merck Frosst in Montreal Quebec was also the first to clone Caspase-5 or ICE_{rel}-III (Munday et al., 1995). ICE_{rel}-III mRNA was found at a tenth of the abundance of Caspase-4 in placenta, lung, liver, pancreas, kidney, and skeletal muscle by Northern blot analysis. Moreover, like Caspase-4, ICE_{rel}-III was not detected in brain samples, could not cleave IL-1β, or lead to apoptosis in the absence of self-processing. It is possible that Caspase-4 and -5 have always been grouped together because of their co-discovery in 1995 and because both enzymes are the only closest relatives of Caspase-1.

Like Caspase-3, Caspase-6 was cloned Dr. Alnemri at the Thomas Jefferson University in Philadelphia. Researchers used a nested PCR approach targeting the conserved regions identified in Caspase-1, -2, and -3 on a cDNA library from Jurkat T lymphocytes (Fernandes-Alnemri et al., 1995a). These regions included the QACRG motif and the glycine-serine-tryptophan-phenylalanine-isoleucine (GSWFI) motif found within the small subunit. This method led to the discovery of mammalian Ced-3 homologues (Mch) 2α and the alternatively spliced isoform Mch2β. The expression of both isoforms was confirmed by Northern blot

analysis on human pre-B lymphocytes. Mch2α is more closely related to Caspase-3 and Ced-3 than the other caspases. In terms of activity, recombinant Mch2α, but not Mch2β, self-processed into smaller subunits, cleaved aspartate-glutamate-valine-aspartate-7-amino-4-methylcoumarin (DEVD-AMC), cleaved poly(adenosine diphosphate(ADP)-ribose) polymerase (PARP), and induced apoptosis in infected sf9 insect cells. Needless to say, it was branded as yet another pro-apoptotic caspase.

Mch3/Caspase-7 was the next to be cloned from the Jurkat T-cell cDNA library using the previously published method by Dr. Alnemri for Caspase-6 coupled to data available in GenBank for EST (Fernandes-Alnemri et al., 1995b). Two alternatively spliced mRNA were identified encoding isoforms Mch3α and Mch3β. Mch3α encoded a protein of 303 amino acids, however, Mch3β lacked the QACRG motif found in all other caspase members suggesting it to be an inactive enzyme. Mch3α is most closely related to Caspase-3 and followed its different tissue expression patterns except for lower levels in the brain. Enzymatically, Mch3α behaved very closely to Caspase-3 with a preference for DEVD over Caspase-1-preferred YVAD substrates and the ability to cleave PARP efficiently. Strikingly, Mch3α induced apoptosis in infected sf9 cells even when the large and small subunits were swapped for a large or small subunit of Caspase-3, respectively. In contrast, Alnemri's research group also found that mixing and matching the subunits of Caspase-3 with those of Caspase-1 did not result in an apoptosis-inducing enzyme (Fernandes-Alnemri et al., 1994). This notion brought the possibility that caspases may regulate their activity by forming heteromeric complexes with subunits from non-parental enzymes. In addition, the researchers discovered that Mch3α is a good substrate of Caspase-3 suggesting that caspases may be activated in a cascade with upstream and downstream components.

Fas-associated death domain-containing protein (FADD)-like ICE (FLICE)/Caspase-8 was cloned by Dr. Dixit and Dr. Peter's groups at the University of Michigan and German Cancer Research Center in Heidelberg, respectively. Nano-electrospray tandem mass spectrometry had just recently been developed (Wilm et al., 1996) to sequence proteins present at femtomole levels and was used to sequence peptides isolated from a 2D-gel electrophoresis of immuno-precipitated complexes containing the death receptor CD95/Fas/Apo-1 (Muzio et al., 1996). One of the isolated proteins was FLICE which contained a QACQG instead of the

QACRG motif, while retaining the amino acids required for aspartate recognition at the P^1 position of the substrate. FLICE was found to be expressed in many tissues, namely blood leukocytes, while under the level of detection in fetal brains as demonstrated by Northern blot analysis. The death effector domain (DED) (Tartaglia et al., 1993) found in FLICE allowed protein-protein interactions with FADD in human embryonic kidney (HEK293T) cells. In addition, Granzyme B, a serine protease found in cytotoxic T lymphocytes cells known to activate Caspase-3 (Darmon et al., 1995) also cleaved FLICE leading to PARP proteolysis. However, it was later found that FLICE cannot be activated in the absence of oligomerization (Boatright et al., 2003). Moreover, FLICE overexpression resulted in the death of human breast adenocarcinoma cells which could be prevented with inhibition by benzyloxycarbonyl-valine-alanine-aspartate-fluoromethyl ketone (Z-VAD-FMK) (Thornberry et al., 1992) or cowpox response modifier A (CrmA) (Ray et al., 1992), a pan-caspase small molecule irreversible peptide inhibitor or a serine protease protein inhibitor, respectively. The identification of FLICE as an intermediate molecule between the activation of death receptors and the activation of Caspase-3/7 formed the foundation for the elaboration of the extrinsic apoptotic pathway.

Caspase-9 was also cloned by Dr. Dixit's laboratory at the Michigan School of Medicine. ICE-like apoptotic protease 6 (ICE-LAP6)/Caspase-9 was discovered using a probe based on EST from a human genome private database to screen a chronic myelogenous leukemia cell line (K562) cDNA library. (Duan et al., 1996). ICE-LAP6 was found to be more closely related to Caspase-3, -6, and -7, than to Caspase-1, -4, and -5. Like Caspase-8, ICE-LAP6 did not have the conserved pentapeptide sequence around the catalytic cysteine, QACRG, but instead had QACGG. In terms of tissue expression, Northern blot analysis revealed two alternatively spliced isoforms of Caspase-9 in most tissues. Overexpression of ICE-LAP6, but not the catalytic mutant, induced apoptosis in human breast adenocarcinoma cells. Moreover, like several members of the caspase family, ICE-LAP6 can be cleaved by Granzyme B, although dimerization was required for activation (Boatright et al., 2003), and can cleave PARP. However, unlike FLICE, ICE-LAP6 was not considered an upstream caspase in the signaling cascade leading apoptosis.

Caspase-10 was initially cloned in the laboratory of Dr. Alnemri who had gained significant recognition in the field of caspases at the Thomas Jefferson University due to his

previous descriptions of Caspase-3, -6, and -7. In the publication that described Mch4/Caspase-10, the researchers had also cloned Mch5 which was actually Caspase-8 (Fernandes-Alnemri et al., 1996). The method used to clone Caspase-6 was employed with additional information from the GenBank EST database to screen the cDNA library of Jurkat cells. Mch4 and Caspase-8 were found to be closely related and shared sequence similarity with CED-3 specifically in their small subunits. The scientists demonstrated that the pentapeptide motif of Mch4 was QACQG which is identical to that of Caspase-8 (Muzio et al., 1996) and that Mch4 contained FADD-like DED suggesting that it interacted with death receptors. Mch4 mRNA expression was found in most tissues although at low levels in some including the brain. In contrast to Caspase-1 or -3, YVAD-AMC and DEVD-AMC were equally susceptible to cleavage by Mch4. Moreover, the DEVD-aldehyde (CHO) reversible inhibitor blocked Mch4 with nanomolar affinity. Overexpression of Mch4 in insect sf9 cells resulted in apoptosis. Granzyme B, but not other caspases, cleaved Mch4 and activation was subsequently shown to be dependent on oligomerization (Boatright et al., 2003). In fact, Mch4 was thought to be an upstream caspase just like Caspase-8 because of its potential to interact with death receptors through FADD-like DED and because it could process and activate Caspase-3 and -7.

Since Caspase-11, a caspase with high sequence identity to human Caspase-4, was found to be exclusively expressed in rodents (Wang et al., 1998), it will not be discussed in detail. Similarly, Caspase-12 was cloned in rodent cells and showed high homology to human Caspase-4 and -5 (Van de Craen et al., 1997). Surprisingly, Caspase-12 is present in the human genome and expressed as nine different alternatively spliced variants (Fischer et al., 2002). However, each one of the variants encodes a premature stop codon resulting in the translation of non-functional truncated proteins in descendants from Eurasia and African populations. Only a small subset of sub-Saharan Africans encode a single nucleotide polymorphism (SNP) that replaces the stop codon with that of an arginine (Saleh et al., 2004). The resulting full length Caspase-12 leads to endotoxin hypo-responsiveness, increased incidence of severe sepsis, and mortality (Saleh et al., 2004; Saleh et al., 2006). Therefore, both Caspase-11 and -12 are considered murine homologs of human Caspase-4 and -5, respectively.

Caspase-13 or evolutionarily related ICE (ERICE) was cloned by Dr. Dixit's group at the Michigan School of Medicine using a database of EST (Humke et al., 1998). ERICE was

highly related to Caspase-4 and its expression was restricted to human peripheral blood lymphocytes, the spleen, and the placenta as detected by Northern blot analysis. Overexpression of ERICE led to apoptotic morphology in both MCF7 and HEK 293. Caspase-8, but not Granzyme B, was capable of activating ERICE. A few years later, two subsequent studies were unable to detect Caspase-13 expression in human tissues by RT-PCR and discovered that Caspase-13 was not a human caspase but a bovine caspase (Lin et al., 2000; Koenig et al., 2001). In fact, it is believed that the original study by Humke et al. detected Caspase-4 or -5 mRNA by Northern blot and not Caspase-13. Thus, like Caspase-11, Caspase-13 is not a human caspase either.

Caspase-14 was cloned by three different research groups. Dr. Vandenabeele's group from Belgium identified two clones of Caspase-14 in a mouse cDNA library when searching for homologs of caspases using the translation basic local alignment search tool for nucleotides algorithm (Van de Craen et al., 1998). Murine Caspase-14 was unique because it was not highly homologous to neither the Caspase-3 nor Caspase-1 subfamilies, it could not be processed efficiently by other caspases, it did not show any enzymatic activity on fluorogenic peptide substrates, it could not self-process upon overexpression in bacteria or yeast, and it did not induce cell death when overexpressed in human cervical adenocarcinoma cells. Most of these results were confirmed by the researchers in Dr. Alnemri's group from the Thomas Jefferson University (Ahmad et al., 1998). Detailed Caspase-14 characterization showed that overexpression in bacteria did not lead to dimerization, which is a unique trait among caspases (Mikolajczyk et al., 2004). For enzymatic activity, Caspase-14 requires dimerization while processing enhances its activity (Mikolajczyk et al., 2004). In terms of expression, murine Caspase-14 seemed to be restricted to stages of embryogenesis and in adult skin. This made sense since the cDNA clones identified by the researchers were from a mouse embryo and whole adult skin, although oddly enough one group did suggest expression in the liver (Ahmad et al., 1998). Scientists from Dr. Dixit's laboratory at the Michigan School of Medicine working with researchers from Dr. Salvesen's group at the Burnham Institute also cloned mouse Caspase-14 and found it expressed in the skin and during development (Hu et al., 1998). In addition, the scientists found that Caspase-14 induced cell death of MCF7 cells and had enzymatic activity on an acetylated (Ac-DEVD-AFC) substrate, which was in contradiction with the two other

groups (Ahmad et al., 1998; Van de Craen et al., 1998). Regardless, a human Caspase-14 homolog was identified with 72 % identity to murine Caspase-14 (Van de Craen et al., 1998; Eckhart et al., 2000a). The reason behind the discrepancies in the characterization of Caspase-14 are unclear, however, one fact remains, Caspase-14 is a member of the caspase family.

Phylogenetic analyses revealed Caspase-15 (Eckhart et al., 2005), -17, and -18 (Eckhart et al., 2008) as mammalian caspases which do not have human orthologs. Caspase-15 is most highly related to Caspase-14 and is found in pigs, dogs, and cattle. In the primary amino acid sequence of Caspase-15 there is a pyrin domain that resembles that from the apoptosis-associated speck-like protein containing a caspase activation and recruitment domain (ASC). Caspase-15 overexpression induced apoptosis in HEK293T cells through the activation of Caspase-3. Caspase-17 resembles Caspase-3, while Caspase-18 shares sequence identity with Caspase-8. However, neither caspase has been studied biochemically. On the other hand, Caspase-16 shares 45 % sequence identity with the catalytic domain of Caspase-14 and is found in humans (Eckhart et al., 2008), but the biochemical characterization of the enzyme has also not been performed. Moreover, it is not clear whether the Caspase-16 sequence in humans encodes a functional protein (Sakamaki and Satou, 2009). All in all, 11 *bona fide* human caspases (Caspase-1 to -10, and -14) have been presented in this section. Their classification based on sequence similarity, substrate preference, and function will be presented next.

1.3 Caspases are classified based on sequence similarities, substrate preferences, or function

Following their discovery, caspases have been classified into several different groups. The method of classification has differed based on the method of analysis. Different approaches looking at sequence similarity, substrate preference, and biological functions have been used to group caspases together. Analyzing sequence similarity gives clues as to the evolutionary relationship between caspases. In contrast, identifying substrate preferences highlight similarities between active site tertiary structures. Lastly, assigning biological function allows the identification of molecular pathways or signaling cascades.

1.3.1 Phylogenetic classification of human caspases

Phylogenetic analysis has helped to establish a link between the different caspases. Caspase genes can be clustered together based on similarities between their amino acid sequences and domains (**Fig. 1.3**) (Thornberry, 1997; Lamkanfi et al., 2002). Cluster I groups together Caspase-1 with Caspase-4 and Caspase-5. All three caspases contain a long prodomain which encodes a caspase recruitment domain (CARD) (Hofmann et al., 1997) that is necessary for homotypic protein-protein interactions. A slightly more distant phylogenetic relative is Caspase-2, although it does bear a CARD. Cluster II includes Caspase-3, -6, and -7. The sequence similarity between Caspase-3 and -7 is more pronounced than with Caspase-6. Cluster II caspases are closely related because of a very short amino-terminal sequence that lacks any domains important for protein-protein interaction. Cluster III is composed of Caspase-8, -9, and -10. Unlike the other caspase clusters, cluster III caspases differ in their prodomain sequences and are separated into two distinct branches. The first branch includes Caspase-8 and -10 which share two N-terminal DED, while the second branch includes Caspase-9 which contains a CARD. Cluster III caspases share sufficient sequence similarity in their large and small subunits to overcome the differences in their prodomains. Finally, Caspase-14 can be thought as belonging to a distant branch of cluster I caspases (Sakamaki and Satou, 2009). This is counterintuitive as Caspase-14 does not contain a CARD because its prodomain is as short as cluster II caspases. Nevertheless, human caspases can be clustered into three main groups based on sequence similarity.

1.3.2 Substrate preference-based classification of human caspases

Another method for classification of caspases is based on their substrate preferences. This was possible by the development of positional scanning synthetic combinatorial libraries (Pinilla et al., 1992). Using this method, a library of different peptides was generated with differing amino acids at positions P^4 to P^2 while maintaining the crucial P^1 aspartic acid residue coupled to a fluorogenic molecule (Rano et al., 1997) (**Fig. 1.2**). This was done using AMC or *p*-nitroaniline (pNA) coupled peptides for fluorogenic and absorbance assays (Talanian et al., 1997; Thornberry et al., 1997). From this analysis, three main groups emerged. Group I is composed of Caspase-1, -4, and -5, which is identical to the results from the phylogenetic

analysis. The consensus sequence for group I is WEHD. This is interesting, since the natural substrate of Caspase-1, interleukin-1β, is cleaved at YVHD (Thornberry et al., 1992). However, the synthetic inhibitor Ac-WEHD-CHO was 14-fold more potent than Ac-YVAD-CHO and crystal structure analysis revealed the preference of the Caspase-1 P^4 subsite for large aromatic amino acids (Rano et al., 1997). Several years later, it was found that Caspase-14 also belonged to group I caspases as it cleaves (W/Y)XXD sequences preferentially (Mikolajczyk et al., 2004). Group II includes Caspase-3, -7, and -2 with a consensus sequence of DEXD, where X can be any amino acid. This optimal sequence is in agreement with known cellular substrates of Caspase-3 and -7 like PARP and SREBP (Lazebnik et al., 1994; Wang et al., 1995). Furthermore, unique to Caspase-2 is its inability to cleave tetrapeptides and the requirement of a hydrophobic residue at P5 leading to an optimal sequence of VDVAD (Talanian et al., 1997). Group III members, Caspase-6, -8, -9, and -10, prefer the substrates (T/L/V)EXD which have a β-branched amino acid in the P^4 position (Talanian et al., 1997; Thornberry et al., 1997). Recent studies have demonstrated that caspases cleaved after glutamate and phosphorylated serine residues in substrates, undermining the notion that caspases were aspartic specific proteases (Seaman et al., 2016). Identification of the optimal sequence for group III caspases coupled to the sequences of processing sites within Group II caspases, chiefly Caspase-3 and -7, suggested that group III caspases were upstream activators within the signalling cascade. Another interesting observation is that even though Caspase-6 shares higher sequence similarity with Caspase-3 and -7, Caspase-6 has optimal substrate preferences more closely related to Caspase-8, -9, and -10. These results suggest that Caspase-6 may be more functionally related to these upstream caspases.

1.3.3 Functional classification of human caspases

More recently, caspases have been grouped by their two classically defined functions in apoptosis and inflammation (**Fig. 1.4**). Caspase-1 has always been the prototypical inflammatory caspase because of its ability to cleave IL-1β (Thornberry et al., 1992) and interleukin-18 (Ghayur et al., 1997; Gu et al., 1997). Studies in Caspase-1 deficient mice emphasized the importance of Caspase-1 in inflammatory processes and not apoptosis (Kuida et al., 1995; Li et al., 1995). However, the Caspase-1 was found to be responsible for cell death in mouse models of amyotrophic lateral sclerosis and potentially through cleavage of the pro-

apoptotic BH3-only protein Bid (Friedlander et al., 1997; Li et al., 1998; Guegan et al., 2002). Despite these results, Caspase-1 has maintained its designation as an inflammatory caspase. The other two inflammatory caspases are Caspase-4 and -5 which have historically been grouped with Caspase-1 based on their sequence similarities, substrate preferences, and recruitment to molecular platforms called inflammasomes (Rano et al., 1997; Thornberry, 1997; Martinon et al., 2002). In contrast, mice that were depleted of Caspase-3 (Kuida et al., 1996) or Caspase-9 (Hakem et al., 1998; Kuida et al., 1998) showed an excess of neurons in the brain and died shortly after birth (Kuida et al., 1996), although mice backgrounds could affect the phenotype displayed (Zheng et al., 1999). Due to sequence similarities, Caspase-3 and -9 were gathered with Caspase-6, -7, -8, and -10 and termed apoptotic caspases. Initiator caspases (Caspase-8, -9, and -10) are upstream in the signalling cascade that leads to apoptosis and have been grouped together because of their long prodomains capable of homotypic protein-protein interactions. The prodomain is crucial for monomeric initiator caspase activation by dimerization at molecular platforms (see section **1.4**). Initiator or inflammatory caspases then proteolytically activate effector caspases (Caspase-3, -6, and -7) (Slee et al., 1999; Guo et al., 2006; Inoue et al., 2009; Akpan et al., 2011; Edgington et al., 2012), which have very short prodomains and systematically dismantle the cell (Thornberry, 1997). Effector caspases exist as dimers in solution making it reasonable for them to have short prodomains that lack protein-protein interactions motifs (Rotonda et al., 1996; Wei et al., 2000; Kang et al., 2002).

As for Caspase-2, it is typically grouped with initiators of apoptosis since *in vivo* results from Caspase-2 deficient mice point towards a pro-apoptotic function (Bergeron et al., 1998). In addition, Caspase-2 can be downstream of death receptor signalling (Duan and Dixit, 1997) which is similar to Caspase-8 and -10.

Caspase-14 is unique as it is not a mediator of apoptosis or inflammation. Caspase-14 expression is confined to the stratum corneum where it plays an important role in terminal keratinocyte differentiation (Eckhart et al., 2000b; Lippens et al., 2000).

1.4 Molecular platforms for apoptotic and inflammatory pathways

Many types of cell death have emerged since the discovery of apoptosis and accidental cell death (necrosis) which include, but is not limited to, regulated necrosis (necroptosis),

anoikis, mitotic catastrophe, and cornification (Kroemer et al., 2009). Cell death was originally classified by morphological analyses as either apoptosis, autophagy, or necrosis. Yet, the ability to modify morphological changes in the absence of cytoprotection led to a more biochemistry-based classification of cell death (Galluzzi et al., 2015). Using this approach, cell death is characterized primarily by molecular pathways. In this thesis, only the main types of cell death mechanisms will be discussed.

1.4.1 The death-inducing signaling complex and the extrinsic pathway

Death receptors, proteins found in the cell membrane, transduce death signals following ligand-binding and receptor trimerization (Banner et al., 1993). The most studied receptors belong to the tumor necrosis factor α (TNFα) receptor (TNFR) superfamily and include TNFR1, Fas, death receptor 3 (DR3), TNF-related-apoptosis-inducing ligand receptor 1 (TRAIL-R1) or DR4, and TRAIL-R2 or DR5. In the case of Fas, binding of Fas ligand (FasL) leads to receptor trimerization and recruitment of the adaptor protein FADD (**Fig. 1.5**) (Boldin et al., 1995; Chinnaiyan et al., 1995). While FADD is recruited to activated Fas through homotypic interactions between their death domains (DD), FADD also recruits caspases through its DED to form the death-inducing signaling complex (DISC) (Kischkel et al., 1995; Los et al., 1995; Muzio et al., 1996). The DED of Caspase-8 and 10 promote their oligomerization at the DISC which leads to their activation (Muzio et al., 1998; Salvesen and Dixit, 1999; Boatright et al., 2003).

During extrinsic apoptosis, the DISC activates Caspase-8/10 by proximity induced oligomerization which then proteolytically cleave either the BH3-only protein Bid or Caspase-3 to follow two converging pathways. In type I cells, like lymphocytes and thymocytes, activated Caspase-8/10 process Caspase-3 directly into its fully mature form (Fernandes-Alnemri et al., 1996; Srinivasula et al., 1996a). Caspase-3 then activates downstream caspases and cleaves many substrates. In type II cells, like hepatocytes and pancreatic β cells, Caspase-8 cleaves the BH3-only protein Bid (Li et al., 1998; Luo et al., 1998). Truncated B-cell lymphoma (Bcl-2) homology domain 3-interacting domain death agonist (tBid) then translocates to the mitochondria where it activates the proapoptotic Bcl-2 family members Bax/Bak to initiate the intrinsic apoptosis pathway which eventually activates Caspase-3 (see section **1.4.2**). The

importance of both FADD and Caspase-8 in apoptosis is corroborated by the embryonic lethality of mice deficient in either protein (Juo et al., 1998; Varfolomeev et al., 1998; Yeh et al., 1998; Zhang et al., 1998).

In contrast, binding of TNFα to TNFR1 leads to binding of TNFR1-associated death domain protein (TRADD) (Hsu et al., 1995), TNFR2-associated factor 2 (TRAF2), and serine/threonine poly-ubiquitinated receptor interacting protein kinase 1 (RIP1) to form the pro-survival complex I (Micheau and Tschopp, 2003). Complex I signals through nuclear factor κ B (NFκB) to promote cell survival. TRAF2 recruits cellular inhibitors of apoptosis proteins (cIAPs) for its E3 ubiquitin-ligase activity. Ubiquitination of Caspase-8 leads to its proteasomal degradation (Gonzalvez et al., 2012), while the addition of poly-ubiquitin chains onto RIP1 promotes its signalling through NFκB (Bertrand et al., 2008). In addition to cIAP, the proteolytic activity of Caspase-8 can also be reduced by heterodimerization with cellular FLICE-like inhibitory protein (cFLIP) (Thome et al., 1997). In fact, the cFLIP long form ($cFLIP_L$)/Caspase-8 heterodimer prevents apoptosis and necroptosis (see section **1.4.5**) signalling (Pop et al., 2011). This is because the heterodimer possesses an active site and catalytic activity that preferentially cleave and inactivate RIP1, but not Bid or effector caspases (Oberst et al., 2011). On the other hand, cFLIP short form ($cFLIP_S$) completely inhibits Caspase-8 processing (Thome et al., 1997) which terminates apoptotic signalling while allowing RIP1 to initiate necroptosis (see section **1.4.5**). Thus, in the context of abundant cFLIP and cIAP, complex I primarily mediates pro-survival signals.

When cIAP and cFLIP levels are reduced, a cytosolic pro-apoptotic complex IIa forms. This complex is composed of TRADD, RIP1, FADD, and Caspase-8. Within complex IIa, Caspase-8 is a fully processed homodimer that can initiate both the cleavage of Bid and effector caspases. In cells that are deficient for Caspase-8 and treated with cIAP antagonists, Caspase-10 can form a complex with RIP1 to mediate apoptosis (Tanzer et al., 2017). The formation and regulation of the complex IIb is necessary for necroptosis (see section **1.4.5**). Therefore, death receptor signaling can activate a plethora of signaling cascades that are integrated by the cell to determine the outcome.

1.4.2 The apoptosome and the intrinsic apoptotic pathway

Mitochondria are at the root of the apoptosome signaling pathway. The core of the apoptosome is composed of apoptotic protease-activating factor-1 (Apaf-1), which is a cytosolic protein with an N-terminal CARD and a member of the nucleotide-binding oligomerization domain (NOD)-like receptors (NLRs), followed by an oligomerization domain, and several C-terminal WD40 repeats (Li et al., 1997; Zou et al., 1997). In normal cells, Apaf-1 is bound to ADP resulting in auto-inhibition through its WD40 domains (Srinivasula et al., 1998). During apoptosis, oligomerization of Apaf-1 is primed by binding of cytochrome C (CytC) to WD40 repeats (Srinivasula et al., 1998), an inter-mitochondrial space protein part of complex IV of the electron transport chain. Once ADP is exchanged for adenosine triphosphate (ATP) or deoxyadenosine triphosphate (dATP), seven copies of the Apaf-1-CytC heterodimer form a heptameric complex called the apoptosome (**Fig. 1.5**). Monomeric Caspase-9 is then recruited to the central hub of the apoptosome and dimerizes (Acehan et al., 2002). The Caspase-9 homodimer has a single active site that is 100-fold more active than the monomeric counterpart (Renatus et al., 2001).

During intrinsic apoptosis, signalling from DNA damage, reactive oxygen species generation, ischemia, or other insults converge onto the outer mitochondrial membrane to trigger cell death. Pro-survival (Bcl-2, Bcl-XL, Mcl-1, etc.) or proapoptotic (Bax, Bak, Bid, Puma, Noxa, etc.) Bcl-2 family members are carefully regulated ultimately to determine whether CytC can escape the inter mitochondrial space (Liu et al., 1996). For example, in a context where tBid is present, the oligomerization of Bax is activated and translocates to the outer mitochondrial membrane. Meanwhile, Bak is released from Bcl-2-mediated inhibition and oligomerizes with Bax to form a pore that leads to mitochondrial outer membrane permeabilization (MOMP). Following MOMP, CytC leaks to the cytosolic compartment where it heterodimerizes with Apaf-1 to form the apoptosome. CytC is not the only protein conducive to caspase activity. Second mitochondria-derived activator of caspase (SMAC/DIABLO) release results in IAP sequestration and degradation through interactions with a tetrapeptide IAP-binding motif (IBM) (Srinivasula et al., 2001). Moreover, high temperature requirement protein A2 (HtrA2) is an IBM-containing serine protease that cleaves IAPs to induce intrinsic apoptosis (Suzuki et al.,

2001). Thus, MOMP allows the apoptosome to activate Caspase-9 which then activates the effector Caspase-3 to initiate cellular demolition (Rodriguez and Lazebnik, 1999).

1.4.3 The inflammasomes and pyroptosis

The mammalian inflammasomes are responsible for the innate immune response and culminate in the activation of Caspase-1. The nucleotide-binding site family comprises several members including NLRs, absent in melanoma 2-like, and pyrin receptors. NLRs come in two flavours, NLRPs have a pyrin domain (PYD) at the amino terminus, while NLRCs have a CARD. In addition, NLRs have a nucleotide-binding NACHT domain required for oligomerization and a leucine-rich repeat (LRR) domain. These intracellular receptors are activated by diverse agonists including muramyl dipeptide, pathogen-associated molecular patterns or damage-associated molecular patterns, bacterial flagellin, and double-stranded DNA targeting NLRP1, NLRP3, NLRC4, and AIM-2, respectively (Sharma and Kanneganti, 2016). Once activated, NLRP1 undergoes oligomerization and recruits Caspase-1 using ASC. ASC couples NLRP1 oligomers to monomeric Caspase-1 by interacting with the NLRP1 PYD and the Caspase-1 CARD. The binding of several Caspase-1 monomers to the inflammasome is believed to induce proximity-induced autoproteolysis and activation (Broz et al., 2010). Surprisingly, in the same study, researchers found that unprocessed dimers of Caspase-1 are less efficacious in cleaving pro-IL-1β and induce-rapid cell death (Broz et al., 2010). In contrast, inflammasomes complexes containing NLRC4 bypass the need for ASC and interact directly with Caspase-1 (Poyet et al., 2001). Caspase-1 activation can lead to the maturation of pro-inflammatory cytokines (IL-1β and IL-18) and to pyroptosis (Fink and Cookson, 2006). Recent evidence from human monocytic cell lines suggests that Caspase-4 and -5 may be involved in NLRP3 or non-classical inflammasome activation to generate mature IL-1β leading to pyroptosis (Baker et al., 2015; Vigano et al., 2015).

Pyroptosis is a form of necrosis wherein cells undergo rapid swelling followed by a rupturing of the cell membrane and release of the cytosolic contents (Fink et al., 2008). Recent studies have identified Gasdermin D as a substrate of Caspase-1/4/5 and the effector of pore formation during pyroptosis (Kayagaki et al., 2015; Shi et al., 2015). Following Caspase-1 activation, IL-1β is released into the extracellular space and signals to neighbouring cells to

coordinate an inflammatory response. This is in stark contrast to apoptosis where the cell is neatly dismantled from within and broken apart into smaller apoptotic bodies with intact membranes (Taylor et al., 2008).

1.4.4 The PIDDosome and mitotic catastrophe

The PIDDosome is a multi-protein complex that serves as a regulator of cell growth and survival during mitosis by regulating Caspase-2 activation. Caspase-2 was found to cleave Bid which could activate apoptosome signaling in cells (see section **1.4.2**) (Guo et al., 2002), but the mechanism of Caspase-2 activation took a few years to unravel. Components of the apoptosome were not required for Caspase-2 activation, although Caspase-2 was found to be part of a large multi-protein complex (Read et al., 2002). RIP-associated Ich-1/CED homologous protein with a DD (RAIDD) is known to interact with Caspase-2 through homotypic CARD interactions (Duan and Dixit, 1997). The DD of RAIDD contacts the homologous domain of p53-induced protein with a DD (PIDD) (Tinel and Tschopp, 2004). PIDD binding to RAIDD is rate-limiting and can be primed by processing or phosphorylation of PIDD (Tinel et al., 2007; Ando et al., 2012). The complex of PIDD/RAIDD/Caspase-2 is termed the PIDDosome and is responsible for Caspase-2 activation. However, unlike the DISC or the apoptosome, PIDDosome formation does not lead to cell death in the absence of another stress (Tinel and Tschopp, 2004).

During the cell cycle, cells in interphase copy their DNA in preparation for division. Yet, to commit to mitosis, several checkpoints must be cleared. In a situation where DNA damage is sensed, ataxia telangiectasia mutated (ATM) is activated and phosphorylates PIDD (Ando et al., 2012). Phosphorylated-PIDD can recruit the RAIDD/Caspase-2 complex. Caspase-2 is activated by proximity-induced oligomerization which also results in self-processing. Active Caspase-2 cleaves Bid and activates extrinsic apoptosis type II cell signaling which results in mitotic catastrophe (Castedo et al., 2004). To give cells a chance to complete mitosis, budding uninhibited by benzimidazoles 1-related protein 1, a subunit of the mitotic checkpoint complex, directly binds to the DD of phosphorylated PIDD at the kinetochore which effectively prevents PIDDosome formation (Thompson et al., 2015). Thus, PIDDosome activation is necessary for the elimination of damaged cells during mitosis.

1.4.5 The Ripoptosome at the crossroads between apoptosis and necroptosis

Necrosis is no longer considered accidental cell death. Regulated necrosis, or necroptosis, involves the formation of the Ripoptosome as a signalling platform. The Ripoptosome is composed of RIP1, FADD, Caspase-8, and cFLIP. High levels of cFLIP and reduced Caspase-8 activity (Thome et al., 1997), low levels of cIAP, or increased deubiquitinase activity from cylindromatosis (CYLD) release RIP1 from complex I (Moquin et al., 2013). This allows RIP1 to autophosphorylate and then subsequently phosphorylate RIP3 (Feoktistova et al., 2011). Because Caspase-8 can cleave Rip1 and CYLD (Lin et al., 1999; O'Donnell et al., 2011), the Ripoptosome will determine if Rip1 is allowed to continue down its signaling cascade. The RIP1/RIP3 complex is known as complex IIb or the necrosome. The phosphorylation cascade continues with mixed lineage kinase domain-like protein (MLKL), which undergoes trimerization and pore formation at the plasma membrane (Cai et al., 2014). MLKL availability at the necrosome is tightly controlled by both TRAF2 and CYLD (Petersen et al., 2015). Consistent with this pathway, the embryonic lethality of FADD or Caspase-8 deficient mice is believed to be due to excess necrosis since depletion of RIP3 rescues this phenotype (Kaiser et al., 2011). Thus, when RIP1 is degraded, the DISC is formed leading to apoptosis. Alternatively, when Caspase-8 is inhibited or degraded, the Ripoptosome is formed leading to necroptosis. However, if RIP1 is poly-ubiquitinated and remains bound to death receptors, RIP1 promotes cell survival through NFκB. Clearly, cell death pathways undergo a complex array of signal integration before cell fate decisions are made.

1.5 Caspase functions in apoptosis and beyond

For many years following their initial discovery, caspases were thought to exclusively function in cell death and inflammatory signaling events. Although the evidence supporting caspase function in apoptosis and inflammation is undeniable and deserves continued effort, it is conceivable that these enzymes, which are expressed in all cells, are responsible for other functions. In fact, most caspase knockout animals did not exhibit overt defects in apoptosis (Zheng et al., 1999) suggesting redundancy in caspase function and the existence of non-apoptotic roles. The value of caspases in other pathways required for cellular homeostasis only emerged starting from the late 90's. In fact, different cell types were discovered to harness

caspase proteolytic activity to achieve a myriad of functions. A description of caspase function in apoptosis will be followed by a few functions in the immune system, nervous system, and other organs.

1.5.1 Caspase functions in systematic dismantling of dying cells

Apoptosis is a controlled process of cell retraction, rounding, membrane blebbing, nuclear fragmentation, chromatin condensation, DNA fragmentation, and phagocytosis (Kerr et al., 1972). Caspases coordinate to dismantle adhesion molecules to initiate retraction from neighbouring cells. An example is Caspase-3-mediated cleavage of focal adhesion kinase which normally inhibits caspases when interacting with integrins (Wen et al., 1997). Caspases also cleave proteins associated with the actin, microtubule, and the intermediate filament networks which weakens the plasma membrane causing cell rounding. This is highlighted by the abundance of Caspase-6-mediated cleavage of cytoskeletal proteins in human neuronal extracts, which include α-tubulin and microtubule associated protein Tau cleavage (Klaiman et al., 2008). These proteolytic events weaken the plasma membrane and promote blebbing. Rho-associated protein kinase 1 cleaved by Caspase-3 phosphorylates myosin light chain which increases contractile forces on actin filaments pushing the cytosol against the vulnerable plasma membrane resulting in blebbing (Sebbagh et al., 2001). Similar actin and microtubule dynamics are required to pull apart the nuclear envelope. First the nuclear envelope is weakened by Caspase-6-mediated cleavage of nuclear lamins (Orth et al., 1996; Takahashi et al., 1996). Caspase-6 and Caspase-3 also cleave the nuclear mitotic apparatus protein at distinct sites (Hirata et al., 1998), then actin and myosin provide contractile force to disintegrate the nuclear envelope while microtubules are used to transport the fragments into the apoptotic bodies (Croft et al., 2005; Moss et al., 2006). Chromatin condensation is thought to depend on histone (H2B) phosphorylation by mammalian sterile twenty kinase following Caspase-3 cleavage and nuclear translocation (Ura et al., 2001; Cheung et al., 2003). DNA fragmentation is also dependent on Caspase-3-mediated cleavage of the inhibitor of caspase-activated deoxyribonuclease (DNAse) which releases caspase-activated DNAse allowing it to translocate into the nucleus (Liu et al., 1997; Enari et al., 1998). Finally, phosphatidylserine is also flipped from the inner leaflet to the outer leaflet early during apoptosis to promote recognition and phagocytosis. The protein responsible for flipping phosphatidylserine remained elusive for several years (Martin et al.,

1996). A few years ago, Xk-family related protein 8, a transmembrane protein with a Caspase-3 cleavage site, was found to be responsible for phosphatidylserine flipping in human and mouse cells (Suzuki et al., 2013). Thus, caspases coordinate all the different aspects of apoptosis from cell retraction to apoptotic body engulfment.

1.5.2 Non-apoptotic caspase functions in immune cells

Considering that most caspases were originally cloned in human monocytic or lymphocytic cell lines, it is not surprising that caspases play an important role in immune cell proliferation and differentiation. In fact, upon encountering an antigen, T cells become stimulated to mount an immune response. This stimulation leads to Caspase-3 processing and activity in the absence of apoptosis (Miossec et al., 1997). In fact, during T helper 2 cell differentiation, Caspase-3 is inhibited by the action of interleukin-4 (Rautajoki et al., 2007). Similarly, treating activated T cells with a pan-caspase inhibitor reduces their ability to expand in culture (Alam et al., 1999). The proliferative ability of T cells depends on the levels of $cFLIP_L$ which heterodimerizes with Caspase-8 to modulate Fas signalling to prevent apoptosis, while favouring NFκB signalling (Lens et al., 2002; Zhao et al., 2014). The generation of mice with T cell-specific depletion of Caspase-8 revealed its role in T cell homeostasis, proliferation, and activation (Salmena et al., 2003).

Dendritic cell and macrophage differentiation following exposure to macrophage-colony stimulating factor or granulocyte-monocyte CSF is dependent on Caspase-8 (Kang et al., 2004). In contrast, Caspase-3 activity keeps dendritic cells in an immature state (Santambrogio et al., 2005), whereas Caspase-3 is necessary for differentiation of macrophages (Sordet et al., 2002). Caspase-6 plays an important role in activating innate immunity in the lung by cleaving IL-1 receptor-activated kinase M in alveolar macrophages (Kobayashi et al., 2011). Furthermore, Caspase-6 upregulation is necessary for the anti-inflammatory M2 phenotype of macrophages and the increased invasiveness of tumor-associated macrophages (Yao et al., 2016).

B cell activation and proliferation is promoted by Caspase-3-mediated cleavage of cyclin-dependent kinase inhibitor p21 (Woo et al., 2003). B cell activation by double-stranded RNA or LPS may require Caspase-8 signalling (Beisner et al., 2005; Lemmers et al., 2007). Stimulating resting B cells with CD40 results in Caspase-6-mediated cleavage of special AT-

rich sequence binding protein 1 and B cell proliferation is arrested by Caspase-6 inhibition with benzyloxycarbonyl-valine-glutamate-isoleucine-aspartate-fluoromethyl ketone (Z-VEID-FMK) (Olson et al., 2003). When Burkitt lymphoma line BL41 undergoes proliferation, Caspase-6 cleaves 5-lipoxygenase which is necessary to initiate leukotriene synthesis from arachidonic acid (Werz et al., 2005). Moreover, terminally differentiated plasma cells have suppressed Caspase-6 activity (Underhill et al., 2003). This is because Caspase-6 blocks entry of B cells into the G_1 stage of the cell cycle leading to decreased plasma cell generation (Watanabe et al., 2008).

1.5.3 Non-apoptotic caspase functions in the nervous system

Many neurons in the developing brain perish due to Bcl-2-regulated Bax-mediated apoptosis and this is exemplified by increased mouse neurons in brains overexpressing Bcl-2 (Martinou et al., 1994). Yet, Bcl-2 overexpression leads to normal mice brain formation while Caspase-3 and Caspase-9 deficiency leads to supernumerary neurons with abnormal brain formation (Kuida et al., 1996; Kuida et al., 1998). These results suggest that caspase activity may be important for normal brain development and led to the hypothesis that sub-lethal caspase activity may be an important factor for different signalling pathways in the nervous system (Li et al., 2010).

Dendritic and axonal pruning are mechanisms by which signalling between neurons can be refined. In *Drosophila melanogaster*, class IV sensory neuron dendritic arborisation is complex during the larval stage, but is completely destroyed in the adult (Truman, 1990). This remodeling is mediated by DRONC, the Caspase-9 ortholog in fruit flies, and is tightly regulated by *Drosophila* IAP 1 which targets DRONC for proteasomal degradation (Wilson et al., 2002; Kuranaga et al., 2006). Mouse sensory, motor, and dorsal root ganglion neurons undergo axonal pruning in response to neurotrophic factor deprivation (Ernsberger, 2009). Caspases became implicated in axonal degeneration following a study which identified amyloid precursor protein (APP) processing and DR6 signalling in nerve growth factor (NGF)-deprived mouse sensory and motor neurons (Nikolaev et al., 2009). For example, during development, embryos undergo robust axonal pruning in the dorsal root ganglion and this process required Caspase-6 and -3 to cleave tubulin (Sokolowski et al., 2014). Although the caspases involved in mouse axonal

degeneration have been studied in great detail (Geden and Deshmukh, 2016; Simon et al., 2016), it is not clear which caspases are important in human neurons (see section **1.11**).

Synaptic plasticity can be modulated by sub-lethal caspase activation. In rat hippocampal slices, Caspase-3 suppression by pharmacological inhibitors leads to a time-dependent block of long-term potentiation, a form of synaptic strengthening associated with learning and memory (Gulyaeva et al., 2003). This could be explained by the constitutive activation of protein kinase C zeta (PKCζ) following cleavage by Caspase-3 to generate PKMζ (Ling et al., 2002). In contrast, other groups have found Caspase-3 to be necessary in mediating the long-term potentiation counterpart, long-term depression (Li et al., 2010). Mechanisms behind long-term depression through Caspase-3 could rely on α-amino-3-hydroxy-5-methyl-4-isoxazolepropionic (AMPA) receptor internalization or cleavage (Chan et al., 1999; Li et al., 2010). In fact, the complex signalling pathway instigated by Caspase-3 starts from the inactivating cleavage of Akt which then activates GSK3β that phosphorylates and destabilizes clusters of post-synaptic density protein 95 (PSD95) ultimately leading to the breakdown of synapses (Nelson et al., 2013). Concomitantly, Caspase-3 activates the phosphatase Calcineurin which can itself lead to Caspase-3 activation by Bad de-phosphorylation and lead to AMPA receptor internalization (Wang et al., 1999; Beattie et al., 2000; Mukerjee et al., 2000).

Other forms of synaptic plasticity are also thought to be mediated through the action of caspases. Heterosynaptic plasticity, which occurs when an active synapse initiates a signalling cascade to downregulate nearby inactive synapses, is dependent on Calcineurin activity (Oh et al., 2015). Caspase signalling could modulate Calcineurin activity during heterosynaptic plasticity, although this needs to be investigated further. Metaplasticity is a consequence of initial neuronal activity on subsequent activity within the same synapse (Huang et al., 1992). This process was found to be dependent on Caspase-9, -3, and -7 activity in developing tadpoles which led to the cleavage of the transcription factor myocyte enhancer factor-2, an activity-dependent synapse function and structure regulator (Chen et al., 2012). On a larger scale, extensive synaptic remodeling occurs at birth in mice at the neuromuscular junction (Sanes and Lichtman, 1999). Acetylcholine receptor clusters form in the post-synaptic muscle tissue and can be removed by the action of Caspase-3 on disheveled 1 (Wang et al., 2014), a protein involved in Wnt signalling and cholinergic receptor clustering.

1.5.4 Other non-apoptotic functions

Apart from cytokine maturation, Caspase-1 can also mediate NFκB signalling through its prodomain independent of catalytic activity (Lamkanfi et al., 2004), anti-angiogenesis by preventing endothelial cell activation (Lopez-Pastrana et al., 2015; Yin et al., 2015), and protein secretion by regulating exosomes (Keller et al., 2008). For those suffering from androgenetic alopecia, or androgen-dependent hair loss, Caspase-1 mRNA is increased in the scalp (de Rivero Vaccari et al., 2012). Treatment with finasteride, a 5α reductase inhibitor, lowers dihydrotestosterone and Caspase-1 levels suggesting the involvement of inflammasome components in androgenetic alopecia.

Caspase-2 is activated following several cellular stressors including DNA damage, cytoskeletal disruption, metabolic perturbation, and heat shock (Harvey et al., 1997). Caspase-2 is protective in instances of DNA-damage (Shi et al., 2009), cancer development (Ho et al., 2009), and motor neuron, sympathetic neuron, and oocyte development in mice (Bergeron et al., 1998). More recent studies have identified a role for Caspase-2 in osteoclastogenesis (Callaway et al., 2016), hematopoietic stem cell differentiation (Dawar et al., 2016), and negative modulation of autophagy (Tiwari et al., 2014).

Caspase-3 and -7 activation by endoplasmic-reticulum stress response is suppressed by the unfolded protein response (UPR) in human uterine cells. Caspase-3 and -7 cleave the gap junction protein α1 to promote uterine cells quiescence, decrease contractile strength, and increase gestational length (Kyathanahalli et al., 2015). Non-apoptotic Caspase-7 activity is also necessary for the development of hair follicles and mast cells (Vesela et al., 2015), osteogenesis (Svandova et al., 2014), tooth development (Matalova et al., 2012), and recently spermatogenesis (Lei et al., 2017).

Caspase-6 cleaves proteins involved in cell structure, signalling, cell cycle, protein folding, transcription, nuclear matrix structure, DNA repair/binding, protein synthesis and elongation, metabolism, proteolysis, and membrane and lipid binding (Klaiman et al., 2009; Graham et al., 2011; Julien et al., 2016; Riechers et al., 2016). Recent studies found Caspase-6 to be secreted from sensory axons following inflammation and trigger TNFα release in microglia residing in the spinal cord (Berta et al., 2014). Microglial TNFα caused increased synaptic

plasticity in the dorsal horn which led to pain hypersensitization. This is corroborated in mice injected intrathecally with recombinant Caspase-6 which led to mechanical allodynia specifically in male mice (Berta et al., 2014). The reason behind sex differences in pain hypersensitization in mice is unknown. In addition, Caspase-6 can negatively regulate cellular growth and survival by preventing downstream signalling from the mammalian target of rapamycin complex 1 (Martin et al., 2016). Apoptosis induction in lymphoma cell lines led to Caspase-6 activation and cleavage of the regulatory-associated protein of mTOR (raptor). Raptor was necessary for recruiting mTOR substrates, but this was prevented following Caspase-6-mediated processing of raptor's N- and C-termini (Martin et al., 2016). In this pathway Caspase-6 prevented cells from entering an anabolic state by inhibiting mTOR signalling. In addition, epithelial cells lining the intestines are subjected to detachment-mediated cell death termed anoikis. Many caspases are activated in this process, but may require Caspase-6-mediated cleavage of focal adhesion kinase (Grossmann et al., 2001). Thus, Caspase-6 can have several functions outside of the immune and nervous systems.

Additional Caspase-8 physiological roles came from characterizing mice with tissue-specific deletions. Caspase-8 knockout mice suffer from cardiac deformations, neural tube defects, and hematopoietic progenitor deficiency resulting in embryonic lethality (Varfolomeev et al., 1998; Sakamaki et al., 2002). To elucidate the mechanisms further, tissue-specific deletions were generated (Kang et al., 2004). Caspase-8 was found to play an important role in endothelial cell development during embryogenesis which is necessary for proper formation of the circulatory system and death of hepatocytes. A recent study identified sorting nexins as Caspase-8 substrates (Duclos et al., 2017). During apoptosis, Caspase-8-mediated cleavage of sorting nexins resulted in reduced endosomal trafficking to the trans-Golgi network because interactions with the retromer complex was lost. Researchers propose that cancer cells may use Caspase-8-mediated cleavage of sorting nexins to increase receptor tyrosine kinase signalling by reducing Met/hepatocyte growth factor receptor endocytosis.

Finally, Caspase-14 has been known to play a fundamental role in keratinocyte differentiation almost since its discovery (Eckhart et al., 2000b; Lippens et al., 2000). Apart from arbitrating differentiation, Caspase-14-mediated processing of profilaggrin is required for water retention and photoprotection against ultraviolet B irradiation (Denecker et al., 2007).

There is one important caveat in studies investigating non-apoptotic caspase function. Most findings do not explain how strong effector caspases could be active yet restricted from dismantling the cell. This is especially interesting for Caspase-3 and -7 considering that they cleave a plethora of substrates important for apoptosis. Additional information on caspase activation related to temporal and spatial restrictions could provide some insight.

1.6 Caspase-6 transcriptional control, alternative splicing, and tissue expression

Following the general literature review on caspases (caspase discovery, family members, classification, signalling platforms, and diverse apoptotic and non-apoptotic functions), the remainder of the literature review will be dedicated to present the current knowledge on Caspase-6. My thesis is an extension of several decades of research from Dr. LeBlanc's laboratory who identified Caspase-6 as an instigating factor in the cognitive impairment seen during aging and Alzheimer disease (AD). For that reason, my research activities revolved around identifying inhibitory mechanisms and molecules to target Caspase-6 to achieve neuroprotection and delay or prevent the onset of cognitive deficits. Thus, prior to presenting my findings, a thorough review on Caspase-6 is necessary.

1.6.1 Little is known about *CASP6* gene transcriptional regulation

There is limited knowledge on the *CASP6* gene promoter found on chromosome 4q25 reverse strand in humans. Based on the Ensembl genome database, the human *CASP6* gene is 15 459 bp in length with 1 548 bp and 1 347 bp encoding the two different Caspase-6 isoforms. A complete bioinformatics and biochemical analysis of the *CASP6* promoter has not been conducted yet. There is an annotated core promoter region (2001 bp) starting 728 bp upstream of the transcription start site (TSS) and ending within the first intron. Transcription factor binding site prediction software[1] reveals 22 potential sites upstream of the TSS and four sites

[1] Based on SABiosciences' Text mining application and the UCSC Genome Browser

downstream (**Fig. 1.6**). These include, but are not limited to, the glucocorticoid receptors α and β, peroxisome proliferator-activator receptor α, myocyte enhancer factor-2, sex determining region Y-box 5 (Sox5), signal transducer and activator of transcription 3 (STAT3), acute myeloid leukemia 1, forkhead box F2, and myeloid ecotropic viral integration site homeobox 1. Interestingly, *CASP6* mRNA is dependent on Sox11 and Sox4 expression in cell lines and mice (Bhattaram et al., 2010; Wang et al., 2010a). Additional experiments designed to test the transcriptional activity of these predicted binding sites using luciferase assays is warranted.

Away from the promoter, two studies have reported that the tumor suppressor p53 transcriptionally upregulates Caspase-6 expression by binding to intronic regions. p53 overexpression upregulates *CASP6* mRNA levels in several different human cancer cell lines possibly by binding to a site within *CASP6*'s third intron (MacLachlan and El-Deiry, 2002). This leads to an increase in both Caspase-6 mRNA and protein. Similarly, treatment with Adriamycin, a DNA intercalating agent, enhances Caspase-6 levels and processing into the active enzyme. However, in these experiments, p53 was only shown to interact with synthetic oligonucleotides representing the predicted p53 binding site. Cultured human astrocytes exposed to human immunodeficiency virus (HIV) viral protein R have increased p53 and Caspase-6 expression (Noorbakhsh et al., 2010). In mice, the *Casp6* gene (12 678 bp) is found on chromosome 3H1 and lacks 78% of the 5'- sequence of exon 1 compared to human *CASP6*. p53 binds to the first C*asp6* intron in response to cisplatin treatment and direct evidence was shown by chromatin immunoprecipitation, electro-mobility shift assay, and quantitative PCR (qPCR) (Yang et al., 2008). Furthermore, in mouse embryonic fibroblasts expressing mutant huntingtin protein *CASP6* mRNA is increased by p53 activation, and this increase is sensitive to pifithrin-α, a p53 inhibitor (Ehrnhoefer et al., 2014). However, a unique DD containing protein found exclusively in the nucleus, p84N5, was shown to activate Caspase-6 in p53 deficient cells treated with adeno-associated virus DNA (Garner et al., 2007). Considering that p84N5 belongs to a multiprotein complex responsible for mRNA transport from the nucleus to the cytoplasm, it is possible that Caspase-6 expression is controlled by multiple transcriptional and post-transcriptional mechanisms.

A recent study identified increases in *CASP6* mRNA expression following pleiotrophin (PTN) deficiency or depletion in mouse hippocampi or primary neuron cultures, respectively

(Gonzalez-Castillo et al., 2016). These data from an *in vivo* RNA microarray, *in vivo* qPCR, and *in vitro* qPCR suggest PTN to be a negative regulator of *CASP6* expression in mice neurons. More work is needed to determine whether PTN regulation occurs in human cells and whether the upregulation of Caspase-6 mRNA translates to increased Caspase-6 protein activity. Thus, although the technologies required for in-depth analysis are available, the mysteries behind *CASP6* gene regulation have not piqued the curiosity of the scientific community.

Considering that apoptosis is a tumor suppressive mechanism, mutational analysis has been performed on several *CASP* genes in relation to various cancers. However, compared to other tumor suppressors, like p53, mutation rates in *CASP* genes are relatively low. *CASP6* mutational analysis has identified two missenses mutations and one splice site mutation in human colorectal carcinomas and gastric carcinomas (Lee et al., 2006a). The prevalence of these mutations was 2% in both cancers, and Caspase-6 immunoreactivity could be detected in greater than 50% of gastric carcinomas, and almost all colon carcinomas (Lee et al., 2006a; Godefroy et al., 2013). Caspase-6's potential role in colon carcinogenesis was studied using Caspase-6-deficient and Caspase-6-overexpressing mice and no increase in tumors was detected (Foveau et al., 2014). Mutational analysis in lung and breast carcinomas detected no mutations in the *CASP6* gene (Lee et al., 2006b). Thus, Caspase-6 may not be pro-apoptotic enough to merit mutations in cancers.

1.6.2 The alternatively spliced Caspase-6 isoform

All caspases have alternatively spliced sequences. In the case of Caspase-6, two protein-coding transcripts were identified in human pre-B lymphocyte and T lymphocyte cell lines (see **section 1.2.4**) (Fernandes-Alnemri et al., 1995a). The canonical Caspase-6α is encoded in 7 exons, whereas the splice variant, Caspase-6β, lacks exons 2-4, leading to a truncated protein that retains the catalytic cysteine and histidine (**Fig. 1.7**). However, recombinant Caspase-6β was shown to have little to no catalytic activity. A more detailed analysis of Caspase-6β revealed that it could act as an inhibitor of Caspase-6α activation/activity when overexpressed in mammalian cells through asymmetrical dimerization or through competition for intermolecular activation (see section **1.14.1**) (Lee et al., 2010).

1.6.3 Caspase-6 is expressed at low levels in the healthy brain

In the original study that described Caspase-6, tissue-specific Caspase-6 expression was not characterized. Caspase-6 was only studied in human pre-B lymphocyte and T lymphocyte cell lines (Fernandes-Alnemri et al., 1995a). A thorough investigation of Caspase-6 protein expression in humans was only performed nearly two decades later (Godefroy et al., 2013). Most human fetal tissues expressed pro-Caspase-6 with the highest levels found in the stomach and colon. Pro-Caspase-6 and processed Caspase-6 followed an age-dependent expression pattern in fetal stomach extracts as determined by western blot analysis. Caspase-1, but not Caspase-3, had a similar expression pattern. In the fetal brain, only very low levels of pro-Caspase-6 could be detected.

The high levels of pro-Caspase-6 expression was maintained in human adult gastro-intestinal tissues (Godefroy et al., 2013). Adult lung and kidney maintained higher pro-Caspase-6 expression ratios normalized to colon, whereas splenic pro-Caspase-6 levels decreased compared to their fetal equivalents. In the adult brain, pro-Caspase-6α expression was nearly undetectable in the temporal cortex and the cerebellum, while pro-Caspase-6β was detected in the temporal cortex, frontal cortex, and the cerebellum (Lee et al., 2010; Godefroy et al., 2013).

Cultures from human fetal tissues revealed Caspase-6 mRNA and protein expression in neurons and astrocytes (Godefroy et al., 2013; Kaushal et al., 2015). Moreover, brain sections from AD patients showed strong Caspase-6 expression in neurons (Guo et al., 2004), while brain sections from HIV encephalitis patients showed Caspase-6 localized into astrocytes, (Noorbakhsh et al., 2010). Yet, Caspase-6 is nearly undetectable in healthy adult brains (Guo et al., 2004; Godefroy et al., 2013), suggesting Caspase-6 expression to be inducible in the central nervous system (CNS) under pathological conditions. In cultured human microglia, immune cells residing in the brain, Caspase-6 mRNA expression could not be detected, although upregulation could occur upon microglial activation (Kaushal et al., 2015). In rat brains, Caspase-6 expression is found in cytosolic, nerve endings, and myelin fractions, suggesting possible Caspase-6 expression in oligodendrocytes, the myelinating cells of the brain (Shimohama et al., 2001). Thus, Caspase-6 is expressed in many cell types in the brain although it is found at low levels under homeostatic conditions.

1.7 Caspase-6 enzyme structural analysis

Caspase-6 is produced as an inactive dimeric zymogen that undergoes cleavage at three distinct sites within the polypeptide chains to yield a mature heterodimeric protein (Kang et al., 2002). The large (p20) and the small (p10) subunits are separated by a 14 amino acid long linker. A small 23 amino acid long prodomain is found at the N-terminus of the p20 subunit. Complete pro-Caspase-6 maturation requires enzymatic processing at the $TETD^{23}$ site to remove the prodomain, while the linker is removed by processing at both $DVVD^{179}$ and $TEVD^{193}$ sites. Proteolysis of the linker operates a rearrangement of four surface loops that forms the catalytic site and the substrate-binding pocket. Through this process, Caspase-6 retains the heterodimer conformation with rotational symmetry, that is, the p20 subunits flank the central p10 subunits (**Fig. 1.8**). Unlike Caspase-3 and -7, Caspase-6 has a bulky phenylalanine at the dimer interface and lacks a "safety catch" regulatory tripeptide DDD sequence (Roy et al., 2001; Fuentes-Prior and Salvesen, 2004). X-ray diffraction on Caspase-1 crystals (Walker et al., 1994; Wilson et al., 1994) paved the way for three-dimensional structure determination on other caspase family members.

1.7.1 The 3D structure of Caspase-6 and its active site

Caspase-6 has a 12-stranded β-sheet at its core flanked by five α-helices on either side to form an overall globular shape that is reminiscent of all the other caspases (**Fig. 1.8**) (Baumgartner et al., 2009). Emanating from the central β-sheet are loop bundles that form the substrate binding subsites (S1-S4) and the catalytic machinery also referred to as the active site (**Fig. 1.8**). The S1 subsite has conserved arginine and asparagine residues responsible for selecting substrates with an aspartate, glutamate, or phosphorylated serine at position P^1 (Walker et al., 1994; Seaman et al., 2016). Two active sites are present on opposing ends of Caspase-6. Loops L1 and L4 are at two extremities of the active site, whereas L3 forms the groove (Shi, 2002). As an analogy, think of a tunnel, where the walls on either side represent the L1 and L4 loops, and the floor is the L3 loop. As you move deeper into the tunnel, away from the opening, you will reach the L2 loop with the side chain of cysteine 163 (C163) pointed towards the opening. Finally, the L2' loop is used to stabilize the L2 loop. Caspase-6's enzymatic activity is possible through the catalytic C163 and histidine (H121) residues which both have pK_a values

near neutral pH. This biochemical property allows these residues to participate as an acid or a base during catalysis (Gutteridge and Thornton, 2005). Thus, following binding of the substrate, H121 acts to de-protonate C163 and stabilize the tetrahedral intermediate that is formed following nucleophilic attack at the scissile carbonyl by the C163 thiol. Water molecules then displaces the thiol which can be re-protonated by H121 resulting in peptide substrate cleavage and active site regeneration (Stennicke and Salvesen, 1999; Fuentes-Prior and Salvesen, 2004).

1.7.2 Unprocessed inactive Caspase-6

The Caspase-6 zymogen structure has been difficult to solve due to the self-activating propensity of recombinant Caspase-6 (see section **1.7.3** & **1.9**) and the flexible nature of the prodomain. For that reason, only one study has thoroughly analyzed the structure of pro-Caspase-6 (Cao et al., 2014). To prevent removal of the prodomain during the purification process, H121 was mutated to alanine (pro-Caspase-6H121A). From their studies, Cao et al. found that the structure of zymogen Caspase-6 is similar to that of prodomain-less Caspase-6 (ΔproCaspase-6) such that the active loop bundles are clearly defined and the linker site $TEVD^{193}$ is found buried within the active site cleft (Wang et al., 2010b; Cao et al., 2014). Moreover, the prodomain was shown to inhibit Caspase-6 intramolecular cleavage at D^{193} and was preferentially cleaved during intermolecular cleavage events, a property conferred in part by the length of the pro-peptide. This result was supported with pro-Caspase-6 transfection experiments in HEK293T cells where the D23A mutant could not be self-processed (Cowling and Downward, 2002; Klaiman et al., 2009). In addition, the Caspase-6 prodomain is also necessary for increasing the stability of the enzyme as its removal decrease Caspase-6's thermal stability (Vaidya et al., 2011).

1.7.3 Caspase-6 processing by inter- and intramolecular cleavage

There are several published Δpro-Caspase-6 structures (Baumgartner et al., 2009; Wang et al., 2010b; Liu et al., 2011; Muller et al., 2011a; Muller et al., 2011b; Vaidya and Hardy, 2011). During recombinant Caspase-6 purification, it was found by mass spectrometry that fragments containing a polypeptide from amino acid 180-293 was never observed. This result suggested that cleavage primarily occurred at $TEVD^{193}$ (Srinivasula et al., 1996b; Baumgartner et al., 2009). Using D to A Caspase-6 mutants, it was found that D193A or D23A/D193A

mutations prevented processing at D179, emphasizing the D193 cleavage priority over D179 *in vitro* (Klaiman et al., 2009). Another research group corroborated the finding with a Caspase-6 structure that highlighted the linker region forming a β-strand within Caspase-6's active site (Wang et al., 2010b). In this structure, the catalytic C163 was very close to D193 and could easily initiate intramolecular cleavage upon a subtle change in conformation. This is inline with previous observations that uncleavable Caspase-6 mutant D23A/D179A/D193A still retained activity above the catalytic mutant C163A on the synthetic fluorophore-labelled substrate, Ac-VEID-7-amino-4-trifluoromethylcoumarin (AFC), suggesting that it could self-process at D193 (Klaiman et al., 2009). Moreover, Caspase-6 could only remove the prodomain of the catalytically inactive Caspase-6C163A suggesting that $DVVD^{179}$ was not a suitable substrate and that the $TEVD^{193}$ was not accessible. This is supported using synthetic polypeptides that showed $TEVD^{193}$ was a better Caspase-6 substrate than $DVVD^{179}$ (Thornberry et al., 1997; Baumgartner et al., 2009). Cleavage at the inter-subunit linker is necessary for active site formation by releasing the N-terminus of the p10 subunit and increases Caspase-6's stability (Chai et al., 2001; Vaidya et al., 2011). Hence, intermolecular Caspase-6 activation proceeds preferentially through the removal of the prodomain and cleavage at $DVVD^{179}$ since the D193 site is buried within the active site rendering it inaccessible (Wang et al., 2010b). In contrast, intramolecular Caspase-6 activation occurs through cleavage at $TEVD^{193}$.

1.7.4 Changes in the Caspase-6 active site upon substrate binding and pH

Apart from the unique conformation that precipitates intramolecular self-cleavage, Caspase-6 can also adopt unique but controversial active site conformations. In the original structure, unliganded processed Caspase-6 was found to have a non-canonical misaligned active site that distanced the H121 and C163 from each other (Baumgartner et al., 2009; Vaidya et al., 2011). This latent conformation arose as a consequence to the increased helical propensity of processed Caspase-6 (Vaidya and Hardy, 2011). The unique salt-bridge network between H121 and other amino acids and the lack of helix breaking amino acids, such as glycine and proline, compared to other caspases allow Caspase-6 to adopt a more helical conformation. Yet when researchers crystalized Caspase-6 under physiological pH, Caspase-6 was folded in a canonical caspase conformation (Muller et al., 2011b). Furthermore, upon substrate binding, Caspase-6 undergoes conformational changes observed by circular dichroism that reduces the helical

propensity transitioning from the non-canonical to the canonical conformation (Vaidya et al., 2011). Again, other researchers were able to crystalize Caspase-6 at acidic pH with the proposed latent conformation, but they observed an increase, not a decrease, in helical propensity (Muller et al., 2011a). These results put in question the physiological significance of previously described latent Caspase-6 structures. A recent study used a more dynamic approach to understand the unliganded Caspase-6 structure. Hydrogen/deuterium exchange mass spectrometry unveiled that Caspase-7 maintained a canonical fold before and after substrate binding, although this is different from a previous report using a different substrate (Chai et al., 2001). Similar to the work by Chai et al. for Caspase-7, Caspase-6 underwent a conversion between helical and strand conformations after substrate binding at neutral pH (Dagbay et al., 2017). Furthermore, the protonation of E135 helped stabilize the more helical state. Hence, there is sufficient evidence to propose that Caspase-6 undergoes conformational changes upon ligand binding and that a proportion of Caspase-6 molecules may adopt a less helical state at physiological pH due to reduced protonation.

1.8 Caspase-6 post-translation modifications (PTMs)

Caspase activation is tightly regulated by the assembly of multimeric protein complexes involved in initiator and inflammatory caspase oligomerization (see section **1.4**). Despite that, additional regulation occurs through PTMs that regulate caspase activation, stability, subcellular localization, and enzymatic activity (Zamaraev et al., 2017). These modifications include phosphorylation, ubiquitination, sumoylation, N-acetylation, S-nitrosylation, and S-gluthathionylation, and other oxidative mechanisms. Also, with respect to Caspase-3, it has been previously shown to be glutathionylated and S-nitrosylated. Glutathionylation prevents Caspase-3 activation and activity, in part by making it a poor substrate for Caspase-8 (Pan and Berk, 2007; Huang et al., 2008). S-nitrosylation blocks Caspase-3's active site but can also prime it for degradation by the proteasome (Jiang et al., 2009; Lai et al., 2011). Such oxidative mechanisms have not been previously described for Caspase-6. In addition, prediction software are not always useful in determining potential PTM sites as shown by the identification of threonine 229, serine 187, serine 74 as possible phosphorylation sites in Caspase-6 (Sattar et al.,

2003), but did not identify the phosphorylated serine 257 observed in cells (Suzuki et al., 2004). Only the experimentally observed PTMs observed for Caspase-6 will be presented.

1.8.1 Caspase-6 phosphorylation at serine 257

Based on a study in human colon cancer cell lines subjected to FasL, there is protection against cell death in cell lines which express the adenosine monophosphate (AMP) kinase (AMPK)-related kinase 5 (ARK5) (Suzuki et al., 2004). This protection resulted from increased cFLIP levels which could be reduced with antisense RNA interference targeting ARK5. Caspase-6 cleavage of cFLIP was found to be responsible for the decreased cell survival following FasL treatment. The colon cancer cell line SW480 avoided cellular demise by recruiting ARK5 to phosphorylate serine 257 (S257) of Caspase-6 which effectively inhibited its activation and activity. Mutating S257 to alanine prevented ARK5-mediated Caspase-6 inhibition and resulted in increased sensitivity to FasL (Suzuki et al., 2004).

The structural determinants for Caspase-6 inhibition following phosphorylation at S257 were the topic two subsequent studies (Cao et al., 2012; Velazquez-Delgado and Hardy, 2012a). Both studies made similar observations despite using different Caspase-6 phosphorylation mimics, that is, substituting S257 with either aspartate (S257D) or glutamate (S257E). The phosphorylation mimics were unable to self-process at D193 because of interaction networks that distanced D193 from the catalytic dyad and locked the enzyme in a more rigid conformation (Cao et al., 2012). Although Caspase-3 could process all three sites, the processed Caspase-6S257D/E had significantly lower activity than wild-type Caspase-6 (Cao et al., 2012; Velazquez-Delgado and Hardy, 2012a). Steric clash between the S257D with the side chain of proline 201 was found to be one of the main culprits preventing proper loop bundle formation and substrate binding (Velazquez-Delgado and Hardy, 2012a). Thus, phosphorylation can block Caspase-6 activation and activity.

1.8.2 Caspase-6 palmitoylation at cysteine residues

HIP14 is a neuronal palmitoyl acytltransferase that is important for the palmitoylation of a number of protein substrates in the context of Huntington's disease (HD) (Singaraja et al., 2011). Specifically, HIP14 is responsible for reversibly adding an 18 carbon long fatty acid

chain, palmitate, to cysteine residues through thioester bonds. When mice are deficient in HIP14, they display HD-like phenotypes (Singaraja et al., 2011). Moreover, Caspase-6 plays an important role in HD-like phenotypes in mice (see section **1.13.1**), therefore the possibility that Caspase-6 was palmitoylated by HIP14 was investigated (Skotte et al., 2017).

In their study, the researchers found high levels of Caspase-6 palmitoylation at baseline when overexpressed in COS7 cells (Skotte et al., 2017). HIP14 overexpression, but not the catalytic inactive form, led to increased Caspase-6 palmitoylation. Palmitoylation resulted in decreased Caspase-6 self-processing and activity. Cysteines 264 and 277 (C264/277) were identified as palmitoylated residues, although other cysteines were suspected to be palmitoylated in the C264/277S double mutant. Mechanistically, molecular dynamic simulations predicted that C264 palmitoylation would block entry of substrates into the loop bundle and increase the distance between D193 and the catalytic dyad. In contrast, C277 palmitoylation was predicted to sterically prevent Caspase-6 dimerization. Although palmitoylation can change membrane association and subcellular localization (Huang and El-Husseini, 2005), there was no observable change in Caspase-6 subcellular localization in the C264/277S double mutant (Skotte et al., 2017). Since this Caspase-6 mutant is still palmitoylated, subcellular localization in cells treated with the palmitoylation inhibitor, 2-bromopalmitate, would remove confounding factors.

1.9 Caspase-6 activation follows canonical activation cascades and can self-activate

Caspase-6's ability to intramolecularly self-activate stems from the unusual L2 loop length which is not present in other executioner caspases (Wang et al., 2010b). This extended L2 loop allows the $TEVD^{193}$ C-terminal linker site to reside within Caspase-6's active site. Considering that the catalytic cysteine is only a few angstroms away from D193 (Wang et al., 2010b), a small shift in conformation is believed to initiate processing at the linker, yielding a more stable and active enzyme (Vaidya et al., 2011). Despite these results from recombinant Caspase-6 protein, it is important to understand how Caspase-6 is activated in cells.

1.9.1 Caspase-6 is activated both downstream and upstream of other caspases

In the early model, the caspase activation cascade was determined in extracts from Jurkat T lymphocytes treated with CytC (Slee et al., 1999). This led to apoptosome formation and Caspase-9 processing (Li et al., 1997). Using ^{35}S labeled proteins, it was found that Caspase-2, -3, -6, -7, -8, and -10 were processed downstream of Caspase-9, but not the inflammatory caspases (Slee et al., 1999). In addition, using the Caspase-3 inhibitor Ac-DEVD-FMK, Caspase-3 activity was shown to be necessary for 1) the processing of Caspase-2, -6, -8, and -10, 2) autocatalytic processing of its prodomain, and 3) positive feedback Caspase-9 processing to amplify the signal. Caspase-7 was not involved in additional processing in these extracts. Immuno-depletion experiments outlined Caspase-6's role in processing Caspase-2, and finally, Caspase-8 and -10. Extrinsic initiator caspase activation during intrinsic apoptosis caused by CytC addition is supported by perturbed Caspase-8 activation in mice deficient in Caspase-9 or Apaf-1 (Hakem et al., 1998; Yoshida et al., 1998). From these studies, it appeared that the activation cascade was dissected out.

It took nearly a decade to revisit the paradigm set forth by Slee et al. using human T lymphocyte extracts. To understand whether the cascade held true in intact cells, various cytotoxic reagents were used to induce intrinsic apoptosis in live Jurkat cells (Inoue et al., 2009). The main difference was that Caspase-7 played a more important role in intact cells. In Caspase-3 deficient MCF7 cells, Caspase-7 was responsible for Caspase-6 and -2 activation (Inoue et al., 2009). Moreover, during death receptor-mediated apoptosis, Caspase-8 activated Caspase-6, while the opposite was true during mitochondrial cell death. Despite all these refinements, caspase activation cascades can vary significantly with cell type and insults. This is supported by instances of, but is not limited to, Caspase-6-mediated Caspase-3 activation in trophic factor-deprived rodent cerebellar granule cells (Allsopp et al., 2000), Caspase-1-mediated Caspase-6 activation in serum-deprived human primary neurons in the absence of Caspase-3 (LeBlanc et al., 1999; Guo et al., 2006), and even more remarkable, Caspase-9 activation in the absence of Apaf-1 in NGF-deprived mouse sympathetic neurons (Cusack et al., 2013). Thus, Caspase-6 follows Caspase-3 or -7 activation during apoptotic signalling, but may engage in parallel pathways during sub-lethal conditions.

1.9.2 Caspase-6 self-activates in mammalian cells

Only one study performed a complete biochemical Caspase-6 analysis in human cells. Caspase-6 overexpression in HEK293T cells led to its complete self-processing at the three cleavage sites (D23, D179, and D193) in the absence of upstream protease activation (Klaiman et al., 2009). However, mutating D179, but not D193, to alanine had an inhibitory effect on Caspase-6 self-processing in cells (Klaiman et al., 2009). This is in contrast to *in vitro* analysis with recombinant protein as described (see section **1.7.2**) (Klaiman et al., 2009; Wang et al., 2010b). Another difference between *in vitro* and cellular analysis lies in the inactivity of uncleavable D23A/D179A/D193A in cells. Even following serum-deprivation, Caspase-6 activity could not be detected from cellular extracts overexpressing the triple mutant suggesting that the uncleavable Caspase-6 mutant, just like the catalytic C163A mutant, inhibits endogenous Caspase-6 activity (Hermel et al., 2004; Klaiman et al., 2009). Nevertheless, like with recombinant Caspase-6, Caspase-6 activity was enhanced in cells by cleavage at a single linker site, but not by prodomain removal (Klaiman et al., 2009; Vaidya et al., 2011). Human Caspase-6 can also self-activate in human colorectal carcinoma (HCT116) cells following transfection (Lee et al., 2010), and in mice neurons when overexpressed (LeBlanc et al., 2014). Therefore, Caspase-6 can be activated by caspases upstream during signaling cascades or by self-processing following overexpression.

1.10 Caspase-6 substrates and protein interaction analysis

Determining protease function requires analysis of activated pathways through cleaved substrates. Several physiological Caspase-6 functions have been described (see section **1.5**), but several more functions are predicted based on substrate identification. In this section, Caspase-6's role based on proteomic studies and yeast-two hybrid (Y2H) screens will be presented.

1.10.1 Caspase-6 cleaves many cytoskeletal proteins in human neurons

Human neuron extracts were treated with recombinant Caspase-6 and separated on a two-dimensional sodium dodecyl sulfate (SDS) gel. Samples that shifted following recombinant Caspase-6 digestion were sent for liquid chromatography and tandem mass spectrometry (LC/MS/MS) (Klaiman et al., 2008). From the analysis, most substrates were cytosolic, with

many cytoskeleton and cytoskeleton-associated proteins (**Fig. 1.9**). Four of the 24 potential protein substrates were validated *in vitro*. These included α-tubulin, Drebrin, Spinophilin, and α-actinin-1 and -4. Caspase-6 cleaves α-tubulin at amino acid D438 and antibodies generated against cleaved α-tubulin recognizes degenerating axons in AD brains and in mice (Klaiman et al., 2008; LeBlanc et al., 2014). Drebrin is enriched in dendritic spines where it interacts with the actin network to regulate PSD95 clustering (Aoki et al., 2005). Spinophilin binds actin and modulates dendritic spine morphology and function (Satoh et al., 1998; Feng et al., 2000), while α-actinin-4 interacts with densin 180 to maintain trans-synaptic adhesion (Walikonis et al., 2001). Hence, in human neurons Caspase-6 may play an important role in axonal degeneration and synapse homeostasis.

1.10.2 Caspase-6 signalling pathways in human T lymphocytes

Although adding recombinant caspases to cellular extracts may provide a starting point to which substrates are cleaved, this interpretation assumes that all substrates are cleaved with similar efficiency. To address this, researchers employed a subtiligase-based N-terminomics technology in cells extracts (Mahrus et al., 2008). Briefly, a biotin-labelled peptide containing a tobacco etch virus cleavage sequence was ligated to primary α-amines by the engineered subtiligase enzyme. This would N-terminally label newly generated α-amines in substrates after enzymatic cleavage. Then, biotin-tagged peptides are precipitated with avidin beads, which bind to biotin, and the biotin-tag is removed by the tobacco etch virus protease. The remaining peptide is sequenced by mass spectrometry revealing sites C-terminal to enzyme cleavage which can be matched to peptide sequences to identify substrates. Using this method, 871 proteins were identified as Caspase-6 substrates in immortalized human T lymphocytes (Julien et al., 2016). These proteins were mainly localized in the cytosol and nucleus, with biological functions in cytoskeleton, cell death, cell cycle, transcriptional regulation, RNA splicing, and DNA damage response.

To measure the reaction rate, selection reaction monitoring was performed on a triple quadrupole mass spectrometer (Julien et al., 2016). Essentially, recombinant Caspase-6 was added to Jurkat cell extracts for different durations before completely inhibiting the enzyme activity using Z-VAD-FMK. Only peptides showing several strong transitions observed by mass

spectrometry were analyzed by selection reaction monitoring, which represented 471 peptides and 276 values for catalytic efficiency. Most substrates were cleaved at a rate of 10^{-3} $M^{-1}s^{-1}$ with very few substrates above and below this rate. However, this analysis highlighted the pre-existing hierarchy rendering some substrates more prone to cleavage by Caspase-6 than others. In addition, the reaction rate was dictated by the primary amino acid sequence and not the overall tertiary structure (Julien et al., 2016). One confounding factor of adding recombinant caspases to extracts is that these caspases may activate other caspases directly or indirectly (see section **1.9**) or other proteases leading to indirect substrate cleavage events. All in all, substrates identified by mass spectrometry offer a greater understanding of the overall biological pathways affected by Caspase-6, yet detailed molecular biology experiments are required to validate substrates.

1.10.3 Caspase-6 protein-protein interaction network

Very few studies have investigated Caspase-6 protein interactors. The interaction between Caspase-6 and chromodomain helicase DNA binding protein 3 was found by Y2H screen used to determine the human protein-protein interaction network (Stelzl et al., 2005). Another Y2H screen using the catalytic inactive Caspase-6C163A as bait was done against a human fetal cDNA library. Sox11, FEZ1, and COP1 were identified as inactive Caspase-6 binding partners, although Caspase-6 inhibition data for FEZ1 and COP1 were not extensive (Waldron-Roby et al., 2015). Using co-immunoprecipitation, Caspase-6 was shown to interact with Caspase-3 and heat shock protein 60 in campthothecin-treated Jurkat cells (Xanthoudakis et al., 1999). Heat shock protein 60 was thought to promote Caspase-3 cleavage by upstream caspases. Ocular lens cell terminal differentiation requires an apoptosis-like pathway that gets rid of all organelles (Bassnett, 2002). During this process, αA-crystallin was found to interact with Caspase-6 by co-immunoprecipitation and inhibited Caspase-6 activity (Morozov and Wawrousek, 2006). Finally, Caspase-6 phosphorylation at S257 is mediated by interactions with ARK5 as shown using recombinant proteins (Suzuki et al., 2004). It is interesting that direct Caspase-6 inhibition by Sox11 or αA-crystallin using recombinant proteins was not determined.

A recent study aimed to identify Caspase-6 interactors important in HD using a Y2H screen (Riechers et al., 2016). In this screen, pro-Caspase-6 or the individual subunits, p20 or

p10, were used as bait. Following several quality control steps, 87 interactors were identified with 61% of interactors containing a predicted Caspase-6 cleavage sequence. The pathways involved included insulin/insulin-like growth factor, phosphatidylinositol-4,5-bisphosphate 3-kinase (PI3K), and p53 signalling. Using their unique approach, researchers could easily identify potential substrates by analyzing interactions that occur specifically with the Caspase-6 subunits and not pro-Caspase-6 (Riechers et al., 2016). Nine targets from the Y2H screen were tested by adding recombinant Caspase-6 to mice cortex samples. Caspase-6 cleavage sites were present in six of the nine interactors predicted to be cleaved by Caspase-6, namely, death domain-associated protein, palmdelphin, serine threonine kinase 3, RNA binding motif 17, syntaxin 16, and ubiquitin-specific peptidase 32 (Riechers et al., 2016). Considering that Caspase-6 can activate other caspases (Slee et al., 1999; Inoue et al., 2009), recombinant or purified proteins should have been used to prevent other caspases from mediating cleavage events. Moreover, there are additional confounding factors with the employed Y2H screen: 1) expressing Caspase-6 subunits alone exposes amino acids that normally would be buried within the holoenzyme thus increasing the odds of false-positive interactions, 2) Caspase-6 is suggested to cleave 871 proteins suggesting that serendipitous findings are possible, and 3) inactive enzymes may have reduced affinity for their substrates. Nevertheless, Caspase-6 interactions with proteins does not always result in proteolytic processing which points to Caspase-6's complex signalling potential.

1.11 Caspase-6 mediates axonal degeneration

From section **1.5.1**, we can conclude that Caspase-3, but not Caspase-6, is the main effector of apoptosis. The only functions that are restricted to Caspase-6 during apoptosis are Lamin A/B/C, and RIP1 cleavage (Orth et al., 1996; Takahashi et al., 1996; Chandler et al., 1997; van Raam et al., 2013; Hill et al., 2016). However, increased Caspase-6 expression or activity in human cells does not induce apoptosis (Klaiman et al., 2009; Gray et al., 2010; Sivananthan et al., 2010b). Serum-deprivation or recombinant Caspase-6 microinjection in human primary neurons only leads to apoptosis several days after the insult (LeBlanc et al., 1999; Zhang et al., 2000). This suggests Caspase-6 to be a weak apoptotic effector and may require the recruitment of other caspases before cell death ensues. Moreover, Caspase-6

deficient mice do not have any overt phenotype pertaining to defects in apoptosis (**Table 1.2**) (Zheng et al., 1999; Watanabe et al., 2008; Gafni et al., 2012; Uribe et al., 2012), although compensation by other effector caspases is possible (Zheng et al., 2000). Unlike apoptosis, there is strong evidence for Caspase-6's role in breaking down the neuronal cytoskeleton and mediating axonal degeneration (**Table 1.3**).

1.11.1 Caspase-6 is activated in peripheral neurons leading to axonal degeneration

Axonal degeneration involves cytoskeletal dismantling, membrane blebbing, and fragmentation which resembles apoptosis. The idea that programmed cell death could be involved in neurons that were deprived of neurotrophic factors was shown by seminal works by Eugene M. Johnson (Martin et al., 1988; Deckwerth and Johnson, 1993; Deshmukh et al., 1996). Yet, caspase involvement in the process was refuted by the lack of Caspase-3 activity or staining in sympathetic neurons, sciatic nerves, and dorsal root ganglion neurons following transection or local neurotrophin deprivation (Finn et al., 2000). Research in the field exploded only following the discovery that Caspase-6 mediated axonal pruning in sensory and motor neurons following NGF-deprivation (Nikolaev et al., 2009). It was found that APP was processed following NGF withdrawal, which released an extracellular DR6 ligand initiating a caspase signalling cascade. Yet, α-tubulin fragmentation, a marker of axonal degeneration, was specifically inhibited following treatment with pharmacological Caspase-6, but not Caspase-3, inhibitors and small interfering RNAs (siRNA) (Nikolaev et al., 2009). Tubulin was found cleaved in NGF-deprived sympathetic neurons suggesting both Caspase-6 and -3 activities (Sokolowski et al., 2014). Others recapitulated Caspase-6's role in axonal degeneration following trophic factor deprivation in dorsal root ganglion neurons using siRNA and identified dynactin 1 as an important mediator of NGF retrograde signalling (Vohra et al., 2010). Caspase-6 activation was specific to removal of trophic support, not other insults, in mouse primary sympathetic neuron cultures (Uribe et al., 2012), and Caspase-6 deficiency only prevented axonal degeneration during axon-targeted trophic factor withdrawal and not other insults (Cusack et al., 2013).

The same group that ignited the field revisited their findings using mice deficient in Caspase-3 and Caspase-6. Dorsal root ganglion neurons lacking Caspase-6 or Caspase-3 were both protected from NGF-deprivation and active Caspase-6 in axons could not be detected in Caspase-3 deficient neurons (Simon et al., 2012). These results were explained by inefficient Caspase-3 inhibition or knockdown using Z-DEVD-FMK or siRNA in the original study (Nikolaev et al., 2009). Not only Caspase-3, but Bax, CytC, and Caspase-9 were necessary to activate Caspase-6 in axons in sympathetic neuron cultures from deficient mice (Cusack et al., 2013). The pathway was further expanded by elegant studies dissecting the interaction between the cell body and axons during axonal degeneration (Simon et al., 2016). It was found that NGF-deprivation results in reduced Akt signalling, which upregulates c-jun N-terminal kinase signalling, which activates the transcription factor forkhead box O3a, resulting in Puma expression that promotes mitochondria-mediated caspase activation in degenerating axons. Furthermore, Caspase-3 is prevented from mediating axonal degeneration in locally deprived neurons by the x-linked inhibitor of apoptosis protein (XIAP) and the proteasome (Cusack et al., 2013; Unsain et al., 2013). The possibility that Caspase-3 may also be responsible for axonal retraction following axotomy lacks strong experimental support (Ozturk et al., 2013). It is mostly accepted that nicotinamide dinucleotide (NAD+) regeneration by nicotinamide mononucleotide adenylyltransferase (NMAT1) is important for axotomy induced degeneration, whereas caspases are mediators of axonal degeneration caused by trophic factor withdrawal (Geden and Deshmukh, 2016). The results described are an accurate depiction of the mouse peripheral nervous system, but do not reflect the realities in human neurons and Alzheimer disease.

1.11.2 Caspase-6-mediated axonal degeneration in the CNS

In the CNS, Caspase-6 also plays an important role in axonal degeneration. Following nerve lesions, it is known that inhibitors found on myelin are the first obstacle to neurite regeneration (Huang et al., 1999). Neurites contacting myelin undergo axonal degeneration in a p75 neurotrophin receptor-Rho guanosine diphosphate dissociation inhibitor(Rho-GDI)-Caspase-6 dependent manner (Park et al., 2010). This was shown in mouse septal cholinergic neurons growing on myelin where pharmacological Caspase-6 inhibition prevented axonal degeneration without affecting axon growth. In addition, immunocytochemistry demonstrated

that active Caspase-6 was present in septal cholinergic neurons only when grown on myelin (Park et al., 2010). Yet, in this study, the possibility that other caspases were involved was not investigated. Septal cholinergic neurons from Caspase-6 deficient mice were also resistant to myelin-mediated degeneration *in vivo* as seen by increased number of healthy neurites found in the corpus callosum (Uribe et al., 2012). Olfactory sensory neurons send their axons to glomeruli in the olfactory bulb and are subject to lifelong turnover through degeneration and neurogenesis. These degenerating axons are positive for cleaved actin and TubΔCasp6 suggesting both Caspase-6 and -3 activities (Sokolowski et al., 2014). Moreover, subcutaneous ethanol injection in day seven pups resulted in striatal neuron degeneration that showed Caspase-6- and -3-mediated cleavage of cytoskeletal proteins that was dependent on the presence of Bax (Sokolowski et al., 2014). Also, pharmacological Caspase-6 and -8 inhibition resulted in increased neurite growth in rat retinal explants grown on myelin (Monnier et al., 2011). In contrast to septal cholinergic neurons, Caspase-6 in retinal ganglion cells promotes axonal degeneration and suppresses axon growth. Following optic nerve crush in rats, Caspase-6 in conjunction with Caspase-2 suppressed retinal ganglion cell neurite regeneration (Vigneswara et al., 2014). However, in this context, Caspase-6 prevents astrocyte and Müller cell activation, CNTF release and Janus kinase/STAT signalling pathways. Thus, Caspase-6 can control neurite physiology in both cell-autonomous and non-cell-autonomous pathways.

In human CNS neurons, serum-deprivation resulted Caspase-6 activity in the absence of all other effector caspases and led to protracted apoptosis (LeBlanc et al., 1999; Zhang et al., 2000). Upon APP^{WT}-overexpression, a condition that is relevant to AD (Rovelet-Lecrux et al., 2006), human neurons undergo neurite degeneration as observed by enhanced green fluorescent protein (EGFP), ubiquitin-tagged with red fluorescent protein, and Tau-red fluorescent protein agglomerates (Sivananthan et al., 2010b). This beading process increased with time and can be inhibited by treatment with Z-VEID-FMK or using Caspase-6C163A as a dominant negative inhibitor, suggesting that human neurite degeneration following APP^{WT}-overexpression is dependent on Caspase-6 activity. Moreover, neurons transfected with APP^{WT} experienced amyloid β_{42} (Aβ)-dependent cell death since transfection with a APP^{MV} mutant, which cannot generate additional Aβ, reduced the percentage of neurons with condensed chromatin back to

baseline levels (Sivananthan et al., 2010b). These results suggest that Caspase-6 plays a primary role in neurite degeneration in human CNS neurons.

1.12 Caspase-6 is activated early in Alzheimer disease

Alzheimer disease (AD) is an age-related neurodegenerative disease that is the leading cause memory loss, cognitive deficits, and behavioural changes in the elderly with genetic underpinnings. The main histopathological hallmarks of AD are hippocampal atrophy, the presence of extracellular Aβ plaques, and intracellular hyper-phosphorylated Tau aggregates forming neurofibrillary tangles (NFTs) (Duyckaerts et al., 2009). Cognitive decline in AD is best correlated with decreased synaptic connections, then by increased NFTs, and finally increased soluble amyloid load (Braak and Braak, 1997; Scheff and Price, 2003; Bennett et al., 2004). Genetically, dominant mutations in APP, presenilin 1 and 2 (PS1, PS2) are known to cause increased Aβ production and early-onset AD (Selkoe, 1997). However, these mutations represent a fraction of AD cases worldwide. Recent genome-wide association studies have revealed several polymorphisms that increase AD risk. These SNPs are associated with mediators of the innate immune response (Mhatre et al., 2015). Molecular biology analysis of these protein variants will help determine the significance of the innate immunity in sporadic AD.

Therapeutic strategies have focused on interfering with Aβ production, degradation, clearance, and aggregation (Graham et al., 2017). Tau aggregation and phosphorylation are also being targeted in clinical trials. Unfortunately, recent data point to the ineffectiveness of targeting Aβ and Tau in AD patients (Wischik et al., 2014; Karran and De Strooper, 2016). Although some suspect that the long prodromal stage in AD renders treatment following diagnosis obsolete, this warrants advances in biomarkers and cognitive tests to identify at-risk populations. The fact remains that the only therapeutic options available for AD patients is symptomatic treatment using acetylcholinesterase inhibitors and NMDA receptor antagonists. Scientists have begun searching for novel biochemical pathways to develop disease-modifying therapies for AD. This search highlights the importance of discovering that Caspase-6 has an instigating role in AD pathogenesis.

1.12.1 Caspase-6 is activated in sporadic and familial AD brains

The development of neoepitope antibodies against active Caspase-6 and Tau-cleaved by Caspase-6 (TauΔCasp6) precipitated the unveiling of active Caspase-6 in AD brains (**Fig. 1.10**) (Guo et al., 2004). Active Caspase-6 and TauΔCasp6 was found in neuropil threads, NFTs, and neuritic plaques in both sporadic and familial AD cases (Guo et al., 2004; Albrecht et al., 2009). TauΔCasp6 levels increased with AD severity from mild, moderate, severe, to very severe (Albrecht et al., 2007; Ramcharitar et al., 2013b). Moreover, TauΔCasp6 appeared before PHF-1 staining, a marker for Tau phosphorylation at S396 and S404, in some neurons from the entorhinal cortex (ERC), the first area of the brain affected by Tau pathology (Braak and Braak, 1997), of non-cognitively impaired (NCI) and mild cognitively impaired (MCI) individuals (Albrecht et al., 2007). Yet, TauΔCasp6 and PHF-1 co-localized in the hippocampus (Albrecht et al., 2007), the main structure of the brain responsible for short-term memory (Scoville and Milner, 1957). Considering these results, it was undeniable that Caspase-6 was activated in AD.

1.12.2 Caspase-6 is activated early during AD pathogenesis

An instigating role for Caspase-6 in AD came from studying NCI individuals. As a pilot analysis, the TauΔCasp6 levels observed by immunohistochemistry were correlated to the cognitive scores of six NCI patients. The results demonstrated a negative correlation between Caspase-6 activity and cognition in cognitively normal individuals (Albrecht et al., 2007). To expand on these results, 17 NCI cases were analyzed by active Caspase-6, TauΔCasp6, PHF-1, and Aβ staining of the ERC and hippocampus. Active Caspase-6 staining correlated strongly with TauΔCasp6 in both brain regions (Ramcharitar et al., 2013a). TauΔCasp6 also correlated with PHF-1 staining, whereas Aβ did not correlate with any of the markers tested. There was a strong negative correlation between global cognitive scores, based on a battery of 19 different tests, and TauΔCasp6 in the ERC and hippocampus (Ramcharitar et al., 2013a). Further analysis showed an inverse relationship between TauΔCasp6 levels and episodic or semantic memory scores (Ramcharitar et al., 2013a). TauΔCasp6 can also be detected in the post-mortem cerebrospinal fluid (CSF) from NCI, MCI, and AD by enzyme-linked immunosorbent assay (ELISA) and correlated with disease severity (Ramcharitar et al., 2013b). In addition, TauΔCasp6 is found in CSF from Parkinson's disease and Multiple sclerosis cases, but the

values were not different from NCI levels and 55% less than TauΔCasp6 in CSF from AD (Ramcharitar et al., 2013b). The levels measured by ELISA are consistent with TauΔCasp6 immunoreactivity in the brain and predicted cognitive performance. In view of episodic memory being the first type of memory and the ERC being the first region affected in AD (Hyman et al., 1984; Rodrigue and Raz, 2004), Caspase-6 seems to be activated during very early stages of AD pathology.

1.12.3 Caspase-6 activity can increase Aβ production, disrupt the cytoskeleton, and impair the ubiquitin-proteasome system

Once activated, Caspase-6 is involved in several pathways important in AD. Serum-deprived primary human neurons have increased Caspase-6 activity that led to increased APP cleavage and Aβ generation (LeBlanc et al., 1999). Increased APP processing was a result of caspase-mediated cleavage of Golgi associated gamma adaptin Ear containing ARF binding protein 3 which increased β-site APP cleaving-enzyme (BACE) trafficking to the plasma membrane to meet its membrane-bound substrate APP (Tesco et al., 2003; Tesco et al., 2007). In AD brains, tubulin-cleaved by Caspase-6 (TubΔCasp6) neoepitope antibodies stained the neuropil threads, NFTs, and neuritic plaques (Klaiman et al., 2008). Caspase-6 removes α-tubulin's C-terminal amino acids which are important for binding to Tau, microtubule-associated protein 2, and dynein (Maccioni et al., 1989; Paschal et al., 1989). However, results could be confounded by Granzyme B and subtilisin since they also cleave tubulin at the Caspase-6 cleavage site which also dysregulates tubulin polymerization dynamics (Serrano et al., 1984; Sackett et al., 1985; Adrain et al., 2006). As mentioned (see section **1.10.1**), Caspase-6 cleaves α-actinin-1 and -4, Drebrin, and Spinophilin (Klaiman et al., 2008). Intracellular aggregates of actin and actin-associated proteins, such as α–Actinin-4, were found in Hirano bodies which accumulate in AD brains (Gibson and Tomlinson, 1977). Developing a neoepitope antibody will determine if cleaved-α-Actinin-4 is preferentially aggregated in Hirano bodies. Drebrin knockdown in rats resulted in cognitive impairment (Kobayashi et al., 2004), and Drebrin levels are decreased in hippocampal synapses in AD (Harigaya et al., 1996). Spinophilin levels were also found to be decreased in elderly individuals with cognitive decline (Akram et al., 2008).

However, Caspase-6's effect on Drebrin and Spinophilin protein stability and function remains to be elucidated.

Valosin-containing protein (VCP/p97) is another important Caspase-6 target in AD brains (Klaiman et al., 2008). VCP/p97 is a chaperone-like ATPase that oversees endoplasmic-reticulum misfolded protein ubiquitination and degradation by the proteasome (Halawani and Latterich, 2006). In AD, there is an accumulation of poly-ubiquitinated proteins suggesting an impaired ubiquitin-proteasome system (Dickson et al., 1990). Concordant with this, active Caspase-6, but not Caspase-3 or -7, cleaved p97 at $VAPD^{179}$ when not bound by ATP and released an N-terminal peptide capable of inhibiting full length p97 function (Halawani et al., 2010). Using a neoepitope antibody for p97-cleaved by Caspase-6 (p97ΔCasp6) was detected in severe AD cases. Caspase-6 and p97ΔCasp6 immunoreactivity co-localized to the cytosol of hippocampal neurons (Halawani et al., 2010). Thus, Caspase-6 can participate in impairing the degradation of misfolded proteins by the proteasome in AD by enzymatically processing p97.

1.12.4 Caspase-6 is part of a pro-inflammatory cycle in AD brains

Inflammasomes are the molecular platform necessary for Caspase-1 activation (see section **1.4.3**) and are activated in AD brains. In AD mouse models, Aβ levels were increased due to NLRP3 inflammasome activation which impaired microglial phagocytic activity and decreased insulin-degrading enzyme expression (Heneka et al., 2013). On the neuronal side, NLRP1, absent in melanoma 2, and ICE protease activating factor, but not NLRP3, were found to be expressed in human CNS neurons (Kaushal et al., 2015). The inflammasomes were functional as assessed with classical ligands or cellular stressors that increased Caspase-1 activity. Downstream targets, such as IL-1β and Caspase-6 were only processed by Caspase-1 as processing was lost following treatment with NLRP1 and Caspase-1-targeting siRNA. Mice deficient in Caspase-1 or NLRP1 were also incapable of processing Caspase-6 or IL-1β in the brain following lipopolysaccharide injections. Moreover, serum-deprivation-mediated increase in Aβ secretion from human primary neurons was dependent on Caspase-1 and NLRP1 immunoreactivity was increased 25 to 30-fold in AD brains (Kaushal et al., 2015). Moreover, mice that overexpress human Caspase-6 in the CA1 region of the hippocampus suffer from neuronal degeneration, early glial inflammation, and age-dependent spatial and episodic

memory impairment (LeBlanc et al., 2014). Taken together, these findings linked neuronal inflammation to Caspase-1-mediated glial activation and to Caspase-6-mediated axonal degeneration.

1.13 Caspase-6 activation in other neurodegenerative diseases

Caspase-6 activity is not found only in AD brains. Some studies suggest that Caspase-6-cleaved targets in Huntington's disease, Parkinson's disease, and in ischaemic stroke. The evidence for Caspase-6's involvement in these neurodegenerative diseases or conditions will be presented briefly.

1.13.1 Caspase-6 cleaves mutant huntingtin protein in mouse models

Huntington's disease (HD) is a neurodegenerative disease manifesting through motor and cognitive deterioration. Genetic analysis showed cytosine-adenine-guanine repeat expansion in the Huntingtin gene causing a poly-glutamine expansion in mutant Huntingtin protein (mhtt). HD brain pathology is characterized by loss of γ-aminobutyric acid (GABA)-ergic medium spiny neurons in the striatum and neurons from cortical layers V and VI. Neuron loss is believed to be a consequence of mhtt cleavage since cleaved N-terminal mhtt fragment overexpression is toxic to cells (Martindale et al., 1998; Saudou et al., 1998) and cleavage fragments can be detected in affected HD brain regions (DiFiglia et al., 1997). Researchers speculated that caspases were involved in mhtt cleavage because DNA strands breaks were detected in HD patient brains (Portera-Cailliau et al., 1995), a process that occurs during apoptosis.

Several studies suggest that mhtt cleavage by caspases is toxic to neurons. Caspase-3 was the first apoptotic protease identified to cleave mhtt (Goldberg et al., 1996). A following study identified the Caspase-3 cleavage sites, but also mhtt cleavage at amino acid 586 by Caspas-6 (Wellington et al., 2000). Mutating D586 to A in mhtt resulted in protection against neuronal toxicity and decreased caspase activation *in vitro*, and *in vivo* (Graham et al., 2006). Caspase activation downstream of mhtt proceeded through Bax activation and the intrinsic apoptosis pathway or through decreased palmitoylation (Ehrnhoefer et al., 2016; Skotte et al., 2017). In addition, mice expressing the mhtt fragment generated by Caspase-6 cleavage showed

HD-like phenotypes in mice (Tebbenkamp et al., 2011; Waldron-Roby et al., 2012). These results suggested that Caspase-6 mediated cleavage of mhtt was sufficient to cause cytotoxicity, mhtt intranuclear aggregation, and increased susceptibility to excitotoxicity. Experiments done in HD mouse models crossed with Caspase-6 depleted mice support the hypothesis that N-terminal mhtt fragments were neurotoxic (Uribe et al., 2012). Similarly, pharmacological Caspase-6 inhibition rescued motor and cognitive deficits in mice (Leyva et al., 2010; Aharony et al., 2015).. A novel therapeutic approach targeted mhtt mRNA with antisense oligonucleotides to promote exon 12 skipping prevented mhtt expression containing D586 in mice (Evers et al., 2014). Exon skipping treatments in HD mouse models will provide additional information on N-terminal mhtt fragments following cleavage by Caspase-6. Apart from mhtt, other substrates were identified including serine threonine kinase 3, a pro-apoptotic kinase, that was activated by Caspase-6 to affect Akt signalling in striatal cells expressing mhtt (Riechers et al., 2016). In contrast, other groups found only partial rescue of HD phenotypes (Wong et al., 2015), or continued cleavage at D586 in Caspase-6 deficient mice (Gafni et al., 2012). Although there is strong evidence for Caspase-6 in HD in mice, there is very limited data on Caspase-6's role in humans which warrants further investigations.

1.13.2 Caspase-6 cleaves DJ-1 in PD

Parkinson's disease (PD) is the second most prevalent neurodegenerative disease in the world with both familial and sporadic forms. PD is characterized by motor dysfunction due to loss of dopaminergic neurons from the substantia nigra pars compacta and the presence of Lewy bodies which are aggregates of the molecular chaperone α-synuclein. Mutations in the E3-ubiquitin ligase Parkin, the serine/threonine protein kinase Pink-1, and the protein deglycase DJ-1 are found in both recessive and dominant early-onset PD patients. DJ-1 is a homodimeric protein that loses protein stability when exons 1-5 are deleted or if leucine 166 is mutated to proline (L166P). The L166P mutation causes a helix-breaking conformational change in DJ-1 that prevents homodimerization resulting in decreased protein stability (Moore et al., 2003; Takahashi-Niki et al., 2004). Loss of DJ-1 protein stability is linked to PD pathogenesis, yet the mutation in D149 to A (D149A) maintains protein levels while leading to early-onset PD (Abou-Sleiman et al., 2003).

A single study found a crucial interaction between Caspase-6 and DJ-1 to mediate p53 downregulation and neuroprotection. Experiments in telencephalon-specific murine 1 neurons and human neuroblastoma cell line found a loss of DJ-1's neuroprotective function in DJ-1 mutants L166P and D149A (Giaime et al., 2010). That was because DJ-1 mutants could not downregulate p53 through an Akt-dependent pathway. In fact, wild-type, but not mutant, DJ-1 activated Akt and NFκB, which led to p53 inactivation in the cytosol by Mdm-2-mediated ubiquitination and proteasomal degradation. Moreover, wild-type DJ-1 prevented transcriptional p53 upregulation by reducing p53 protein levels. For the L166P mutant, the reduced protein stability prevented DJ-1's neuroprotective signalling. In contrast, D149A DJ-1 was stable, but was resistant to caspase-mediated cleavage (Giaime et al., 2010). A similar study showed that Caspase-3 and Caspas-6 were capable of cleaving Synphilin, an α-synuclein binding protein, to generate a neuroprotective C-terminal fragment that inhibited p53 signalling (Giaime et al., 2006). The same pathway was investigated for DJ-1 mutants. Only Caspase-6, not Caspase-3 or -7, cleaved DJ-1 which generated a C-terminal fragment capable of inhibiting p53 and Caspase-3 induction in staurosporine or 6-hydroxy-dopamine-treated primary neuron cultures (Giaime et al., 2010). Furthermore, western blot analysis showed higher Caspase-6 and DJ-1 protein levels in sporadic PD cases suggesting that this protective mechanism is upregulated but not sufficient to halt disease progression (Giaime et al., 2010). Thus, Caspase-6 may also confer neuroprotection in neurodegenerative diseases.

1.13.3 Caspase-6 is activated following ischemic stroke

Stroke is the third leading cause of death in the world affecting nearly 15 million people worldwide (Hemphill et al., 2015). More than half of stroke patients die or are left disabled following an attack. Ischemic stroke pertains to embolism leading to focal cerebral blood flow interruption normally in the middle cerebral artery. Experimentally, ischemic stroke can be induced by middle cerebral artery occlusion (MCAo) in rats. Following MCAo, necrotic cell death occurs at the ischemic core, whereas apoptosis is detected in the penumbra, the surrounding tissue (Linnik et al., 1993). In human stroke cases, there is evidence of cleaved-Caspase-3 and axonal degeneration in the penumbra (Thomalla et al., 2004; Mitsios et al., 2007). Furthermore, ischemia-induced injury also happens following reperfusion which results in

inflammatory cytokine release such as IL-1β (Mazzotta et al., 2004). Hence, there is supporting evidence for caspase activation following ischemic stroke.

Caspase-6, among other caspases, is activated during ischemic stroke and leads to axonal degeneration. Following MCAo, Caspase-1, -2, -3, -6, and -8 mRNA or protein were increased in neurons, astrocytes, or microglia at different timepoints (Krupinski et al., 2000; Harrison et al., 2001; Chang and Wu, 2016). Increased active Caspase-6 immunoreactivity was detected in degenerating axons in white matter tracts from hypoxia-ischemia neonatal rat and preterm human brains (Guo et al., 2004; Baburamani et al., 2015). Similarly, in a 4-vessel occlusion global ischemia model, pre-conditioning, and post-conditioning had a protective effect that was reflected by decreased cleaved Caspase-3, -6, and -9 levels (Ding et al., 2012). In addition, prophylactic treatment with a histone H3 phosphorylation inhibitor ameliorated behavioural deficits, but not back to baseline, following transient MCAo and reduced Caspase-9 and -3 mRNA upregulation with no effect on Caspase-6 (Chang and Wu, 2016). In human stroke cases, Caspase-6 was localized to the nucleus, and TubΔCasp6 clearly defined zone of axonal degeneration (Guo et al., 2004; Sokolowski et al., 2014). These results suggest that Caspase-6 activity during stroke is deleterious, yet a recent study found that Caspase-6-deficiency had no impact on white matter loss and brain injury in neonatal ischemia (Baburamani et al., 2015). Thus, Caspase-6 is increased following ischemic injury, but it may not be the only relevant caspase.

Caspase-6's role in reperfusion injury and retinal ganglion cell survival following ischemia has also been investigated. Active Caspase-9 was observed in rat brains two hours following reperfusion in a transient MCAo model in rodents and Caspase-9 inhibition increased the number of neurons in the penumbra and neurofunctional scores (Akpan et al., 2011). At later timepoints, Caspase-6 protein was increased in neuronal processes and cell bodies. Caspase-9 inhibition also prevented Caspase-6 activation and Caspase-6-deficient mice had higher neuronal counts in the cortex compared to controls following ischemic stroke (Akpan et al., 2011). These experiments suggested that Caspase-9-mediated Caspase-6 activation led to axon and neuron loss which triggered neurological deficits. Meanwhile, Caspase-6 or -8 inhibition resulted in decreased cerebral infarct volume, brain edema, neurological deficits, and seizure activity following MCAo (Shabanzadeh et al., 2015). Moreover, NF-200, a protein involved in

maintaining cell shape and facilitating axonal transport, and proliferating cells numbers increased following Caspase-6 and -8 inhibition. Thus, targeting caspases in the penumbral region may have therapeutic potential in cerebral ischemia.

Blindness following retinal ischemia in diabetic patients is common (Rahmani et al., 1996) and may result from Caspase-6 activity. Ophthalmic artery ligation serves as a retinal stroke model in rats and leads to retinal ganglion cell (RGC) death (Lafuente et al., 2002). RGC survival was increased following pharmacological Caspase-6 or -8 inhibition or silencing by siRNA (Shabanzadeh et al., 2015). In addition, Caspase-6 inhibition prevented Caspase-8 and -3 activation in retinal and brain lysates following ischemia. This is in contrast to findings in Caspase-3-deficient mice which demonstrated no Caspas-6 activation during MCAo suggesting that Caspase-3 activated Caspase-6 (Le et al., 2002). Scientists need to understand the limitations of the commercially available caspase inhibitors since they are sold under the false pretence that they are specific against individual caspases. Moreover, in biological settings there exist an inevitable caveat where even selective caspase inhibition will result in inhibition of downstream caspases. Therefore, it is possible that the inhibitors used in the study were not selective and warrant the use of multiple approaches to dissect out the activation cascade. Caspase-null mice, siRNA, selective inhibitors (Merck Caspase-3, Vertex Caspase-1), or even immuno-depletion experiments could help further elucidate the signalling cascade in both retinal and cerebral ischemia models and consolidate the results in the field.

1.14 Caspase-6 inhibitors: proteins, peptides, and small molecules

To date, caspase inhibitors come in several forms, from viral proteins, endogenous proteins, to pharmacological inhibitors (**Table 1.4 & 1.5**). PTMs such as phosphorylation and palmitoylation also inhibit Caspase-6 activity (see section **1.8**). Endogenous protein inhibitors are also regulated during apoptosis, whereas pharmacological inhibitors can be subdivided into reversible or irreversible, competitive, non-competitive, or uncompetitive inhibitors based on their mechanisms of inhibition. Due to the attention Caspase-6 has garnered as an effector of neurodegeneration, inhibitors with varying levels of potency and selectivity have been developed. Before my results can be presented, an overview of current Caspase-6 inhibitors is essential.

1.14.1 Endogenous protein Caspase-6 inhibitors

The first caspase inhibitors to ever be described were the viral proteins p35 and cow pox virus response modifier A (CrmA). CrmA was originally classified as a serine protease inhibitor when it was discovered in 1986 (Pickup et al., 1986). Shortly after Caspase-1 was cloned, CrmA was shown to inhibit Caspase-1 by acting as a suicide inhibitor, that is, a protein that is cleaved but remains irreversibly bound to the enzyme to prevent further activity (Ray et al., 1992). This was surprising since caspases are cysteine proteases, which for the first time, suggested that protein inhibitors targeted enzymes based on the geometry of their active sites, and not by their catalytic mechanism. Subsequently, CrmA demonstrated inhibitory activity on the serine protease Granzyme B (Quan et al., 1995), Caspase-1, and -8 (Zhou et al., 1997). CrmA was not considered a physiologically relevant Caspase-6, -3, or -7 inhibitor. When p35, a protein found in *Autographa californica* nuclear polyhedrosis virus, was discovered, it could inhibit apoptosis in insect and mammalian cells (Clem et al., 1991; Rabizadeh et al., 1993). Soon after caspases were identified, p35 was found to be a suicide Caspase-1, -2, -3, and -4 inhibitor (Bump et al., 1995). This list grew to include Caspase-6, -7, -8, and -10 (Zhou et al., 1998), while the baculoviral protein p49 inhibited Caspase-9 (Zoog et al., 2002). Unlike, CrmA, p35 showed specificity towards caspases as it did not inhibit Granzyme B, and other serine or cysteine proteases significantly (Bump et al., 1995; Zhou et al., 1998). Thus, p35 is a viral protein with inhibitory activity against Caspase-6.

Inhibitors of apoptosis proteins (IAPs) are endogenous caspase inhibitors that lack the ability to inhibit Caspase-6 and only one IAP is an actual caspase inhibitor (**Table 1.5**). The discovery of the first IAP came from viral DNA lacking p35 that still prevented apoptosis (Crook et al., 1993). This IAP was not homologous to p35, but did contain a roughly 80 amino acid baculoviral IAP repeat (BIR) motif that was capable of binding zinc. The search for mammalian homologous led to the identification of eight IAPs. Neuronal apoptosis inhibitory protein (NAIP) belonged to the NLR family with functions in innate immunity (Liston et al., 1996; Damiano et al., 2004). Survivin participated in mitosis as shown by its localization to centromeres (Ambrosini et al., 1997; Li et al., 1999). Initially, both NAIP and Survivin were thought to directly bind and inhibit Caspase-3 and -7 (Shin et al., 2001; Maier et al., 2002), yet this inhibitory activity was not relevant physiologically due to the absence of key structural

elements (Banks et al., 2000; Eckelman and Salvesen, 2006). XIAP is the best characterized IAP with three consecutive BIR domains and a C-terminal RING domain (Duckett et al., 1996; Deveraux et al., 1997; Deveraux et al., 1998). BIR2 and a N-terminal linker region led to direct Caspase-3 and -7 inhibition (Sun et al., 1999; Riedl et al., 2001), whereas the BIR3 domain prevented Caspase-9 homodimerization (Sun et al., 2000). Cellular IAP (cIAP1) and cIAP2 contain a CARD, in addition to three tandem BIR repeats and a RING domain (Rothe et al., 1995). The cIAP1 and cIAP2 proteins showed direct caspase inhibitory activity (Roy et al., 1997; Deveraux et al., 1998), yet in a physiological setting cIAPs bound to caspases without inhibiting them (Eckelman and Salvesen, 2006). Using their RING domains, XIAP, cIAP1, and cIAP2 were found to auto-ubiquitinate leading to their degradation during apoptosis (Yang et al., 2000). This mechanism may allow the degradation of bound SMAC/DIABLO or HtrA2 accidentally released from the mitochondria. BRUCE/Apollon is a roughly five thousand amino acid long E2 ubiquitin-conjugating enzyme found on the trans-Golgi membrane that showed anti-apoptotic function (Hauser et al., 1998; Hao et al., 2004). Melanoma-IAP and IAP-like protein 2 possessed anti-apoptotic activities linked to Caspase-9 inhibition (Vucic et al., 2000; Richter et al., 2001). Future experiments suggested that melanoma-IAP may have signalled through alternate cell survival pathways (Sanna et al., 2002), while IAP-like protein 2 did not have a BIR domain capable of directly inhibiting caspases (Shin et al., 2005). IAPs most likely promote cell survival by acting as decoy molecules to IBM-containing proteins, namely, SMAC/DIABLO and HtrA2. This would help XIAP to keep Caspase-3, -7, and -9 activities at bay. Therefore, although IAPs are anti-apoptotic molecules, only XIAP may be considered a physiological caspase inhibitor, yet it lacked the ability to inhibit Caspase-6 directly (Deveraux et al., 1997).

A few other proteins have been observed to inhibit Caspase-6 activity. In human neurons, treatment with 17β-estradiol led to the activation of caspase inhibitory factor (CIF) that inhibited Caspase-6, -3, -7, and -8 (Zhang et al., 2001). CIF mediated ubiquitin-independent but proteasome-dependent degradation of active Caspase-6 subunits, although this was not necessary for CIF's inhibitory activity (Tounekti et al., 2004). The alternatively spliced Caspase-6 isoform, Caspase-6β, did not inhibit active Caspase-6, but through asymmetrical dimerization, prevented Caspase-6α activation (Lee et al., 2010). Sox11, Sox4, and Sox7 inhibited nuclear

Caspase-6 activity and self-activation (Waldron-Roby et al., 2015). Sox11 also inhibited effector Caspase-3 and -7. During lens formation, αA-crystallin directly bound and inhibited Caspase-6 (Morozov and Wawrousek, 2006). Finally, a nucleophosmin mutant accumulated in the cytosol where it inhibited Caspase-6 and -8 through by binding directly, resulting in decreased myeloid differentiation (Leong et al., 2010).

1.14.2 Zinc-mediated Caspase-6 inhibition

Caspases are susceptible to zinc-mediated inhibition. During the early characterization of caspase biochemical properties, it was noted that caspase activity was sensitive to zinc, but not calcium, ions (Stennicke and Salvesen, 1997). Later, apoptosis-inducing agents were shown to chelate zinc, suggesting that intracellular zinc concentrations were sufficient to keep caspases inhibited (Chai et al., 2000; Sarkar et al., 2016) and apoptosis could be prevented by caspase inhibition in zinc-chelated cells (Shindler et al., 2000). The mechanism for zinc-mediated Caspase-6 inhibition was solved by identifying zinc binding sites by anomalous diffraction. A unique site was observed away from the Caspase-6 active site where three residues formed a cage where one zinc molecule could bind per monomer (Velazquez-Delgado and Hardy, 2012b). Zinc-binding essentially locked Caspase-6 in the helical unliganded conformation which prevented substrate hydrolysis.

1.14.3 Pharmacological Caspase-6 inhibitors

Competitive small molecule peptide inhibitors bind to Caspase-6's active site and prevent protein substrates from entering. Most commercial Caspase-6 inhibitors are based on peptide screening libraries that were initially used to understand the substrate specificities of different caspases (Rano et al., 1997; Talanian et al., 1997; Thornberry et al., 1997). From these early studies, the aldehyde and the FMK conjugated Z-VEID became the classical reversible and irreversible Caspase-6 inhibitors, respectively. Yet, to this day, the selectivity of these inhibitors has been put into question (McStay et al., 2008; Pereira and Song, 2008). The identification of transcription factor activator protein 2α as a Caspase-6 substrate led to the development of Z-DRHD-FMK as a Caspase-6 inhibitor (Nyormoi et al., 2003). However, the activator protein 2α-based inhibitor also showed strong inhibitory activity against Caspase-8 and -9. Aza-peptide Michael acceptors screened for different caspases revealed IETD and

VEVD as the preferred Caspase-6 tetrapeptides (Ekici et al., 2006). Yet, the irreversible inhibitors lacked selectivity as it showed strong Caspase-8 and -3 inactivation. In contrast, aza-peptide epoxides based on IETD with optimized stereochemistry achieved 3- to 10-fold greater specificity for Caspase-6 compared to Caspase-1 and -8, respectively (James et al., 2004). Both irreversible inhibitors, aza-peptide Michael acceptors and epoxides, showed little reactivity against other cysteinyl, aspartyl, or serine proteases (James et al., 2004; Ekici et al., 2006). Acyloxymethylketone irreversible inhibitors based on the Z-EKD tripeptide showed strong Caspase-3 but not Caspase-6 inhibition, although the inhibitor had sufficient affinity to extract Caspase-6 from overexpressing cells (Henzing et al., 2006). A fusion peptide, ED11, based on the Caspase-6's cleavage sequence in htt protein and HIV's transactivation of transcription (TAT)-peptide was shown to potently inhibit Caspase-6 activity and rescue HD-like phenotypes in mice (Aharony et al., 2015). However, ED11 inhibited Caspase-1, -2, and -10-mediated htt cleavage and increased Caspase-5 activity. Hence, all competitive peptide-based inhibitors against Caspase-6 have compromised selectivity.

Nonpeptidic small molecule inhibitors require further optimization. Anilinoquinazolines were developed as potent Caspase-3 inhibitors to overcome the drawbacks of peptide-based inhibitors (Scott et al., 2003). However, in enzyme assays, some anilinoquinazolines also inhibited Caspase-6 with nanomolar inhibitory constants. The presumed serine protease inhibitors N-α-Tosyl-L-LysinylChloromethylketone (TLCK) and N-Tosyl-LPhenylalaninyl-Chloromethylketone (TPCK) showed inhibitory activity on recombinant human effector caspases with μM efficacy against Caspase-6 (Frydrych and Mlejnek, 2008a). TLCK and TPCK inhibited Caspase-3 and -7 with greater potency than against Caspase-6, and inhibited catalytic activity, not activation or processing, in cells treated with cytotoxic agents (Frydrych and Mlejnek, 2008b). Sulfonamide isatin Michael acceptors (IMA) were synthesized as novel Caspase-6 inhibitors and achieved high nanomolar IC_{50} values (Chu et al., 2009). IMA were identified as reversible inhibitors that could distinguish between Caspase-6 and Caspase-1, -3, -7, and -8. Although this is promising, selectivity against Caspase-9, and -10 needs to be tested to warrant continued development of IMAs as Caspase-6 inhibitors. Using an alternate approach, researchers sought to develop highly efficient substrates that would be converted into inhibitors by the addition of a 2,4,5,6-tetrafluorophenoxymethyl chemical warhead. Starting

with a library of 1,4-disubstituted-1,2,3-triazole substrates, scientists developed irreversible pan-caspase inhibitors capable of preventing mhtt cleavage by Caspase-6 and -3 *in vitro* and in primary neuron cultures (Leyva et al., 2010). Thus, although these inhibitors are potent and show efficacy in biological settings, they lack selectivity for Caspase-6.

To finally tackle the issue of selectivity, research groups targeted regions outside Caspase-6's active site. N-furoyl-phenylalanine derivatives showed exceptional inhibitory activity against Caspase-6 cleaving the caged rhodamine (R110) substrate $VEID_2R110$, especially when the R enantiomer was used (Heise et al., 2012). This novel inhibitor was selective to Caspase-6, compared to Caspase-3 and -7, but also depended on VEID and R110 being present on the substrate. This was because this new inhibitor was uncompetitive and bound to the enzyme-substrate complex. Changing the cleavage sequence in the tetrapeptide or the fluorophore weakened the inhibitory potency significantly. In addition, although VEID-CHO prevented Lamin A cleavage at VEID, the N-furoyl-phenylalanine inhibitor was ineffective at the highest concentration tested (Heise et al., 2012). Another group employed fragment based discovery using modeling and X-ray crystallization to identify a novel drug-binding site in zymogen pro-Caspase-6 (Murray et al., 2014). The investigators identified several different compounds capable of increasing Caspase-6 zymogen stability, effectively preventing L2 loop rearrangement during Caspase-6 self-activation. Although the compounds have dissociation constants in the nanomolar range, the effect on Caspase-6 self-activation or activity and selectivity against other caspases were not shown (Murray et al., 2014). Zymogen Caspase-6 was also subjected to a peptide phage library. This screen identified two peptides, pep419 and pep440c, that strongly bound Caspase-6 zymogen, but also inhibited active Caspase-6 activity (Stanger et al., 2012). However, neither peptide was selective for Caspase-6. Pep419 was found to induce both zymogen and active Caspase-6 tetramerization. Active Caspase-6 tetramerization was behind the noncompetitive mode of inhibition which resulted in substrate binding but not turnover (Stanger et al., 2012). In addition, pep419 was effective in inhibiting Lamin A cleavage in neuroblastoma cells treated with staurosporine. Therefore, targeting Caspase-6 away from the active site shows promise, but additional pharmacokinetic and pharmacodynamic experiments *in vivo* are necessary.

1.15 Hypothesis and Thesis objectives

Based on the literature review, Caspase-6 is a unique enzyme among caspases that plays an important role in axonal degeneration and in neurodegenerative diseases. In pre-clinical AD, there is a strong correlation between Caspase-6 activity and cognitive decline (Ramcharitar et al., 2013a), while Caspase-6-overexpression in the CA1 region of the hippocampus leads to age-dependent spatial and episodic memory deficits (LeBlanc et al., 2014). Caspase-6 cleaves a multitude of cytoskeletal proteins which could impact axonal integrity and synaptic structures (Klaiman et al., 2008). Thus, we believe Caspase-6 to be a novel and important target to combat cognitive decline in the elderly.

The thesis objective is to characterize novel Caspase-6 inhibitors to help develop therapeutic interventions for AD. To achieve this, two inhibitory mechanisms have been investigated. In Chapter 2, methylene blue and its derivatives were studied to assess if cysteine oxidation could result in Caspase-6 inhibition. The possibility that methylene blue behaved as a caspase inhibitor was assessed *in vitro*, in cells, and *in vivo*. In Chapter 3, vinyl sulfone inhibitors are characterized as a new line of chemical warheads for use *in vivo*. Vinyl sulfones were tested in primary human neuron and mouse Caspase-6 models to assess safety and efficacy. Together, both studies reveal a novel mechanism for Caspase-6 inhibition and a proof-of-concept for targeting Caspase-6 to reverse memory deficits. With these contributions to the field, there is hope that a potent, non-toxic, and selective Caspase-6 inhibitor will one day reach clinical trials to combat cognitive decline in the elderly.

1.16 Figures and legends

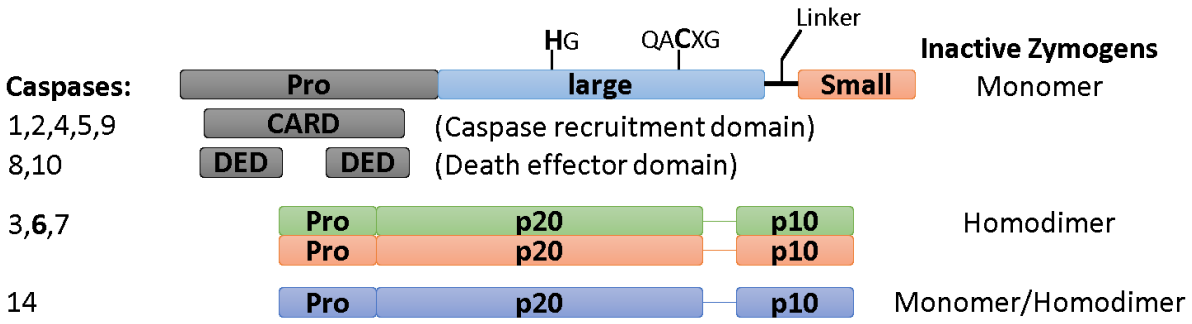

Figure 1.1 General caspase structure.

All caspases have a prodomain (pro), a large domain (large or p20 for Caspase-6), and small domain (small or p10 for Caspase-6). The large domain contains both catalytic residues, and cleavage events to remove the prodomain and the linker must occur to maximize catalytic activity. Caspase-1, -2, -4, -5, -8, -9, and -10 exist as monomers in solution and have either caspase recruitment domains (CARD) or death effector domains (DED) within their prodomains. In contrast, Caspase-3, -6, and -7 have smaller prodomains lacking any protein-protein interaction motifs and exist as dimers in solution. Caspase-14 also has a small prodomain although it can be found as both monomeric and dimeric species.

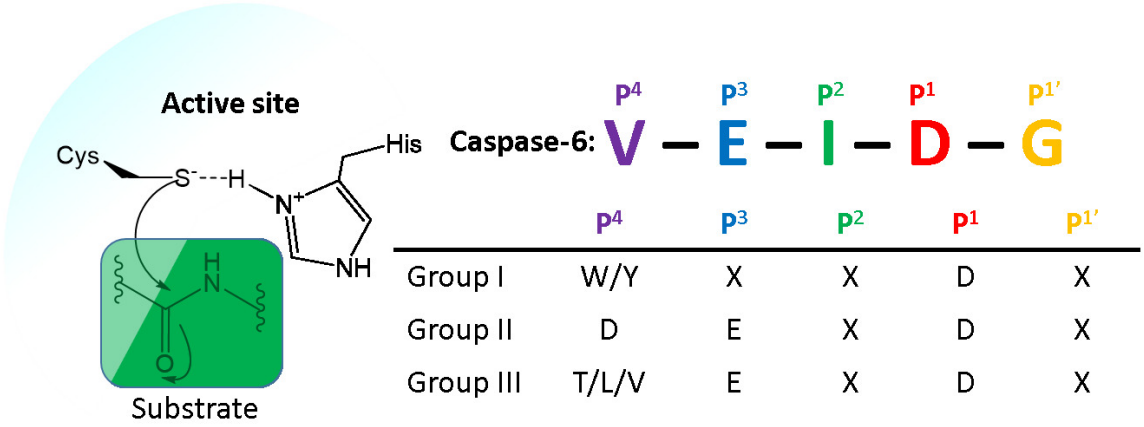

Figure 1.2 Preferred substrate cleavage sequences for different caspase groups.

Caspases are cysteinyl proteases that with the help of a histidine residue within the active site hydrolyze peptide bonds in substrates. Early studies have identified that caspases cleave specifically after aspartic acid residues at the P^1 position, although recent evidence suggests that glutamate and phosphorylated serine may also be accommodated in this position. Group I caspases prefer large aromatic amino acids at position P^4, whereas Group II caspases prefer aspartic acid residues. Group III caspases prefer smaller non-charged amino acids position P^4.

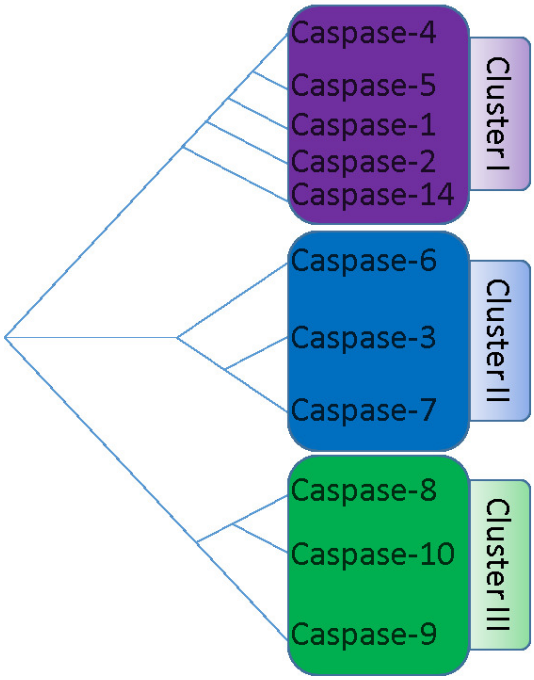

Figure 1.3 Phylogenetic relationship between caspases.

Caspases can be separated into three clusters based on their sequence homology. Cluster I is populated mostly by CARD-containing Caspase-1, -2, -4, and -5, but also includes Caspase-14. Cluster II contains all three short prodomain-containing caspases (3, 6, 7), while Cluster III includes DED- and CARD-containing caspases (8, 9, 10).

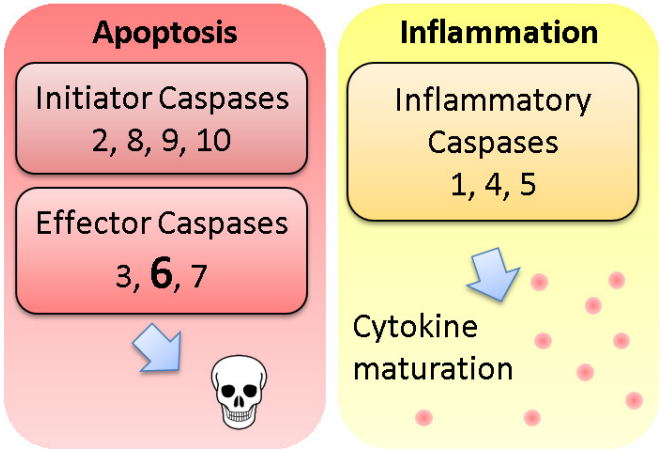

Figure 1.4 Classically-defined roles for caspases in apoptosis and inflammation.

Early studies on caspases have focused primarily on apoptotic and inflammatory pathways. Initiator caspases (2, 8, 9, 10) are activated by cell death signals either extrinsic or intrinsic to the cell and then proteolytically process effector caspases (3, 6, 7) leading to apoptosis. On the other hand, inflammatory caspases (1, 4, 5) are activated by damage or pathogen-associated molecular patterns and proteolytically process cytokines leading to an inflammatory response.

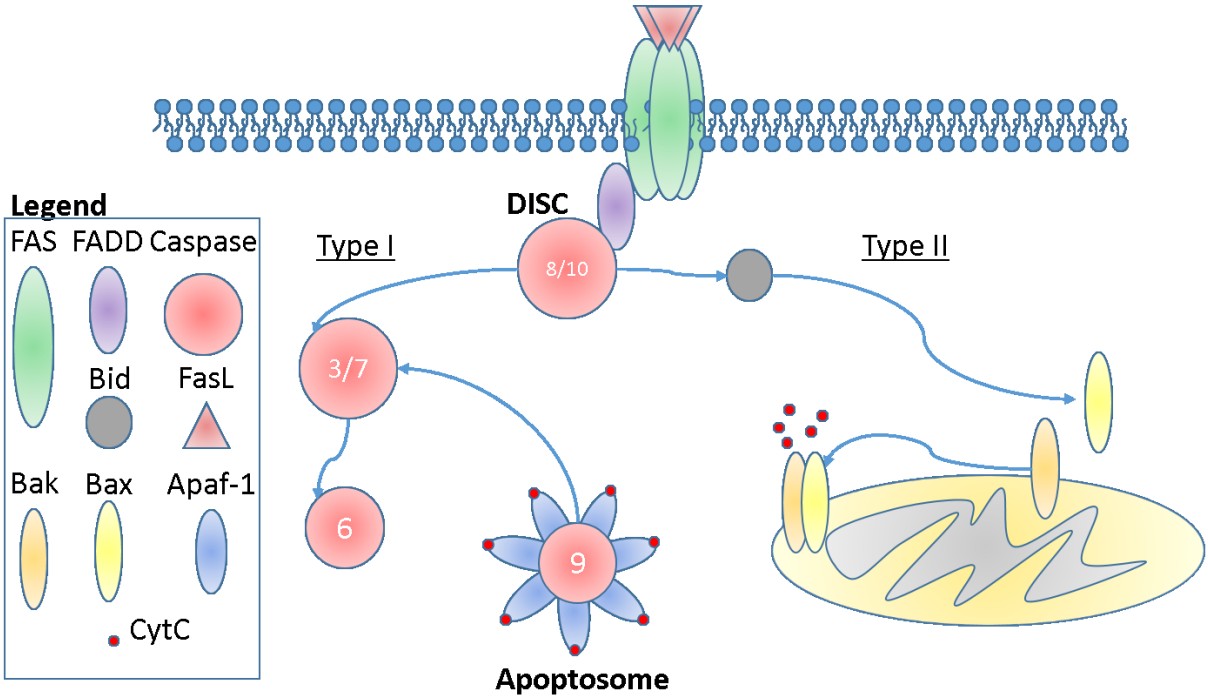

Figure 1.5 Schematic of extrinsic and intrinsic apoptotic signaling cascades.

Extrinsic apoptosis is induced by death receptors binding to death ligands. Following FasL binding to Fas, the adapter molecule FADD is recruited to the plasma membrane. FADD then recruits Caspase-8/10 through its CARD domain forming the DISC and induces caspase oligomerization. In type I cells, activated Caspase-8/10 proteolytically activates effector Caspase-3/7 to induce apoptosis. In type II cells, Caspase-8 cleaves Bid. In this scenario, intrinsic apoptotic signaling is activated. Truncated Bid translocates to the mitochondria where it promotes Bax and Bak oligomerization inducing mitochondrial outer membrane permeabilization. Many proteins escape mitochondria including CytC which binds to Apaf-1 to form the heptameric apoptosome. The apoptosome activates Caspase-9 through oligomerization. Active Caspase-9 then proteolytically activates Caspase-3/7 to induce apoptosis.

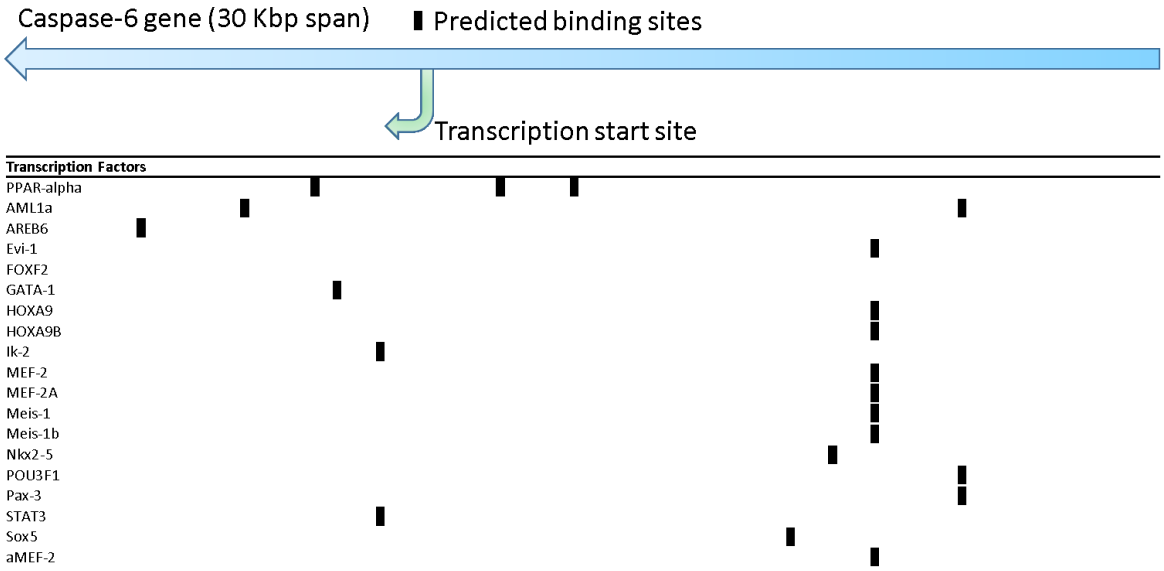

Figure 1.6 Schematic of predicted transcription factor binding sites on the *CASP6* gene.

List of transcription factors predicted to bind upstream and downstream of the transcription start site (30 Kbp range) in *CASP6*. Potential binding site locations are depicted by black boxes along *CASP6*.

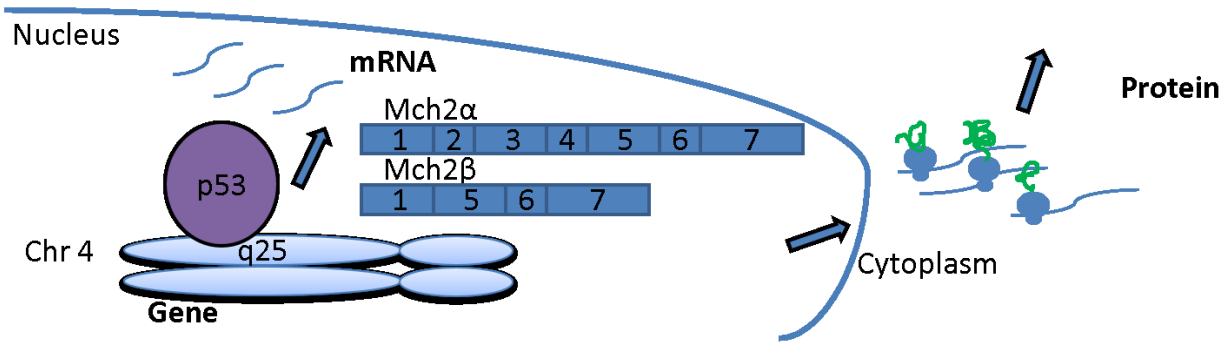

Figure 1.7 Caspase-6 transcription can be upregulated by p53 with two splice variants.

CASP6 is found on chromosome 4q25 with p53 binding sites in an intronic region. Little else is known about *CASP6* transcriptional regulation. Caspase-6 mRNA can be spliced into the canonical Caspase-6α (Mch2α) which contains all seven exons or the truncated isoform Caspase-6β (Mch2β) which lacks exons 2-4 inclusively. Both mRNA can be transcribed into protein. Although both Caspase-6α and Caspase-6β contain active site residues, only Caspase-6α is enzymatically active.

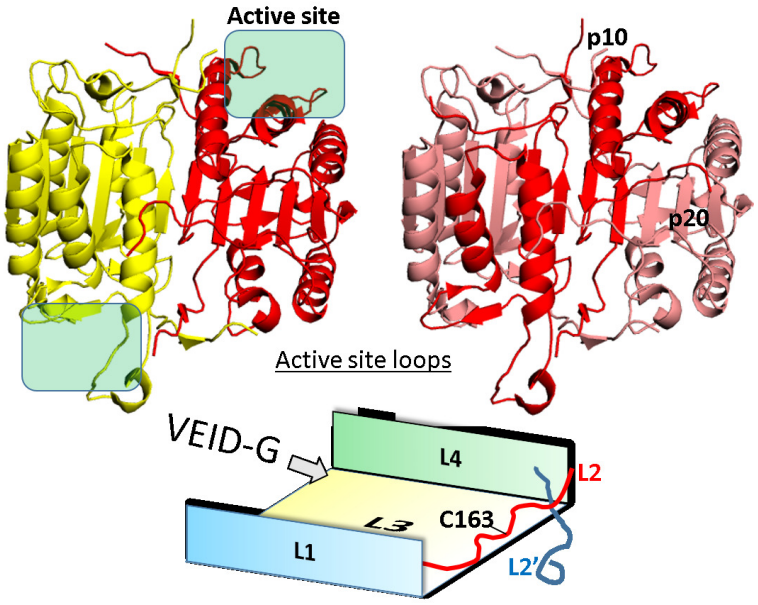

Figure 1.8 Caspase-6 crystal structures.

Caspase-6 structure on the left displays each monomer of the homodimer in different colors (yellow and red). Active sites are formed by loops emanating from the α-helices and β-strands and are identified with transparent boxes. The Caspase-6 structure on the right demonstrates that the p10 subunits (red) form the dimerization interface, while the p20 subunits (pink) are on the outer edges.

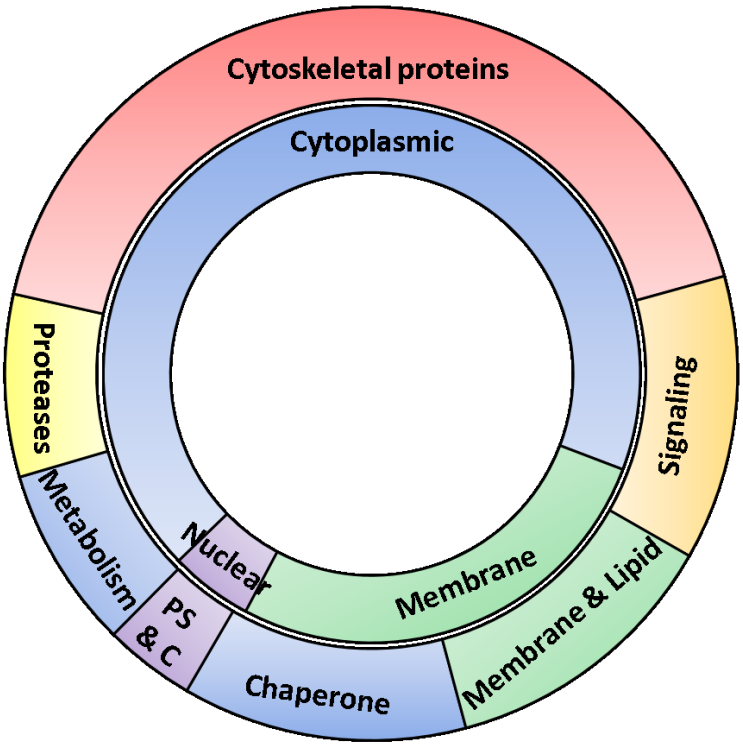

Figure 1.9 Caspase-6 substrates in human neuronal extracts.

Caspase-6 substrates are mostly located within the cytoplasmic and membrane compartments in human neurons. Listed in order of abundance, Caspase-6 cleaves cytoskeletal proteins, signaling proteins, membrane and lipid-associated proteins, chaperones, proteases, metabolism-related proteins, protein synthesis and conjugation-associated proteins (PS & C).

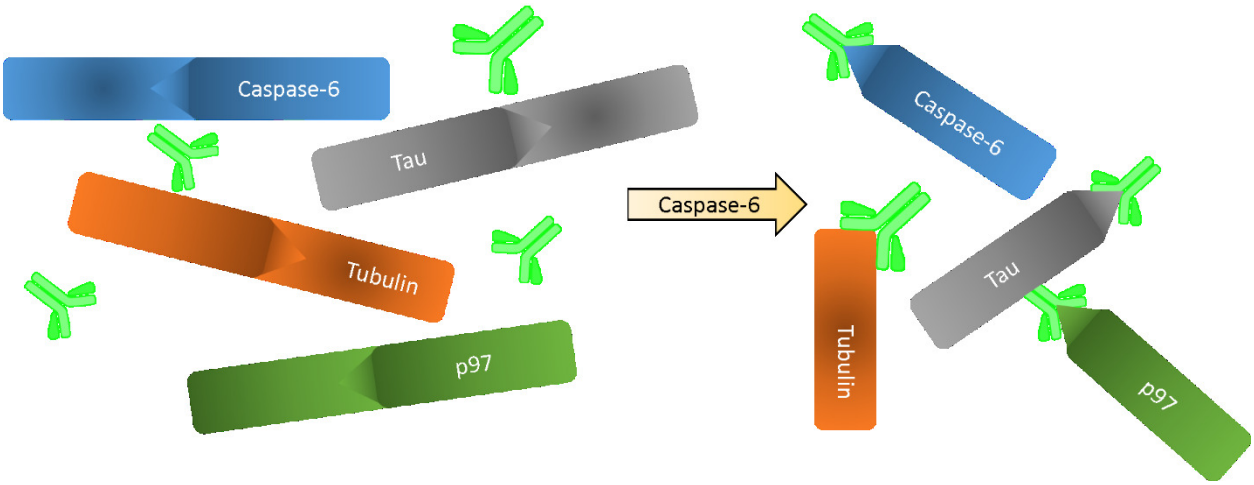

Figure 1.10 Neoepitope antibodies distinguish between full length and cleaved substrates.

A surrogate marker for active Caspase-6 are the identification of Caspase-6 cleaved substrates. This is possible by the generation of neoepitope antibodies that have higher affinity for epitopes generates following cleavage by Caspase-6 than for the full length protein.

1.17 Tables

Table 1.1 Clan CD proteases.

Clan	Family	Peptidase
CD	C11	Clostripain
	C13	Legumain
	C14	Caspases
	C25	Gingipain RgpA
	C50	Separase
	C80	RTX self-cleaving toxin
	C84	prtH peptidase

Table 1.2 Caspase-6 deficient models and their phenotypes.

Model	Experimental model	Phenotype	Reference
Caspase-6 Knock-Out	Mouse	Normal (viable)	Zheng et al., *Nat. Med.* 2000
	Mice and NPC culture from embryos	No effect on DNA-damaged-induced NPC cell death	D'Sa et al., *J Neurosci Res* 2003
	Lens from the eye	No effect on organelle clearance	Zandy et al., *J Biol Chem* 2005
	Ex vivo B Cell culture	↓ Proliferation ↑ Differentiation	Watanabe et al., *J Immunol* 2008
	AOM-DSS model of colon carcinogenesis	No effect on tumorigenesis	Foveau et al., *Plos One* 2014
Removal of Casp6 exons 2-5	Mouse	Protects against excitotoxicity ↑ Cortical and striatal volume Deficits in learning Hypokinetic	Uribe et al., *Hum Mol Genet* 2012

Table 1.3 Caspase-6 leads to axonal degeneration in several different models.

Model	References
Serum-deprivation of human primary neurons	LeBlanc et al. *J Biol Chem* 1999
NGF-deprivation models (DRG axons, sympathetic, sensory, commissural, motor, cervical ganglion)	Nikolaev et al. *Nature* 2009 Schoenmann et al. *J Neurosci* 2010 Vohra et al. *J Neurosci* 2010 Uribe et al. *Hum Mol Genet* 2012 Simon et al. *J Neurosci* 2012 Cusack et al. *Nat Commun* 2013 Unsain et al. *Cell Rep* 2013 Simon et al. *Cell* 2016
Optic nerve injury and retinal ganglion cells Optic nerve crush retinal ganglion cells	Monnier et al. *J Neurosci* 2011 Vigneswara et al. *Brain* 2014
Middle Carotid Artery occlusion Thromboembolic stroke	Akpan et al. *J Neurosci* 2011 Shabanzadeh et al. *Cell Death Dis* 2015
Mouse sympathetic or rat septal cholinergic neurons grown on myelin	Park et al. *Nat Neurosci* 2010 Uribe et al. *Hum Mol Genet* 2012
Human primary neurons overexpressing Amyloid precursor protein	Sivananthan et al. *Cell Death Differ* 2010

Table 1.4 Different types, targets, and mechanisms developed for Caspase-6 inhibition.

Type of Inhibitor	Target	Mechanisms	Examples	References
Peptide	Active site	Competitive reversible and irreversible	Z-VEID-fmk VEID-CHO	Talanian et al. 1997 JBC Thornberry et al. 1997 JBC Nyormoi et al. 2003 Apoptosis Ekici et al. 2006 J. Med. Chem. Henzing et al. 2006 J. Med. Chem. Aharony et al. 2015 HMG
	Allosteric site	Non-competitive reversible	Pep419	Stanger et al. 2012 Nat. Chem. Biol.
Small molecule	Active site	Competitive reversible and irreversible	1,4-disubstituted-1,2,3-triazole	Flydrych & Mlejnek 2008 J Cell Biochem. Chu et al. 2009 J. Med. Chem. Leyva et al. 2010 Chem. Biol.
	Allosteric site	Uncompetitive reversible	N-Furoyl-phenylalanine	Heisce et al. 2012 PLOS One Murray et al. 2014 Chem Med Chem
Protein	Unknown	Unknown	CIF	Zhang et al. 2001 J. Neurosci. Tounekti et al. 2004 J. Neurochem.
	Allosteric site	Asymmetrical dimerization	Mch2	Lee et al. 2010 JBC
	Allosteric site	Asymmetrical dimerization	PEN-C163A	Vigneswara et al. 2014 Brain
Post-translational modifications	Ser 257	Phosphorylation	ARK5	Suzuki et al. 2004 Oncogene Velazquez-Delgado et al. 2012 Structure
	Cys264/277	Palmitoylation	HIP14	Skotte et al. 2016 CDD
Cofactors	Allosteric site	Non-competitive reversible	Zinc	Velazquez-Delgado et al. 2012 JBC

Table 1.5 Baculoviral and inhibitors of apoptosis proteins and their caspase targets.

Caspase Inhibitor	Organism	Target Caspases	References
CrmA	Cowpox Virus	1, 8, 10	Zhou et al. 1997 JBC
p35	Baculovirus	1, 2, 3, 4, **6**, 7, 8, 10	Bump et al. 1995 Science Zhou et al. 1998 Biochemistry
p49	Baculovirus	9	Zoog et al. 2002 EMBO
XIAP	Mammalian	3, 7, 9	Deveraux et al. 1997Nature Sun et al. 1999 Nature Sun et al. 2000 JBC Riedl et al. 2001 Cell
cIAP1	Mammalian		Eckelman & Salvesen. 2006 JBC
cIAP2	Mammalian		
ILP-2	Mammalian		Shin et al. 2005 Biochem J
ML-IAP	Mammalian		Sanna et al. 2002 MCB
Survivin	Mammalian		Banks et al. 2000 Blood Eckelman & Salvesen. 2006 JBC
NAIP	Mammalian		
BRUCE/Apollon	Mammalian		Hauser et al. 1998 JCB Hao et al. 2004 NCB

2. Methylene blue inhibits caspases by oxidation of the catalytic cysteine

2.1 Preface

Caspase-6 activity can be inhibited by phosphorylation at serine 257 and palmitoylation at cysteine residues. Phosphorylation locks the enzyme in an inactive conformation, while palmitoylation prevents self-activation or Caspase-6 dimerization. Despite experimental evidence for inhibitory PTMs, no Caspase-6 inhibitor has been described to function through modulating PTMs. The present study describes methylene blue and its derivatives as pan-caspase inhibitors *in vitro*, in cells, and *in vivo*. Moreover, Caspase-6's catalytic C163, among other cysteine and methionine residues, is reversibly oxidized as detected by LC-MS/MS. These findings are the first to identify oxidation as a novel PTM for Caspase-6 and describe compounds that can inhibit Caspase-6 by acting through PTMs.

2.2 Abstract

Methylene blue, currently in phase 3 clinical trials against Alzheimer Disease, disaggregates the Tau protein of neurofibrillary tangles by oxidizing specific cysteine residues. Here, we investigated if methylene blue can inhibit caspases via the oxidation of their active site cysteine. Methylene blue, and derivatives, azure A and azure B competitively inhibited recombinant Caspase-6 (Casp6), and inhibited Casp6 activity in transfected human colon carcinoma cells and in serum-deprived primary human neuron cultures. Methylene blue also inhibited recombinant Casp1 and Casp3. Furthermore, methylene blue inhibited Casp3 activity in an acute mouse model of liver toxicity. Mass spectrometry confirmed methylene blue and azure B oxidation of the catalytic Cys163 of Casp6. Together, these results show a novel inhibitory mechanism of caspases via sulfenation of the active site cysteine. These results indicate that methylene blue or its derivatives could (1) have an additional effect against Alzheimer Disease by inhibiting brain caspase activity, (2) be used as a drug to prevent caspase activation in other conditions, and (3) predispose chronically treated individuals to cancer via the inhibition of caspases.

2.3 Introduction

Methylene blue, a tricyclic phenothiazine (also known as methylthionine hydrochloride), has a history of diverse medical applications stretching over a century for treatment of enzymopenic hereditary methemoglobinemia, acute acquired methemoglobinemia, urinary tract infections, malaria, septic shock, and hepatopulmonary syndrome (Schirmer et al., 2011). Alzheimer disease (AD) is a progressive neurodegenerative disorder showing abundant deposits of β -amyloid peptide (Aβ) plaques, intracellular neurofibrillary tangles (NFTs) consisting of Tau protein, and the loss of synapses (Goedert and Spillantini, 2006). Presently, inhibitors of Tau aggregation are being considered as therapeutic interventions against AD, and methylene blue disaggregates Tau NFTs. Methylene blue, and its demethylated derivatives azure A and azure B, were initially identified as blocking in vitro Tau-Tau aggregation identified as paired helical filaments by electron microscopy (Wischik et al., 1996). Methylene blue was also shown to prevent heparin-induced Tau filament formation (Hattori et al., 2008). More recently, several studies have demonstrated the ability of methylene blue to prevent Tau aggregation in transgenic mouse models expressing the P301L or P301S Tau mutations associated with the formation of NFTs in mice and in human disease. Treatment of the rTg4510 human P301L transgenic mouse with methylene blue improved behavior slightly in treated 3 month old mice, reduced brain total Tau and phospho-Tau, and increased neuronal survival (O'Leary et al., 2010). However, treatments in 16 month old rTg4510 mice did not have any effect on Tau levels, neuronal survival or brain atrophy (Spires-Jones et al., 2014). The preventative nature of methylene blue was also observed in TauΔK280 and TauRDK transgenic mice where treatments started in 1.5 or 9 month old mice, but not in 15 month old mice, showed improved cognitive behavior and a decrease in pathological Tau at 18 months of age (Hochgrafe et al., 2015). Similarly, methylene blue treatment of the JNPL3 human P301L or the P301S transgenic mice decreased Tau pathology in brains (Hosokawa et al., 2012; Stack et al., 2014). Reduced Tau aggregation was also observed in JNPL3 organotypic brain slices (Congdon et al., 2012). Furthermore, methylene blue improved behavioral deficits and Tau pathology in C. elegans and Drosophila models (Fatouros et al., 2012; Mohideen et al., 2015). Accordingly, methylene blue is currently in phase III clinical trials in human AD patients in the hope of stopping the progression of cognitive deficits and dementia (Wischik et al., 2014).

Methylene blue has been shown to clear Tau pathology through increased autophagy in JNPL3 organotypic slices (Congdon et al., 2012). Molecularly, methylene blue, and its mono and di-N-demethylated forms, azure B and azure A, were shown to interact with and promote the oxidation of Tau cysteine residues, retaining Tau in a monomeric conformation, thus preventing formation of fibrils and their toxic precursors (Akoury et al., 2013; Crowe et al., 2013). The identification of this mechanism prompted us to ask whether methylene blue may modulate the activity of caspases, a group of cysteinyl proteases involved in inflammation and cell death.

One of the effector caspases, Caspase-6 (Casp6), has been highly implicated in age-dependent cognitive decline and in sporadic and familial AD pathology (Guo et al., 2004; Albrecht et al., 2007; Albrecht et al., 2009; Ramcharitar et al., 2013a; LeBlanc et al., 2014). Furthermore, the expression of a self-activated form of Casp6 in the hippocampal CA1 of mice induces age-dependent cognitive deficits in episodic and spatial memory (LeBlanc et al., 2014). While Casp6 in cells and neurons does not induce the expected effector caspase-mediated rapid cell death (Klaiman et al., 2009; Gray et al., 2010), Casp6 cleaves a number of cytosolic neuronal cytoskeleton or cytoskeleton-associated proteins, including Tau and α -tubulin (Klaiman et al., 2008). Casp6 is implicated in axonal degeneration of developing and injured neurons (Sokolowski et al., 2014), nerve growth factor deprived mouse sensory neurons (Nikolaev et al., 2009; Simon et al., 2012; Uribe et al., 2012; Cusack et al., 2013), and primary human CNS neurons transfected to over-express AD-associated mutant amyloid precursor proteins (Sivananthan et al., 2010a). Because of our expertise with in vitro and cellular Casp6 activity analyses, we initially studied the effect of phenothiazines on Casp6 activity, and further extended the research to Casp1 and Casp3.

Similar to other caspases, Casp6 is translated as a zymogen, comprised of a short prodomain, a p20 subunit containing the catalytic cysteine (Cys163), a linker region, and a p10 subunit (Fernandes-Alnemri et al., 1995a). The zymogen is cleaved at three distinct sites to remove the prodomain and linker regions in order to obtain an active enzyme. Interestingly, Casp6 can self-activate by intramolecular cleavage of its C-terminal linker-processing site (Wang et al., 2010b). Once activated, Casp6 forms a covalent tetrahedral intermediate where the de-protonated sulfur of the catalytic Casp6 Cys163 launches a nucleophilic attack on the

scissile carbonyl of the substrate to generate an acyl enzyme intermediate (Fuentes-Prior and Salvesen, 2004). Therefore, the catalytic cysteine must be in a reduced state to efficiently cleave protein substrates.

Since methylene blue inhibits the activity of Tau protein through its pro-oxidant activity on cysteines, here, we tested if it can also inhibit the cysteinyl caspase proteases. Our results showed that methylene blue and its derivatives efficiently inhibited active caspases in vitro, in cells, and in vivo at concentrations allowing phenothiazine-mediated Tau disaggregation. These results indicate that methylene blue or its derivatives could (1) have an additional effect in AD by inhibiting caspases, (2) be used as a drug to prevent caspase activation in other degenerative conditions, and (3) predispose chronically treated individuals to cancer via the inhibition of effector Casp3.

2.4 Results

2.4.1 Methylene blue and its derivatives inhibit the activity of caspases in vitro

To assess if methylene blue (**Fig. 2.1a**) can inhibit Casp6 activity through oxidation, the amount of dithiothreitol (DTT) required for measurable RCasp6, RCasp1, and RCasp3 activity was titrated on their preferred peptide substrate in an in vitro assay. Caspase activities were sufficiently retained with 10 μM DTT (**Fig. 2.1b**). Under these conditions, methylene blue and its mono- and di-demethylated derivatives, azure B and azure A (**Fig. 2.1a**), inhibited Casp6 activity in a dose dependent manner (**Fig. 2.1c**). Reduction in Casp6 activity was observed with only 100 pM methylene blue and azure B while 10 nM azure A was necessary for a significant inhibition. Because phenothiazines above the concentration of 100 μM exert a quenching effect on the caspase fluorogenic assays (**Fig. S2.1**), the IC_{50} was calculated with an in vitro tubulin cleavage assay. The tubulin cleaved by Casp6 (TubΔCasp6) was detected with a neoepitope antiserum whereas full length uncleaved tubulin (upper tubulin band) and TubΔCasp6 (lower protein band) were detected with a full-length tubulin antibody by western blot analyses (**Fig. 2.1d**). The results show that methylene blue, azure A and azure B inhibit cleavage of tubulin by RCasp6 in a dose dependent manner (**Fig. 2.1d**). Quantitation of the TubΔCasp6

relative to total tubulin yielded an IC_{50} of 10.6 μM ($r^2 = 0.87$), 0.5 μM ($r^2 = 0.89$), and 34.4 μM ($r^2 = 0.90$) with methylene blue, azure A, and azure B, respectively (**Fig. 2.1e**). Methylene blue exhibited an IC_{50} of 14.2 μM on RCasp3-cleaved tubulin (**Fig. 2.1f**), confirming the dose dependent inhibition of RCasp6, RCasp3, and RCasp1 observed in the fluorogenic assay (**Fig. 2.1g**).

2.4.2 Competitive mode of inhibition for phenothiazines on Caspase-6

To determine the mechanism of methylene blue-mediated Casp6 inhibition, inhibitor kinetic studies were conducted with non-interfering concentrations of phenothiazine in the fluorogenic assay. Increasing concentrations of methylene blue (**Fig. 2.2a**), azure A (**Fig. 2.2b**) and azure B (**Fig. 2.2c**), resulted in increasing K_m values whereas the V_{max} values remained the same. A reciprocal (Lineweaver Burk) plot (inset) shows that the data intersect the y axis at the same point, indicating a competitive mode of inhibition. Fitting the data to the competitive inhibition model, and using nonlinear regression analysis, we determined the K_i values to be 50.5 μM ± 2.3 μM for methylene blue, 0.42 μM ± 0.02 for azure A, and 7.89 μM ± 0.2 μM for azure B, respectively. These results suggest that methylene blue, azure A, and azure B prevent binding of substrate in a competitive manner.

2.4.3 Methylene blue and its derivatives inhibit the activity of caspases in cell lines and primary cultures of human neurons

HCT116 and human primary neurons were first observed by phase contrast microscopy after treatment with increasing concentrations of methylene blue and its derivatives (**Fig. 2.3a,b**). At 100 μM methylene blue, 50 μM azure A, and 100 μM azure B, HCT116 cells retained a morphology and confluence comparable to PBS-treated controls (**Fig. 2.3a**). Toxicity of high concentrations of phenothiazines was observed microscopically as rounded cell morphology, cell loss, and increased cellular debris in HCT116 cultures (**Fig. 2.3a**). Moreover, in human primary neurons, concentrations above 100 μM of methylene blue, 50 μM azure A, and 10 μM azure B increased cell body size and axonal fragmentation (**Fig. 2.3b**). The toxicity of phenothiazines was verified in MTT assays (**Fig. 2.3c,d**). Methylene blue treatment of HCT116 cells at concentrations of up to 1 mM had similar absorbance in the MTT assay as the

PBS-treated cells, thereby indicating healthy mitochondrial function. However, 10 mM methylene blue decreased MTT absorbance to almost nothing, indicating toxicity. Azure A showed toxicity above 50 μM, while azure B was well tolerated up to 100 μM concentrations. Similar results were obtained on human primary neurons although the phenothiazines were more toxic on these cells than on HCT116 cells. The MTT signal represents reduced cell viability and not modulation of the oxidation-reduction state of MTT by phenothiazines because non-toxic concentrations of phenothiazines on HCT116 cells were observed to be toxic to human primary neurons in the MTT assay. Furthermore, the MTT results were consistent with the toxicity observed by microscopy.

To test the ability of phenothiazines to inhibit Casp6 in live cells, HCT116 cells, transfected with a self-activating form of Casp6 (Casp6p20p10) to induce high levels of Casp6 activity (Klaiman et al., 2009) were treated for 2 hrs with 100 μM and 1 mM methylene blue, 50 μM azure A, and 10 μM and 100 μM azure B, concentrations determined to be non-toxic on non-transfected HCT116 cells. Methylene blue and azure B significantly inhibited Casp6 activity on the Ac-VEID-AFC peptide substrate (**Fig. 2.4a**). At 50 μM, azure A also showed a trend towards inhibition but it did not reach statistical significance. Western blot analyses revealed that while the levels of the cellular active p20 subunit of Casp6 were maintained, the tubulin cleaved by Casp6 (TubΔCasp6) was significantly decreased in the cells treated with phenothiazines, thus clearly indicating functional inhibition of the cellular Casp6 activity (**Fig. 2.4b,c**).

To determine if these phenothiazines might inhibit caspases in the chief cell type affected in AD brains, human primary CNS neuron cultures were serum-deprived, a condition known to activate endogenously expressed Casp6 (LeBlanc et al., 1999), and treated with phenothiazines. Higher concentrations of methylene blue and derivatives were more toxic to serum-treated human neuron cultures (**Fig. 2.3d**) than to the cell line so the lower concentrations were assessed. As previously observed, serum deprivation induced a 2-3 fold increase in Casp6 activity (**Fig. 2.4d**). Treatment of serum-deprived neurons for 2 hrs with 100 μM methylene blue, 50 μM azure A, or 10 μM azure B, significantly inhibited VEIDase activity in vitro (**Fig. 2.4d**), and TubΔCasp6 in cells (**Fig. 2.4e**). Quantitation of 3 independent experiments indicated an increase in TubΔCasp6/Tub in serum deprivation, but it did not reach statistical

significance because of variability in human neurons (**Fig. 2.4f**). Nevertheless, methylene blue returned the levels to the basal levels observed in serum-treated neurons and azure A and azure B significantly decreased the levels compared to PBS-treated serum-deprived neurons. The levels of the active p20 Casp6 subunit remained the same with or without phenothiazine treatments, consistent with inhibition of the enzyme rather than increased turnover of active Casp6 (**Fig. 2.4g**). There is a slight discrepancy in the inhibition measured by VEIDase activity and that reported by the TubΔCasp6/Tub level in the human neurons. The levels of TubΔCasp6 are much lower in azure A and azure B-treated neurons compared to the methylene blue. This is likely due either an effect on the turnover of TubΔCasp6, on the ability of the TubΔCasp6 to bind to the caspase or to oxidative effects on the Tubulin. Nevertheless, together, these results demonstrate that phenothiazines can inhibit caspase activity in live cells, and importantly in human neurons.

2.4.4 Methylene Blue and its derivatives inhibit the activity of Casp3 in vivo

To determine if methylene blue has the ability to inhibit caspases in vivo, wild type male C57BL6/J mice were given 3 mg/kg of methylene blue by gavage and injected with lipopolysaccharides (LPS)/galactosamine (GALN), a well-known model to assess drugs against liver Casp3 activity (Amir et al., 2013). As expected, while control- and methylene blue-treated mouse livers did not show significant Casp3 DEVDase activity, control mice injected with LPS/GALN showed strong liver Casp3 DEVDase activity (**Fig. 2.5a**). Mouse liver protein extracts from mice pre-treated with methylene blue and injected with LPS/GALN showed significantly less Casp3 activity (**Fig. 2.5a**).

Caspase substrates can be cleaved by the caspases-like activity of the proteasome. Therefore, we tested Ac-nLPnLD-AMC as a specific substrate for the caspase-like activity of the proteasome (Kisselev et al., 2003). RCasp3 was unable to cleave Ac-nLPnLD-AMC, whereas human neuronal extracts did possess the expected nLPnLDase proteasomal activity (**Fig. S2.2**). Treatment with LPS/GALN had no effect on nLPnLDase activity in mouse liver protein extracts in the presence or absence of the irreversible proteasome inhibitor epoxomicin (**Fig. 2.5b**), nor was Casp3 DEVDase activity affected by epoxomicin (**Fig. S2.2**). In addition, the reversible proteasome inhibitor, bortezomib, did not inhibit RCasp3 activity in vitro

(**Fig. 2.5c**) nor did it prevent DEVDase activity in LPS/GALN-treated mouse liver protein extracts (**Fig. 2.5d**). However, nLPnLDase proteasomal activity was significantly inhibited by bortezomib (**Fig. S2.2**). Furthermore, the pan-caspase inhibitor Q-VD-OPh abrogated RCasp3 activity (**Fig. 2.5c**) and DEVDase activity in mouse liver protein extracts (**Fig. 2.5d**). Therefore, the DEVDase activity observed in the mice livers after LPS/GALN challenge is not due to the proteasome activity but to caspase activity. These results strongly support methylene blue inhibition of Casp3 *in vivo*.

The possibility that the lower Casp3 activity was the result of less Casp3 enzyme in the methylene blue-treated LPS/GALN mice livers was excluded since both the proCasp3 enzyme and its active p17/p19 subunits were elevated in the methylene blue/LPS/GALN treated mice compared to the other three treatments (**Fig. 2.5e**). Higher levels of enzyme may indicate that methylene blue delays turnover of the proCasp3 and its active subunits despite reducing the activity. Casp3 can also cleave β-actin (Yang et al., 1998), therefore levels of cleaved β-actin were used to assess the functional inhibition of Casp3 *in vivo*. Consistent with the lower levels of caspase DEVDase activity, the levels of cleaved β-actin relative to total β-actin were significantly lower in methylene blue/LPS/GALN-treated mouse liver protein extracts compared to LPS/GALN treatment alone (**Fig. 2.5f,g**). These results show that methylene blue can inhibit active caspases in vivo.

2.4.5 Methylene blue inhibits Casp6 by oxidation of catalytic cysteine Cys163

Mass spectrometric analyses of Casp6 showed the catalytic Cys163 of Casp6 to be oxidized into sulfenic acid (R-SOH) by both methylene blue and azure B (**Fig. 2.6a,b**). LC/MS/MS analyses did not reveal any peptide containing oxidized Cys163 in untreated recombinant Casp6, but 15% and 7.7% of sequenced peptides contained oxidized Cys163 in recombinant Casp6 treated with methylene blue and azure B, respectively (**Fig. 2.6a**). The levels of oxidation are consistent with the reversibility of sulfenation (Lo Conte and Carroll, 2013). The sulfenation of Cys163 by methylene blue and azure B thus prevents the sulfur from attacking the scissile carbonyl of the peptide substrate, thereby rendering the caspase inactive (**Fig. 2.6c**).

2.5 Discussion

Our study provides the identification of a post-translational regulatory modification of the caspase catalytic cysteine and adds a new group of cysteinyl enzymes that are regulated by sulfenation. Oxidation-dependent inhibition of caspases, mainly Casp3, has been demonstrated previously, but the chemical modification was not identified (Mohr et al., 1997; Nobel et al., 1997; Kohler et al., 2009). Our results add caspases to the list of 47 other proteins, including five other cysteinyl proteases, regulated post-translationally by sulfenation (Lo Conte and Carroll, 2013). Sulfenation could transiently or locally regulate caspase activity, since all caspases are cysteinyl proteases. While cellular Casp3 is under strong regulation by the inhibitor of apoptosis proteins (Deveraux et al., 1997), Casp1 and Casp6 do not have known cellular protein inhibitors, although Casp6 can be inhibited in an allosteric fashion by phosphorylation and zinc (Velazquez-Delgado and Hardy, 2012a, b).

The inhibition of Casp1, Casp3, and Casp6 could have a major influence on inflammation, apoptosis and neurodegeneration, respectively. Casp1 is the main producer of interleukin-1-beta, which can mediate several neuroinflammatory processes (Walsh et al., 2014), and is elevated early in AD brains (Griffin et al., 1989; Griffin et al., 1995). Casp3 is an executioner caspase essential to apoptotic cell death and is also involved in neuronal function (D'Amelio et al., 2010). Casp6 is associated with axonal degeneration (Nikolaev et al., 2009; Sivananthan et al., 2010a). Oxidative stress increases in most cells of the body with aging and thus the oxidation of caspase catalytic cysteines could depress caspase-mediated functions in vivo. Similarly, inhibition of Casp1 and Casp6 by methylene blue could have beneficial effects by reducing inflammatory processes and axonal degeneration, but inhibition of Casp3 could alter neuronal function or promote cancer cell survival and be detrimental to tissue homeostasis. It is therefore important to monitor patients who are chronically treated with phenothiazines for deregulated inflammatory responses and cancers, especially in individuals at risk for these conditions.

Beneficial effects observed in AD clinical trials will have to consider the possibility that phenothiazines may benefit cognitive decline in AD not only by disaggregating Tau but by inhibiting Casp6-mediated axonal degeneration. The IC_{50} against Tau aggregation ranges from

2 μM (Wischik et al., 1996) to 31 μM (Schirmer et al., 2011) for both methylene blue and azure B. The IC_{50} of methylene blue and azure B against Casp6 cleavage of tubulin are 10.6 μM and 34.4 μM, respectively, whereas azure A is 0.5 μM. Therefore, the abundant levels of active Casp6 observed in AD brains (LeBlanc, 2013) may be inactivated by phenothiazines used at clinical concentrations to promote Tau disaggregation.

Compared to other caspase inhibitors, which have IC_{50} in the nM or pM range, phenothiazines are weak inhibitors (Callus and Vaux, 2007), phenothiazines are weak inhibitors. However, the fact that phenothiazines are non-toxic at high concentrations in humans and can reach mean plasma levels of 5 μM, traverse the blood brain barrier, and are over 70% bioavailable after an oral ingestion (Oz et al., 2011) indicate that concentrations capable of inhibiting caspases could be reached in the brain.

Methylene blue and its derivatives have other pleiotropic effects that could benefit AD (reviewed by (Schirmer et al., 2011)). Phenothiazines inhibit acetyl-cholinesterase and butyrylcholinesterase, thereby possibly increasing levels of acetylcholine (Sezgin et al., 2013; Tacal et al., 2013; Petzer et al., 2014). Interestingly, reversible acetylcholinesterase inhibitors are the main drugs used against AD presently. Methylene blue also inhibits monoamine oxidase thereby increasing the levels of 5-hydroxytryptamine involved in several nervous system functions including mood and cognition (Petzer et al., 2012). Methylene blue enhances mitochondrial function (Atamna and Kumar, 2010), which is impaired in AD brains, and reduces levels of amyloid beta peptide in transgenic mice models (Medina et al., 2011). The inhibitory function of methylene blue against Casp6 activity may also benefit Huntington disease (Graham et al., 2006), axonal degeneration of the nervous system (Nikolaev et al., 2009; Sivananthan et al., 2010a; Simon et al., 2012; Uribe et al., 2012; Cusack et al., 2013; Sokolowski et al., 2014), or other conditions where Casp6 activity mediates pathogenesis. Thus, it will be important to dissect out the exact mechanism of methylene blue in vivo to fully understand how phenothiazines benefit age-dependent cognitive deficits and AD. Autopsied brains from AD individuals treated with phenothiazines will be invaluable to assess the effect of methylene blue on neurofibrillary tangles and Casp6 activity and obtain more selective therapies against AD.

These results imply that methylene blue or its derivatives could (1) have an additional positive effect against AD by inhibiting caspases, (2) be used as a drug to prevent caspase

activation in other degenerative conditions, and (3) predispose chronically treated individuals to cancer via the inhibition of caspases. In conclusion, this study identifies an important mechanism of action of methylene blue against activity of caspases that could impact tissue homeostasis in pathological and age-dependent conditions.

2.6 Materials and methods

DNA constructs: The pET23b (+) recombinant human Casp6-His*tag containing the pro-domain was a kind gift from Dr Guy Salvesen (Sandford-Burnham Medical Research Institute, CA) and the mammalian construct encoding human Casp6p20p10 in pCep4β vector was previously cloned in our laboratory (Klaiman et al., 2009).

Protein expression and purification: pET23b (+) recombinant pro-Casp6-His*tag was transformed in *E. Coli* BL21 (DE3)pLysS (Stratagene, La Jolla, CA, USA) and purified as described (Denault and Salvesen, 2002). Briefly, cells were grown to OD_{600} = 0.6 at 37°C. Protein expression was induced with 40 μM isopropyl-beta-D-thiogalactopyranoside (IPTG: BioShop Canada Inc, Burlington, Ontario, CA) at 20°C for 21 h. The bacteria were harvested by centrifugation, resuspended in Buffer 1 (50 mM Tris-HCl pH 8.0, 100 mM NaCl), and stored at -80 °C. Cell pellets were thawed and lysed by sonication on ice with a Branson S-450A sonifier (Branson Ultrasonic Corporation, Danbury, CT, USA) for 2 min at 50% duty cycle. The lysate was centrifuged at 18000 x g for 30 min at 4 °C, filtered through a 45 μm filter, loaded on nickel Sepharose 6 Fast-flow resin (GE Healthcare, Uppsala, Sweden), and washed extensively with Buffer 1 supplemented to 500 mM NaCl. Bound proteins were eluted with a 0-200 mM imidazole (BioShop Canada Inc, Burlington, Ontario, CA) linear gradient in Buffer 1. The fractions were evaluated for recombinant protein purity by Coomassie blue staining. Pure fractions were pooled together, buffer was exchanged in Buffer1 to remove imidazole and the proteins were concentrated on a 3000 Da molecular cut off Amicon Ultra centrifugal filter (Millipore Corporation, Billerica, MA, USA). Protein concentration was determined by the Bradford protein assay (BioRad, Mississauga, ON, CA). Active Casp6 and Casp3 represented > 99% of the purified enzyme, as verified by titration against their respective inhibitors (Denault and Salvesen, 2002) (**Fig**. **S2.2**). RCasp1 (0.15 units) (specific activity = 5000 U/mg) was added per 50 μL reaction yielding a 20 nM concentration.

Caspase activity assays: Casp6 activity was assessed by *in vitro* fluorogenic assays with the Ac-Val-Glu-Ile-Asp-7-Amino-4-trifluoromethyl-couramin substrate (Ac-VEID-AFC: Enzo LifeSciences, NY, USA) in Stennicke's buffer [SB: 20 mM piperazine-N, N-bis (2-ethanesulfonic acid (BioShop Canada Inc, Burlington, Ontario, CA) pH 7.2, 30 mM NaCl, 10 mM EDTA, 0.1% CHAPS, 10% sucrose] (Stennicke and Salvesen, 1997). Briefly, the reaction mix consisted of 20 nM RCasp6 or 20-30 μg cellular protein extracts, 1 X SB, 10 μM DTT, 10 μM Ac-VEID-AFC substrate and deionized water. Methylene Blue (Sigma-Aldrich, St. Louis, MO, USA), azure A (MP Biomedicals, Solon, OH, USA), and azure B (MP Biomedicals, Solon, OH, USA) were added in increasing concentrations (0-100 μM) to the reaction mix and the activity was measured in a black clear bottom 96-well plate (Costar, Corning, NY, USA) at 37 °C in the Synergy H4 plate reader (BioTek) every two minutes for 100 minutes. An AFC (Sigma-Aldrich, St. Louis, MO, USA) standard curve was used for data conversion to pmol AFC released and the assay was gain adjusted to 12.5 μM AFC (ex: 380 nm, em: 505 nm). Activity assays for RCasp1 (Biovision, Millpitas, CA, USA) and RCasp3 (Enzo LifeSciences, NY, USA) were done similarly to RCasp6, except the substrate used were Z-Tyr-Val-Ala-Asp-7-Amino-4-trifluoromethylcoumarin (z-YVAD-AFC: Enzo LifeSciences, NY, USA), and Ac-Asp-Glu-Val-Asp-7-Amino-4-trifluoromethylcouramin (Ac-DEVD-AFC: Enzo LifeSciences, NY, USA), respectively. To confirm that these substrates report caspase activity and not proteasomal caspase-like enzyme activity, 1 μM pan-caspase inhibitor, Q-VD-OPh (Sigma-Aldrich, St. Louis, MO, USA) or 0.1 μM proteasome inhibitor, bortezomib (Calbiochem, MA, USA) were tested on 20 nM RCasp3 or 40-60 μg of mouse liver protein extracts.

IC_{50} determination using an in vitro tubulin cleavage assay: The IC_{50} for methylene blue, azure A, and azure B was determined by performing an *in vitro* tubulin cleavage assay because concentrations of phenothiazines above 100 μM interfered with both fluorescence (**Fig. S2.1**) and luminescence (data not shown) enzyme assays. Phenothiazines, ranging from 10 nM to 1 mM, were mixed with 20 nM RCasp6 or RCasp3, 10 μM DTT, and 7.5 nM BSA in SB and 36 μg HCT116 protein extracts added before incubation at 37°C for 10 hours, western blot analysis, and densitometry for tubulin-cleaved by Casp6 (TubΔCasp6) and total tubulin as described in the western blot section. Data represent the mean and SD of 3 independent experiments. The

IC_{50} was determined by a non-linear regression fit for log inhibitor vs caspase activity with a Hill slope of -1 using GraphPad Prism 5.0.

Lineweaver-Burk Plot: To analyze the mode of methylene blue and azure B inhibition on RCasp6, 10 μM and 25 μM methylene blue, and 1 μM and 5 μM azure B were added to 10 nM RCasp6 and enzyme activity was measured on nine different Ac-VEID-AFC concentrations (2.5 μM to 200 μM) as described in the caspase activity assay section. To estimate K_i values for the inhibition of RCasp6 by methylene blue and azure B, the apparent K_m and V_{max} values for the Ac-VEID-AFC substrate in the presence and absence of methylene blue and azure B were determined via non-linear regression analysis of the corresponding Michaelis-Menten graphs (v vs. [S]). The K_i values and type of inhibition of RCasp6 by methylene blue and azure B was subsequently estimated from the x-axis (K_m values) and y-axis (V_{max}) intercepts of plots of these versus inhibitor concentrations. Linear and non-linear regression analyses were performed using the Prism version 5.0 software package.

Cell culture treatments with methylene blue and derivatives: Human colon carcinoma (HCT116) cells (ATCC: Manassas, VA, USA), were cultured in McCoy's 5A modified media (Invitrogen, Burlington, VT, USA) supplemented with 10% fetal bovine serum (ThermoSci, Mississauga, ON, CA), transfected with 1 μg of pCep4βCasp6p20p10 and 8 μg of polyethyleneimine (Polysciences Inc., Warrington, PA, USA), and grown 24 hrs before treatment with phosphate buffered saline (PBS), 100 μM to 10 mM methylene blue, 50 μM to 5 mM azure A or 10 μM to 1 mM azure B for 2 hours. Human primary neurons were cultured from fetal brain cortical areas obtained under ethical guidelines and approved by the McGill University's institutional review board as previously described (LeBlanc, 1995). Human primary neurons plated in poly-L-lysine -coated 6-well plates at a density of $3x10^6$ cells/mL were serum-deprived for 2 hours in the presence of 100 μM methylene blue, 50 μM azure A, 100 μM azure B, or an equivalent volume of PBS. Proteins were harvested in cell lysis buffer (CLB; 50mM HEPES, 0.1% CHAPS, 0.1mM EDTA). Protein concentration was determined with Bradford reagent (BioRad, Mississauga, ON, CA)

Cell viability assays*: *Microscopic analysis: HCT116 cells were plated at a density of $1x10^5$ cells/well in an uncoated 6-well plate, and human neurons were plated at a density of $6x10^6$ cells/well in a 6-well plate coated with poly-L-lysine. Cells were treated with PBS, 100 μM, 1

mM, or 10 mM methylene blue, 50 μM, 500 μM, or 5 mM azure A, or 10 μM, 100 μM, or 1 mM azure B for 2 hours at 37ºC in 5% CO2. The media was removed and replaced with fresh media before acquiring images with the Nikon Eclipse Ti microscope and the NIS-Elements (Version 3.10) software. ***MTT assays***: HCT116 cells and human primary neurons were plated in 96-well plates at a density of $1x10^4$ and $1x10^5$ cells per well, respectively. After 24 hours, the cells and neurons were treated with methylene blue, azure A, azure B, or equal volume of PBS in fresh media. After 2 hours, fresh media containing 0.5μg/ml MTT (3-(4,5-dimethylthiazol-2-yl)-2,5-diphenyltetrazolium bromide) (Sigma-Aldrich, St. Louis, MO, USA) was added and the cells were incubated for 4 hours at 37ºC in 5% CO_2. The media was removed, formazan crystals were dissolved in DMSO, and the absorbance was measured at 560 nm and 670 nm using the Synergy H4 plate reader from BioTek (Winooski, VT, USA).

Proteasome assay: The caspase-like activity of the proteasome was measured using 10 μM Ac-Nle-Pro-Nle-Asp-AMC (Ac-nLPnLD-AMC, Enzo LifeSciences, NY, USA) as described for caspase activity assays except for the use of 10 mM DTT and a 7-amino-4-methylcoumarin (AMC, Sigma-Aldrich, St. Louis, MO, USA) standard curves. To confirm mouse liver protein extracts contained Casp3 activity, 0.1 μM of the proteasome inhibitors epoxomicin (Enzo LifeSciences, NY, USA) or bortezomib or 1 μM of the pan-caspase inhibitor Q-VD-OPh, or equal volumes of DMSO was incubated with the extracts for 20 mins on ice before analysis.

Western blot analyses: The 10630 (1:10,000) and GN60622 (1:10,000) neoepitope antibodies against the p20 subunit of active Casp6 (Guo et al., 2004) and TubΔCasp6 (Klaiman et al., 2008), respectively, were generated in our laboratory. The β-actin clone AC-15 (1:5000, Sigma-Aldrich, Oakville, ON, CA), Casp6 p10 clone B93-4 (1:250, BD Canada, Mississauga, ON, CA), Casp3, and full-length α-tubulin (1:1000, Cell Signaling Technology Inc., Danvers, MA, USA) antibodies were diluted in 5% non-fat dry milk in Tris-buffered saline containing 0.1 % Tween-20 (Sigma-Aldrich, ON, CA). Secondary anti-mouse (1:5000, GE Healthcare Life Sciences, Baie D'Urfe, QC, CA) and anti-rabbit antibodies (1:5000, Dako, Burlington, ON, CA) conjugated to horseradish peroxidase (HRP) were used to detect immunoreactive proteins using ECL prime western blotting detection reagent (GE Healthcare Life Sciences, Baie D'Urfe, QC, CA) and Kodak BioMax MR film (Kodak, Rochester, NY, USA). Secondary anti-mouse conjugated to alkaline phosphatase (AP, Jackson Immunoresearch Laboratories Inc., West

Grove, PA) was developed with nitro-blue tetrazolium (ThermoSci, Mississauga, ON, CA) and 5-bromo-4-chloro-3'-indolyphosphate (ThermoSci, Mississauga, ON, CA). The western blots were scanned with an HP scanner and densitometry was performed using ImageJ software (NIH, Bethesda, MD) by rendering tiff images into an 8 bit format and measuring the intensity values above background. Images were not modified except to adjust the contrast for the entire blot.

LPS/galactosamine treatment of C57BL6/J mice*:* All animal procedures followed the Canadian Council on Animal Care guidelines and were approved by the McGill Animal care committees. Male C57BL6/J mice (10-12 weeks old) were purchased from Jackson Laboratories (Bar Harbor, ME, USA). Mice were gavaged with 3 mg/kg dose of methylene blue or vehicle (0.5% methylcellulose (Sigma)) for 3 consecutive days. On the 3rd day, following the gavage, a mixture of 100 mg/kg of LPS (Sigma) and 700 mg/kg of D-(+)-galactosamine (GALN) (Sigma) or PBS was injected i.p. as described (Amir et al., 2013). The mice were sacrificed using isofluorane/CO_2 5.5 hours after the i.p. injection. Small sections of the left lobe of the liver were harvested and frozen rapidly. Frozen liver samples between 50-150 mg were homogenized on ice in a ground glass homogenizer with 10x the volume of CLB supplemented with fresh protease inhibitors (38 μg/mL AEBSF (4-(2-Aminoethyl)benzenesulfonyl fluoride hydrochloride), 0.5 μg/mL leupeptin, 0.1 μg/mL TLCK (Tosyl-L-lysyl-choromethane hydrochloride), 0.1 μg/mL pepstatin; Sigma). The homogenates were centrifuged at 1000 x g at 4ºC and the supernatant analysed for caspase activity in a blind fashion.

Electrospray ionization mass spectroscopy**:** RCasp6 (1 mg/ml) in 50 mM Tris, pH 8.0, 100 mM NaCl, 1 mM DTT was incubated for 15 min at 37ºC, divided equally in three tubes, and 2 mM methylene blue, 2 mM azure B or buffer were added to each tube and incubated for 45 min at 37 ºC. The samples were snap-frozen immediately in dry ice and ethanol, and stored at -80 ºC until analysis at the IRIC Mass Spectrometry core facility by Eric Bonneil (U. de Montreal, Montreal, Quebec, Canada). Briefly, 10 μg RCasp6 was digested with 1 μg of trypsin for 8 h at 37°C. Samples were desalted with Ziptips and loaded on a homemade C18 pre-column (0.3 mm i.d. x 5 mm) connected directly to the switching valve and separated on a homemade reversed-phase column (150 μm i.d. x 150 mm) with a 56-min gradient from 10–60% acetonitrile (0.2% FA) and a 600 nl/min flow rate on a NanoLC-2D system (Eksigent) connected to an LTQ-Orbitrap Elite (Thermo Fisher Scientific). Each full MS spectrum acquired with a 60,000

resolution was followed by 12 MS/MS spectra, where the 12 most abundant multiply charged ions were selected for MS/MS sequencing. Tandem MS experiments were performed using collision-induced dissociation in the linear ion trap. Peaks were identified using Mascot version 2.4 (Matrix science) and peptide sequence were blasted against the Human Uniprot database (301,754 sequences). Tolerance was set at 15 ppm for precursor and 0.5 Da for fragment ions during data processing. For the post-translational modification of proteins, occurrence of cysteine oxidations was considered.

Statistical Analyses: The number of independent experiments and statistical analyses conducted with one-way ANOVA and post hoc Bonferroni or Dunnett's tests were indicated in the figure legends.

2.7 Acknowledgements

We thank Eric Bonneil at the IRIC for his services with mass spectrometry and Véronique Michaud for her technical help with the in vivo study. This work was supported by the Canadian Foundation of Innovation, Canadian Institutes of Health Research (CIHR) MOP-243413-BCA-CGAG-45097, and the JGH Foundation. Dr Vikas Kaushal was a recipient of McGill's CIHR Neuroinflammation Training Program award (2010-2012); Prateep Pakavathkumar is the recipient of a Fonds de recherche Québec Santé M.Sc. scholarship (2011-2013) and a Fonds de recherche Québec-Santé/Alzheimer Society of Canada doctoral award (2014-2017).

2.8 Figures and legends

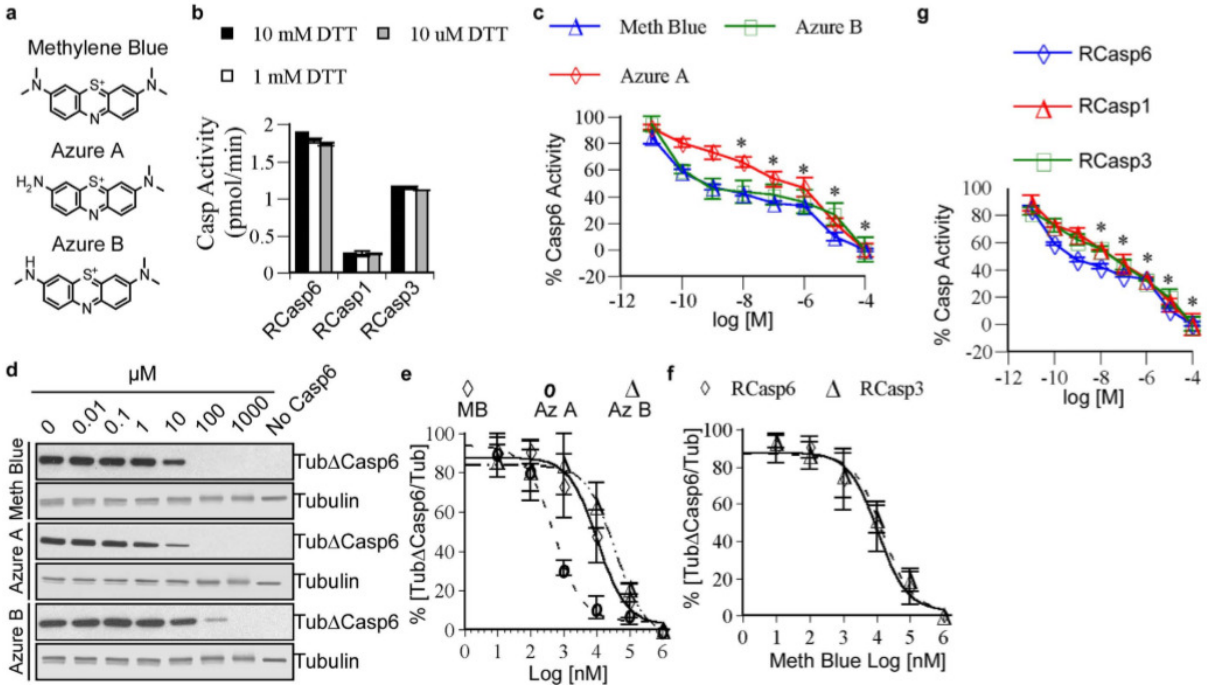

Figure 2.1 Inhibition of caspases in vitro by phenothiazines.

a Chemical structures of methylene blue, azure A and azure B. **b** Activity of RCasp6, RCasp3, and RCasp1 with different dithiothreitol (DTT) concentrations. Data represent mean and SD of 3 independent experiments. **c** Dose-dependent inhibition of Casp6 in presence of methylene blue, azure A, and azure B. Each data point represents the mean and SD of 3 independent experiments. Statistical difference between no phenothiazines and addition of phenothiazines was determined by one-way ANOVA $p < 0.0001$ and post-hoc Bonferroni $^*p < 0.001$. **d** Western blot analysis of the in vitro tubulin cleavage assay showing dose-dependent inhibition of Casp6 activity in the presence of methylene blue, azure A, and azure B. **e** Non-linear regression curve for dose-dependent inhibition of RCasp6 cleavage of tubulin in the presence of methylene blue and its derivatives. **f** Dose-dependent inhibition of RCasp6 and RCasp3 with methylene blue. For e and f, Data represent mean and SD of 3 independent experiments. **g** Dose-dependent inhibition of RCasp6, RCasp3, and RCasp1 with methylene blue. Data represent the mean and SD of 3 independent experiments. Statistical analyses conducted as in c.

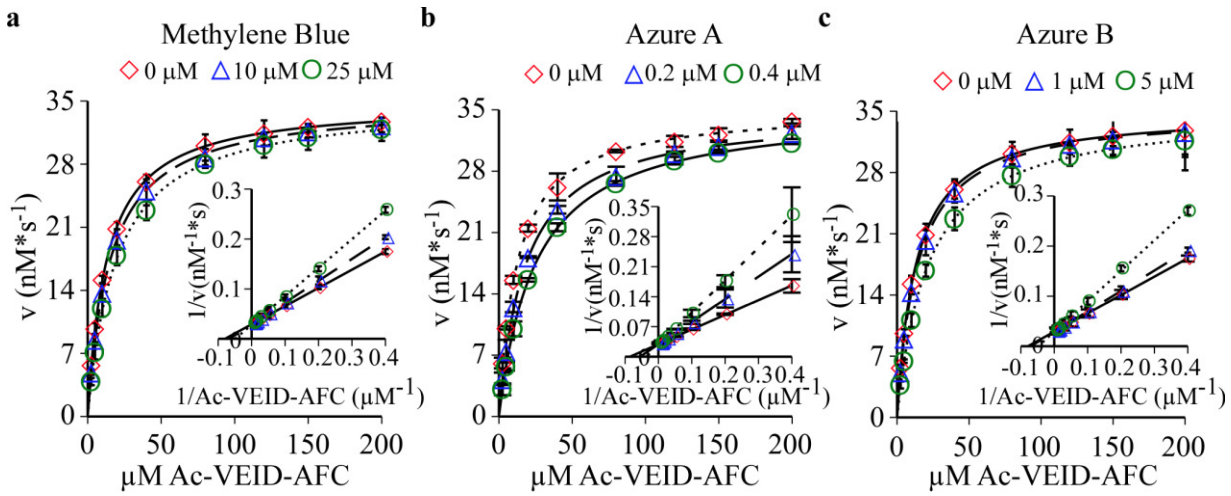

Figure 2.2 Michaelis-Menten kinetic analyses of phenothiazines on RCasp6.

Initial enzyme velocity of Casp6 plotted against indicated concentrations of Ac-VEID-AFC substrate in presence of 0, 10 μM, and 25 μM methylene blue (a), 0, 0.2 μM, and 0.4 μM azure A (b), or 0, 1 μM, and 5 μM azure B (c). The inset represents the Lineweaver-Burk plot for methylene blue (a), azure A (b), and azure B (c) with Ac-VEIDAFC substrate showing competitive mode of inhibition. Data represent the mean ± S.D. of three independent experiments.

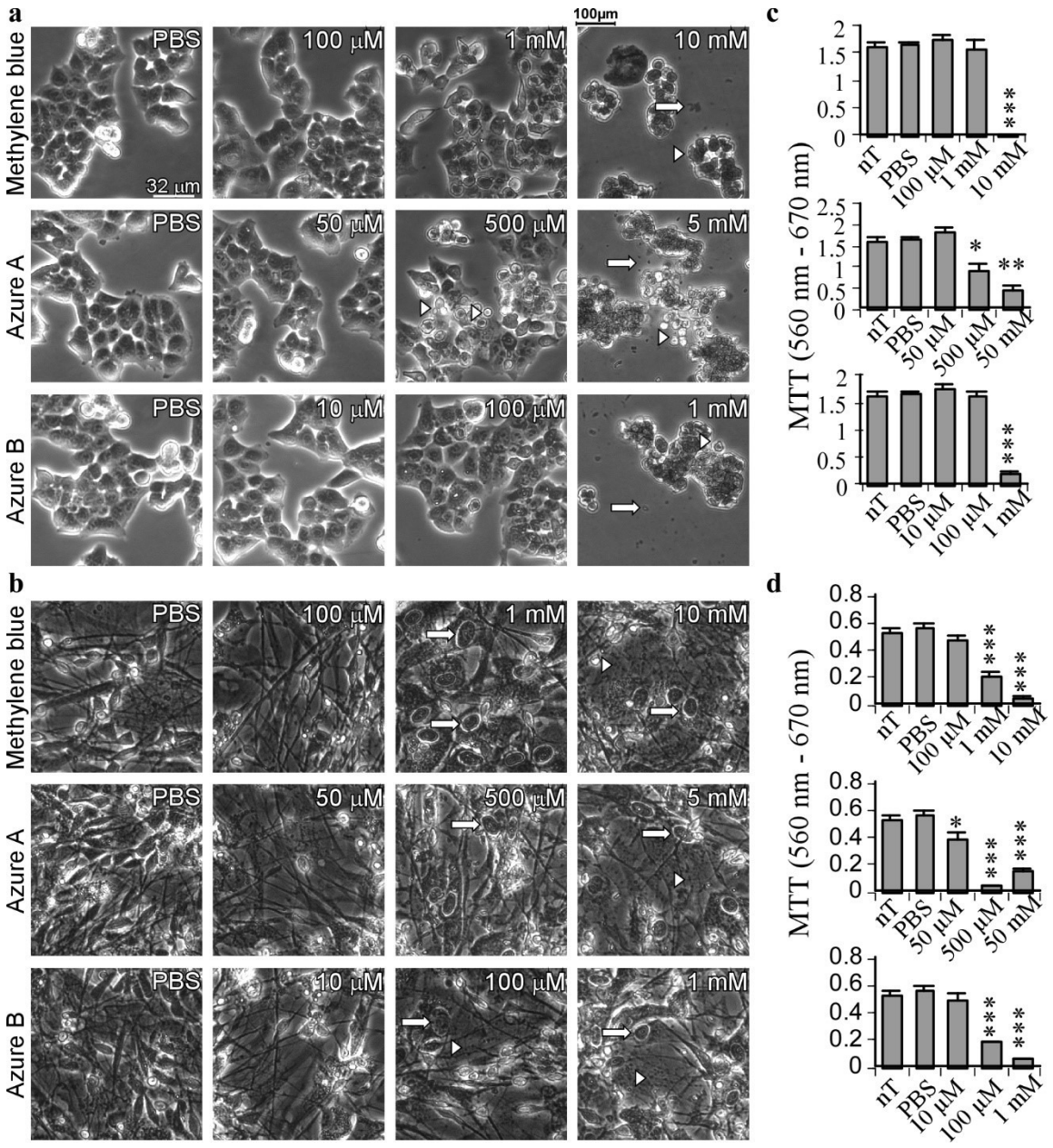

Figure 2.3 Toxicity of methylene blue, azure A, and azure B in HCT116 cells and human primary neurons.

a & b Phase contrast images of (a) HCT116 cells and (b) human primary CNS neurons treated with an increasing concentration of methylene blue, azure A, or azure B for 2 hours. Round cells (white arrowheads) and cellular debris (white arrows) are indicated in (a), while fragmented axons (white arrowheads) and swollen cell bodies (white arrows) are shown for (b). **c & d** The mitochondrial reductive potential of HCT116 cells and human primary neurons was measured

by MTT assay in the presence or absence of methylene blue, azure A or azure B. HCT116 cells (c) or human primary neurons (d) were either nontreated (nT), treated with PBS, treated with 100 μ M to 10 mM methylene blue, 50 μ M to 50 mM azure A, or 10 μ M to 1 mM azure B for 2 hours. Data represent the mean and SEM of 3 (c) or 4 (d) independent experiments. Statistical difference between phenothiazine treated samples and the PBS control was measured with a one-way ANOVA ($p < 0.0001$) and post hoc Dunnett's analysis compared to PBS: $*p < 0.05$, $**p < 0.01$, $***p < 0.001$.

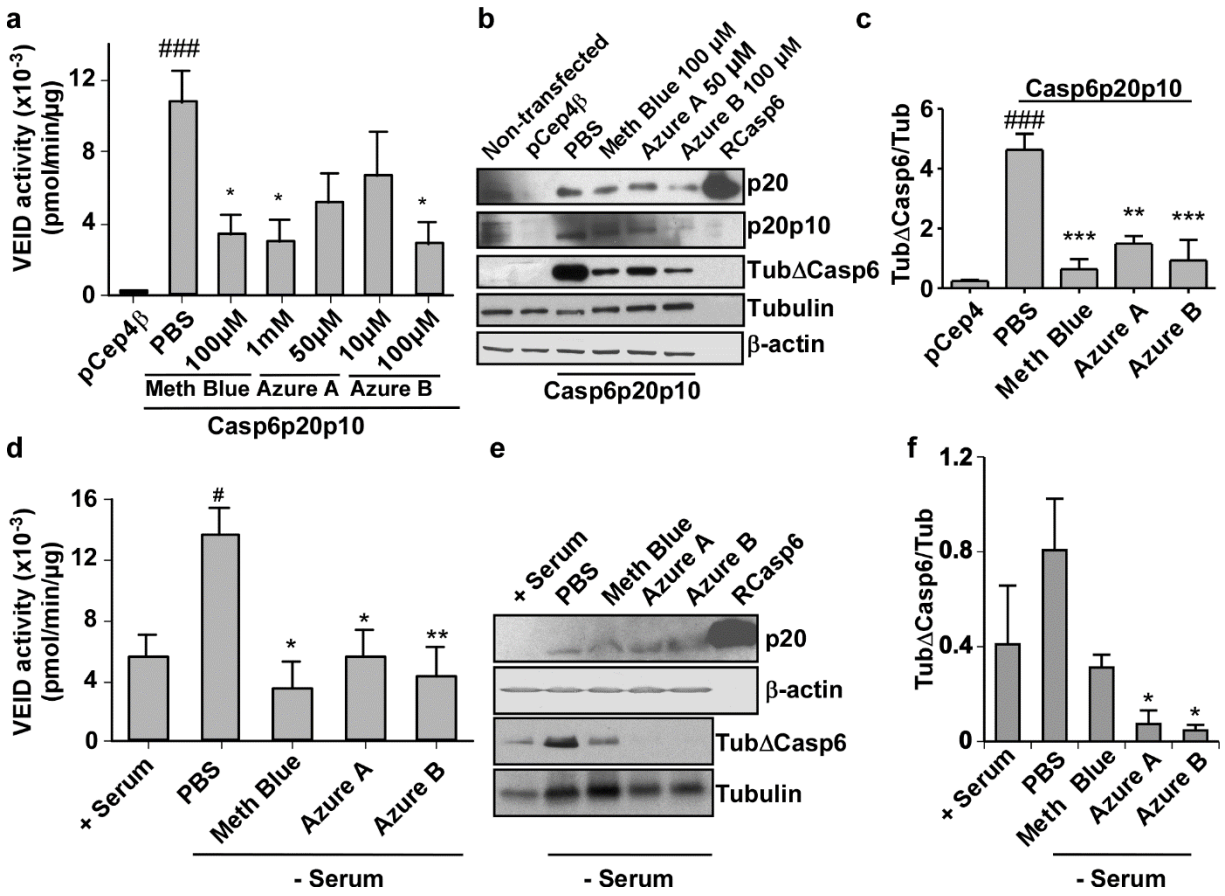

Figure 2.4 Methylene blue, azure A, and azure B inhibit active Casp6 in HCT116 cells and human primary neurons.

a Casp6 VEIDase enzymatic activity in pCep4β vector- and pCep4β Casp6p20p10transfected HCT116 cells treated with PBS, methylene blue (Meth blue), azure A, and azure B for 2 hours. Data represent the mean and SEM of 4 independent experiments. Statistical differences were evaluated with one-way ANOVA ($p \leq 0.0001$) and post hoc Bonferroni test comparing PBS or phenothiazine-treated cells with pCep4β (#) or pCep4β Casp6p20p10-transfected HCT116 cells (*). ###$p < 0.001$, *$p < 0.05$. **b** Western blot analysis of transfected- or non-transfected HCT116 cells shown in panel a for active Casp6p20 subunit (p20), full length Casp6 lacking its pro-domain; Casp6p20p10 (p20p10), Tubulin-cleaved by Casp6 (TubΔCasp6), full length Tubulin and β-actin. **c** Densitometric quantification of the levels of TubΔCasp6 in three independent experiments as shown in panel b. Data represent the mean and SEM of 3 independent experiments. Statistical evaluation conducted as described in a. ###$p < 0.001$, **$p < 0.01$, ***$p < 0.001$. **d** Casp6 VEIDase enzymatic activity in serum-deprived primary human neuron cultures

treated with 100 μM methylene blue, 50 μM azure A, and 10 μM azure B or PBS for 2 hours. Data represent the mean and SEM of 4 independent experiments. Statistical differences were conducted with a one-way ANOVA ($p < 0.041$) followed by a post hoc Bonferroni test comparing PBS or phenothiazine-treated cells with serum-treated (+ serum; #) or serum-deprived PBS-treated cells (PBS; *) #$p < 0.05$, *$p < 0.05$, **$p < 0.01$). **e** Western blot analysis of neuronal protein extracts shown in panel d for levels of TubΔCasp6 and full length tubulin. **f** Quantification of the levels of TubΔCasp6/total tubulin shown in panel e. Data represent the mean and SEM of 3 independent experiments. Statistical evaluations by one-way ANOVA ($p = 0.0315$) followed by post hoc Dunnett's test comparing to serum-treated (no significant difference) and serum deprived PBS-treated neurons (*$p < 0.05$). **g** Western blot analysis of the p20 active subunit of Casp6 (p20) and β-actin in proteins from serum-deprived human neurons.

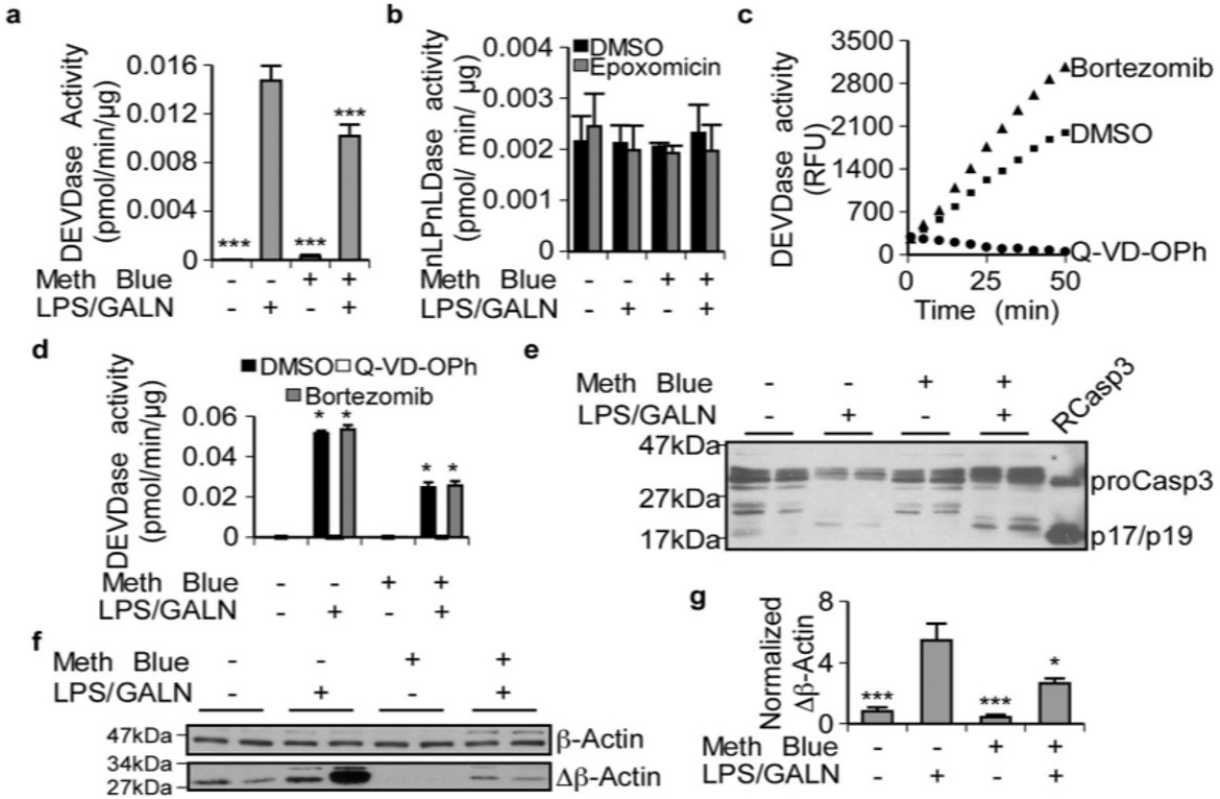

Figure 2.5 Methylene Blue inhibits Casp3 activity in liver of mice treated with LPS/GALN.

a Casp3 activity was assessed in liver protein extracts from mice treated 3 days with methylene blue (3 mg/kg) or vehicle and then injected with LPS/GALN or PBS. Data represent the mean and SEM of 8 independent experiments. Statistical differences were assessed with one-way ANOVA ($p < 0.0001$) and a post hoc Dunnett's test comparing all conditions to LPS/GALN-treated conditions ***$p < 0.001$. **b** Proteasomal nLPnLDase activity measured in liver protein extracts from mice treated with methylene blue and/or LPS/GALN in the presence or absence of 0.1 μM proteasome inhibitor epoxomicin. Data represent the mean and SEM of 3 independent experiments. No statistical differences were observed. **c** RCasp3 activity after treatment with DMSO, 1 μM of the pan-caspase inhibitor Q-VD-OPh, or 0.1 μM of the reversible proteasome inhibitor bortezomib. (d) DEVDase activity in liver protein extracts from mice treated with or without methylene blue and LPS/GALN after addition of DMSO, 1 μM Q-VD-OPh, or 0.1 μM bortezomib. Data represent the mean and SEM of 3 independent experiments. Statistical differences were assessed in a one-way ANOVA ($p < 0.0001$) followed with a post hoc Dunnett's test comparing all conditions to DMSO in control-treated mice (*). DEVDase activity

in DMSO treated protein extracts from LPS/GALN (no methylene blue)-treated mice did not change significantly in the presence of bortezomib. **e** Western blot of liver protein extracts from two different mice per group showing levels of proCasp3 and cleaved-Casp3 (p17/p19). **f** Western blot of liver protein extracts from two different mice per group showing levels of cleaved β-actin and β-actin. (g) Quantitative analyses of cleaved β-actin over full-length β-actin levels in liver protein extracts from mice treated with methylene blue or vehicle in the presence or absence of LPS/GALN. Data represent the mean and SEM of 8 independent experiments. Statistical evaluations were conducted as described in a.

a

	Peptide sequences	# peptides Cys 163	# peptides $Cys163_{ox}$	% peptide oxidized
Ctl	IFIIQACR (9), IFIIQACRG (1), IFIIQACRGNQHDVPVIPLDVVDNQTEK (6)	16	0	0%
MB	IFIIQACR (15), IFIIQACRG (14), IFIIQACRGNQH (3), IFIIQACRGNQHDV (1), IFIIQACRGNQHDVPVIPLDVVDNQTEK (5), CHSLVGKPKFIIQACRGNQHDVPVIPLDVVDNQTEK (1), CRGNQHDVPVIPLDVVDNQTEK (1)	40	6	15%
Azure B	IFIIQACR (5), IFIIQACRG (1), IFIIQACRGNQH (1), IFIIQACRGNQHDVPVIPLDVVDNQTEK (19)	26	2	7.7%

b

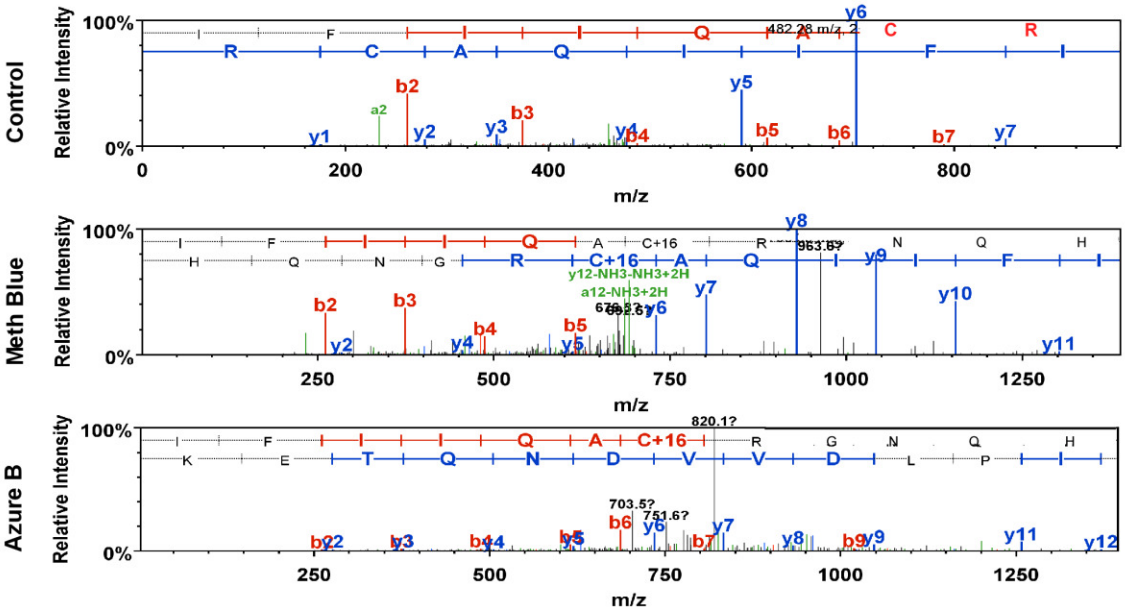

c

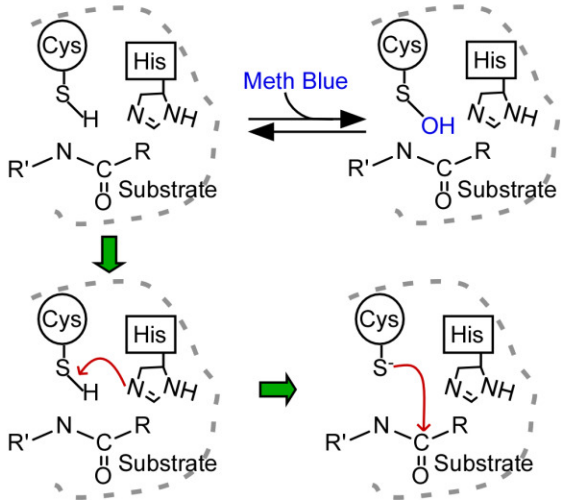

Figure 2.6 Methylene blue and azure B oxidizes the catalytic Cys163 of active Casp6.

a The table represents the number of peptide sequences containing Cys163 obtained by MS/MS and the number of peptides showing Cys163 oxidation. The underlined peptide sequence spectrums are represented in panel b. The percentage of peptides oxidized represents the number

of peptides containing an oxidized Cys163 divided by the total number of peptides containing the Cys163 in its sequence. **b** MS/MS spectra showing the oxidized (+16) catalytic Cys163 of Casp6 in the presence of methylene blue or azure B. **c** Schematic representation of Casp6 active site (top left panel). The catalytic mechanism of Casp6 is a multi-step process. The first step (bottom left panel) involves the de-protonation of the active site cysteine thiol by a histidine residue (His 121), thus activating the enzyme. The next step is a nucleophilic attack by the thiolate on the substrate's peptide carbonyl carbon that subsequently leads to cleavage of the substrate (bottom right panel). However, in presence of methylene blue, the Cys163 thiol group is sulfenated and unable to attack the substrate (top left and right panels).

2.9 Supplemental material

2.9.1 Materials and methods

Active Enzyme Measurements: Active RCasp6 and RCasp3 concentration was measured as previously described in (Denault and Salvesen, 2002). Briefly, it is a two-step assay. First the enzyme (final concentration 20 nM) is incubated with the titrant in concentrations ranging from 0 to 4 times the estimated caspase concentration in a low volume (25 μL) in assay buffer for 15 min at 37 °C. The titrant of choice is the irreversible caspase inhibitor benzoxycarbonyl-Val-Ala-Asp-fluoromethylketone (z-VAD-FMK) (Enzo LifeSciences, NY, USA). After the enzyme-titrant equilibrium is reached, the assay is diluted by the addition of excess substrate, VEID-AFC and DEVD-AFC and the remaining activity is determine with a simple enzymatic assay. The concentration of the active enzyme is determined by plotting the relative hydrolysis rate against the concentration of the titrant. The x-axis intercept of the tangent to the slope at low titrant concentration gives the active caspase concentration in the assay.

Fluorescence Quenching*:* AFC (12.5 μM) in Stennicke buffer was mixed with varying concentrations of methylene blue, Azure A and Azure B (10 mM, 1 mM, 0.1 mM, and 100 μM). A fluorescence emission spectrum was generated between 400 to 700 by exciting at 380 nm for each phenothiazine compound. The AFC fluorescence was gain-adjusted to 45000 relative fluorescence units.

Caspase activity assays: Casp6 activity was assessed by *in vitro* fluorogenic assays using Ac-Val-Glu-Ile-Asp-7-Amino-4-trifluoromethyl-couramin) (Ac-VEID-AFC: Enzo LifeSciences, NY, USA) as the Casp6 substrate. The activity was measured using Stennicke's buffer (SB) (20 mM piperazine-N, N-bis (2-ethanesulfonic acid) (PIPES: BioShop Canada Inc, Burlington, Ontario, CA) pH 7.2, 30 mM NaCl, 1 mM EDTA, 0.1% CHAPS, 10% sucrose) (Stennicke and Salvesen, 1997). Briefly, the reaction mix consisted of 20 nM recombinant Casp6, 1 X SB, 10 μM DTT, 10 μM VEID-AFC substrate and deionized water. Methylene Blue, azure A, and azure B were added in increasing concentrations (0-100 μM) to the reaction mix and the activity was measured in a black clear bottom 96-well plate (Costar, Corning, NY, USA) at 50 μL/well in

duplicate at 37 °C in the Synergy H4 plate reader (BioTek) at excitation 380 nm and emission 505 nm every two minutes for 100 minutes. Fluorescence units were converted to the amounts of moles of AFC released based on standard curve of 0 - 12.5 μM free AFC. Cleavage rates were calculated from the linear phase of the assay. The activity is considered on a percentage scale where no inhibitor present is equated at 100% activity of the enzyme. Activity assays for recombinant Casp3 was done similarly to recombinant Casp6, except the substrate used was Ac-Asp-Glu-Val-Asp-7-Amino-4-trifluoromethylcouramin (Ac-DEVD-AFC: Enzo Life Sciences, NY, USA).

Proteasome assay: The caspase-like activity of the proteasome was measured using the substrate Ac-Nle-Pro-Nle-Asp-AMC (Enzo LifeSciences, NY, USA) at a final concentration of 10 μM in Stennicke's buffer in the presence of 10 mM DTT. The assay was setup similarly to the caspase activity assay except for the use of a 7-amino-4-methylcoumarin (AMC, Sigma-Aldrich, St. Louis, MO, USA) standard curve. Mouse extracts were incubated with the irreversible proteasome inhibitor, 0.1 μM epoxomicin (Enzo LifeSciences, NY, USA), or 0.1 μM bortezomib (Calbiochem, MA, USA), 1 μM the pan-caspase inhibitor Q-VD-OPh (Sigma-Aldrich, St. Louis, MO, USA) or equal volumes of DMSO for 20 mins on ice before starting the assay. Recombinant Casp3 (20 nM) was used to test the specificity of the proteasomal substrate.

Statistical Analysis: For Caspase-3 activity assays, data represent the mean ± SEM of 3 livers from 3 animals and was analyzed using a one-way ANOVA with Dunnett's post hoc test (*** $p < 0.001$ in DMSO, and ### $p < 0.001$ in bortezomib) comparing all samples to LPS/GALN-treated mice in the absence of methylene blue, while proteasome assays were analyzed using Dunnett's post hoc test (*** $p < 0.001$ for mice not-treated with methylene blue or LPS, and # for mice treated with LPS only) compared all samples to DMSO.

2.9.2 Figures and legends

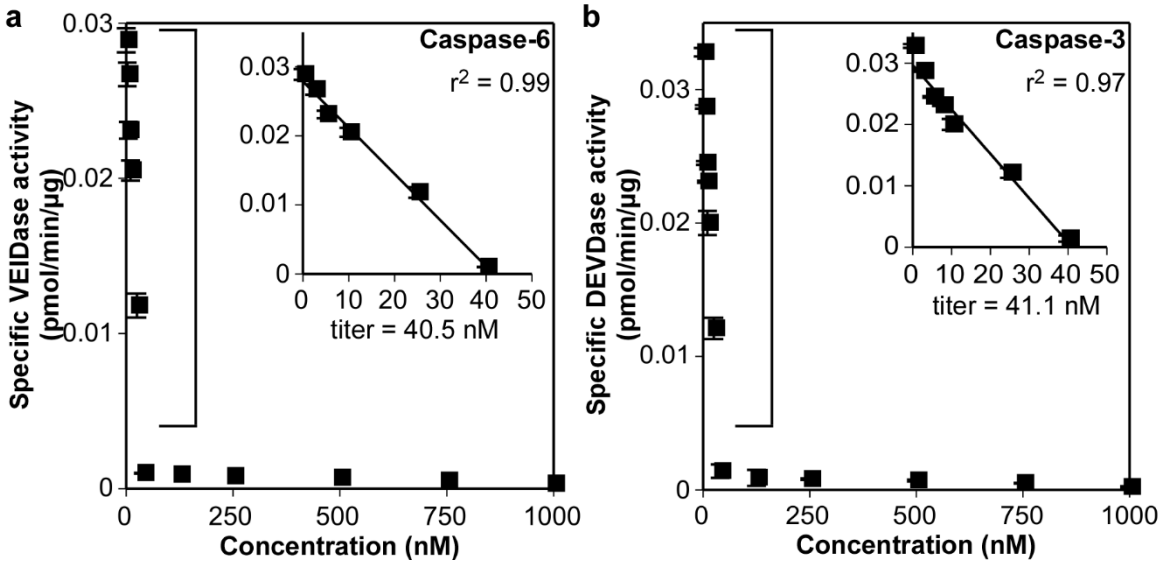

Supplemental Figure S2.1 Recombinant Caspases are highly active and functional.

a & b The active-enzyme concentration for RCasp6 and RCasp3 was calculated by titrating the enzymes with the irreversible inhibitor, Z-VAD-fmk, using Ac-VEID-AFC and Ac-DEVD-AFC as substrates, respectively. The bracket in panel a and b indicate the values used to obtain the active RCasp6 and RCasp3 concentration by linear regression (inset). The x-axis intercept (titer) represents the concentration of the active enzyme in the assay. Data represent the mean ± S.D. of three independent experiment

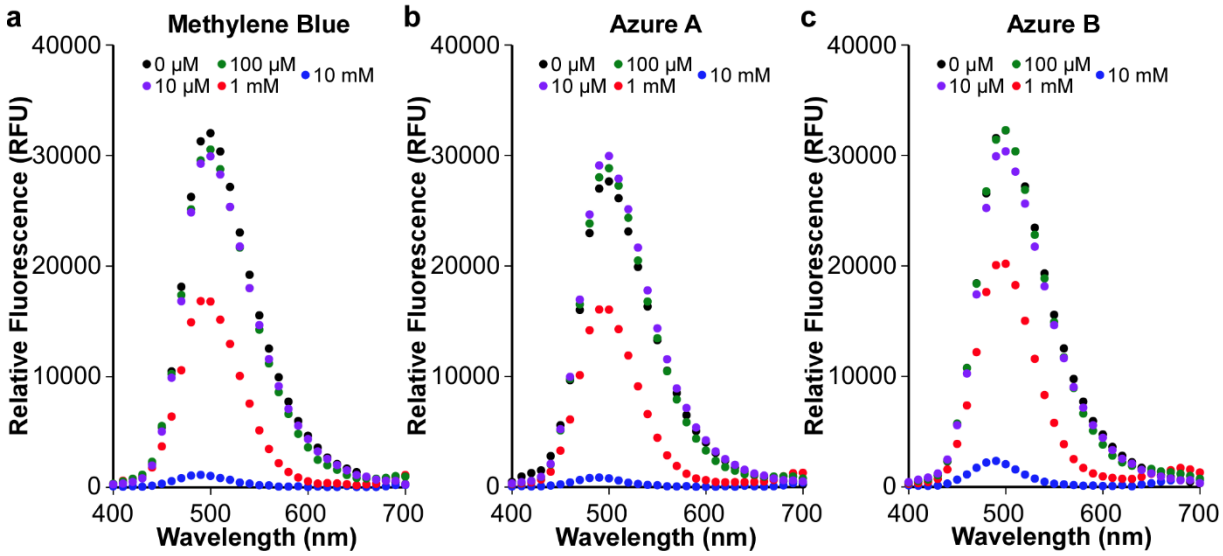

Supplemental Figure S2.2 Phenothiazines inhibit fluorescence in a dose-dependent manner.

a-c Fluorescence emission spectrum of AFC in presence of 0, 10 µM, 100 µM, 1mM, 10 mM of methylene Blue (a), azure A (b), and azure B (c), respectively.

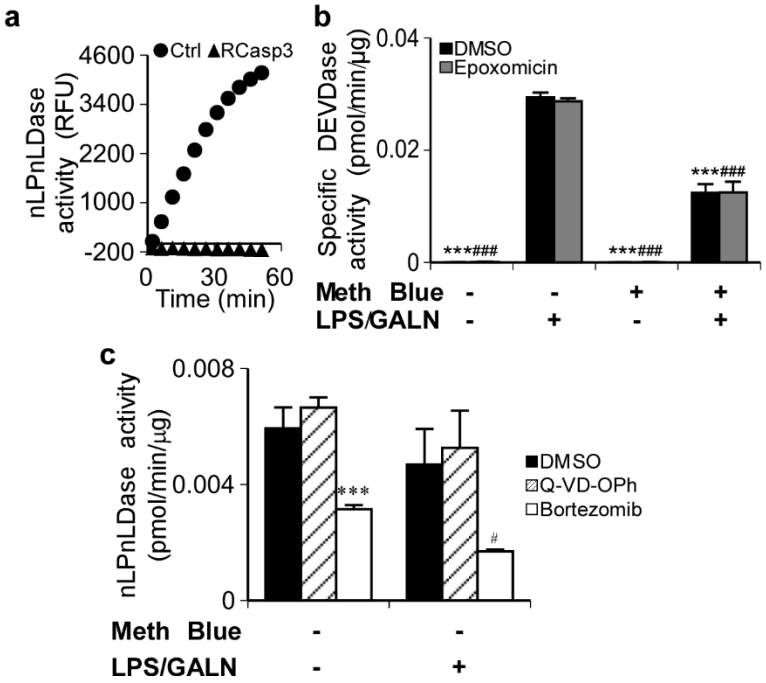

Supplemental Figure S2.3 Proteasome inhibitors do not inhibit DEVDase activity in mice liver extracts.

a Proteasomal caspase-like activity measured by fluorescence of cleaved Ac-nLPnLD-AMC substrate in human neuronal extracts (Ctrl) and by recombinant active Caspase-3 (RCasp3). **b** Casp3 DEVDase activity measured in liver protein extracts from mice treated with methylene blue and/or LPS/GALN in the presence or absence of 0.1 µM of the irreversible proteasome inhibitor, epoxomicin. **c** nLPnLDase activity in liver protein extracts from mice treated with or without methylene blue and LPS/GALN after addition of DMSO, 1 µM Q-VD-OPh, or 0.1 µM bortezomib.

3. Caspase vinyl sulfone small molecule inhibitors prevent axonal degeneration in human neurons and reverse cognitive impairment in Caspase-6-overexpressing mice

3.1 Preface

Caspase-6 activation is found in non-cognitively impaired individuals and correlates inversely with cognitive performance. In AD brain tissue, extensive Caspase-6-mediated axonal degeneration is evident by increased Tau and α-tubulin cleavage. Therefore, it is important to know whether human neurons can be protected from Caspase-6 activity and whether cognitive deficits due to Caspase-6 activity can be reversed. To answer this question adequately, a more specific approach than methylene blue treatment to inhibit Caspase-6 activity was required. Thus, our research group collaborated with New World Laboratories Inc. (NWL) to investigate novel caspase inhibitors with promising pharmacological properties such as favourable *in vivo* toxicity, sub-micromolar potency, and blood-brain barrier permeability. Using these caspase inhibitors, the neuroprotective potential of Caspase-6 inhibition was addressed.

3.2 Abstract

The activation of the aspartate-specific cysteinyl protease, Caspase-6, is proposed as an early pathogenic event of Alzheimer disease (AD) and Huntington's disease. Caspase-6 inhibitors could be useful against these neurodegenerative diseases but most Caspase-6 inhibitors have been exclusively studied in vitro or show acute liver toxicity in humans. Here, we assessed vinyl sulfone small molecule peptide caspase inhibitors for potential use in vivo. The IC_{50} of NWL vinyl sulfone small molecule caspase inhibitors were determined on Caspase-1 to 10, and Caspase-6-transfected human colon carcinoma HCT116 cells. Inhibition of Caspase-6-mediated axonal degeneration was assessed in serum-deprived or amyloid precursor protein-transfected primary human CNS neurons. Cellular toxicity was measured by phase contrast microscopy, mitochondrial and lactate dehydrogenase colorimetric activity assays, or flow cytometry. Caspase inhibition was measured by fluorogenic activity assays, fluorescence microscopy, and western blot analyses. The effect of inhibitors on age-dependent cognitive

deficits in Caspase-6 transgenic mice was assessed by the novel object recognition task. Liquid chromatography coupled to tandem mass spectrometry assessed the blood-brain barrier permeability of inhibitors in Caspase-6 mice. Vinyl sulfone NWL-117 caspase inhibitor has a higher selectivity against Caspase-6, −4, −8, −9, and −10 whereas NWL-154 has higher selectivity against Caspase-6, −8, and −10. The half-maximal inhibitory concentrations (IC_{50}) of NWL-117 and NWL-154 is 192 nM and 100 nM against Caspase-6 in vitro, and 4.82 μM and 3.63μM in Caspase-6-transfected HCT116 cells, respectively. NWL inhibitors are not toxic to HCT116 cells or to human primary neurons. NWL-117 and NWL-154 inhibit serum deprivation-induced Caspase-6 activity and prevent amyloid precursor protein-mediated neurite degeneration in human primary CNS neurons. NWL-117 crosses the blood brain barrier and reverses age-dependent episodic memory deficits in Caspase-6 mice. NWL peptidic vinyl methyl sulfone inhibitors are potent, non-toxic, blood-brain barrier permeable, and irreversible caspase inhibitors with neuroprotective effects in HCT116 cells, in primary human CNS neurons, and in Caspase-6 mice. These results highlight the therapeutic potential of vinyl sulfone inhibitors as caspase inhibitors against neurodegenerative diseases and sanction additional work to improve their selectivity against different caspases.

3.3 Introduction

Alzheimer disease (AD) is a neurodegenerative condition characterized by cognitive impairments leading to dementia with no disease-modifying treatments. Pathologically, AD is defined by an accumulation of extracellular plaques containing mostly amyloid-beta peptide (Aβ) and intracellular neurofibrillary tangles (NFT) composed of a hyperphosphorylated form of the microtubule-associated protein Tau. Clinical trials targeting Aβ plaques have been unsuccessful in restoring cognitive function (Karran and De Strooper, 2016), while trials on disaggregating NFTs are currently ongoing (Wischik et al., 2014). The results from the current clinical trials suggest that therapeutic intervention against AD could be improved by targeting earlier pathogenic events.

One emerging potential disease-modifying therapeutic target is Caspase-6 (Casp6), a cysteinyl protease that cleaves protein substrates specifically after an aspartic acid residue (Fernandes-Alnemri et al., 1995a). Casp6, but not Casp3 or Casp7, is activated in neurites

interspersing Aβ plaques, NFTs, and neuropil threads of familial and sporadic AD brains (Guo et al., 2004; Albrecht et al., 2009; LeBlanc, 2013). In brains from some aged non-cognitively impaired individuals, Casp6 activity levels correlates negatively with episodic and semantic memory performance (Ramcharitar et al., 2013a), two types of memory first affected in AD. Tau-cleaved by Casp6 (TauΔCasp6) levels in post-mortem cerebrospinal fluid correlate inversely with episodic, semantic, and working memory performance (Ramcharitar et al., 2013b). Overexpression of human Casp6 in the CA1 region of mice hippocampi results in age-dependent episodic and spatial memory loss (LeBlanc et al., 2014). These findings suggest that early Casp6 activation in the hippocampus of aged pre-symptomatic individuals leads to cognitive impairment.

When activated, Casp6 can impair the microtubule network within neuronal axons and lead to degeneration. Casp6 cleaves the C-terminus of several neuronal cytoskeletal or associated proteins including Tau and α-tubulin (Guo et al., 2004; Klaiman et al., 2008). In human CNS neuron cultures, overexpression of wild type amyloid precursor protein (APP^{WT}), a condition associated with familial AD (Rovelet-Lecrux et al., 2006), results in Casp6-dependent, but Aβ-independent, neuritic degeneration (Sivananthan et al., 2010a). Therefore, inhibiting Casp6 activity could prevent axonal degeneration. Caspases play an important role in other neurodegenerative conditions. Casp6 is associated with motor impairment in the Huntington mouse model (Wellington et al., 2000; Graham et al., 2006; Uribe et al., 2012; Waldron-Roby et al., 2012; Aharony et al., 2015; Wong et al., 2015). Casp6-dependent tubulin fragmentation is associated with neuritic degeneration in mouse sympathetic, retinocollicular, dorsal root ganglion sensory, commissural, and motor neurons following nerve growth factor (NGF)-deprivation (Nikolaev et al., 2009; Cusack et al., 2013; Simon et al., 2016). Casp6 participates in axonal degeneration of neurturin-deprived dorsal root ganglion cells (Vohra et al., 2010), myelin-mediated sympathetic and septal cholinergic neurons (Park et al., 2010), ischemic neurons (Akpan et al., 2011; Shabanzadeh et al., 2015), and retinal ganglion cells in models of optic nerve injury in rodents (Monnier et al., 2011). In these conditions, Casp6 is activated in the presence of other caspases, including Casp9 and Casp3. Similarly, human neonatal, infant, and adult hypoxic-ischemic brain injury results in increased levels of active

Casp6, active Casp3, and tubulin cleaved by Casp6/3 (TubΔCasp6/3) (Guo et al., 2004; Sokolowski et al., 2014).

Natural caspase inhibitors either do not inhibit Casp6 or are non-selective. Viral proteins p35 and CrmA inhibit several caspases (Zhou et al., 1997; Zhou et al., 1998). The mammalian inhibitors of apoptosis proteins (IAP) do not inhibit Casp6 (Deveraux et al., 1997; Roy et al., 1997). There are two natural Casp6 protein inhibitors: the alternatively spliced Casp6β isoform, which only prevents Casp6 activation and the caspase inhibitory factor (CIF), which is reactive against other caspases (Zhang et al., 2001; Lee et al., 2010). Many competitive small molecule Casp6 inhibitors have been developed but most have not been tested for cellular toxicity, blood brain barrier permeability and in vivo inhibition. Aza-peptides specifically inhibit caspases and not other cysteine proteases (Ekici et al., 2006). Casp6 specificity is improved with sulfonamide isatin Michael acceptors (Chu et al., 2009). Aldehyde or fluoromethyl ketones (fmk)-conjugated peptides obtained from positional scanning libraries or natural AP-2α and Lamin A Casp6 substrates have been used as Casp6 inhibitors (Orth et al., 1996; Talanian et al., 1997; Thornberry et al., 1997; Garcia-Calvo et al., 1998; Nyormoi et al., 2003; Edgington et al., 2012; Aharony et al., 2015). The commercially available Casp6 inhibitor benzyloxycarbonylVal-Glu-Ile-Asp-fmk (Z-VEID-fmk) is toxic to mammals because the fmk moiety can be metabolized into fluorocitrate, an inhibitor of aconitase that depletes tricarboxylic acid cycle intermediates (Eichhold et al., 1997). Nevertheless, a Huntington-based peptide inhibitor conjugated to TAT to enhance membrane permeability and delivered to the brain with an osmotic pump protects against behavioral and motor deficits in a mutant Huntingtin mouse model (Aharony et al., 2015).

New World Laboratories Inc. (NWL) has developed novel peptidomimetic irreversible small molecule inhibitors that retain Casp6's Z-VEID preferred substrate, but have a methyl vinyl sulfone chemical warhead which 1) is selective for cysteinyl proteases, 2) is unreactive with circulating thiols or non-active site cysteines, 3) forms a hydrogen bond with the active site histidine (Palmer et al., 1995), and (4) is safe in rats, dogs, and primates (Abdulla et al., 2007). Here, we describe a non-toxic and blood-brain permeable NWL caspase inhibitor that prevents axonal degeneration of primary human neurons, and reverses Casp6-dependent episodic

memory impairment in mice. These findings highlight vinyl sulfones as viable caspase inhibitors for pre-clinical studies.

3.4 Results

3.4.1 NWL-117 and −154 are potent peptide-based vinyl methyl sulfone inhibitors of recombinant active Casp6

NWL-117 and NWL-154 are peptide-based inhibitors flanked by a lipophilic moiety and a vinyl methyl sulfone chemical warhead (**Fig. 3.1a**). NWL-117 and −154 showed a dose-dependent Casp6 inhibition with half-maximal inhibitory concentrations (IC_{50}) of 192 nM and 100 nM, respectively (**Fig. 3.1b**). The peptide backbone of NWL inhibitors binds to the active site of Casp6, which allows the vinyl sulfone warhead to hydrogen bond with the protonated imidazole ring of histidine, while the catalytic cysteine attacks the β-carbon of the vinyl group (**Fig. 3.1c**). The reaction is irreversibly stabilized under physiological conditions by histidine de-protonation by the α-carbon of the vinyl group (Palmer et al., 1995). Thus, peptide-based vinyl sulfones are potent, irreversible, and competitive Casp6 inhibitors.

3.4.2 NWL inhibitors inhibit recombinant initiator caspases and Casp6 at sub-micromolar concentrations

NWL inhibitor specificity was tested on recombinant Casp1 to Casp10 (**Table 3.1**). NWL-117 inhibited effector Casp6, but not Casp3 or −7. NWL-117 inhibited initiator Casp8, Casp9, and Casp10, and inflammatory Casp4 but not Casp1 and Casp5. NWL-154 inhibited most strongly Casp6, Casp8 and Casp10, but not Casp3, Casp7, Casp9, Casp1, Casp4, or Casp5. Neither compounds showed inhibitory activity on Casp2. Casp6 IC_{50} in Fig. 3.1b differs slightly from these results because the recombinant Casp1-10 were not active site titrated as done for Casp6 purified in-house. These results indicate that NWL-117 and NWL-154 are strong Casp6 inhibitors although their selectivity requires improvement.

3.4.3 NWL-117 and −154 are non-toxic and potent inhibitors of Casp6 activity in Casp6-transfected HCT116 cells

To address NWL inhibitor efficacy in a cellular context, human colon carcinoma HCT116 cells were treated with 100 μM NWL-117, NWL-154 or staurosporine as a cell death control for 24 h (**Fig. 3.2a**). NWL inhibitor-treated cells looked morphologically normal. The mitochondrial reductive potential of cells treated with 20, 50, or 100 μM NWL-117 or −154 for 24 (**Fig. 3.2b**) or 48 h (**Fig. 3.2c**) was comparable to vehicle-treated cells. NWLtreated cells did not release lactase dehydrogenase (LDH) (**Fig. 3.2d**) nor did the cells show increased sub-G1 levels of DNA (**Fig. 3.2e**), excluding necrosis and apoptosis, respectively. Therefore, unlike staurosporine, NWL inhibitors are not toxic to HCT116 cells at the tested concentrations.

Casp6 overexpression in HCT116 increases Casp6 activity fivefold (**Fig. 3.2f**), and 100 μM NWL-117 or −154 treatments for 2 h decreased Casp6 activity by 80% (IC_{50} 4.82 μM; r2 =0.94) and 96% (IC_{50} 3.63 μM; r2 =0.91), respectively (**Fig. 3.2g-h**). Functional inhibition of Casp6 activity was confirmed by a substantial decrease in TubΔCasp6 and a modest reduction of active Casp6 p20 subunit in cells treated with 100 μM NWL inhibitors (**Fig. 3.2i**). These findings suggest a functional inhibition of Casp6 by NWL inhibitors within HCT116 cells.

3.4.4 NWL inhibitors block Casp6 activity within minutes in Casp6-transfected HCT116 cells

To assess the kinetics of NWL-117 and −154-mediated Casp6 inhibition, Casp6-expressing HCT116 cells were treated with 100 μM NWL-117 or NWL-154 for 15 to 120 min after 24 h of transfection. Within 15 min of treatment, Casp6 VEIDase activity decreased significantly by 88% with NWL-117 and 95% with NWL-154 and the inhibition continued for 2 (**Fig. 3.3a**) and 48 h (**Fig. S3.1**). TubΔCasp6 and Casp6p20 levels were decreased within 15 min of treatment (**Fig. 3.3b, c**).

To assess Casp6 activity recovery, transfected cells were treated with 100 μM NWL-117 or NWL-154 for 2 h and subsequently replaced with fresh media. Casp6 activity rose by 43%±5.0 within the first 15 min of NWL-117 removal and recovered 85%±2.5 of the initial activity after 2 h (**Fig. 3.3d**). In contrast, NWL-154 withdrawal increased by 21%±2.2 within

15 min, reaching 30%±15 after 2 h. Western blot analysis showed that the levels of TubΔCasp6 and Casp6p20 (**Fig. 3.3e–f**) were consistent with the VEIDase activity restoration (**Fig. 3.3d**). Together, these results indicate that the NWL inhibitors rapidly inhibit Casp6 activity and that this inhibition can be rapidly washed out in transfected HCT116 cells.

3.4.5 NWL inhibitors are non-toxic and prevent Casp6dependent neuritic degeneration in APP^{WT}-transfected human CNS neurons

Human primary neurons are primary targets for caspase inhibitors in neurodegenerating brains, and therefore these were cells of choice to examine the potential toxicity and caspase inhibition by these vinyl sulfone caspase inhibitors. Treatment with 100 μM NWL-117 or NWL-154 for 24 h did not change neuronal morphology (**Fig. 3.4a**), and showed mitochondrial reductive potential comparable to vehicle-treated neurons at 24 (**Fig. 3.4b**) or 48 h (**Fig. S3.2a**). These results indicate that neither NWL-117 nor −154 is toxic at concentrations up to 100 μM in human neurons.

Casp6 fluorogenic (**Fig. 3.4c**) and fluorochrome-labelled inhibitor of caspases (FLICA)-measured activity (**Fig. 3.4d**) and TubΔCasp6 (**Fig. 3.4e**) were decreased by both inhibitors in serum-deprived human neurons, thus supporting the ability of NWL-117 and −154 to inhibit intraneuronal Casp6 activity. Co-expression of APP^{WT} and enhanced green fluorescent protein (EGFP) induced neuritic beading and somatic swelling after 48 h (**Fig. 3.4f,g**), as previously observed (Sivananthan et al., 2010a). NWL-117, NWL-154, or 5 μM Z-VEIDfmk prevented neuritic beading (**Fig. 3.4h**). To study this effect over time, pBudEGFP- (**Fig. S3.3a**) or pBudEGFP/APP^{WT} − transfected neurons treated with vehicle (**Fig. 3.4i**) or NWL-117 (**Fig. S3.3b**) were assessed for beading by live fluorescent microscopy for a 72 h period. The percentage of beaded neurons increased significantly by 1.52 fold ± 0.07 with APP^{WT} compared to EGFP-alone (1.00±0.05) and decreased to 0.84 fold ± 0.13, 1.07 fold ± 0.08, 0.97 fold ± 0.14 with NWL-117, −154, or 5 μM Z-VEID-fmk treatment, respectively (**Fig. 3.4j**). Analyses with time indicate that the NWL-117-treated neurons have less beading compared to both pBudEGFP-transfected and pBudEGFP/APP^{WT} − transfected neurons (**Fig. 3.4k**). This protection is attenuated after 24 h because media was not replenished with the NWL-117 to avoid losing the settings for the time-lapse microscopy. Similarly, neuronal soma rounding was

inhibited by NWL-117 (**Fig. 3.4l**). Finally, a measure of neurons with homogeneously distributed EGFP as a measure of health shows that NWL-117 significantly increases neuronal survival under these conditions (**Fig. 3.4m**) Therefore, NWL-117 showed stronger neuroprotective effects than NWL-154 against neuronal beading and rounding in the APP^{WT} -transfected human neurons.

3.4.6 NWL-117 penetrates the blood-brain barrier and reaches high nanomolar concentrations in mouse brains

To assess the blood-brain barrier permeability of NWL117, 18 month old Casp6-expressing transgenic mice were injected via the carotid artery. Liquid chromatography/tandem mass spectrometry (LC/MS-MS) analyses showed hippocampal concentrations ranging from 67.9 nM to 879 nM, while plasma concentrations ranged from 3.4 μM to 48μM, after 5 minutes of injection (**Table 3.2**). The ratio between hippocampal and plasma concentrations suggested low brain penetrance, although levels greater than the in vitro IC_{50} against Casp6 (192 nM) and some initiator caspases (**Table 3.1**) were reached. Variability was expected due to the unpredictable effects of surgery on old mice. Blood-brain barrier integrity was confirmed with Evan's blue. These results demonstrate the ability of NWL-117 to cross the blood-brain barrier in mice.

3.4.7 Treatment of human Casp6 knock-in mice with NWL-117 improves their performance in the novel object recognition (NOR) task

Human Casp6 overexpression in the CA1 region of the hippocampus results in age-dependent episodic memory impairments measured by NOR (LeBlanc et al., 2014). Casp6 KI/Cre mice were tested following the experimental paradigm shown in **Fig. 3.5a**. Control mice spent more time with the novel object (70%±1.6), while KI/Cre mice did not (47%±3.6) (**Fig. 3.5b**) in the pre-test. Total path length (**Fig. 3.5c**), the percentage of time moving (**Fig. 3.5d**), and total number of entries in each part of the arena (**Fig. 3.5e**) were equivalent in control and KI/Cre mice indicating comparable locomotor and exploratory activities. Following two intraperitoneal injections, NWL-117-treated control mice performed equally to saline-treated mice (**Fig. 3.5f**). In contrast, saline-treated KI/Cre mice remained impaired (**Fig. 3.5g**), whereas

NWL-117-treated mice regained normal NOR performance (**Fig. 3.5h**). Injections had no effect on the locomotor or exploratory activities (**Fig. 3.5i–k**). Hence, age-dependent Casp6-mediated deficits in NOR can be overcome by an acute treatment with NWL-117.

3.4.8 Casp6 substrates, synaptic proteins, and glial inflammation markers are unchanged in mice hippocampi following NWL-117 treatment

Western blot analyses (**Fig. 3.6a**) showed that old KI/Cre mice overexpressed Casp6 but TubΔCasp6 levels remained below detection, as expected since neurons are likely degenerated. TubΔCasp6 positive immunohistochemical staining in the CA1 region (**Fig. 3.6b,c**) was slightly higher in saline KI/Cre mice compared to controls (**Fig. 3.6d**). NWL-117-treatment non-significantly decreased TubΔCasp6 levels threefold in control, but increased nonsignificantly in KI/Cre mice. Valosin-containing protein p97 cleaved by Casp6 (Δp97) (**Fig. 3.6e**) was not different in saline and NWL-117 treatments (**Fig. 3.6f**).

Synapsin, synaptophysin, and post-synaptic protein (PSD95) hippocampal protein levels were unchanged with NWL-117 treatment (**Fig. 3.6g–I & Fig. S3.4**). Synaptophysin immunoreactivity in the hippocampal CA1 region was slightly higher in saline-treated control than KI/Cre mice, and unchanged in NWL-117treated mice (**Fig. 3.6j–l**).

Protein analyses of mouse hippocampi showed a nonsignificant reduction in microglial ionized calcium binding adapter molecule 1 (Iba1) levels in KI/Cre mice, whether treated or not with NWL-117 (**Fig. 3.6m-o**). Astroglial glial fibrillary acidic protein (GFAP) levels also did not change with NWL-117 treatment (**Fig. 3.6p-q**). Thus, analyses could not detect changes in synaptic proteins, Casp6 substrates, or inflammatory markers that account for the behavioral improvement seen in NWL-117-treated KI/Cre mice.

3.5 Discussion

Our study demonstrates that NWL inhibitors are 1) non-toxic, but non-selective, strong Casp6 inhibitors in vitro, in colon cancer cells, and in primary CNS human neurons, 2) protective against Casp6-mediated neuritic degeneration in serum-deprived or APP^{WT} expressing human neurons, 3) blood-brain barrier permeable, and 4) reversing episodic memory impairments in transgenic Casp6 mice.

There are several advantages to these vinyl sulfone inhibitors. NWL-117 and NWL-154 are potent, non-toxic, but non-selective Casp6 inhibitors. Both NWL-117 and NWL-154 inhibited 1) recombinant Casp6 activity (IC_{50} =192 nM and 100 nM, respectively), 2) Casp6 activity in Casp6-transfected HCT116 cells (IC_{50} =4.82 μM and 3.63 μM, respectively), and 3) Casp6 activity in serumdeprived human neurons. In contrast to Z-VEID-fmk (Eichhold et al., 1997), vinyl sulfone inhibitors remain intact after target engagement (Palmer et al., 1995), and are not toxic to mammals (Abdulla et al., 2007). Similarly, NWL vinyl sulfone inhibitors do not cause cellular toxicity measured by mitochondrial activity, cell morphology, LDH release, or sub-G1 populations, or any gross physiological or anatomical changes in vivo (**Appendix 1**). Furthermore, NWL inhibitors non-covalently interact with the substrate-binding pocket of Casp6 and effectively block other substrates from entering the active site. In addition, by bringing the weak vinyl sulfone electrophilic warhead, near the catalytic histidine and cysteine residues of Casp6, Casp6 enzymatic activity is irreversibly blocked. Compared to reversible inhibitors, irreversible inhibitors can achieve higher potency by completely inhibiting their target and require less frequent and lower doses resulting in higher safety profiles (Singh et al., 2011). Therefore, the potential that NWL vinyl sulfone inhibitors could be used in humans is high. On the other hand, as with other active-site directed Casp6 inhibitors (Talanian et al., 1997; Nyormoi et al., 2003; Ekici et al., 2006; Henzing et al., 2006; Chu et al., 2009; Leyva et al., 2010; Edgington et al., 2012; Aharony et al., 2015), NWL inhibitors remain nonselective for Casp6 since they inhibit many other caspases. Reducing the concentration of NWL inhibitors can increase selectivity, but significant enhancements in potency and specificity are still required before these inhibitors reach clinical trials. To overcome this limitation, the unique inactive conformation of Casp6 was targeted by others (Vaidya and Hardy, 2011). The peptide inhibitor, pep419, targets and stabilizes the tetrameric inactive form of Casp6 in a pH-dependent non-competitive manner in vitro and in cells (Stanger et al., 2012). Similarly, non-competitive ligands that stabilize the L2 loop of Casp6, which normally rearranges during activation (Murray et al., 2014), and a potent uncompetitive inhibitor targeting the caspase-substrate interface (Heise et al., 2012), in vitro, are effective Casp6 inhibitors. Through these innovative mechanisms, highly specific inhibitors have emerged, yet remain to be tested for toxicity and efficiency in cells and in mice. Nevertheless, active site inhibitors can be chemically modified to reach exquisite selectivity against specific caspases (Methot et al., 2004).

The selectivity of VEID is controversial but it remains the best candidate for targeting the active site of Casp6. The study by McStay et al. (McStay et al., 2008) does suggest that VEID can be cleaved by recombinant Caspase-3 or by Caspase-3 in extracts from Jurkat cells undergoing intrinsic apoptosis after the addition of cytochrome c and ATP, which activates the apoptosome pathway. However, other groups have shown that Casp6 is better at cleaving VEID than Caspase-3 (Takahashi et al., 1996; Ehrnhoefer et al., 2011). In fact, the MichaelisMenten constant (K_m) for VEID is 8-fold lower for recombinant Casp6 (30 μm) than it is for Caspase-3 (250 μm) (Talanian et al., 1997). This suggests that VEID binds the active site of Casp6 with greater affinity than that of Caspase-3. Similarly, the IC_{50} and the inhibitory constant (K_i) of zVEID-CHO (aldehyde) are 2-fold smaller for Casp6 than they are for Caspase-3 (Heise et al., 2012). These data suggest that VEID is a preferred substrate of Casp6, although not specific. Apart from the peptide sequence, the other components of the small molecule also influence its selectivity. This is evident in (Berger et al., 2006) where screening of peptide acyloxymethyl ketones (AOMK) inhibitors resulted in the identification of TETD as the preferred peptide sequence for Casp6 over Caspase-3 (Edgington et al., 2012). Yet, in the same study, they found that Cy5 labeled VEID-AOMK was a better substrate for Casp6 than the TETD version. Similarly, chemical warheads can affect the selectivity of inhibitors bearing the same peptide sequence. In fact, VEID-CHO was more selective for Casp6 than −3 compared to the fluoromethyl ketone (FMK) counterpart (Pereira and Song, 2008). Exosites also modulate substrate binding (Boucher et al., 2012). It is possible that exosites are responsible for limiting the cleavage of lamin A at the VEID sequence to Casp6 (Takahashi et al., 1996). In our study, we find Z-VEID vinyl methyl sulfone inhibitors are 10-fold more selective against Casp6 than Caspase-3 (**Table 3.1**). It is possible that interactions of the lipophilic moiety or the chemical warhead with natural substrate exosites increase selectivity of the NWL inhibitors further towards Casp6.

Our results demonstrate that the NWL vinyl sulfone caspase inhibitors are non toxic to human neurons and neuroprotective against serum deprivation or APP overexpression. NWL inhibitors prevent serum-deprivation or APP^{WT}-expression induced TubΔCasp6 and neuritic degeneration in human neurons, as shown previously with Z-VEID-fmk and Casp6 dominant negative inhibitors (Sivananthan et al., 2010a). Maintaining full-length α-tubulin is essential to

stabilize microtubules (Maccioni et al., 1989), and intact microtubules are critical for neuronal function. Since active Casp6 or TubΔCasp6 are increased in human AD and hypoxia-induced ischemia (Guo et al., 2004; Klaiman et al., 2008; Sokolowski et al., 2014), inhibition of Casp6 and other caspases in these conditions may help maintain neuronal function. Even if Casp6 has been implicated in axonal degeneration of NGF-dependent neurons, recent evidence suggests that Casp3 also participates in axonal degeneration (Nikolaev et al., 2009; Park et al., 2010; Schoenmann et al., 2010; Vohra et al., 2010; Akpan et al., 2011; Monnier et al., 2011; Uribe et al., 2012; Cusack et al., 2013; Shabanzadeh et al., 2015; Simon et al., 2016). In our study, the possibility that NWL inhibitors are acting on Casp3 to protect neurons was excluded because only Casp1 and Casp6 are co-activated in our cellular model (Guo et al., 2006; Sivananthan et al., 2010a; Kaushal et al., 2015), and both NWL-117 and NWL-154 are more effective against Casp6 than Casp1 and Casp3. Moreover, in AD brains, active Casp6 is detected in the absence of Casp3 (Selznick et al., 1999; LeBlanc, 2013). Thus, although studies in mouse peripheral neuron cultures implicate Casp3 to be an important regulator of axonal degeneration, the pathways involved in human CNS neurons seem to converge on Casp6. Nevertheless, given the strong inhibition of initiator caspases by the NWL vinyl sulfone caspase inhibitors, it is not possible in these experiments to conclude that the effect observed was uniquely due to Casp6. The ability of short term treatment with NWL-117 to reverse episodic memory impairments in our mice suggests that Casp6mediated damage is reversible in aged mice. We did not determine whether other caspases are activated downstream of Casp6 in our mouse model and it remains a possibility that the inhibition of other caspases such as Casp4, 8, 9, and 10 additionally contributed to the improvement of cognitive deficits mediated by the overexpression of Casp6. Nevertheless, the development of specific Casp6 inhibitors and assessment of target engagement will help determine whether it is Casp6 inhibition alone, a combination of Casp6 with other caspases activated as a consequence of Casp6 activation in the mice brains, or a non-caspase effect that is responsible for the behavioural improvement. Most importantly, our findings suggest that vinyl sulfone NWL caspase inhibitors are permeable to the blood-brain barrier with concentrations in the hippocampus reaching in vitro IC_{50} values. Intra-carotid injections were used as a proof of principle as it limits exposure to peripheral tissues and is the most rapid path to the brain. Rapid exposure was necessary as the LC/MS/MS method can only detect free NWL-117. Pharmacokinetic and pharmacodynamic detailed analyses should be conducted in

order to determine dosing regimens for chronic administration studies. Only one other Casp6 inhibitor, ED11, was shown to be brain permeable and have a significant effect against behavioral and cognitive deficits in an Huntington's mouse model (Aharony et al., 2015). ED11 was delivered by subcutaneous pump delivery of 4 mg/kg/ day for 28 days or more. In contrast, NWL-117 reversed Casp6-induced memory deficits after only 2 intraperitoneal injections of 20 mg/kg within 72 h in the Casp6 transgenic mouse. These results support delivery of the NWL inhibitors to the brain and suggest that Casp6-mediated functional impairment can be rapidly reversed.

Compared to ED11 (Aharony et al., 2015), NWL have several advantages. ED11 is a 24 amino acid peptide (GRKKRRQRRR PPQSSEIVLDGTDN) containing part of the human immunodeficiency virus (HIV) TAT-peptide and huntingtin protein sequences. The TAT-peptide confers permeability to plasma membranes and the blood-brain barrier, while the huntingtin sequence is used to target Casp6. NWL inhibitors have 1) lower molecular weight, 2) lower IC_{50} against VEID substrates, and 3) no activity enhancing effect on caspases compared to ED11. Lower molecular weight is associated with several different parameters that determine the oral bioavailability of compounds as well as their production cost (Veber et al., 2002). In addition, large peptides have lower half-lives in the body due to extensive degradation and clearance by the liver and kidneys. This often leads to the use of parenteral routes of administration, like injections for insulin, which subsequently leads to reduced patient compliance. Thus, the development of small molecules is often preferred. In addition, although the IC_{50} against mutant huntingtin cleavage determined by fluorescence resonance energy transfer (FRET) was 12.12 nM for ED11, ED11 did not inhibit the cleavage of VEID aminoluciferin as potently (>10 μM). Like NWL inhibitors, ED11 showed inhibition of other caspases, but the IC_{50} of ED11 against all caspases on their preferred substrates has not been determined. Therefore, it is not possible to compare the selectivity of ED11 to that of NWL. Furthermore, ED11 showed a significant enhancement of Caspase-5 activity on the FRET assay. Deregulated Caspase-5 activation could perturb inflammasome signalling (Baker et al., 2015). No activation of caspases was observed with NWL inhibitors. Finally, ED11 is a competitive reversible inhibitor that gets cleaved by Casp6. Although it has not been measured, the affinity of cleaved ED11 could be lower than the parent compound. Thus, the efficacy of ED11 will be

reduced over time. In contrast, irreversible NWL inhibitors can completely inhibit the target enzyme, require less frequent dosing, and have better safety profiles than reversible inhibitors (Singh et al., 2011). In theory, both these caspase inhibitors are in the early phases of development and will need much improvement before being considered for clinical use.

The underlying molecular mechanism(s) involved in the restoration of cognitive function remain unclear. NWL-117 had no effect on hippocampal levels of TubΔCasp6 or p97ΔCasp6, synaptic protein expression, or glial inflammation markers. Our inability to detect changes may be a consequence of the short treatment period. Furthermore, Casp6 expression and activation is limited to the pyramidal neurons of the CA1 region of the hippocampus and this does not provide sufficient material to assess Casp6-cleaved protein substrates by western blot, especially since neurons will not all degenerate at the same time. In addition, the rapid reversal of cognitive deficits suggest that the effect is possibly mediated through neuronal plasticity which re-establishes neuronal function, therefore, different tools encompassing synaptic plasticity need to be developed to assess how NWL reverses cognitive deficits in these mice. In other mice studies, cognitive amelioration was measured in the absence of changes in synaptic protein expression or brain volume (Tong et al., 2012; Aharony et al., 2015). Future long-term prophylactic treatment studies may enlighten us to the effects of NWL-117 in the context of age and Casp6-dependent cognitive impairment and allow proper identification of target engagement. In addition, NWL inhibitors need to be administered to different AD mouse models which display an aggravated pathological phenotype, such as high Aβ load or NFTs, to determine the efficacy of this treatment in re-establishing memory function in other models of neurodegeneration.

NWL inhibitors have advantages over current research tools as they are permeable to the blood brain barrier and are less toxic than the commercially available fluoromethylketone based tools (cell permeable inhibitors and FLICA reagents) without any compromise in selectivity. As NWL Inc. improves on their small molecules Casp6 inhibitors, experiments on non-human primates, clinical trials, and the development of radio-ligands for positron emission tomography will become reality.

This study reveals the potential for vinyl sulfone caspase inhibitors to effectively inhibit Casp6 activity and promote neuronal axonal integrity. Also, our results suggest that Casp6-

mediated damage can be reversed in aged brains. Much work still needs to be done to confirm target engagement, measure selectivity, potency, and blood-brain-barrier permeability in animal models. However, with the increasing number of research groups focusing on Casp6 as a therapeutic target against neurodegenerative diseases, the possibility that Casp6 inhibitors will one day reach human trials is promising. Whether Casp6 inhibitors will be sufficient as a monotherapy, or whether they will become part of a combinatorial approach with Tau, amyloid, and other emerging therapies is a question that will be answered in the years to come.

3.6 Materials and methods

DNA constructs: The mammalian constructs encoding human Casp6p20p10 in the pCep4β vector (Thermo Fisher Scientific, Waltham, MA, USA) (Klaiman et al., 2009), and enhanced green flurorescent protein (EGFP) or EGFP and amyloid precursor protein (APP^{WT}) in the double promoter-containing pBudCE4.1 vector (Thermo Fisher Scientific, Waltham, MA, USA) (Sivananthan et al., 2010a) were previously cloned in our laboratory. A synthetic Escherichia coli codon-optimized gene (GenScript, Piscataway, NJ, USA) coding for human Casp6 large subunit (amino acids 24-179, flanked by start (ATG) and stop (TAA) codons) and small subunit (amino acids 194-293, preceded by a start codon), separated by GAATTCAATAATTTTGTT TAACTTTAAGAAGGAGATATACAT containing an internal ribosome binding site (underlined), was ligated into the XbaI/XhoI sites of the pET23b(+)-Casp6-His plasmid (a kind gift from Dr. Guy Salvesen, Sanford Burnham Prebys Medical Discovery Institute, CA, USA), under the control of a single T7 promoter. All plasmids were sequenced by the Sanger method (McGill University and Genome Quebec Innovation Center, Montreal, Quebec, CA).

Recombinant Casp6 Expression and purification: Casp6 was expressed from the pET23b(+)-Casp6-His plasmid in E. coli BL21(DE3)pLysS strain (Promega, Fitchburg, WI, USA) at 37 °C in 2xYT medium (16 g/l tryptone, 10 g/l yeast extract, 5 g/l NaCl) supplemented with 0.1 mg/ml ampicillin and 0.034 mg/ml chloramphenicol under vigorous shaking according to (Denault and Salvesen, 2002). Casp6 expression was induced with 50 µM isopropyl βD-1-thiogalactopyranoside (IPTG) when cell cultures reached OD595 nm of 0.6 and cells cultured at 22 °C for 16 h under vigorous shaking. Cells were harvested by centrifugation, resuspended

in buffer A (50 mM Tris pH 8.5, 300 mM NaCl, 5% glycerol, 2 mM imidazole), and lysed by sonicating on ice with a Vibra-Cell ultrasonic processor (Sonics and Materials, Newtown, CT, USA) for 2 min at 50% duty with output control set to four. The lysate was clarified by centrifugation (30,000 x g for 30 min at 4 °C) and loaded on Ni Sepharose Fast Flow 6 medium (GE Healthcare Life Sciences, Baie D'Urfe, QC, CA) pre-equilibrated with buffer A, washed with buffer B (50 mM Tris pH 8.5, 500 mM NaCl, 5% glycerol, 20 mM imidazole), and bound proteins eluted with a 50-300 mM linear imidazole gradient in buffer A. Fractions were assessed for recombinant Casp6 purity by SDS-PAGE and Coomassie blue staining. Fractions containing pure Casp6 were pooled together, dialyzed against storage buffer (20 mM Tris pH 8.5, 200 mM NaCl, 10 mM DTT, 5% glycerol), concentrated by dialysis against polyethylene glycol (PEG) 20,000 (Sigma-Aldrich, Oakville, ON, CA), and stored at -80 °C in small aliquots. Protein concentration was measured using Quick Start Bradford 1x Dye Reagent (Bio-Rad Laboratories, Hercules, CA, USA). Active site titration assay: The concentration of Casp6 active sites was determined by active site titration assay using Z-VAD-fmk (N-benzyloxycarbonylVal-Ala-Asp-(O-methyl)-fluoromethylketone, MP Biomedicals, Santa Ana, CA, USA) inhibitor (Denault and Salvesen, 2002). Casp6 (398 nM) was incubated in SB with 0 to 1.25 µM Z-VAD-fmk for 2 h at room temperature in a final volume of 10 µl, diluted 20fold with SB, and 25 µl of aliquots transferred to a black clear bottom 96-well microplate (Costar, Corning, NY, USA). Casp6 VEIDase activity (see below) was plotted as a function of Z-VAD-fmk concentration; the intersection at the X-axis in the linear region of the curve indicates the concentration of active sites of Casp6.

Cell cultures and NWL inhibitor treatments HCT116: Human colon carcinoma (HCT116) cells (ATCC, Manassas, VA, USA) were cultured in McCoy's 5A modified media (Thermo Fisher Scientific, Waltham, MA, USA) supplemented with 10% fetal bovine serum (Thermo Fisher Scientific, Waltham, MA, USA) and transfected with 1 µg of pCep4 βCasp6p20p10 mixed with 8 µg of polyethyleneimine (Polysciences Inc., Warrington, PA, USA) (Boussif et al., 1995). Protein expression was allowed for 24 h before treating with vehicle (PBS), 100 µM NWL-117, or 100 µM NWL-154 for 2 h. For NWL inhibitor kinetic experiments, 100 µM of NWL-117 or NWL-154 was added at 120, 90, 60, 30, 15, or 0 min before harvest. For the extended time course from 2 to 48 h, NWL inhibitors were dissolved in PEG400 (Sigma-Aldrich, Oakville,

ON, CA) (50% v/v), anhydrous ethanol (20% v/v), and 154 mM NaCl (BioShop Canada Inc, Burlington, Ontario, CA) (30% v/v)). For recovery time course experiments, after the initial treatment with 100 μM of NWL-117 or−154 for 2 h, the media was replaced with fresh media for 120, 90, 60, 30, 15, or 0 min before harvest. Primary Human CNS neurons: Cortical tissues were obtained from the Birth Defects Research Laboratory (BDRL, University of Washington, Seattle, USA) in accordance with NIH ethical guidelines approved by McGill University's institutional review board and primary neurons cultured as previously described (LeBlanc, 1995). Primary human neurons were seeded on poly-L-lysine-coated (5 μg/mL) 6-well plates or glass coverslips coated with poly-L-lysine and laminin (5 μg/mL) (Sigma-Aldrich, Oakville, ON, CA) at a density of $3x10^6$ cells/mL. Primary human neurons were pre-treated with 0.1 μM epoxomicin (Enzo LifeSciences, Farmingdale, NY, USA) and 100 μM NWL-117, 100 μM NWL-154, or vehicle (PBS) for 2 h, and serum-deprived for 2 h in the presence of epoxomicin and vehicle (PBS), 100 μM NWL117, or 100 μM NWL-154 before harvesting or measuring caspase activity with FLICA, as described below.

Casp6 activity assays: *Recombinant or extracted cellular Casp6 activity:* Casp6 activity was assessed by in vitro fluorogenic assays using Ac-Val-Glu-Ile-Asp-(7-Amino-4-trifluoromethylcouramin) (Ac-VEID-AFC: Enzo LifeSciences, NY, USA) as the Casp6 substrate. The activity was measured in Stennicke's buffer (SB) (20 mM piperazine-N, N-bis (2-ethanesulfonic acid) (PIPES: BioShop Canada Inc, Burlington, Ontario, CA) pH 7.2, 30 mM NaCl, 1 mM ethylenediaminetetraacetic acid (EDTA), 0.1% 3-[(3-cholamidopropyl)-dimethylammonio]-2-hydroxy-1-propanesulfonic acid (CHAPS), 10% sucrose) (Stennicke and Salvesen, 1997). The reaction mix consisted of either 20 nM RCasp6 or 20–30 μg cellular protein extracts, SB, 10 mM DTT, 10 μM VEID-AFC substrate and deionized water. The activity was measured in a black clear bottom 96-well plate (Costar, Corning, NY, USA) at 50 μL/well in triplicate at 37 °C in the Synergy H4 plate reader (BioTek) at excitation 380 nm and emission 505 nm every two minutes for 100 min. Fluorescence units were converted to the moles of AFC released based on a standard curve of 0–625 picomoles of free AFC. Cleavage rates were calculated from the linear phase of the assay. The activity is considered on a percentage scale where no inhibitor present is equated to 100% activity of the enzyme. *Cellular Casp6 activity assay by FLICA:* Active Casp6 was labeled within primary human neurons using

the fluorescent inhibitor of Casp6 (FLICA) (FAM-VEID-fmk, ImmunoChemistry, Bloomington, MN, USA) following the manufacturer's protocol. Briefly, FLICA reagent and Hoechst 33342 were added to a black clear bottom 96-well plate containing 100,000 of the treatedprimary human neurons for 2 h at 37 °C in 5% CO2. The cells were rinsed twice with wash buffer and fresh media was added to the cells. The fluorescence of FAM-VEIDfmk was measured at 490 nm excitation and 520 nm emission with bandwidth reduced to 8 nm in the Synergy H4 plate reader (BioTek). The Hoechst signal was measured by excitation at 360 nm and emission at 485 nm.

IC_{50} determination of NWL inhibitors on recombinant proteins or in cells: The half-maximal inhibitory concentrations (IC_{50}) for NWL inhibitors (Patent publication # WO/2009/140765, WO/2010/133000, and WO/2012/140500) was determined by incubating 0 to 20 μM NWL-117 and NWL-154 with 20 nM of active site-titrated Casp6 in SB at room temperature for 5 minutes. Then, 10 μM Ac-VEID-AFC was added and fluorescence measured for 20 min at 37 °C as described above. New World Laboratories performed the IC_{50} determination for NWL inhibitors dissolved in dimethyl sulfoxide (DMSO) against recombinant Casp1-10 using the Caspase Inhibitor Drug Screening Kits (BioVision, San Francisco, CA) following the manufacturer's instructions and the preferred substrates for the caspases (Caspase-1: WAD-AFC, Caspase-2: VDVAD-AFC, Caspase-3: DEVD-AFC, Caspase-4: LEVD-AFC, Caspase-5: WEHDAFC, Casp6:VEID-AFC, Caspase-7: DEVD-AFC, Caspase8: IETD-AFC, Caspase-9: LEHD-AFC, Caspase-10: AEVD-AFC). In transfected HCT116 cells, 0 to 100 μM NWL inhibitors were added in the culture media and left on the cells for 2 h. Cells were washed once with 1 mL ice-cold PBS, incubated on ice for 5 min with 200 μL cell lysis buffer (CLB) (50 mM HEPES, 0.1% CHAPS, 0.1 mM EDTA), and gently scraped off. Protein concentrations were determined by Bradford assay (BioRad, Mississauga, ON, CA) by measuring the absorbance at 595 nm using the BioTek Synergy H4 plate reader. Caspase-6 activity was measured in 40–60 μg total protein as described above. The IC_{50} for recombinant and cellular caspases were determined using GraphPad Prism 5.0 (La Jolla, CA, USA) using a log (inhibitor) – response curve with a Hill slope of −1.

Microscopy analyses: *Immunofluorescence on human neuron cultures:* Primary human neurons were pre-treated 2 h and serum-deprived in the presence of 100 μM NWL-117, 100 μM NWL-

154, or 5 μM Z-VEID-fmk (Biomol, Plymouth meeting, PA, USA) for 24 h. Following treatment, human neurons were washed once with warm PBS, fixed for 20 min at room temperature with 4% paraformaldehyde (Sigma, Oakville, ON, CA)/4% sucrose (BioRad, Mississauga, ON, CA) for TubΔCasp6 or 2% formaldehyde (Thermo Fisher Scientific, Waltham, MA, USA)/0.2% glutaraldehyde (Sigma, Oakville, ON, CA) for pBudEGFP or pBudEGFP/APP^{WT}-transfected neurons (Nybo, 2012), incubated in permeabilization buffer (0.1% Triton X-100, 0.1 sodium citrate) for 1 min on ice, washed with PBS, blocked for 20 min at room temperature with 10% goat serum (Sigma, Oakville, ON, CA), and incubated with primary antibodies diluted in 10% goat serum in PBS overnight at 4 °C in a humid chamber. The glass coverslips were washed with PBS, and incubated with goat anti-rabbit secondary antibody coupled to Alexa 488 (Molecular Probes, Eugene, OR, USA) or Cy3 (GE Healthcare Life Sciences, Baie D'Urfe, QC, CA) and Hoechst 33342 (ImmunoChemistry, Bloomington, MN, USA) at 1 μg/mL for 2 h at room temperature. The coverslips were washed with PBS and rinsed in Milli-Q water before mounting in fluoromount (Dako, Burlington, ON, CA). Images were acquired by fluorescence microscopy and quantified using the ImageJ software (NIH, Bethesda, MD, USA) for TubΔCasp6 and manually counted for transfected EGFP(+)-neurons. *Time lapse-imaging by live fluorescence microscopy:* Primary human neurons were transfected with gold beads coated with pBudEGFP or pBudEGFP/APP^{WT} using a Helios Gene gun (BioRad, Mississauga, ON, CA) (Sivananthan et al., 2010a). Briefly, cells were pretreated with 100 μM NWL inhibitors or 5 μM Z-VEID-fmk for 2 h. The media was removed and the neurons were shot at 100 psi. The media was quickly replaced with the inhibitors present. The plasmid was expressed for 16 h before setting up the fluorescence microscope (Nikon Eclipse Ti) to acquire 20 images per condition every hour for 72 h at 37 °C with 5% CO2. The images were analyzed by counting the total number of neurons (50–100 neurons per condition per independent experiment), and the number of beaded, swollen soma, and healthy neurons. In addition, the time at which cells beaded was noted. Phase contrast microscopy: HCT116 cells, plated at a density of 1×105 cells/well and human neurons, plated at a density of 6×106 cells/well on poly-L-lysine were treated with PBS, 100 μM NWL-117, 100 μM NWL-154, or 2 μM staurosporine (Biomol, Plymouth meeting, PA, USA) for 24 h. Images were acquired with the Nikon Eclipse Ti microscope and the NIS-Elements (Version 3.10) software.

Cellular toxicity assays: *MTT assay:* HCT116 cells or primary human neurons were seeded in 96-well plates at a density of 1x104 and 1x105 cells per well, respectively. The next day, cells and neurons were treated with vehicle (PBS), or 20, 50, or 100 μM of NWL-117, NWL-154, or 2 μM staurosporine for 24 or 48 h. The media was replaced with 0.5 μg/ml MTT (3-(4,5-dimethylthiazol-2-yl)-2,5-diphenyltetrazolium bromide) (Sigma-Aldrich, Oakville, ON, CA) and the cells were incubated for 4 h at 37 °C in 5% CO2. The media was removed before dissolving the formazan crystals in 100 μL DMSO while shaking for 30 min. Once dissolved, the absorbance of each sample was measured at 560 nm and 670 nm using the Synergy H4 plate reader from BioTek (Winooski, VT, USA). *LDH Assay:* HCT116 cells were seeded in a 6-well plate at a density of 1×105 cells/well and treated the following day with 100 μM NWL-117 or −154 or equal volumes of vehicle (PBS) for 24 h. As a positive control, some cells were lysed for 2 h in 0.9% Triton X-100 (BioShop Canada Inc, Burlington, Ontario, CA). Media was collected and stored at −20 °C or assayed right away using the Cytotox 96 kit (Promega, Madison, WI, USA) following the manufacturer's protocol. Hydrochloric acid (1 N) was added for 10 min to stop the reaction, which was read at 490 nm (signal) and 520 nm (background) using the Synergy H4 plate reader from BioTek. Media without cells were also used to correct the absorbance. *SubG1 population analysis:* HCT116 cells were seeded in a 6-well plate at a density of 1x105 cells/well and treated the following day with 100 μM NWL-117, 100 μM NWL-154, equal volumes of vehicle (PBS), or 2 μM staurosporine for 24 h. The media was recovered and the cells were trypsinized in 0.25% Trypsin-EDTA (Thermo Fisher Scientific, Waltham, MA, USA). Both the media and the cells were combined and centrifuged for 5 min at 4 °C and washed with cold PBS-EDTA (5 mM). Cells were resuspended in 1 mL cold PBS-EDTA (5 mM), fixed by the dropwise addition of 3 mL of ice cold 100% ethanol and stored at −20 °C overnight. After centrifugation, the ethanol was removed and the cells were washed with cold PBS-EDTA (5 mM). Then, 1 mL of staining solution was added (5 mM PBS-EDTA, 50 μg/mL propidium iodide, 20 μg/ mL RNAse A (Sigma-Aldrich, Oakville, ON, CA)). The samples were analyzed by flow cytometry using the FACS Calibur II instrument (BD Biosciences, Mississauga, ON, Canada). The data were interpreted using the cell cycle analysis tool in FlowJo Version 10.0, which determined the DNA content in cells based on propidium iodide intensity (Ashland, OR, USA).

Western blot analyses: Protein extracts from HCT116 cells and human primary neurons were subjected to western blotting analyses. The 10630 (1:10 000) and GN60622 (1:10 000) neoepitope antibodies against the p20 subunit of active Casp6 (Casp6p20) and α-tubulin cleaved by Casp6 (TubΔCasp6) were generated previously in our laboratory (Guo et al., 2004; Klaiman et al., 2008; Halawani et al., 2010). The β-actin clone AC-15 (1:5 000, Sigma-Aldrich, Oakville, ON, CA), Casp6 (1:1 000), Synapsin (1:5 000), full-length α-tubulin (1:1 000, Cell Signalling Technology Inc., Danvers, MA, USA), GFAP (1:3 000, Dako, Burlington, ON, CA), synaptophysin (1:5 000, Sigma, Oakville, ON, CA), and PSD95 clone K28143 (1:5 000, UC Davis/NIH NeuroMab Facility) were purchased. All antibodies were diluted in 5% non-fat dry milk. Secondary anti-mouse (1:5 000, GE Healthcare Life Sciences, Baie D'Urfe, QC, CA) and anti-rabbit antibodies (1:5 000, Dako, Burlington, ON, CA) conjugated to horseradish peroxidase were used to detect immunoreactive proteins using ECL prime western blotting detection reagent (GE Healthcare Life Sciences, Baie D'Urfe, QC, CA) and Kodak BioMax MR film (Kodak, Rochester, NY, USA). Secondary anti-mouse conjugated to alkaline phosphatase (Jackson Immunoresearch Laboratories Inc., West Grove, PA) was developed with nitro-blue tetrazolium (Thermo Fisher Scientific, Waltham, MA, USA) and 5-bromo-4chloro-3-indolylphosphate (Thermo Fisher Scientific, Waltham, MA, USA) for chromogenic detection of proteins. The western blots were scanned with an HP scanner and the images were not manipulated except to adjust the brightness/contrast and this was done simultaneously to the entire blot. Quantification was performed with the ImageJ software (NIH, Bethesda, MD, USA).

NWL caspase inhibitors and Casp6 transgenic mice: Casp6 transgenic mouse model: All animal procedures followed the Canadian Council on Animal Care guidelines and were approved by the McGill Animal care committees. Sixteen to 20 month old C57BL/6 J mice were bred and aged in the pathogen-free Goodman Cancer Research Centre Mouse Transgenic Facility at McGill University. Mice were housed in a temperature-controlled room at 22 °C and were kept on a 12 h light/dark cycle. Food and water were available at libitum. Casp6 overexpressing mice (KI/Cre) express Casp6p20p10 under the CAG promoter (CMV immediate early enchancer/chicken β-actin promoter fusion) in the CA1 pyramidal cell layer of the hippocampus under the control of calmodulin kinase IIa (CAMKIIa)-regulated Cre expression

(LeBlanc et al., 2014). No obvious toxicity was observed after a one month treatment of NWL-117 on mice (**Appendix 1**).

NWL treatments: Only males were used and littermates from each genotype (wild type (WT)/WT, WT/Cre, & knock-in (KI/)Cre) were tested together. The experimenter was blind to genotype and treatment groups. Mice were administered 20 mg/kg NWL-117 or physiological saline (0.9% NaCl) by intraperitoneal injections two times 48 h apart. Injection volumes did not exceed 150 µL of 10 mg/mL NWL-117 prepared in physiological saline. Blood brain barrier permeability of NWL-117 caspase inhibitor: Briefly, 18–22 month old Casp6 mice were anesthetised with isoflurane, warmed with a heating blanket, and their physiological vitals (heart rate, body temperature, and respiration) monitored. The skin over the mouse's neck was shaved, xylocaine applied, and an incision was made along the midline. Under a surgical microscope, the right carotid artery was gently separated from surrounding tissue. Two suture threads were placed at the proximal and distal ends of the carotid, and a small incision was made along the carotid wall. A micro-catheter (attached to a 1 ml syringe controlled by a micropump) was inserted and pushed to the entrance of the internal carotid artery. The catheter was secured in place using suture thread. NWL-117 (20 mg/kg) was infused via the micro-catheter using a pump set at 50 µL/min (total volume between 64 µL and 130 µL). After 5 min, blood was collected by intra-cardiac puncture, the mouse was perfused through the heart with ice cold saline for 2–3 min. The brain was removed and hippocampi were dissected and frozen on dry ice and stored. Samples were sent to the Biopharmacy platform at the University of Montreal (Quebec, Canada) for liquid chromatography and tandem mass spectrometry analysis. The integrity of the blood-brain barrier was confirmed by injecting 3% Evan's blue solution in 20 month old Casp6 mice. Mouse cognitive analysis by novel object recognition: Mice were handled during 5 min for one week prior to behavioral tests. Novel object recognition (NOR) task was administered in three phases: habituation, familiarization (pre-exposure), and test phase. For habituation, mice were placed in the NOR box (80 cm x 80 cm, Stoelting Co, Wood Dale, IL, USA) for 5 min. After 24 h, the pre-exposure phase was initiated by allowing the animals to explore two identical objects inside the NOR box. Then, following a 2 h gap, mice were re-introduced to the NOR box which now contained a familiar and a novel object. The position of the novel object was counterbalanced between animals to avoid any bias related to a

preference in the location of the new object and the use of potential confounding spatial cues. The objects were located in the middle of the NW and SE quadrants of the box, equidistantly from the box corners and from each other. The mice were placed in the middle of the SW quadrant. Washing the box and objects with 70% ethanol eliminated odour cues. The number of times touching each object was manually recorded, while the total distance, percent time moving, and number of entries into virtual cells were recorded using the HVS 2100 automated video tracking system (HVS Image, Buckingham, UK). Animals whose exploration was considered insufficient to allow recognition (<10 s per object) during the familiarization phase were excluded from analysis. Different object sets were used in the pre- and post-tests. Immunohistochemistry on mouse brain slices: Following behavioural analysis, animals were anaesthetized under isoflurane and perfused intracardially with ice cold saline for 7 min and 4% paraformaldehyde for 20 min. Mice brains were removed and stored in 10% neutral-buffered formalin (Thermo Fischer Scientific, Waltham, MA, USA) for 24 h then dehydrated in 70% ethanol for 24 h or less. Brains were embedded in paraffin and cut using a vibratome at the histology platform of the Institute for Research on Immunology and Cancer (U Montreal). Slides containing 4 µm thick sections of the anterior hippocampus were deparaffinized in xylene (Thermo Fisher Scientific, Waltham, MA, USA), and rehydrated before demasking in antigen retrieval buffer (10 mM Tris, 1 mM EDTA, pH 9; or 10 mM tri-sodium citrate, pH 6 for synaptophysin) for 20 min at 97 °C in the Pascal Dako Cytomation (Dako, Burlington, ON, CA). The immunostaining procedure was automated using the Dako Autostainer Plus slide processor and the EnVision Flex system (Dako, Burlington, ON, CA). Slides were treated with peroxidase for 5 min, then rinsed, blocked with Serum-Free Protein Block (Dako, Burlington, ON, CA) for 30 min, and incubated with either Iba1 (1: 2 000, Wako, Richmond, VA, USA), TubΔCasp6 (1: 5 000), or synaptophysin (1: 8 000, Sigma, Oakville, ON, CA) antibodies diluted in EnVision Flex Antibody Diluent (Dako, Burlington, ON, CA) for 30 min. After rinsing, the mouse brain slices were incubated with secondary rabbit-horseradish peroxidase antibody (Dako, Burlington, ON, CA) for 30 min and diaminobenzidine (Dako, Burlington, ON, CA) for 10 min before counterstaining with hematoxylin (Dako, Burlington, ON, CA). Slides were scanned using the MIRAX SCAN (Zeiss, Oberkochen, Germany) and analyzed using the ImageJ software (NIH, Bethesda, MD, USA) by measuring the area of positive immunoreactivity over the total area in square microns.

Statistical analysis: Statistical analysis of data was performed using Graphpad Prism 5.0 (La Jolla, CA, USA). The analyses were done with ANOVA followed by post-hoc analyses as indicated for each test in the figure legends. Alternatively, a student t-test was done to compare between two samples as indicated in figure legends. Significance was set at $p<0.05$ for all experiments.

3.7 Acknowledgements

We would like to thank Dr. Vikas Kaushal, Dr. Joseph Flores, and Andrea Hébert-Losier for culturing human primary neurons, Dr. Benedicte Foveau for technical help with immunohistochemical staining of mice brains against synaptophysin, Dr. Xing-Kang Tong for performing the cardiac puncture and perfusion on mice for the blood-brain barrier permeability experiment, Martin Jutras for analyzing blood and hippocampal samples by liquid chromatography tandem mass spectrometry, the animal quarters staff for maintaining the mice, and New World Laboratories Inc. specifically, Richard Frenette and Dr. Benoit Bachand, for providing NWL-117 and NWL-154 inhibitors.

Prateep Pakavathkumar is the recipient of a Fonds de recherche Québec-Santé scholarship (2011–2013) and the FRQ-S Alzheimer Society of Canada doctoral award (2014–2017). Anastasia Noël received a postdoctoral scholarship from the Alzheimer Society of Canada (2013–2015). This work was supported by funds from the Canadian Institutes of Health Research (CIHR) MOP-142417 to EH and from the Canadian Foundation for Innovation, CIHR MOP-243413-BCA-CGAG45097, and the JGH Foundation to ALB. The funding agencies did not play a role in the design of the study and collection, analysis, and interpretation of data and in writing the manuscript.

3.8 Figures and legends

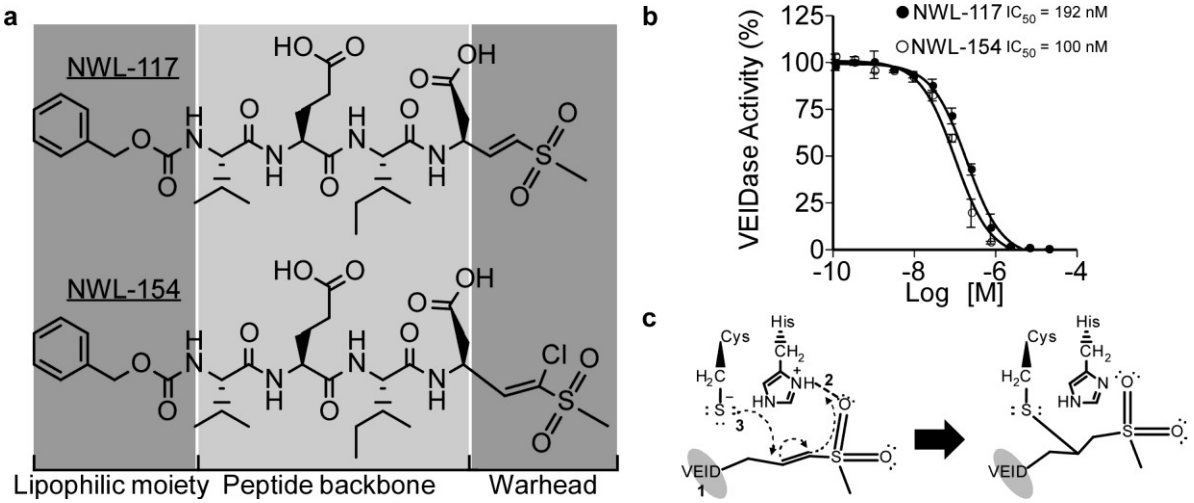

Fig. 3.1 NWL inhibitors are irreversible peptide vinyl sulfone inhibitors of Casp6.

a Chemical structures of NWL-117 and NWL-154 highlighting the lipophilic moiety, the peptide backbone, and the chemical warhead. **b** Dose-response curve for NWL-117 (closed circle, IC50 =192 nM) or NWL-154 (open circle, IC50 =100 nM) against 20 nM recombinant active site-titrated Casp6. Data represent the mean ± S.D. for three independent experiments. **c** Schematic representation of the mechanism for covalent linkage of vinyl sulfone warheads to the catalytic cysteine of Casp6. 1 Peptide (VEID) binds to the substrate-binding pocket. 2 This interaction allows the sulfone moiety to form a hydrogen bond with the protonated imidazole ring of histidine. 3 The sulfur from the catalytic cysteine performs a nucleophilic attack on the β-carbon of the vinyl group, which triggers a movement of electrons leading to the protonation of the α-carbon. The result is a covalent link between the vinyl sulfone inhibitor and Casp6.

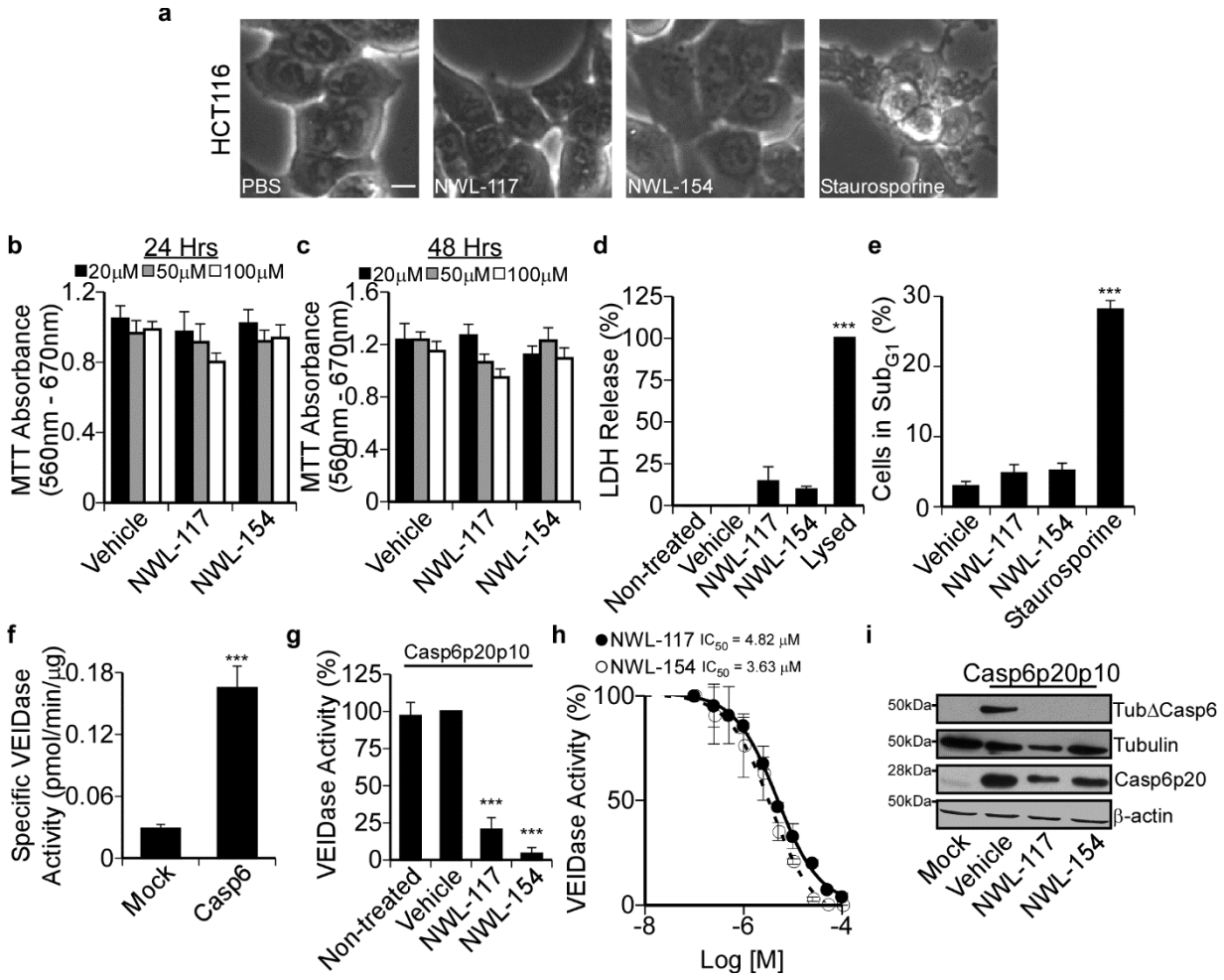

Fig. 3.2 Non-toxic concentrations of NWL-117 and −154 inhibit Casp6 activity in HCT116 cells.

a Phase contrast microscope images of HCT116 cells treated with phosphate-buffered saline, 100 μM NWL inhibitors, or 2 μM staurosporine for 24 h. Scale bar represents 10 μm. **b** & **c** MTT absorbance following treatment with PBS, NWL-117, or NWL-154 at 20, 50, or 100 μM for 24 h (b) or 48 h (c). No statistical differences were found by two-way ANOVA with Bonferroni post-tests. **d** Lactate dehydrogenase activity in untreated cells, or treated with PBS, 100 μM NWL inhibitors, or lysed with 0.9% Triton X-100 for 24 h. **e** Quantification of the sub-G1 population following cell cycle analysis in PBS, 100 μM NWL inhibitors, or 2 μM staurosporine treatment for 24 h. **f** VEIDase activity in pCep4β-transfected (mock) or pCep4β-Casp6p20p10 transfected HCT116 cells. Data represent the mean ± SEM of five independent experiments. Statistical analysis was performed using an unpaired two-tailed t-test (*** $p<0.01$).

g Casp6 VEIDase activity in cellular extracts from pCep4β-Casp6p20p10-transfected HCT116 cells treated with PBS, NWL-117 or NWL-154 at 100 μM for 2 h. **h** Dose-response curve for NWL-117 (closed circle, IC50 =4.82μM) and NWL-154 (open circle, IC50 =3.63 μM) in pCep4β-Casp6p20p10-transfected HCT116 cells treated for 2 h. **i** Western blot analysis of samples from panel f and g for α-tubulin-cleaved by Casp6 (TubΔCasp6), α-tubulin (Tubulin), active Casp6 p20 subunit (Casp6p20), and β-actin. Casp6 expression was allowed for 24 h before treatment with inhibitors in all transfection experiments. For panels b-g, data represent the mean of three independent experiments ± SEM and were analyzed by one-way ANOVA ($p<0.0001$) with post hoc Dunnett's multiple comparison test comparing to vehicle-treated (***denotes $p<0.001$) unless specified otherwise.

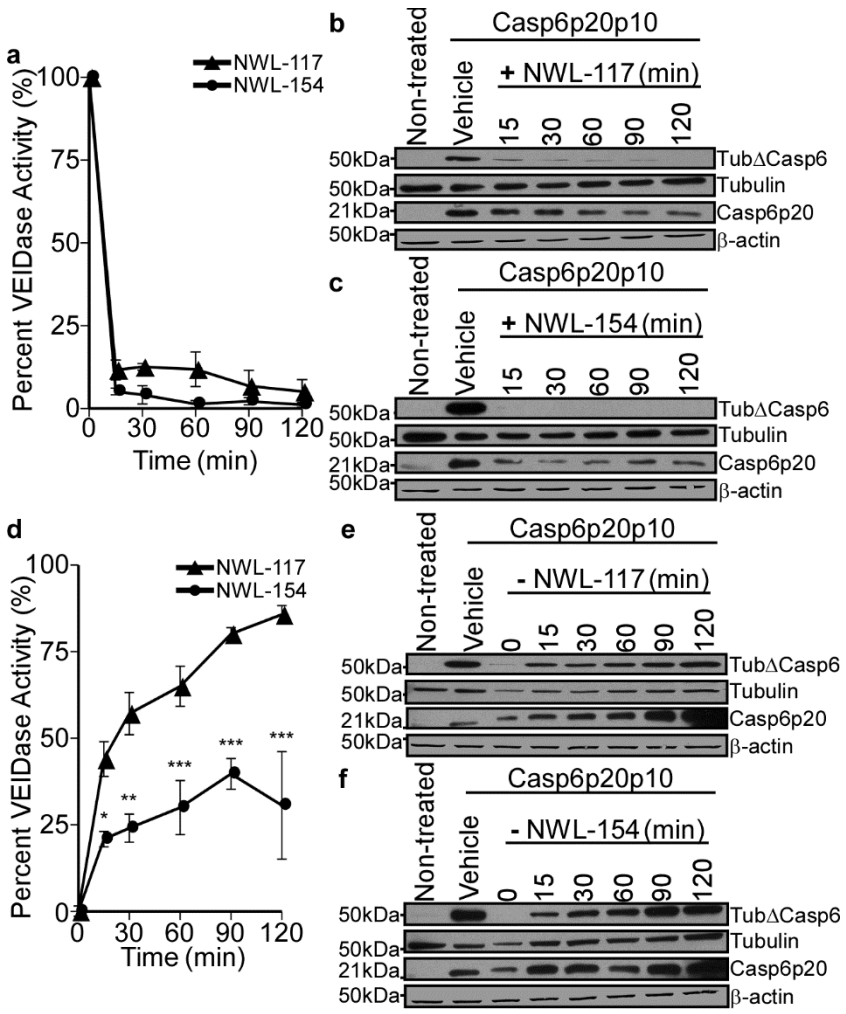

Fig. 3.3 NWL-117 and -154 rapidly inhibit Casp6 activity in HCT116 cells.

a Percent VEIDase activity from cellular protein extracts of Casp6-transfected HCT116 cells treated with either NWL-117 (closed triangle) or -154 (closed circle) at 100 μM for 0, 15, 30, 60, 90, or 120 min. No statistical significant differences were obtained between NWL-117 and NWL-154. **b & c** Western blot analysis of samples from panel (a) of NWL-117 (b) and NWL-154 (c) for α-tubulin-cleaved by Casp6 (TubΔCasp6), α-tubulin (Tubulin), active Casp6 p20 subunit (Casp6p20), and β-actin. **d** Percent VEIDase activity from cellular extracts after 2 h of treatment with 100 μM NWL-117 (closed triangle) or -154 (closed circle) in Casp6-transfected HCT116 cells followed by the removal of the inhibitors for 0, 15, 30, 60, 90, or 120 min. **e & f** Western blot analysis of samples from panel (d) of NWL-117 (e) and NWL-154 (f) for α-tubulin-cleaved by Casp6 (TubΔCasp6), α-tubulin (Tubulin), active Casp6 p20 subunit (Casp6p20), and β-actin. For panels (a) & (d), data represent the mean ± SEM of three

independent experiments. Statistical analysis was performed by two-way ANOVA (((compound ($p=0.0010$), time ($p<0.0001$), interaction ($p=0.4546$)); (compound ($p<0.0001$), time ($p<0.0001$), interaction ($p=0.0054$))), respectively, with Bonferroni post-tests (*$p<0.05$, **$p<0.01$, ***$p<0.001$).

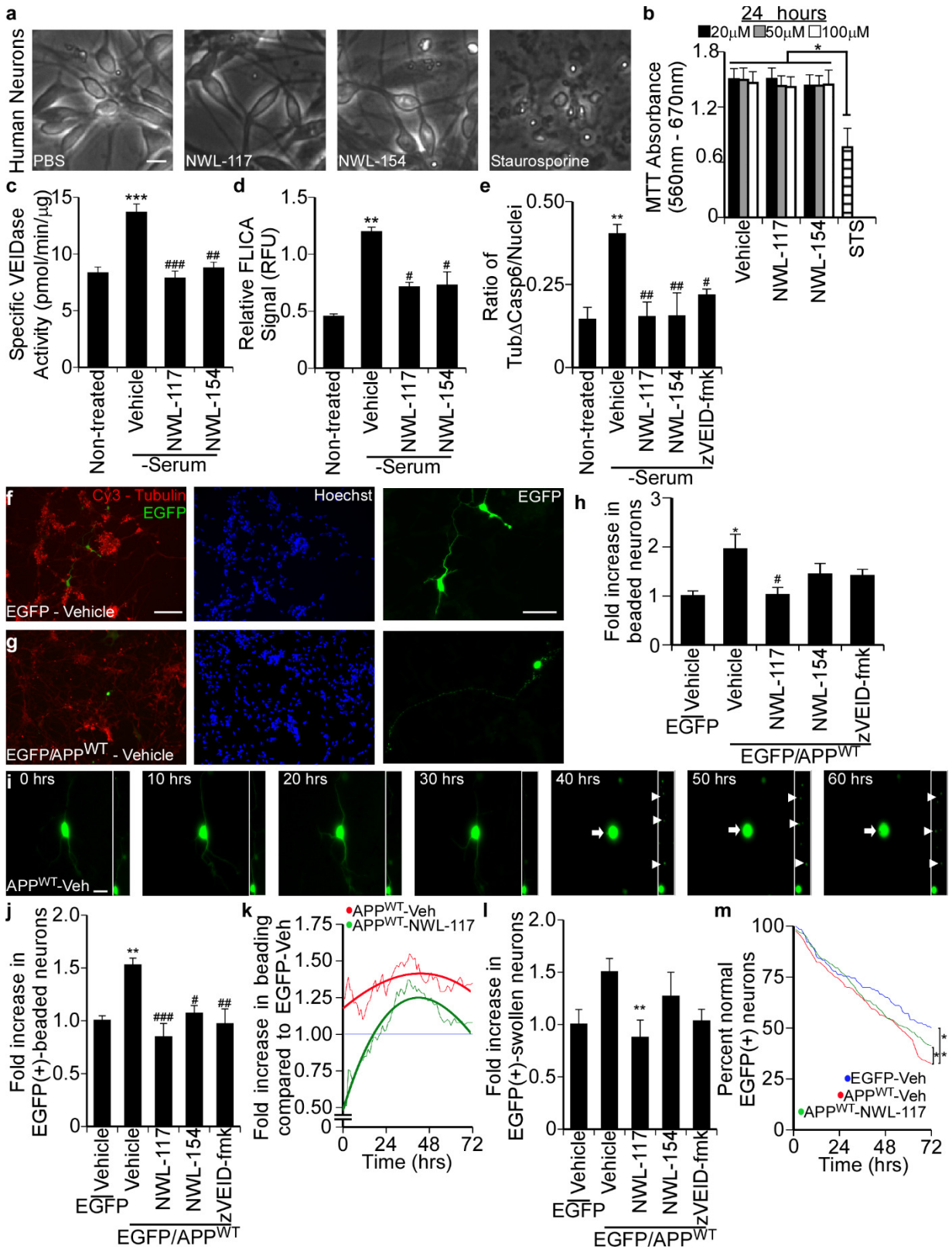
a
Human Neurons
PBS
NWL-117
NWL-154
Staurosporine
b
24 hours
20μM 50μM 100μM
MTT Absorbance (560nm - 670nm)
Vehicle
NWL-117
NWL-154
STS
c
Specific VEIDase Activity (pmol/min/μg)
Non-treated
Vehicle
NWL-117
NWL-154
-Serum
d
Relative FLICA Signal (RFU)
e
Ratio of TubΔCasp6/Nuclei
zVEID-fmk
f
Cy3 - Tubulin
EGFP
Hoechst
EGFP - Vehicle
g
EGFP/APPWT - Vehicle
h
Fold increase in beaded neurons
EGFP
EGFP/APPWT
i
0 hrs
10 hrs
20 hrs
30 hrs
40 hrs
50 hrs
60 hrs
APPWT-Veh
j
Fold increase in EGFP(+)-beaded neurons
k
APPWT-Veh
APPWT-NWL-117
Fold increase in beading compared to EGFP-Veh
Time (hrs)
l
Fold increase in EGFP(+)-swollen neurons
m
Percent normal EGFP(+) neurons
EGFP-Veh
APPWT-Veh
APPWT-NWL-117

Fig. 3.4 Non-toxic concentrations of NWL-117 and -154 inhibit Casp6 activity in primary human neurons.

a Micrographs of primary human neurons treated with PBS vehicle, 100 μM NWL inhibitors, or 2 μM staurosporine for 24 h. Scale bar represents 10 μm. **b** MTT absorbance following treatment with PBS, NWL-117, or NWL-154 at 20, 50, or 100 μM or 2 μM staurosporine for 24 h (n=4, one-way ANOVA ($p=0.0169$), Tukey's multiple comparison test (*$p<0.05$)). **c** VEIDase activity in neuronal extracts following treatment with PBS, 100 μM NWL-117 (n=5), or 154 (n=2) for 2 h (one-way ANOVA ($p<0.0001$)). **d** Casp6 FLICA assay (one-way ANOVA ($p=0.0041$)). **e** Quantification of the number of TubΔCasp6 beads/nuclei in Supplementary Figure S2b (one-way ANOVA ($p=0.0095$)). **f–h** Fluorescence micrographs following transfections with pBudEGFP (f) or pBudEGFP/APP^{WT} (g) stained for α-tubulin (Cy3), Hoechst, and quantified (h) (one-way ANOVA ($p=0.0385$)). Scale bar represents 100 μm for merge and Hoechst panels, and 50 μm for EGFP panel. **i** Live-imaging fluorescence micrographs from 0 to 60 h of a human neuron transfected with pBudEGFP/APP^{WT} and pre-treated with vehicle. The inset highlights the neurite extending upward. Arrowheads indicate agglomerates of EGFP protein within the axonal membrane while arrows mark a rounded cell body. Scale bar represents 10 μm. **j–m** Quantification of panel (i) for overall fold increased beaded neurites (j), fold increased beaded neurons at specific times (k), overall fold increase swollen neuronal soma (l), or normal EGFP positive neurons (m). For panels (c–e, h), and (j–k) data represent the mean ± SEM ($n\geq3$), one-way ANOVA ($p=0.0005$ for j, $p=0.0264$ for k, and post hoc tests were performed with Dunnett's multiple comparison test (*compares to serum (+) or EGFP-vehicle: *$p<0.05$, **$p<0.01$, ***$p<0.001$; # compares to serum (−) with vehicle or to EGFP/APP^{WT}-vehicle: # $p<0.05$, ## $p<0.01$, ### $p<0.001$) unless stated otherwise. For panel (m), log-rank Mantel-Cox test was performed to compare between curves.

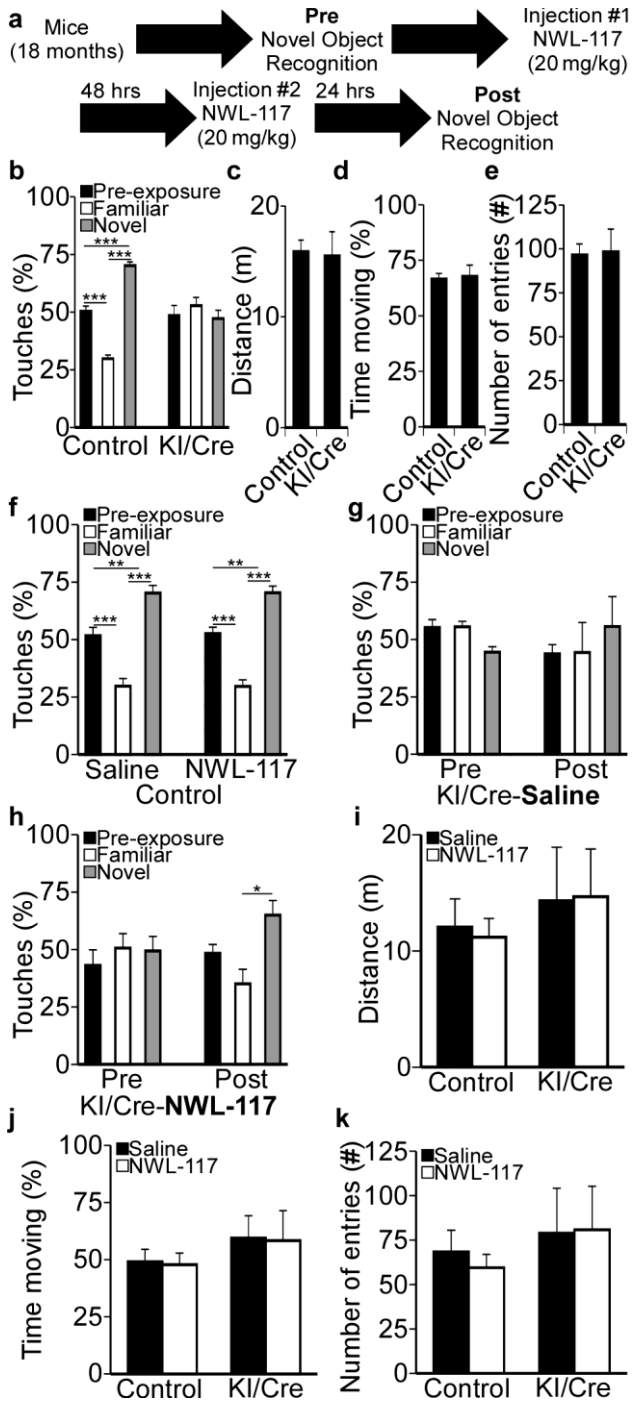

Fig. 3.5 Acute NWL-117 administration reverses novel object recognition deficits in Casp6-overexpressing KI/Cre mice.

a Experimental design for the in vivo study highlighting the novel object recognition (NOR) tests and injections. **b** Percent touches of objects during the NOR task in WT/ WT and WT/Cre

controls (n=16), and Casp6-expressing KI/Cre (n=9) mice prior to injections. Statistical analysis was performed by one-way ANOVA ($p<0.0001$). **c** Distance traveled, (**d**) percent time moving, and (**e**) number of cell entries of control (n=16) and KI/Cre (n=9) mice. Statistical analysis was performed by unpaired two-tailed t test. No significant differences were found in c-e. **f** Percent touches of objects during the NOR task following saline (n=8) or 20 mg/Kg NWL-117 (n=8) injections in control mice. Statistical analysis was performed by one-way ANOVA ($p<0.0001$). **g** Percent touches of objects during the NOR task in pre- and post-injections (n=4) saline injections in KI/Cre mice. Statistical analysis was performed by repeated measures ANOVA ($p=0.7661$). **h** Percent touches of objects during the NOR task in pre- and post- (n=5) 20 mg/Kg NWL-117 injections in KI/Cre mice. Statistical analysis was performed by repeated measures ANOVA ($p=0.0860$) with Bonferroni's multiple comparison test (* $p<0.05$). **i** Distance traveled, (**j**) percent time moving, and (**k**) number of cell entries of control mice injected with saline (n=8) or NWL-117 (n=8) and KI/Cre injected with saline (n=4) or NWL-117 (n=5). Statistical analysis was performed by two-way ANOVA for panels (i) to (k) and no significant differences were found. For panels (a–k), data represent the mean ± SEM and post hoc analyzes were performed using Bonferroni's multiple comparison test (*$p<0.05$, **$p<0.01$, and ***$p<0.001$) unless stated otherwise.

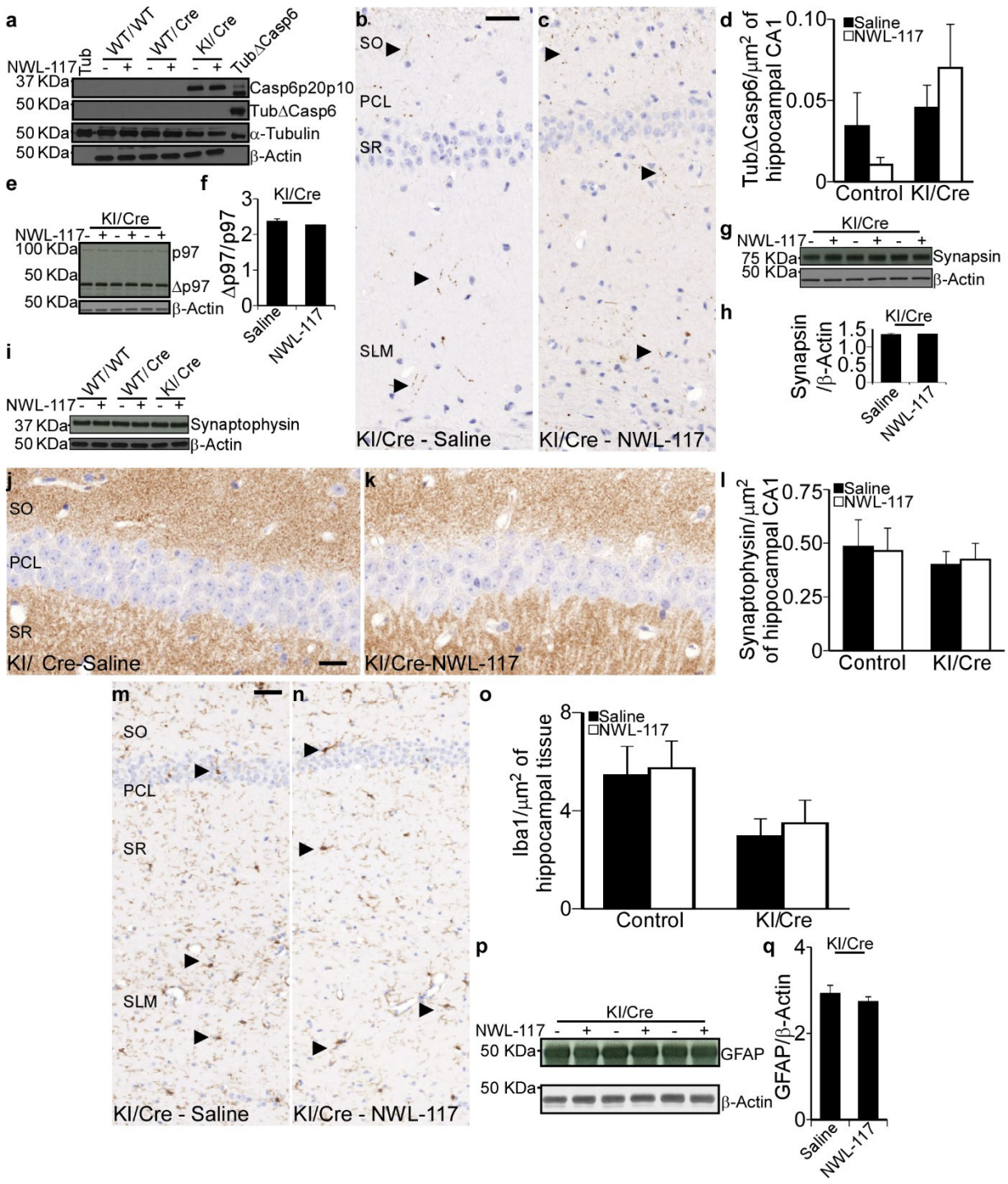

Fig. 3.6 Hippocampal levels of synaptic and glial markers are unchanged with NWL-117 treatment.

a Levels of Casp6 p20p10 (Casp6p20p10), α-tubulin-cleaved by Casp6 (TubΔCasp6), α-tubulin (Tubulin), and β-actin in hippocampal protein extracts WT/WT, WT/Cre, and KI/Cre mice

treated with saline or 20 mg/Kg NWL-117. **b & c** Immunohistochemistry of TubΔCasp6-stained hippocampi from KI/Cre mice treated with saline (b) or NWL-117 (c). Arrowheads mark some positive immunoreactivity. **d** Quantification of positive immunostaining shown in panel (b) and (c). **e** Levels of p97 and p97-cleaved by Casp6 (p97ΔCasp6) in hippocampal protein extracts of KI/Cre mice treated with saline (n=3) or NWL-117 (n=3). **f** Quantification of the levels of p97ΔCasp6/p97 shown in panel (e). **g & h** Levels of synapsin in hippocampal extracts from KI/Cre mice treated with saline (n=3) or NWL-117 (n=3) (g) and quantified in (h). **i** Levels of Synaptophysin in hippocampal protein extracts from WT/WT, WT/Cre, and KI/ Cre (Casp6 overexpressing) mice treated with saline or NWL-117. **j–l** Brightfield scans of KI/Cre-Saline (j) and NWL-117 (k) mice brains stained for synaptophysin by immunohistochemistry and quantification (l). **m & n** Iba1-stained hippocampi from KI/Cre mice treated with saline (m) or NWL117 (n). Arrowheads mark some positive immunoreactivity. **o** Quantification of the area of positive immunostaining for Iba1 over the total area of the tissue. **p** Levels of GFAP in hippocampal extracts from KI/Cre mice treated with saline (n=3) or NWL-117 (n=3). **q** Quantification of the levels of GFAP/β-actin. For panels (d), (l), and (o), data represent the mean ± SEM for each group: Control-saline (n=5), Control-NWL-117 (n=5), KI/Cre-saline (n=5), and KI/Cre-NWL-117 (n=4). Statistical analysis was performed by two-way ANOVA and no significant differences were found. For panels (f), (h), and (q), data represent the mean ± SEM and statistical analysis was performed by unpaired two-tailed t test, no significant differences were found. SO: Stratum Oriens, PCL: Pyramidal Cell layer, SR: Stratum Radiatum, SLM: Stratum Lacunosum.

3.9 Tables

Table 3.1 Half-maximal inhibitory concentrations (IC50) of NWL-117 and NWL-154 against recombinant Caspase-1 to -10*

Cpd No.	MW±	C1	C2	C3	C4	C5	C6	C7	C8	C9	C10
NWL-117	668	2.7	>100	6.96	0.38	19.54	0.60	>100	0.66	0.79	0.13
NWL-154	703	3.85	>100	1.34	1.80	4.19	0.23	>100	0.53	6.40	0.19

* IC_{50} values are measured in μM

± Molecular weight in g/mol

Table 3.2 Hippocampal and plasma concentrations of NWL-117 following injections through the internal carotid artery of mice*

Animal #	Hippocampus	Plasma	Ratio±
1	193	48521	0.004
2	816	3416	0.239
3	67.9	8998	0.008
4	356	7408	0.048
5	879	25425	0.035

*Concentrations are reported in nM
±Ratio of [hippocampal]/[plasma]

3.10 Supplementary information

3.10.1 Figures and legends

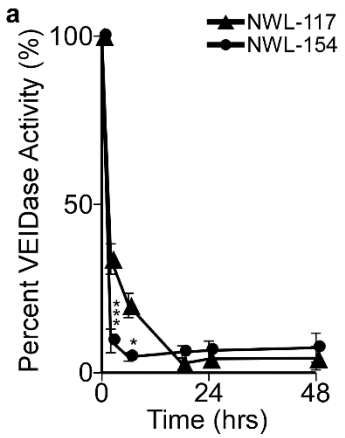

Supplemental Figure S3.1 NWL inhibitors sustain Caspase-6 inhibition up to 48 hours. **a** Percent VEIDase activity from cellular protein extracts of pCep4β-Casp6p20p10-transfected HCT116 cells treated with either PEG-soluble NWL-117 (closed triangle) or -154 (closed circle) at 100 μM for 0, 2, 6, 18, 24, or 48 hours. Data represent the mean ± SEM of three independent experiments. Statistical analysis was performed by two-way ANOVA (compound ($p = 0.0240$), time ($p < 0.0001$), interaction ($p = 0.0018$)) with Bonferroni post tests (* $p < 0.05$, *** $p < 0.001$).

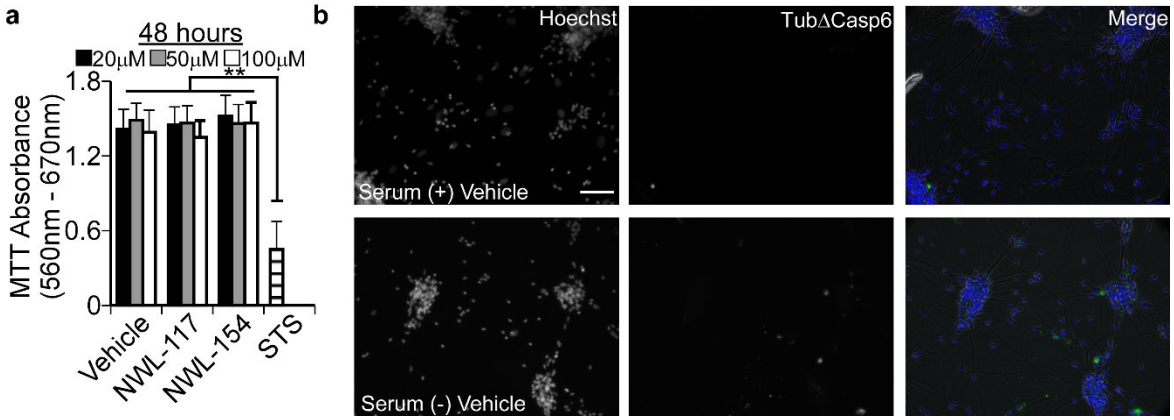

Supplemental Figure S3.2 NWL inhibitors do not alter mitochondrial activity after 48 hours of treatment and serum-deprivation increases TubΔCasp6 immunoreactivity.

a MTT absorbance from human neurons treated with PBS vehicle, water-soluble NWL-117, or NWL-154 at 20, 50, or 100 μM or 2 μM staurosporine for 48 hours. Data represent the mean ± SEM of at least three independent experiments. Statistical analysis was done by one-way ANOVA with Tukey's multiple comparison test ($p = 0.0024$) (* compares to staurosporine treatment: ** $p < 0.01$) unless stated otherwise. **b** Phase contrast and fluorescence micrographs of human neurons transfected with pBudEGFP or pBudEGFP/APP^{WT} treated with vehicle and stained for α-tubulin-cleaved by Casp6 (TubΔCasp6) (Alexa 488) and Hoechst before or after serum-deprivation. Scale bar represents 100 μm.

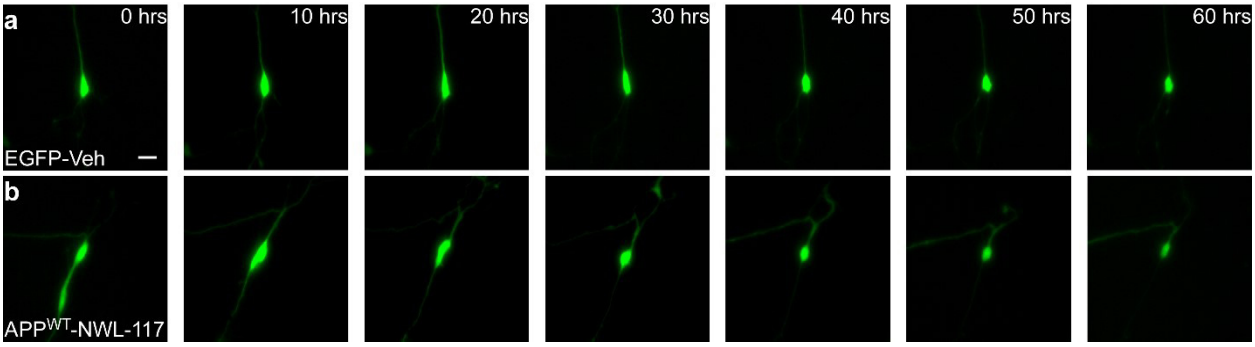

Supplemental Figure S3.3 Time-lapse imaging in EGFP-Veh and APP^{WT}-NWL-117-treated primary human neurons.

a & b Live imaging fluorescence micrographs at 0, 10, 20, 30, 40, 50, and 60 hours of a human neuron transfected with pBudEGFP or pBudEGFP/APP^{WT}. Primary human neurons were pre-treated with vehicle (a) or 100 μM water-soluble NWL-117 (b) starting 2 hours prior to transfection. Scale bar represents 10 μm.

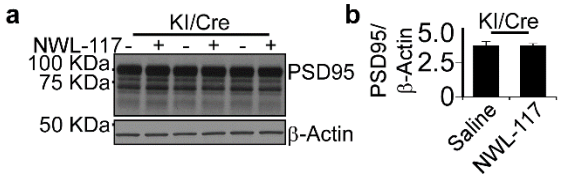

Supplemental figure S3.4 PSD95 levels are unchanged in hippocampi from NWL-117 treated mice.

a & b Levels of PSD95 in hippocampal extracts from KI/Cre mice treated with saline (n=3) or 20 mg/Kg water-soluble NWL-117 (n=3) (a) and quantified in (b). For panel b, data represent the mean ± SEM. Statistical analysis was performed by unpaired two-tailed t test and no significant differences were found.

4. Discussion

As shown in this thesis, Caspase-6 inhibition was achieved by oxidation with methylene blue or irreversible competitive inhibition by NWL compounds *in vitro*, in cells, in human neurons, and *in vivo*. In addition, a proof-of-concept for developing Caspase-6 inhibitors was demonstrated by the neuroprotective effects of NWL inhibitors in human neurons and in mice. Human neurons were protected from axonal degeneration, whereas mice were rescued from cognitive deficits in models driven by Caspase-6 activity. Yet, neither inhibitor could provide strict selectivity for Caspase-6 among all other caspases. This lack of selectivity will hinder progress towards clinical trials due to potential increases in toxicity and ambiguity in interpreting results. Thus, this thesis will discuss what is known about Caspase-6 inhibition and toxicity, mechanisms by which specific Caspase-6 inhibition can be achieved, the overall difficulties in developing drugs for CNS diseases, and the relative importance Caspase-6 holds among other causative hypotheses in AD.

4.1 Assessing whether Caspase-6 inhibition will produce adverse effects

To assess whether Caspase-6 inhibition will result in adverse effects, it is necessary to conduct safety studies in rodents. Very few pharmacological Caspase-6 inhibitors have been tested for pre-clinical toxicity in animal models. However, several Caspase-6-deficient mice have been generated shedding some light on the potential for toxicity (Zheng et al., 1999; Watanabe et al., 2008; Uribe et al., 2012). Yet, genetic compensatory mechanisms present in certain mice strains make it difficult to predict whether Caspase-6 inhibition in humans is a viable therapeutic option (Gafni et al., 2012; Wong et al., 2015). Additional research to assess safety profiles will be required.

4.1.1 Information from genetic Caspase-6 ablation models

Despite the Caspase-6 functions previously described (**see sections 1.5, 1.10, & 1.11**), several different studies have shown that genetic Caspase-6 ablation in mice does not produce an obvious phenotype (Zheng et al., 1999; Watanabe et al., 2008; Gafni et al., 2012; Uribe et

al., 2012). These results should be taken lightly considering that genetic compensation is mouse strain specific and produces different outcomes. This is evident in Caspase-3-ablated animals bred in a mixed background between 129/SvJ and C57BL/6 compared to those bred in a pure C57BL/6 background (Kuida et al., 1996; Zheng et al., 1999). Caspase-3 deficiency is perinatally lethal in the mixed background specifically, whereas C57BL/6 mice develop normally. When analysed in greater detail, Caspase-6 deficient mice had B cells that accelerated into the G1 phase of the cell cycle leading to increased differentiation into antibody producing plasma cells (Watanabe et al., 2008). Moreover, striatal and cortical volumes were increased in another Caspase-6 knockout model which displayed a hypoactive phenotype and learning deficits by NOR (Uribe et al., 2012). Caspase-6-ablated mice shared an indistinguishable phenotype from WT mice in an inflammation-induced tumorigenesis model (Foveau et al., 2014). Taken together, genetic ablation does not produce overtly abnormal phenotypes in mice supporting that Caspase-6 inhibition could be well tolerated. The identification of inactivating Caspase-6 SNPs in humans may provide some clue as to compensatory mechanisms present in developing humans. Nevertheless, more rigorous analysis is required to predict toxicity in a heterogeneous human population.

4.1.2 Caspase-6 inhibitors show few signs of toxicity in mice or humans

Methylene blue has been approved for the treatment of several indications before the advent of the Food and Drug Administration. Methylene blue is used to treat methemoglobinemias, malaria, and ifosfamide-induced encephalopathy because of its oxidation-reduction capacity (Kupfer et al., 1994; Bradberry, 2003; Coulibaly et al., 2009). As a stain, methylene blue is used for parathyroid imaging and lymph node biopsies (Dudley, 1971; Varghese et al., 2007). Studies have shown that methylene blue is toxic only when used outside the therapeutic window especially in neonates (Albert et al., 2003). Yet, a case report described a child treated with 16-fold higher methylene blue amounts than required and found no adverse effects apart from a bluish skin tone (Blass and Fung, 1976). The oral lethal dose in mice and rats is 4-10-fold greater than the therapeutic dose used in human clinical trials (Oz et al., 2011; Wischik et al., 2015). In rodents, methylene blue treatment at high doses up to 24 months slightly increased the incidence of lymphomas (Oz et al., 2011), which may be attributed to Caspase-3 inhibition as shown in this thesis. Indirectly, methylene blue's enviable safety profile suggests

that Caspase-6 inhibition may not lead to clinically relevant adverse effects, albeit in a context where methylene blue exerts several other effects.

More specific Caspase-6 inhibitors have few reported adverse effects in mice and human tissues. NWL compounds, as described in this thesis, did not show toxicity based on mitochondrial reductive potential, LDH release, sub-G_1 populations, and cell morphology in HCT116 and human primary neurons. In mice, acute NWL-117 injections in Caspase-6-overexpressing mice did not result in behavioural or pathological abnormalities. Chronic treatment in CD11 mice also produced few adverse events (**Appendix I**). Moreover, the peptide based Caspase-6 inhibitor ED11 also showed no toxicity in a HD mouse model (Aharony et al., 2015), while a 1,4-disubstituted-1,2,3-triazole showed a rescue from toxicity in rat cortical and striatal neurons (Leyva et al., 2010). Based on these results, Caspase-6 inhibition by small molecules or peptides did not lead to toxicity in human tissue or in rodents. More studies addressing Caspase-6 inhibition by pharmacological agents in biological settings will help establish the therapeutic window for Caspase-6 inhibition in humans. The findings in this thesis contribute significantly in building that framework, but ultimately, a Phase I clinical trial with a selective Caspase-6 inhibitor will provide the most conclusive data.

4.2 Other mechanisms to achieve specific Caspase-6 inhibition

Most of the mechanisms presented in this thesis dealt with inhibiting the active Caspase-6 enzyme. All the active site-directed inhibitors showed overlapping inhibitory activities against different caspases. A few research groups have focused on the unique structure of pro-Caspase-6 to develop selective inhibitors (Stanger et al., 2012; Murray et al., 2014), yet other mechanisms for inhibition are still available to explore. In this section, theoretical approaches based on mechanisms used for other diseases or targets will be presented for use against Caspase-6.

4.2.1 CRISPR-Cas9-mediated transcriptional blockade

Very little is known about transcriptional Caspase-6 regulation (**see section 1.6**). One way to identify important transcription factor binding sites is to use the clustered regularly interspaced palindromic repeats (CRISPR)-Cas9 system. This system was identified as an innate immunity mechanism present in bacteria against bacteriophages (Mojica et al., 2005; Barrangou

et al., 2007). CRISPR worked in conjunction with the nuclease Cas9 through CRISPR RNA duplexing with trans-activating CRISPR RNA to target and cleave DNA near a protospacer adjacent motif (Brouns et al., 2008; Deltcheva et al., 2011). This bacterial system was capable of performing human and mouse genome editing effectively paving the way to a new era of genetic manipulations (Cong et al., 2013). By mutating the Cas9 enzyme, the nuclease activity is abrogated while maintaining the CRISPR-Cas9 complex at a targeted DNA sequence which efficiently represses transcription (Qi et al., 2013). This method was used in a recent study identifying the transcription factor AP-1 as a downstream effector of APOE4-mediated Aβ production (Huang et al., 2017). This approach can be used to identify key transcription factor binding sites in the Caspase-6 promoter. Following those studies, *CASP6* specific and efficient transcriptional repression can be achieved using the nuclease deficient CRISPR-Cas9. This method will overcome the difficulties currently observed against targeting Caspase-6 protein. Moreover, Caspase-6 protein is upregulated with age in humans, with little to no brain immunoreactivity in individuals below the age of 45 (Guo et al., 2004; Godefroy et al., 2013). However, compared to using pharmacological inhibitors, transcriptional repression could suppress non-enzymatic Caspase-6 functions. These functions have not been described for Caspase-6, but they have been suggested for Caspase-2 (Sohn et al., 2011). With respect to delivery, adeno-associated viruses can be packaged with CRISPR-Cas9 and injected intravenously to observe effects in the liver (Ran et al., 2015). If this does not allow brain penetrance, invasive surgery may be required for local delivery. Researchers remain hopeful that novel methods for administering gene therapy will arise soon. Hence, transcriptional *CASP6* repression may become an amenable therapeutic avenue.

4.2.2 Antisense oligonucleotides to destabilize RNA or promote splicing into Caspase-6β

Antisense oligonucleotides (ASOs) may also represent an important therapeutic approach for Caspase-6 inhibition. These DNA polymers heterodimerize to sequence specific RNA to induce cleavage by RNAse H1 in mammalian cells (Walder and Walder, 1988). Akin to RNA interference technology, ASOs lead to translational repression through mRNA degradation with the added advantage of not requiring to be packaged into viruses. In fact, ASOs

can be directly injected into the CSF intrathecally to allow complete brain penetrance without severe adverse events (Miller et al., 2013). ASO treatment doubled the survival of amyotrophic lateral sclerosis mice harboring a superoxide dismutase 1 mutation (Smith et al., 2006). A similar approach has been tested in HD whereby transient infusion with ASOs targeting mhtt mRNA slowed down and reversed HD phenotypes in mice (Kordasiewicz et al., 2012). This method also worked to reduce htt protein expression in the brain of non-human primates. Therefore, it is feasible to target Caspase-6 mRNA in the brain through ASOs injected intrathecally in AD patients.

Another avenue to consider is the use of ASOs to alter Caspase-6 mRNA splicing. Spinal muscular atrophy is an autosomal recessive disease that results from survival of motor neurons (SMN1) loss of function (Lefebvre et al., 1995). Luckily, a similar protein, SMN2, is found in humans, however a nucleotide difference in exon 7 results in exon exclusion during splicing and subsequent degradation of the truncated protein (Cartegni and Krainer, 2002). Therapies have focused on rescuing the splicing in SMN2 mRNA using ASOs. This was successfully performed using a modified ASO intrathecally injected in children and infants suffering from spinal muscular atrophy (Chiriboga et al., 2016; Finkel et al., 2016). It was recently announced during the ADPD 2017 Conference in Vienna that the ASO developed by Ionis pharmaceuticals has been approved by the Food and Drug Administration for spinal muscular atrophy treatment. To apply this to Caspase-6, we need to understand the biology behind Caspase-6 mRNA splicing into Caspase-6α and Caspase-6β. If Caspase-6 mRNA could be manipulated to favour splicing into the catalytically inactive Caspase-6β isoform using ASOs, Caspase-6 activity would be inhibited. In-depth analysis on Caspase-6β signalling pathways may also be required since very little is known about this isoform. Thus, ASOs show a lot of promise in treating patients which could be harnessed to target Caspase-6 in aging brains.

4.2.3 Sequestering Caspase-6 away from its substrates or facilitating its degradation

Changing Caspase-6's subcellular localization is an additional mechanism by which Caspase-6 substrates could be spared from cleavage. A reverse version of this mechanism was investigated in the context of developing BACE inhibitors. BACE is normally found in the

plasma membrane thus undergoes transit from the endoplasmic reticulum and the Golgi before reaching the plasma membrane. BACE's low affinity for APP results in APP processing following endocytosis in late endosomes, whereas BACE processes many of its high affinity targets earlier in the secretory pathway (Ben Halima et al., 2016). A specific inhibitor against BACE-mediated APP processing was engineered by targeting the inhibitor to the plasma membrane using a lipophilic moiety. This resulted in the inhibitor being restricted to the plasma membrane and endosomes leading to specific inhibition of APP processing by BACE and not other targets such as neuregulin (Ben Halima et al., 2016). Using this approach, serious adverse effects could be avoided by preventing a specific cleavage event. Applying this to Caspase-6, it is known that Caspase-6 is localized in both the cytosol and the nucleus where it cleaves its substrates (Klaiman et al., 2008; Waldron-Roby et al., 2015). It is not possible to target Caspase-6 in a specific subcellular compartment as done for BACE, but perhaps Caspase-6 could be tethered to a compartment wherein it does not have access to its substrates. Thus, high affinity ligands could be designed away from the active site, which offers greater chance for selectivity. The ability of these ligands to inhibit the enzyme would be irrelevant once this ligand is linked to another moiety which restricts Caspase-6 localization. Similarly, this high affinity ligand could be tethered to other small molecules that lead to protein degradation via the proteasome. Inhibitor-mediated protein degradation has been described in the past (Long et al., 2012), and may be developed for Caspase-6 as it is already susceptible to proteasomal degradation (Tounekti et al., 2004). The avenues available to inhibit Caspase-6 activity are promising and numerous, but will require a concerted effort from several specialized research groups.

4.3 Difficulties in CNS drug development for AD

CNS drug development is plagued with several obstacles leading to increased attrition rates in clinical trials. In fact, CNS drugs have failed more than cancer drugs in phase III clinical trials between 1990 and 2012 (Kesselheim et al., 2015). This is discouraging for drug development against AD since 50% of CNS drugs target dementia, depression, or are neuroleptics and 46% of CNS drugs failed because they did not meet their efficacy outcomes (Kesselheim et al., 2015). The most obvious hurdle is the presence of a blood-brain barrier that restricts passage of most molecules by inhibiting passive diffusion through tight junctions or by

actively expelling compounds through P-glycoproteins and ABC transporters (Cordon-Cardo et al., 1989). In addition, the inability to assess target occupancy to determine dosing regimens in humans leads to increased risk for toxicity. This explains why serious adverse events are another culprit of attrition in clinical trials for CNS drugs (Kesselheim et al., 2015). The lack of proper imaging tools to assess target engagement in the brain may explain the 36% phase III trial discontinuation since actual reasons are unknown. Thus, basic and translational research need to be prioritized to halt the elevated attrition rates in CNS drug development.

4.3.1 AD animal models do not possess sufficient predictive value and clinical trials have been poorly designed

There are well over one hundred AD animal models[2], yet none of them fully recapitulate the pathophysiology of the disease. Each model displays certain phenotypes such as neuronal loss, Aβ plaques, NFTs, gliosis, synaptic loss, changes in long-term potentiation or depression, or cognitive impairment. In addition, most of these models are based on the genetic mutations associated with dominantly inherited AD or frontotemporal dementias and are overexpression models. This is especially concerning since most AD cases are sporadic with no overexpression or mutations in APP, PS1, or PS2. Somehow ignoring this fact, therapies developed against Aβ or Tau have been tested in clinical trials using sporadic mild- to moderate AD patients (Doody et al., 2014; Wischik et al., 2014). As expected, these clinical trials showed no changes in cognitive performance compared to placebo. Models where APP is expressed under its endogenous promoter are emerging (Saito et al., 2014), which represents a step in the right direction. Future therapies should undergo rigorous preclinical testing in several AD mouse models with non-overlapping pathophysiology at different ages and timepoints. Then, if possible, toxicology information and efficacy should be addressed in non-human primate models. Careful consideration as to not over-interpret findings from AD mouse models is imperative to avoid failures in clinical trials. Ultimately, true efficacy cannot be determined until

[2] Based on the research model database from alzforum.org/research-models/alzheimer-disease

clinical testing, but multi-million-dollar phase III trials should be avoided at all cost when only marginal effects are observed in phase II. Thus, although animal models can recapitulate certain aspects of AD, they lack predictive value as shown by the high incidence of failures in phase III trials.

Despite these relentless failures, the amyloid hypothesis is still considered untested due to poor trial design (Abbott and Dolgin, 2016). Trials designed with better patient stratification, cognitive measures, biomarkers, and imaging techniques are underway (Sevigny et al., 2016). These therapies that originated from mice harbouring genetic disease-causing mutations need to be tested in individuals with dominantly inherited AD. This conceptual advance is obvious by the creation of the dominantly inherited AD network which are testing anti-amyloid therapies (solanezumab, gantenerumab) with results expected to be released in 2019. Therefore, the current struggles with developing disease modifying drugs against AD are due to improper animal models and trial designs.

4.3.2 AD neuropsychiatric symptoms are not a focus of animal models or clinical trials

Pre-clinical studies with new investigational drugs measure reversal in memory impairment and certain AD hallmarks as primary outcomes while ignoring neuropsychiatric symptoms. This is also the case in clinical trials where primary outcomes often rely on a battery of neurocognitive tests. The main concern is that AD is not simply a disease of cognitive and functional memory impairment. Most AD patients (80-90%) suffer from a long list of neuropsychiatric symptoms including delusions, hallucinations, agitation/aggression, depression/dysphoria, anxiety, elation/euphoria, apathy/indifference, disinhibition, irritability/lability, motor disturbances, and changes in night-time behaviour and appetite (Cummings et al., 1994). There is very little research on the interplay between these neuropsychiatric symptoms and cognitive performance. Moreover, animal models are rarely tested for most non-memory-related AD symptoms, while other symptoms are difficult to measure. Considering that research in animal models do not measure these neuropsychiatric symptoms, it may not be so surprising that all drugs that have worked in animals have so far failed in clinical trials. Again, this puts into question the predictive value of the developed AD

mouse models for AD-treatment. It may be that we do not have the knowledge necessary to prevent AD from progressing, let alone reverse the symptoms. Currently, our hope lies in finding the best early biomarkers and treat individuals with neuroprotective agents at the earliest possible timepoint.

4.3.3 Caspase-6-overexpressing mice serve as a model for age-dependent cognitive impairment

The mice used in this thesis were designed to mimic the increased Caspase-6 activity that is detected in NCI hippocampi (Ramcharitar et al., 2013a; LeBlanc et al., 2014). This increase in Caspase-6 activity represents the early changes that occur in the brain before the onset of mild cognitive impairments. As such, Caspase-6 mice do not display Aβ or Tau pathology, but Caspase-6 overexpression in the hippocampus does lead to increased glial inflammation and some synaptic protein expression abnormalities (LeBlanc et al., 2014). Instead of modelling AD, Caspase-6 mice are a better model for age-dependent episodic and spatial memory deficits. Thus, if cognitive scores remain the primary outcome for clinical efficacy against AD, Caspase-6-overexpressing mice should be considered as a model to test anti-inflammatory drugs or drugs with unknown mechanisms of action instead of dominantly inherited AD mouse models.

4.4 Caspase-6 inhibition may combat cognitive decline in AD, but cannot treat all the underlying pathologies

Two major hypotheses for AD pathogenesis have led to successful symptomatic treatment. The oldest is the cholinergic hypothesis that is based on many findings that choline acetyl transferase activity, choline uptake, and muscarinic receptor signalling are decreased in normal aging or AD (Bartus et al., 1982). The second is the excitotoxicity theory which posits that increased extracellular levels of excitatory amino acids leads to neuronal destruction (Whetsell and Shapira, 1993). This can occur due to increased sodium and chloride entry leading to cell swelling or through calcium entry via NDMA receptors leading to oxidative damage and apoptosis (Olney, 1994). These two hypotheses have led to the use of anticholinesterase inhibitors and NMDA receptor antagonist for symptomatic treatment in AD.

4.4.1 There are several risk factors for AD that may or may not lead to Caspase-6 activation

AD has many risk factors that are not directly linked to Caspase-6 activation. Epidemiological studies have identified vascular health, diabetes, hypertension, and high blood cholesterol levels as increasing odds ratio for developing AD (Imtiaz et al., 2014). Additional risk factors include but are not limited to traumatic brain injury (Shively et al., 2012), ischemia or hypoxia (Zhang and Le, 2010), neuroinflammation (Ferreira et al., 2014), exposure to toxins from cyanobacteria (Arif et al., 2014), and decreased brain glucose uptake (Gong et al., 2006). Genome-wide association studies identified variants in pathways involved in cholesterol metabolism and synthesis, innate immunity, and endosomal vesicle trafficking (Hardy et al., 2014). Thus, it will be important to determine whether Caspase-6 activation in the brain can be precipitated by the various risk factors and affected pathways. Most likely, Caspase-6 will not be implicated in all of the risk factors for AD suggesting that Caspase-6 inhibition alone may not be a sufficient therapeutic strategy against AD, but it may still serve as an important target for age-dependent cognitive decline.

4.4.2 Several other caspases are linked to AD

Caspase-6 is not the only caspase to be linked to AD. Work from our lab has identified the NLRP1 inflammasome as an upstream activator of Caspase-1 in AD brains and human neurons (Kaushal et al., 2015). NLRP1, NLRP3, and Caspase 1 mRNA were upregulated in AD monocytes, and this was correlated with increased protein levels in mild AD as well (Saresella et al., 2016). Like Caspase-6, Caspase-2 can also cleave Tau and this leads to Tau mislocalization into dendritic spines (Zhao et al., 2016). Preventing Tau cleavage at D314 prevents defects in synaptic function and restores long-term memory in mice. Caspase-3 has been mostly described in granulovacuolar degeneration of the hippocampus, but not in Aβ plaques or NFTs (Selznick et al., 1999; Stadelmann et al., 1999), yet our lab has not been able to detect active Caspase-3 or -7 in AD tissue (LeBlanc, 2013). However, Caspase-3 can also cleave Tau which creates a fragment that leads to spatial learning and memory deficits and synaptic dysfunction (Kim et al., 2016). These deficits could be rescued by treatment with methylene blue, congo red, and rapamycin. Multiphoton imaging studies revealed that caspase

activation leads to Tau cleavage and that truncated Tau may recruit WT Tau to form aggregates (de Calignon et al., 2010). This mechanism suggests that caspase activation occurs upstream of tangle formation and that Tau aggregation may proceed through prion like conversion (Ozcelik et al., 2016; Goedert et al., 2017).

CASP4 expression is strongly correlated with immune genes such as TREM2 in brain samples from sporadic AD cases (Kajiwara et al., 2016). In mice, Caspase-4 upregulation in microglial cells is thought to increase pro-inflammatory signalling in APP/PS1 mice (Kajiwara et al., 2016). The *CASP7* gene was identified as a genetic risk factor for AD in Caribbean Hispanic individuals in conjunction with APOE, a known risk gene (Shang et al., 2015). Recent studies unveiled that a loss of function *CASP7* variant reduced sporadic AD incidence in APOEε4 carriers in four different cohorts of individuals from European ancestry (Ayers et al., 2016). It is suggested that the neuroprotective effect of reduced Caspase-7 activity is through reduced microglia-mediated neurotoxicity (Burguillos et al., 2011).

Neoepitope antibodies against an active Caspase-8 fragment labelled neurons bearing hyperphosphorylated Tau and Caspase-3 in hippocampal tissue from AD brains (Rohn et al., 2001). The Caspase-8-mediated Caspase-3 activation was thought to initiate neuronal death. Moreover, familial Danish dementia is caused by mutations in BRI2/ITM2B and is believed to converge with AD based on the generation of toxic APP metabolites. Familial Danish dementia can be modeled in mice resulting in synaptic and memory impairment (Giliberto et al., 2009). These mice also have increased Caspase-9 activity in hippocampal fractions and Caspase-9 inhibition reverses both synaptic plasticity and memory deficits (Tamayev et al., 2012). Aβ toxicity can affect synaptic terminals by reducing actin and synaptophysin levels, while causing mitochondrial dysfunction in rat cortical neurons (Mungarro-Menchaca et al., 2002). In the triple transgenic AD mouse model (APP KM670/671NL (Swedish), MAPT P301L, PSEN1 M146V), synaptosomes showed increased Caspase-12 activity that was necessary for Aβ-induced toxicity.

Since many caspases are activated in AD, pan-caspase inhibitors may be a useful therapeutic approach. In a pilot study, TgCRND8 mice which express both Swedish and Indiana mutations in APP under the hamster prion protein promoter were used (Chishti et al., 2001). These mice were shown to display increased Caspase-7 expression and activity leading to Tau

cleavage (Rohn et al., 2009). Treatment with the pan-caspase inhibitor Q-VD-OPh chronically did not lead to any adverse events and prevented Tau cleavage. Pan-caspase inhibitors have been used successfully in several models of neurodegenerative diseases including PD, HD, stroke, and amyotrophic lateral sclerosis (Ona et al., 1999; Schierle et al., 1999; Li et al., 2000; Yang et al., 2004; Braun et al., 2007). A recent study also found that non-steroidal anti-inflammatory drugs strongly inhibited Caspase-4, -5, and -9, with weak inhibition against Caspase-1, and -3 (Smith et al., 2017). Therefore, it may be possible to achieve pan-caspase inhibition, as observed with methylene blue and NWL-117, without worrying about safety issues. This opens the way for multiple caspases inhibition to provide therapeutic benefit in AD.

4.5 Conclusion

AD represents an unmet medical need. The number of individuals that are suffering from and will develop this debilitating disease grows as the population ages and longevity increases. The patients, caregivers, families, and doctors are all waiting for some therapeutic advance. Pharmaceutical giants are spending billions of dollars in testing therapies that have yet to yield any fruit, constantly hammering at an old hypothesis without ever successfully testing it. These companies have learned much in how to design trials. Biomarkers have developed greatly over the years to provide early clinical efficacy measures away from batteries of cognitive tests. Improvements have been made to help generate novel therapies despite the gruelling task of developing CNS drugs.

The situation is not dire. Companies have not been focusing on a singular hypothesis due to the lack of alternatives. Researchers around the world are developing novel theories and approaches to stem or reverse AD pathology. One such hypothesis is that Caspase-6 may be important in mediating the degenerative phenotypes in human neurons. Although it may be but a single mechanism in a plethora of cellular changes that occur in aging brains, Caspase-6 inhibition deserves to be tested in the clinic due to the abundance of supporting human data. The development of potent and non-toxic Caspase-6 inhibitors will provide the opportunity to answer questions several decades in the making. Can Caspase-6 inhibition alone prevent the onset of AD in patients that are developing cognitive impairment? Can Caspase-6 inhibition in

combination with anti-Aβ or Tau therapies stop the progression of AD? The work presented here will hopefully bring these questions to the lips of decision-makers in the future.

References

Abbott, A., and Dolgin, E. (2016). Failed Alzheimer's trial does not kill leading theory of disease. Nature 540, 15-16.

Abdulla, M.H., Lim, K.C., Sajid, M., McKerrow, J.H., and Caffrey, C.R. (2007). Schistosomiasis mansoni: novel chemotherapy using a cysteine protease inhibitor. PLoS Med 4, e14.

Abou-Sleiman, P.M., Healy, D.G., Quinn, N., Lees, A.J., and Wood, N.W. (2003). The role of pathogenic DJ-1 mutations in Parkinson's disease. Ann Neurol 54, 283-286.

Acehan, D., Jiang, X., Morgan, D.G., Heuser, J.E., Wang, X., and Akey, C.W. (2002). Three-dimensional structure of the apoptosome: implications for assembly, procaspase-9 binding, and activation. Mol Cell 9, 423-432.

Adrain, C., Duriez, P.J., Brumatti, G., Delivani, P., and Martin, S.J. (2006). The cytotoxic lymphocyte protease, granzyme B, targets the cytoskeleton and perturbs microtubule polymerization dynamics. J Biol Chem 281, 8118-8125.

Aharony, I., Ehrnhoefer, D.E., Shruster, A., Qiu, X., Franciosi, S., Hayden, M.R., and Offen, D. (2015). A Huntingtin-based peptide inhibitor of caspase-6 provides protection from mutant Huntingtin-induced motor and behavioral deficits. Hum Mol Genet 24, 2604-2614.

Ahmad, M., Srinivasula, S.M., Hegde, R., Mukattash, R., Fernandes-Alnemri, T., and Alnemri, E.S. (1998). Identification and characterization of murine caspase-14, a new member of the caspase family. Cancer Res 58, 5201-5205.

Akoury, E., Pickhardt, M., Gajda, M., Biernat, J., Mandelkow, E., and Zweckstetter, M. (2013). Mechanistic basis of phenothiazine-driven inhibition of Tau aggregation. Angew Chem Int Ed Engl 52, 3511-3515.

Akpan, N., Serrano-Saiz, E., Zacharia, B.E., Otten, M.L., Ducruet, A.F., Snipas, S.J., Liu, W., Velloza, J., Cohen, G., Sosunov, S.A.*, et al.* (2011). Intranasal delivery of caspase-9 inhibitor reduces caspase-6-dependent axon/neuron loss and improves neurological function after stroke. J Neurosci 31, 8894-8904.

Akram, A., Christoffel, D., Rocher, A.B., Bouras, C., Kovari, E., Perl, D.P., Morrison, J.H., Herrmann, F.R., Haroutunian, V., Giannakopoulos, P., and Hof, P.R. (2008). Stereologic estimates of total spinophilin-immunoreactive spine number in area 9 and the CA1 field: relationship with the progression of Alzheimer's disease. Neurobiol Aging 29, 1296-1307.

Alam, A., Cohen, L.Y., Aouad, S., and Sekaly, R.P. (1999). Early activation of caspases during T lymphocyte stimulation results in selective substrate cleavage in nonapoptotic cells. J Exp Med 190, 1879-1890.

Albert, M., Lessin, M.S., and Gilchrist, B.F. (2003). Methylene blue: dangerous dye for neonates. J Pediatr Surg 38, 1244-1245.

Albrecht, S., Bogdanovic, N., Ghetti, B., Winblad, B., and LeBlanc, A.C. (2009). Caspase-6 activation in familial alzheimer disease brains carrying amyloid precursor protein or presenilin i or presenilin II mutations. J Neuropathol Exp Neurol 68, 1282-1293.

Albrecht, S., Bourdeau, M., Bennett, D., Mufson, E.J., Bhattacharjee, M., and LeBlanc, A.C. (2007). Activation of caspase-6 in aging and mild cognitive impairment. Am J Pathol 170, 1200-1209.

Allsopp, T.E., McLuckie, J., Kerr, L.E., Macleod, M., Sharkey, J., and Kelly, J.S. (2000). Caspase 6 activity initiates caspase 3 activation in cerebellar granule cell apoptosis. Cell Death Differ 7, 984-993.

Alnemri, E.S., Livingston, D.J., Nicholson, D.W., Salvesen, G., Thornberry, N.A., Wong, W.W., and Yuan, J. (1996). Human ICE/CED-3 protease nomenclature. Cell 87, 171.

Ambrosini, G., Adida, C., and Altieri, D.C. (1997). A novel anti-apoptosis gene, survivin, expressed in cancer and lymphoma. Nat Med 3, 917-921.

Amir, M., Zhao, E., Fontana, L., Rosenberg, H., Tanaka, K., Gao, G., and Czaja, M.J. (2013). Inhibition of hepatocyte autophagy increases tumor necrosis factor-dependent liver injury by promoting caspase-8 activation. Cell Death Differ 20, 878-887.

Ando, K., Kernan, J.L., Liu, P.H., Sanda, T., Logette, E., Tschopp, J., Look, A.T., Wang, J., Bouchier-Hayes, L., and Sidi, S. (2012). PIDD death-domain phosphorylation by ATM controls prodeath versus prosurvival PIDDosome signaling. Mol Cell 47, 681-693.

Aoki, C., Sekino, Y., Hanamura, K., Fujisawa, S., Mahadomrongkul, V., Ren, Y., and Shirao, T. (2005). Drebrin A is a postsynaptic protein that localizes in vivo to the submembranous surface of dendritic sites forming excitatory synapses. J Comp Neurol 483, 383-402.

Aravind, L., and Koonin, E.V. (2002). Classification of the caspase-hemoglobinase fold: detection of new families and implications for the origin of the eukaryotic separins. Proteins 46, 355-367.

Arif, M., Kazim, S.F., Grundke-Iqbal, I., Garruto, R.M., and Iqbal, K. (2014). Tau pathology involves protein phosphatase 2A in parkinsonism-dementia of Guam. Proc Natl Acad Sci USA 111, 1144-1149.

Atamna, H., and Kumar, R. (2010). Protective role of methylene blue in Alzheimer's disease via mitochondria and cytochrome c oxidase. J Alzheimers Dis 20 Suppl 2, S439-452.

Ayers, K.L., Mirshahi, U.L., Wardeh, A.H., Murray, M.F., Hao, K., Glicksberg, B.S., Li, S., Carey, D.J., and Chen, R. (2016). A loss of function variant in CASP7 protects against Alzheimer's disease in homozygous APOE epsilon4 allele carriers. BMC Genomics 17 Suppl 2, 445.

Baburamani, A.A., Miyakuni, Y., Vontell, R., Supramaniam, V.G., Svedin, P., Rutherford, M., Gressens, P., Mallard, C., Takeda, S., Thornton, C., and Hagberg, H. (2015). Does Caspase-6 Have a Role in Perinatal Brain Injury? Dev Neurosci 37, 321-337.

Baker, P.J., Boucher, D., Bierschenk, D., Tebartz, C., Whitney, P.G., D'Silva, D.B., Tanzer, M.C., Monteleone, M., Robertson, A.A., Cooper, M.A., *et al.* (2015). NLRP3 inflammasome activation downstream of cytoplasmic LPS recognition by both caspase-4 and caspase-5. Eur J Immunol 45, 2918-2926.

Banks, D.P., Plescia, J., Altieri, D.C., Chen, J., Rosenberg, S.H., Zhang, H., and Ng, S.C. (2000). Survivin does not inhibit caspase-3 activity. Blood 96, 4002-4003.

Banner, D.W., D'Arcy, A., Janes, W., Gentz, R., Schoenfeld, H.J., Broger, C., Loetscher, H., and Lesslauer, W. (1993). Crystal structure of the soluble human 55 kd TNF receptor-human TNF beta complex: implications for TNF receptor activation. Cell 73, 431-445.

Barrangou, R., Fremaux, C., Deveau, H., Richards, M., Boyaval, P., Moineau, S., Romero, D.A., and Horvath, P. (2007). CRISPR provides acquired resistance against viruses in prokaryotes. Science 315, 1709-1712.

Bartus, R.T., Dean, R.L., 3rd, Beer, B., and Lippa, A.S. (1982). The cholinergic hypothesis of geriatric memory dysfunction. Science 217, 408-414.

Bassnett, S. (2002). Lens organelle degradation. Exp Eye Res 74, 1-6.

Baumgartner, R., Meder, G., Briand, C., Decock, A., D'Arcy, A., Hassiepen, U., Morse, R., and Renatus, M. (2009). The crystal structure of caspase-6, a selective effector of axonal degeneration. Biochem J 423, 429-439.

Beattie, E.C., Carroll, R.C., Yu, X., Morishita, W., Yasuda, H., von Zastrow, M., and Malenka, R.C. (2000). Regulation of AMPA receptor endocytosis by a signaling mechanism shared with LTD. Nat Neurosci 3, 1291-1300.

Beisner, D.R., Ch'en, I.L., Kolla, R.V., Hoffmann, A., and Hedrick, S.M. (2005). Cutting edge: innate immunity conferred by B cells is regulated by caspase-8. J Immunol 175, 3469-3473.

Ben Halima, S., Mishra, S., Raja, K.M., Willem, M., Baici, A., Simons, K., Brustle, O., Koch, P., Haass, C., Caflisch, A., and Rajendran, L. (2016). Specific Inhibition of beta-Secretase Processing of the Alzheimer Disease Amyloid Precursor Protein. Cell Rep 14, 2127-2141.

Bennett, D.A., Schneider, J.A., Wilson, R.S., Bienias, J.L., and Arnold, S.E. (2004). Neurofibrillary tangles mediate the association of amyloid load with clinical Alzheimer disease and level of cognitive function. Arch Neurol 61, 378-384.

Berger, A.B., Witte, M.D., Denault, J.B., Sadaghiani, A.M., Sexton, K.M., Salvesen, G.S., and Bogyo, M. (2006). Identification of early intermediates of caspase activation using selective inhibitors and activity-based probes. Mol Cell 23, 509-521.

Bergeron, L., Perez, G.I., Macdonald, G., Shi, L., Sun, Y., Jurisicova, A., Varmuza, S., Latham, K.E., Flaws, J.A., Salter, J.C.*, et al.* (1998). Defects in regulation of apoptosis in caspase-2-deficient mice. Genes Dev 12, 1304-1314.

Berta, T., Park, C.K., Xu, Z.Z., Xie, R.G., Liu, T., Lu, N., Liu, Y.C., and Ji, R.R. (2014). Extracellular caspase-6 drives murine inflammatory pain via microglial TNF-alpha secretion. J Clin Invest 124, 1173-1186.

Bertrand, M.J., Milutinovic, S., Dickson, K.M., Ho, W.C., Boudreault, A., Durkin, J., Gillard, J.W., Jaquith, J.B., Morris, S.J., and Barker, P.A. (2008). cIAP1 and cIAP2 facilitate cancer cell survival by functioning as E3 ligases that promote RIP1 ubiquitination. Mol Cell 30, 689-700.

Bhattaram, P., Penzo-Mendez, A., Sock, E., Colmenares, C., Kaneko, K.J., Vassilev, A., Depamphilis, M.L., Wegner, M., and Lefebvre, V. (2010). Organogenesis relies on SoxC transcription factors for the survival of neural and mesenchymal progenitors. Nat Commun 1, 9.

Bidle, K.D. (2016). Programmed Cell Death in Unicellular Phytoplankton. Curr Biol 26, R594-607.

Blass, N., and Fung, D. (1976). Dyed but not dead--methylene blue overdose. Anesthesiology 45, 458-459.

Boatright, K.M., Renatus, M., Scott, F.L., Sperandio, S., Shin, H., Pedersen, I.M., Ricci, J.E., Edris, W.A., Sutherlin, D.P., Green, D.R., and Salvesen, G.S. (2003). A unified model for apical caspase activation. Mol Cell 11, 529-541.

Boldin, M.P., Varfolomeev, E.E., Pancer, Z., Mett, I.L., Camonis, J.H., and Wallach, D. (1995). A novel protein that interacts with the death domain of Fas/APO1 contains a sequence motif related to the death domain. J Biol Chem 270, 7795-7798.

Boucher, D., Blais, V., and Denault, J.B. (2012). Caspase-7 uses an exosite to promote poly(ADP ribose) polymerase 1 proteolysis. Proc Natl Acad Sci USA 109, 5669-5674.

Boussif, O., Lezoualc'h, F., Zanta, M.A., Mergny, M.D., Scherman, D., Demeneix, B., and Behr, J.P. (1995). A versatile vector for gene and oligonucleotide transfer into cells in culture and in vivo: polyethylenimine. Proc Natl Acad Sci USA 92, 7297-7301.

Braak, H., and Braak, E. (1997). Diagnostic criteria for neuropathologic assessment of Alzheimer's disease. Neurobiol Aging 18, S85-88.

Bradberry, S.M. (2003). Occupational methaemoglobinaemia. Mechanisms of production, features, diagnosis and management including the use of methylene blue. Toxicol Rev 22, 13-27.

Braun, J.S., Prass, K., Dirnagl, U., Meisel, A., and Meisel, C. (2007). Protection from brain damage and bacterial infection in murine stroke by the novel caspase-inhibitor Q-VD-OPH. Exp Neurol 206, 183-191.

Brouns, S.J., Jore, M.M., Lundgren, M., Westra, E.R., Slijkhuis, R.J., Snijders, A.P., Dickman, M.J., Makarova, K.S., Koonin, E.V., and van der Oost, J. (2008). Small CRISPR RNAs guide antiviral defense in prokaryotes. Science 321, 960-964.

Broz, P., von Moltke, J., Jones, J.W., Vance, R.E., and Monack, D.M. (2010). Differential requirement for Caspase-1 autoproteolysis in pathogen-induced cell death and cytokine processing. Cell Host Microbe 8, 471-483.

Bump, N.J., Hackett, M., Hugunin, M., Seshagiri, S., Brady, K., Chen, P., Ferenz, C., Franklin, S., Ghayur, T., Li, P., and et al. (1995). Inhibition of ICE family proteases by baculovirus antiapoptotic protein p35. Science 269, 1885-1888.

Burguillos, M.A., Deierborg, T., Kavanagh, E., Persson, A., Hajji, N., Garcia-Quintanilla, A., Cano, J., Brundin, P., Englund, E., Venero, J.L., and Joseph, B. (2011). Caspase signalling controls microglia activation and neurotoxicity. Nature 472, 319-324.

Cai, Z., Jitkaew, S., Zhao, J., Chiang, H.C., Choksi, S., Liu, J., Ward, Y., Wu, L.G., and Liu, Z.G. (2014). Plasma membrane translocation of trimerized MLKL protein is required for TNF-induced necroptosis. Nat Cell Biol 16, 55-65.

Callaway, D.A., Riquelme, M.A., Sharma, R., Lopez-Cruzan, M., Herman, B.A., and Jiang, J.X. (2016). Caspase-2 modulates osteoclastogenesis through down-regulating oxidative stress. Bone 93, 233-234.

Callus, B.A., and Vaux, D.L. (2007). Caspase inhibitors: viral, cellular and chemical. Cell Death Differ 14, 73-78.

Cao, Q., Wang, X.J., Li, L.F., and Su, X.D. (2014). The regulatory mechanism of the caspase 6 pro-domain revealed by crystal structure and biochemical assays. Acta Crystallogr D Biol Crystallogr 70, 58-67.

Cao, Q., Wang, X.J., Liu, C.W., Liu, D.F., Li, L.F., Gao, Y.Q., and Su, X.D. (2012). Inhibitory mechanism of caspase-6 phosphorylation revealed by crystal structures, molecular dynamics simulations, and biochemical assays. J Biol Chem 287, 15371-15379.

Cartegni, L., and Krainer, A.R. (2002). Disruption of an SF2/ASF-dependent exonic splicing enhancer in SMN2 causes spinal muscular atrophy in the absence of SMN1. Nat Genet 30, 377-384.

Castedo, M., Perfettini, J.L., Roumier, T., Valent, A., Raslova, H., Yakushijin, K., Horne, D., Feunteun, J., Lenoir, G., Medema, R.*, et al.* (2004). Mitotic catastrophe constitutes a special case of apoptosis whose suppression entails aneuploidy. Oncogene 23, 4362-4370.

Cerretti, D.P., Kozlosky, C.J., Mosley, B., Nelson, N., Van Ness, K., Greenstreet, T.A., March, C.J., Kronheim, S.R., Druck, T., Cannizzaro, L.A., and et al. (1992). Molecular cloning of the interleukin-1 beta converting enzyme. Science 256, 97-100.

Chai, F., Truong-Tran, A.Q., Evdokiou, A., Young, G.P., and Zalewski, P.D. (2000). Intracellular zinc depletion induces caspase activation and p21 Waf1/Cip1 cleavage in human epithelial cell lines. J Infect Dis 182 Suppl 1, S85-92.

Chai, J., Wu, Q., Shiozaki, E., Srinivasula, S.M., Alnemri, E.S., and Shi, Y. (2001). Crystal structure of a procaspase-7 zymogen: mechanisms of activation and substrate binding. Cell 107, 399-407.

Chan, S.L., Griffin, W.S., and Mattson, M.P. (1999). Evidence for caspase-mediated cleavage of AMPA receptor subunits in neuronal apoptosis and Alzheimer's disease. J Neurosci Res 57, 315-323.

Chandler, J.M., Alnemri, E.S., Cohen, G.M., and MacFarlane, M. (1997). Activation of CPP32 and Mch3 alpha in wild-type p53-induced apoptosis. Biochem J 322 (Pt 1), 19-23.

Chang, C.Z., and Wu, S.C. (2016). 4'-O-beta-D-Glucosyl-5-O-Methylvisamminol, A Natural Histone H3 Phosphorylation Epigenetic Suppressor, Exerts a Neuroprotective Effect Through PI3K/Akt Signaling Pathway on Focal Cerebral Ischemia in Rats. World Neurosurg 89, 474-488.

Chen, S.X., Cherry, A., Tari, P.K., Podgorski, K., Kwong, Y.K., and Haas, K. (2012). The transcription factor MEF2 directs developmental visually driven functional and structural metaplasticity. Cell 151, 41-55.

Cheung, W.L., Ajiro, K., Samejima, K., Kloc, M., Cheung, P., Mizzen, C.A., Beeser, A., Etkin, L.D., Chernoff, J., Earnshaw, W.C., and Allis, C.D. (2003). Apoptotic phosphorylation of histone H2B is mediated by mammalian sterile twenty kinase. Cell 113, 507-517.

Chinnaiyan, A.M., O'Rourke, K., Tewari, M., and Dixit, V.M. (1995). FADD, a novel death domain-containing protein, interacts with the death domain of Fas and initiates apoptosis. Cell 81, 505-512.

Chiriboga, C.A., Swoboda, K.J., Darras, B.T., Iannaccone, S.T., Montes, J., De Vivo, D.C., Norris, D.A., Bennett, C.F., and Bishop, K.M. (2016). Results from a phase 1 study of nusinersen (ISIS-SMN(Rx)) in children with spinal muscular atrophy. Neurology 86, 890-897.

Chishti, M.A., Yang, D.S., Janus, C., Phinney, A.L., Horne, P., Pearson, J., Strome, R., Zuker, N., Loukides, J., French, J.*, et al.* (2001). Early-onset amyloid deposition and cognitive deficits in transgenic mice expressing a double mutant form of amyloid precursor protein 695. J Biol Chem 276, 21562-21570.

Chu, W., Rothfuss, J., Chu, Y., Zhou, D., and Mach, R.H. (2009). Synthesis and in vitro evaluation of sulfonamide isatin Michael acceptors as small molecule inhibitors of caspase-6. J Med Chem 52, 2188-2191.

Clem, R.J., Fechheimer, M., and Miller, L.K. (1991). Prevention of apoptosis by a baculovirus gene during infection of insect cells. Science 254, 1388-1390.

Cong, L., Ran, F.A., Cox, D., Lin, S., Barretto, R., Habib, N., Hsu, P.D., Wu, X., Jiang, W., Marraffini, L.A., and Zhang, F. (2013). Multiplex genome engineering using CRISPR/Cas systems. Science 339, 819-823.

Congdon, E.E., Wu, J.W., Myeku, N., Figueroa, Y.H., Herman, M., Marinec, P.S., Gestwicki, J.E., Dickey, C.A., Yu, W.H., and Duff, K.E. (2012). Methylthioninium chloride (methylene blue) induces autophagy and attenuates tauopathy in vitro and in vivo. Autophagy 8, 609-622.

Cordon-Cardo, C., O'Brien, J.P., Casals, D., Rittman-Grauer, L., Biedler, J.L., Melamed, M.R., and Bertino, J.R. (1989). Multidrug-resistance gene (P-glycoprotein) is expressed by endothelial cells at blood-brain barrier sites. Proc Natl Acad Sci USA 86, 695-698.

Coulibaly, B., Zoungrana, A., Mockenhaupt, F.P., Schirmer, R.H., Klose, C., Mansmann, U., Meissner, P.E., and Muller, O. (2009). Strong gametocytocidal effect of methylene blue-based combination therapy against falciparum malaria: a randomised controlled trial. PLoS One 4, e5318.

Cowling, V., and Downward, J. (2002). Caspase-6 is the direct activator of caspase-8 in the cytochrome c-induced apoptosis pathway: absolute requirement for removal of caspase-6 prodomain. Cell Death Differ 9, 1046-1056.

Croft, D.R., Coleman, M.L., Li, S., Robertson, D., Sullivan, T., Stewart, C.L., and Olson, M.F. (2005). Actin-myosin-based contraction is responsible for apoptotic nuclear disintegration. J Cell Biol 168, 245-255.

Crook, N.E., Clem, R.J., and Miller, L.K. (1993). An apoptosis-inhibiting baculovirus gene with a zinc finger-like motif. J Virol 67, 2168-2174.

Crowe, A., James, M.J., Lee, V.M., Smith, A.B., 3rd, Trojanowski, J.Q., Ballatore, C., and Brunden, K.R. (2013). Aminothienopyridazines and methylene blue affect Tau fibrillization via cysteine oxidation. J Biol Chem 288, 11024-11037.

Cummings, J.L., Mega, M., Gray, K., Rosenberg-Thompson, S., Carusi, D.A., and Gornbein, J. (1994). The Neuropsychiatric Inventory: comprehensive assessment of psychopathology in dementia. Neurology 44, 2308-2314.

Cusack, C.L., Swahari, V., Hampton Henley, W., Michael Ramsey, J., and Deshmukh, M. (2013). Distinct pathways mediate axon degeneration during apoptosis and axon-specific pruning. Nat Commun 4, 1876.

D'Amelio, M., Cavallucci, V., and Cecconi, F. (2010). Neuronal caspase-3 signaling: not only cell death. Cell Death Differ 17, 1104-1114.

Dagbay, K.B., Bolik-Coulon, N., Savinov, S.N., and Hardy, J.A. (2017). Caspase-6 Undergoes a Distinct Helix-Strand Interconversion upon Substrate Binding. J Biol Chem 292, 4885-4897.

Damiano, J.S., Newman, R.M., and Reed, J.C. (2004). Multiple roles of CLAN (caspase-associated recruitment domain, leucine-rich repeat, and NAIP CIIA HET-E, and TP1-containing protein) in the mammalian innate immune response. J Immunol 173, 6338-6345.

Darmon, A.J., Nicholson, D.W., and Bleackley, R.C. (1995). Activation of the apoptotic protease CPP32 by cytotoxic T-cell-derived granzyme B. Nature 377, 446-448.

Dawar, S., Shahrin, N.H., Sladojevic, N., D'Andrea, R.J., Dorstyn, L., Hiwase, D.K., and Kumar, S. (2016). Impaired haematopoietic stem cell differentiation and enhanced skewing towards myeloid progenitors in aged caspase-2-deficient mice. Cell Death Dis 7, e2509.

de Calignon, A., Fox, L.M., Pitstick, R., Carlson, G.A., Bacskai, B.J., Spires-Jones, T.L., and Hyman, B.T. (2010). Caspase activation precedes and leads to tangles. Nature 464, 1201-1204.

de Rivero Vaccari, J.P., Sawaya, M.E., Brand, F., 3rd, Nusbaum, B.P., Bauman, A.J., Bramlett, H.M., Dietrich, W.D., and Keane, R.W. (2012). Caspase-1 level is higher in the scalp in androgenetic alopecia. Dermatol Surg 38, 1033-1039.

Deckwerth, T.L., and Johnson, E.M., Jr. (1993). Neurotrophic factor deprivation-induced death. Ann N Y Acad Sci 679, 121-131.

Deltcheva, E., Chylinski, K., Sharma, C.M., Gonzales, K., Chao, Y., Pirzada, Z.A., Eckert, M.R., Vogel, J., and Charpentier, E. (2011). CRISPR RNA maturation by trans-encoded small RNA and host factor RNase III. Nature 471, 602-607.

Denault, J., and Salvesen, G. (2002). Expression, Purification, and Characterization of Caspases. In Current Protocols in Protein Science, pp. 21.13.21-21.13.15.

Denecker, G., Hoste, E., Gilbert, B., Hochepied, T., Ovaere, P., Lippens, S., Van den Broecke, C., Van Damme, P., D'Herde, K., Hachem, J.P*., et al.* (2007). Caspase-14 protects against epidermal UVB photodamage and water loss. Nat Cell Biol 9, 666-674.

Deshmukh, M., Vasilakos, J., Deckwerth, T.L., Lampe, P.A., Shivers, B.D., and Johnson, E.M., Jr. (1996). Genetic and metabolic status of NGF-deprived sympathetic neurons saved by an inhibitor of ICE family proteases. J Cell Biol 135, 1341-1354.

Deveraux, Q.L., Roy, N., Stennicke, H.R., Van Arsdale, T., Zhou, Q., Srinivasula, S.M., Alnemri, E.S., Salvesen, G.S., and Reed, J.C. (1998). IAPs block apoptotic events induced by caspase-8 and cytochrome c by direct inhibition of distinct caspases. EMBO J 17, 2215-2223.

Deveraux, Q.L., Takahashi, R., Salvesen, G.S., and Reed, J.C. (1997). X-linked IAP is a direct inhibitor of cell-death proteases. Nature 388, 300-304.

Dickson, D.W., Wertkin, A., Mattiace, L.A., Fier, E., Kress, Y., Davies, P., and Yen, S.H. (1990). Ubiquitin immunoelectron microscopy of dystrophic neurites in cerebellar senile plaques of Alzheimer's disease. Acta Neuropathol 79, 486-493.

DiFiglia, M., Sapp, E., Chase, K.O., Davies, S.W., Bates, G.P., Vonsattel, J.P., and Aronin, N. (1997). Aggregation of huntingtin in neuronal intranuclear inclusions and dystrophic neurites in brain. Science 277, 1990-1993.

Ding, Z.M., Wu, B., Zhang, W.Q., Lu, X.J., Lin, Y.C., Geng, Y.J., and Miao, Y.F. (2012). Neuroprotective effects of ischemic preconditioning and postconditioning on global brain ischemia in rats through the same effect on inhibition of apoptosis. Int J Mol Sci 13, 6089-6101.

Doody, R.S., Farlow, M., Aisen, P.S., Alzheimer's Disease Cooperative Study Data, A., and Publication, C. (2014). Phase 3 trials of solanezumab and bapineuzumab for Alzheimer's disease. N Engl J Med 370, 1460.

Duan, H., and Dixit, V.M. (1997). RAIDD is a new 'death' adaptor molecule. Nature 385, 86-89.

Duan, H., Orth, K., Chinnaiyan, A.M., Poirier, G.G., Froelich, C.J., He, W.W., and Dixit, V.M. (1996). ICE-LAP6, a novel member of the ICE/Ced-3 gene family, is activated by the cytotoxic T cell protease granzyme B. J Biol Chem 271, 16720-16724.

Duckett, C.S., Nava, V.E., Gedrich, R.W., Clem, R.J., Van Dongen, J.L., Gilfillan, M.C., Shiels, H., Hardwick, J.M., and Thompson, C.B. (1996). A conserved family of cellular genes related to the baculovirus iap gene and encoding apoptosis inhibitors. EMBO J 15, 2685-2694.

Duclos, C.M., Champagne, A., Carrier, J.C., Saucier, C., Lavoie, C.L., and Denault, J.B. (2017). Caspase-mediated proteolysis of the sorting nexin 2 disrupts retromer assembly and potentiates Met/hepatocyte growth factor receptor signaling. Cell Death Discov 3, 16100.

Dudley, N.E. (1971). Methylene blue for rapid identification of the parathyroids. Br Med J 3, 680-681.

Duyckaerts, C., Delatour, B., and Potier, M.C. (2009). Classification and basic pathology of Alzheimer disease. Acta Neuropathol 118, 5-36.

Eckelman, B.P., and Salvesen, G.S. (2006). The human anti-apoptotic proteins cIAP1 and cIAP2 bind but do not inhibit caspases. J Biol Chem 281, 3254-3260.

Eckhart, L., Ballaun, C., Hermann, M., VandeBerg, J.L., Sipos, W., Uthman, A., Fischer, H., and Tschachler, E. (2008). Identification of novel mammalian caspases reveals an important role of gene loss in shaping the human caspase repertoire. Mol Biol Evol 25, 831-841.

Eckhart, L., Ballaun, C., Uthman, A., Kittel, C., Stichenwirth, M., Buchberger, M., Fischer, H., Sipos, W., and Tschachler, E. (2005). Identification and characterization of a novel mammalian caspase with proapoptotic activity. J Biol Chem 280, 35077-35080.

Eckhart, L., Ban, J., Fischer, H., and Tschachler, E. (2000a). Caspase-14: analysis of gene structure and mRNA expression during keratinocyte differentiation. Biochem Biophys Res Commun 277, 655-659.

Eckhart, L., Declercq, W., Ban, J., Rendl, M., Lengauer, B., Mayer, C., Lippens, S., Vandenabeele, P., and Tschachler, E. (2000b). Terminal differentiation of human keratinocytes and stratum corneum formation is associated with caspase-14 activation. J Invest Dermatol 115, 1148-1151.

Edgington, L.E., van Raam, B.J., Verdoes, M., Wierschem, C., Salvesen, G.S., and Bogyo, M. (2012). An optimized activity-based probe for the study of caspase-6 activation. Chem Biol 19, 340-352.

Ehrnhoefer, D.E., Caron, N.S., Deng, Y., Qiu, X., Tsang, M., and Hayden, M.R. (2016). Laquinimod decreases Bax expression and reduces caspase-6 activation in neurons. Exp Neurol 283, 121-128.

Ehrnhoefer, D.E., Skotte, N.H., Ladha, S., Nguyen, Y.T., Qiu, X., Deng, Y., Huynh, K.T., Engemann, S., Nielsen, S.M., Becanovic, K.*, et al.* (2014). p53 increases caspase-6 expression and activation in muscle tissue expressing mutant huntingtin. Hum Mol Genet 23, 717-729.

Ehrnhoefer, D.E., Skotte, N.H., Savill, J., Nguyen, Y.T., Ladha, S., Cao, L.P., Dullaghan, E., and Hayden, M.R. (2011). A quantitative method for the specific assessment of caspase-6 activity in cell culture. PLoS One 6, e27680.

Eichhold, T.H., Hookfin, E.B., Taiwo, Y.O., De, B., and Wehmeyer, K.R. (1997). Isolation and quantification of fluoroacetate in rat tissues, following dosing of Z-Phe-Ala-CH2-F, a peptidyl fluoromethyl ketone protease inhibitor. J Pharm Biomed Anal 16, 459-467.

Ekici, O.D., Li, Z.Z., Campbell, A.J., James, K.E., Asgian, J.L., Mikolajczyk, J., Salvesen, G.S., Ganesan, R., Jelakovic, S., Grutter, M.G., and Powers, J.C. (2006). Design, synthesis, and evaluation of aza-peptide Michael acceptors as selective and potent inhibitors of caspases-2, -3, -6, -7, -8, -9, and -10. J Med Chem 49, 5728-5749.

Ellis, H.M., and Horvitz, H.R. (1986). Genetic control of programmed cell death in the nematode C. elegans. Cell 44, 817-829.

Enari, M., Sakahira, H., Yokoyama, H., Okawa, K., Iwamatsu, A., and Nagata, S. (1998). A caspase-activated DNase that degrades DNA during apoptosis, and its inhibitor ICAD. Nature 391, 43-50.

Ernsberger, U. (2009). Role of neurotrophin signalling in the differentiation of neurons from dorsal root ganglia and sympathetic ganglia. Cell Tissue Res 336, 349-384.

Evers, M.M., Tran, H.D., Zalachoras, I., Meijer, O.C., den Dunnen, J.T., van Ommen, G.J., Aartsma-Rus, A., and van Roon-Mom, W.M. (2014). Preventing formation of toxic N-terminal huntingtin fragments through antisense oligonucleotide-mediated protein modification. Nucleic Acid Ther 24, 4-12.

Fatouros, C., Pir, G.J., Biernat, J., Koushika, S.P., Mandelkow, E., Mandelkow, E.M., Schmidt, E., and Baumeister, R. (2012). Inhibition of tau aggregation in a novel Caenorhabditis elegans model of tauopathy mitigates proteotoxicity. Hum Mol Genet 21, 3587-3603.

Faucheu, C., Diu, A., Chan, A.W., Blanchet, A.M., Miossec, C., Herve, F., Collard-Dutilleul, V., Gu, Y., Aldape, R.A., Lippke, J.A., and et al. (1995). A novel human protease similar to the interleukin-1 beta converting enzyme induces apoptosis in transfected cells. EMBO J 14, 1914-1922.

Feng, J., Yan, Z., Ferreira, A., Tomizawa, K., Liauw, J.A., Zhuo, M., Allen, P.B., Ouimet, C.C., and Greengard, P. (2000). Spinophilin regulates the formation and function of dendritic spines. Proc Natl Acad Sci USA 97, 9287-9292.

Feoktistova, M., Geserick, P., Kellert, B., Dimitrova, D.P., Langlais, C., Hupe, M., Cain, K., MacFarlane, M., Hacker, G., and Leverkus, M. (2011). cIAPs block Ripoptosome formation, a RIP1/caspase-8 containing intracellular cell death complex differentially regulated by cFLIP isoforms. Mol Cell 43, 449-463.

Fernandes-Alnemri, T., Armstrong, R.C., Krebs, J., Srinivasula, S.M., Wang, L., Bullrich, F., Fritz, L.C., Trapani, J.A., Tomaselli, K.J., Litwack, G., and Alnemri, E.S. (1996). In vitro activation of CPP32 and Mch3 by Mch4, a novel human apoptotic cysteine protease containing two FADD-like domains. Proc Natl Acad Sci USA 93, 7464-7469.

Fernandes-Alnemri, T., Litwack, G., and Alnemri, E.S. (1994). CPP32, a novel human apoptotic protein with homology to Caenorhabditis elegans cell death protein Ced-3 and mammalian interleukin-1 beta-converting enzyme. J Biol Chem 269, 30761-30764.

Fernandes-Alnemri, T., Litwack, G., and Alnemri, E.S. (1995a). Mch2, a new member of the apoptotic Ced-3/Ice cysteine protease gene family. Cancer Res 55, 2737-2742.

Fernandes-Alnemri, T., Takahashi, A., Armstrong, R., Krebs, J., Fritz, L., Tomaselli, K.J., Wang, L., Yu, Z., Croce, C.M., Salveson, G., and et al. (1995b). Mch3, a novel human apoptotic cysteine protease highly related to CPP32. Cancer Res 55, 6045-6052.

Ferreira, S.T., Clarke, J.R., Bomfim, T.R., and De Felice, F.G. (2014). Inflammation, defective insulin signaling, and neuronal dysfunction in Alzheimer's disease. Alzheimers Dement 10, S76-83.

Fink, S.L., Bergsbaken, T., and Cookson, B.T. (2008). Anthrax lethal toxin and Salmonella elicit the common cell death pathway of caspase-1-dependent pyroptosis via distinct mechanisms. Proc Natl Acad Sci USA 105, 4312-4317.

Fink, S.L., and Cookson, B.T. (2006). Caspase-1-dependent pore formation during pyroptosis leads to osmotic lysis of infected host macrophages. Cell Microbiol 8, 1812-1825.

Finkel, R.S., Chiriboga, C.A., Vajsar, J., Day, J.W., Montes, J., De Vivo, D.C., Yamashita, M., Rigo, F., Hung, G., Schneider, E.*, et al.* (2016). Treatment of infantile-onset spinal muscular atrophy with nusinersen: a phase 2, open-label, dose-escalation study. Lancet 388, 3017-3026.

Finn, J.T., Weil, M., Archer, F., Siman, R., Srinivasan, A., and Raff, M.C. (2000). Evidence that Wallerian degeneration and localized axon degeneration induced by local neurotrophin deprivation do not involve caspases. J Neurosci 20, 1333-1341.

Fischer, H., Koenig, U., Eckhart, L., and Tschachler, E. (2002). Human caspase 12 has acquired deleterious mutations. Biochem Biophys Res Commun 293, 722-726.

Foveau, B., Van Der Kraak, L., Beauchemin, N., Albrecht, S., and LeBlanc, A.C. (2014). Inflammation-induced tumorigenesis in mouse colon is caspase-6 independent. PLoS One 9, e114270.

Friedlander, R.M., Brown, R.H., Gagliardini, V., Wang, J., and Yuan, J. (1997). Inhibition of ICE slows ALS in mice. Nature 388, 31.

Frydrych, I., and Mlejnek, P. (2008a). Serine protease inhibitors N-alpha-tosyl-L-lysinyl-chloromethylketone (TLCK) and N-tosyl-L-phenylalaninyl-chloromethylketone (TPCK) are potent inhibitors of activated caspase proteases. J Cell Biochem 103, 1646-1656.

Frydrych, I., and Mlejnek, P. (2008b). Serine protease inhibitors N-alpha-tosyl-L-lysinyl-chloromethylketone (TLCK) and N-tosyl-L-phenylalaninyl-chloromethylketone (TPCK) do not inhibit caspase-3 and caspase-7 processing in cells exposed to pro-apoptotic inducing stimuli. J Cell Biochem 105, 1501-1506.

Fuentes-Prior, P., and Salvesen, G.S. (2004). The protein structures that shape caspase activity, specificity, activation and inhibition. Biochem J 384, 201-232.

Gafni, J., Papanikolaou, T., Degiacomo, F., Holcomb, J., Chen, S., Menalled, L., Kudwa, A., Fitzpatrick, J., Miller, S., Ramboz, S.*, et al.* (2012). Caspase-6 activity in a BACHD mouse modulates steady-state levels of mutant huntingtin protein but is not necessary for production of a 586 amino acid proteolytic fragment. J Neurosci 32, 7454-7465.

Galluzzi, L., Bravo-San Pedro, J.M., Vitale, I., Aaronson, S.A., Abrams, J.M., Adam, D., Alnemri, E.S., Altucci, L., Andrews, D., Annicchiarico-Petruzzelli, M.*, et al.* (2015). Essential versus accessory aspects of cell death: recommendations of the NCCD 2015. Cell Death Differ 22, 58-73.

Garcia-Calvo, M., Peterson, E.P., Leiting, B., Ruel, R., Nicholson, D.W., and Thornberry, N.A. (1998). Inhibition of human caspases by peptide-based and macromolecular inhibitors. J Biol Chem 273, 32608-32613.

Garner, E., Martinon, F., Tschopp, J., Beard, P., and Raj, K. (2007). Cells with defective p53-p21-pRb pathway are susceptible to apoptosis induced by p84N5 via caspase-6. Cancer Res 67, 7631-7637.

Geden, M.J., and Deshmukh, M. (2016). Axon degeneration: context defines distinct pathways. Curr Opin Neurobiol 39, 108-115.

Ghayur, T., Banerjee, S., Hugunin, M., Butler, D., Herzog, L., Carter, A., Quintal, L., Sekut, L., Talanian, R., Paskind, M.*, et al.* (1997). Caspase-1 processes IFN-gamma-inducing factor and regulates LPS-induced IFN-gamma production. Nature 386, 619-623.

Giaime, E., Sunyach, C., Druon, C., Scarzello, S., Robert, G., Grosso, S., Auberger, P., Goldberg, M.S., Shen, J., Heutink, P.*, et al.* (2010). Loss of function of DJ-1 triggered by Parkinson's disease-associated mutation is due to proteolytic resistance to caspase-6. Cell Death Differ 17, 158-169.

Giaime, E., Sunyach, C., Herrant, M., Grosso, S., Auberger, P., McLean, P.J., Checler, F., and da Costa, C.A. (2006). Caspase-3-derived C-terminal product of synphilin-1 displays antiapoptotic function via modulation of the p53-dependent cell death pathway. J Biol Chem 281, 11515-11522.

Gibson, P.H., and Tomlinson, B.E. (1977). Numbers of Hirano bodies in the hippocampus of normal and demented people with Alzheimer's disease. J Neurol Sci 33, 199-206.

Giliberto, L., Matsuda, S., Vidal, R., and D'Adamio, L. (2009). Generation and initial characterization of FDD knock in mice. PLoS One 4, e7900.

Godefroy, N., Foveau, B., Albrecht, S., Goodyer, C.G., and LeBlanc, A.C. (2013). Expression and activation of caspase-6 in human fetal and adult tissues. PLoS One 8, e79313.

Goedert, M., Masuda-Suzukake, M., and Falcon, B. (2017). Like prions: the propagation of aggregated tau and alpha-synuclein in neurodegeneration. Brain 140, 266-278.

Goedert, M., and Spillantini, M.G. (2006). A century of Alzheimer's disease. Science 314, 777-781.

Goldberg, Y.P., Nicholson, D.W., Rasper, D.M., Kalchman, M.A., Koide, H.B., Graham, R.K., Bromm, M., Kazemi-Esfarjani, P., Thornberry, N.A., Vaillancourt, J.P., and Hayden, M.R. (1996). Cleavage of huntingtin by apopain, a proapoptotic cysteine protease, is modulated by the polyglutamine tract. Nat Genet 13, 442-449.

Gong, C.X., Liu, F., Grundke-Iqbal, I., and Iqbal, K. (2006). Impaired brain glucose metabolism leads to Alzheimer neurofibrillary degeneration through a decrease in tau O-GlcNAcylation. J Alzheimers Dis 9, 1-12.

Gonzalez-Castillo, C., Ortuno-Sahagun, D., Guzman-Brambila, C., Marquez-Aguirre, A.L., Raisman-Vozari, R., Pallas, M., and Rojas-Mayorquin, A.E. (2016). The absence of pleiotrophin modulates gene expression in the hippocampus in vivo and in cerebellar granule cells in vitro. Mol Cell Neurosci 75, 113-121.

Gonzalvez, F., Lawrence, D., Yang, B., Yee, S., Pitti, R., Marsters, S., Pham, V.C., Stephan, J.P., Lill, J., and Ashkenazi, A. (2012). TRAF2 Sets a threshold for extrinsic apoptosis by tagging caspase-8 with a ubiquitin shutoff timer. Mol Cell 48, 888-899.

Graham, R.K., Deng, Y., Slow, E.J., Haigh, B., Bissada, N., Lu, G., Pearson, J., Shehadeh, J., Bertram, L., Murphy, Z.*, et al.* (2006). Cleavage at the caspase-6 site is required for neuronal dysfunction and degeneration due to mutant huntingtin. Cell 125, 1179-1191.

Graham, R.K., Ehrnhoefer, D.E., and Hayden, M.R. (2011). Caspase-6 and neurodegeneration. Trends Neurosci 34, 646-656.

Graham, W.V., Bonito-Oliva, A., and Sakmar, T.P. (2017). Update on Alzheimer's Disease Therapy and Prevention Strategies. Annu Rev Med 68, 413-430.

Gray, D.C., Mahrus, S., and Wells, J.A. (2010). Activation of specific apoptotic caspases with an engineered small-molecule-activated protease. Cell 142, 637-646.

Griffin, W.S., Sheng, J.G., Roberts, G.W., and Mrak, R.E. (1995). Interleukin-1 expression in different plaque types in Alzheimer's disease: significance in plaque evolution. J Neuropathol Exp Neurol 54, 276-281.

Griffin, W.S., Stanley, L.C., Ling, C., White, L., MacLeod, V., Perrot, L.J., White, C.L., and Araoz, C. (1989). Brain interleukin 1 and S-100 immunoreactivity are elevated in Down syndrome and Alzheimer's disease. Proc Natl Acad Sci USA 86, 7611-7615.

Grossmann, J., Artinger, M., Grasso, A.W., Kung, H.J., Scholmerich, J., Fiocchi, C., and Levine, A.D. (2001). Hierarchical cleavage of focal adhesion kinase by caspases alters signal transduction during apoptosis of intestinal epithelial cells. Gastroenterology 120, 79-88.

Gu, Y., Kuida, K., Tsutsui, H., Ku, G., Hsiao, K., Fleming, M.A., Hayashi, N., Higashino, K., Okamura, H., Nakanishi, K.*, et al.* (1997). Activation of interferon-gamma inducing factor mediated by interleukin-1beta converting enzyme. Science 275, 206-209.

Guegan, C., Vila, M., Teismann, P., Chen, C., Onteniente, B., Li, M., Friedlander, R.M., and Przedborski, S. (2002). Instrumental activation of bid by caspase-1 in a transgenic mouse model of ALS. Mol Cell Neurosci 20, 553-562.

Gulyaeva, N.V., Kudryashov, I.E., and Kudryashova, I.V. (2003). Caspase activity is essential for long-term potentiation. J Neurosci Res 73, 853-864.

Guo, H., Albrecht, S., Bourdeau, M., Petzke, T., Bergeron, C., and LeBlanc, A.C. (2004). Active caspase-6 and caspase-6-cleaved tau in neuropil threads, neuritic plaques, and neurofibrillary tangles of Alzheimer's disease. Am J Pathol 165, 523-531.

Guo, H., Petrin, D., Zhang, Y., Bergeron, C., Goodyer, C.G., and LeBlanc, A.C. (2006). Caspase-1 activation of caspase-6 in human apoptotic neurons. Cell Death Differ 13, 285-292.

Guo, Y., Srinivasula, S.M., Druilhe, A., Fernandes-Alnemri, T., and Alnemri, E.S. (2002). Caspase-2 induces apoptosis by releasing proapoptotic proteins from mitochondria. J Biol Chem 277, 13430-13437.

Gutteridge, A., and Thornton, J.M. (2005). Understanding nature's catalytic toolkit. Trends Biochem Sci 30, 622-629.

Hakem, R., Hakem, A., Duncan, G.S., Henderson, J.T., Woo, M., Soengas, M.S., Elia, A., de la Pompa, J.L., Kagi, D., Khoo, W.*, et al.* (1998). Differential requirement for caspase 9 in apoptotic pathways in vivo. Cell 94, 339-352.

Halawani, D., and Latterich, M. (2006). p97: The cell's molecular purgatory? Mol Cell 22, 713-717.

Halawani, D., Tessier, S., Anzellotti, D., Bennett, D.A., Latterich, M., and LeBlanc, A.C. (2010). Identification of Caspase-6-mediated processing of the valosin containing protein (p97) in Alzheimer's disease: a novel link to dysfunction in ubiquitin proteasome system-mediated protein degradation. J Neurosci 30, 6132-6142.

Hao, Y., Sekine, K., Kawabata, A., Nakamura, H., Ishioka, T., Ohata, H., Katayama, R., Hashimoto, C., Zhang, X., Noda, T.*, et al.* (2004). Apollon ubiquitinates SMAC and caspase-9, and has an essential cytoprotection function. Nat Cell Biol 6, 849-860.

Hardy, J., Bogdanovic, N., Winblad, B., Portelius, E., Andreasen, N., Cedazo-Minguez, A., and Zetterberg, H. (2014). Pathways to Alzheimer's disease. J Intern Med 275, 296-303.

Harigaya, Y., Shoji, M., Shirao, T., and Hirai, S. (1996). Disappearance of actin-binding protein, drebrin, from hippocampal synapses in Alzheimer's disease. J Neurosci Res 43, 87-92.

Harrison, D.C., Davis, R.P., Bond, B.C., Campbell, C.A., James, M.F., Parsons, A.A., and Philpott, K.L. (2001). Caspase mRNA expression in a rat model of focal cerebral ischemia. Brain Res Mol Brain Res 89, 133-146.

Harvey, N.L., Butt, A.J., and Kumar, S. (1997). Functional activation of Nedd2/ICH-1 (caspase-2) is an early process in apoptosis. J Biol Chem 272, 13134-13139.

Hattori, M., Sugino, E., Minoura, K., In, Y., Sumida, M., Taniguchi, T., Tomoo, K., and Ishida, T. (2008). Different inhibitory response of cyanidin and methylene blue for filament formation of tau microtubule-binding domain. Biochem Biophys Res Commun 374, 158-163.

Hauser, H.P., Bardroff, M., Pyrowolakis, G., and Jentsch, S. (1998). A giant ubiquitin-conjugating enzyme related to IAP apoptosis inhibitors. J Cell Biol 141, 1415-1422.

Heise, C.E., Murray, J., Augustyn, K.E., Bravo, B., Chugha, P., Cohen, F., Giannetti, A.M., Gibbons, P., Hannoush, R.N., Hearn, B.R.*, et al.* (2012). Mechanistic and structural understanding of uncompetitive inhibitors of caspase-6. PLoS One 7, e50864.

Hemphill, J.C., 3rd, Greenberg, S.M., Anderson, C.S., Becker, K., Bendok, B.R., Cushman, M., Fung, G.L., Goldstein, J.N., Macdonald, R.L., Mitchell, P.H.*, et al.* (2015). Guidelines for the Management of Spontaneous Intracerebral Hemorrhage: A Guideline for Healthcare Professionals From the American Heart Association/American Stroke Association. Stroke 46, 2032-2060.

Heneka, M.T., Kummer, M.P., Stutz, A., Delekate, A., Schwartz, S., Vieira-Saecker, A., Griep, A., Axt, D., Remus, A., Tzeng, T.C.*, et al.* (2013). NLRP3 is activated in Alzheimer's disease and contributes to pathology in APP/PS1 mice. Nature 493, 674-678.

Henzing, A.J., Dodson, H., Reid, J.M., Kaufmann, S.H., Baxter, R.L., and Earnshaw, W.C. (2006). Synthesis of novel caspase inhibitors for characterization of the active caspase proteome in vitro and in vivo. J Med Chem 49, 7636-7645.

Hermel, E., Gafni, J., Propp, S.S., Leavitt, B.R., Wellington, C.L., Young, J.E., Hackam, A.S., Logvinova, A.V., Peel, A.L., Chen, S.F.*, et al.* (2004). Specific caspase interactions and amplification are involved in selective neuronal vulnerability in Huntington's disease. Cell Death Differ 11, 424-438.

Hill, M.E., MacPherson, D.J., Wu, P., Julien, O., Wells, J.A., and Hardy, J.A. (2016). Reprogramming Caspase-7 Specificity by Regio-Specific Mutations and Selection Provides Alternate Solutions for Substrate Recognition. ACS Chem Biol 11, 1603-1612.

Hirata, H., Takahashi, A., Kobayashi, S., Yonehara, S., Sawai, H., Okazaki, T., Yamamoto, K., and Sasada, M. (1998). Caspases are activated in a branched protease cascade and control distinct downstream processes in Fas-induced apoptosis. J Exp Med 187, 587-600.

Ho, L.H., Taylor, R., Dorstyn, L., Cakouros, D., Bouillet, P., and Kumar, S. (2009). A tumor suppressor function for caspase-2. Proc Natl Acad Sci USA 106, 5336-5341.

Hochgrafe, K., Sydow, A., Matenia, D., Cadinu, D., Konen, S., Petrova, O., Pickhardt, M., Goll, P., Morellini, F., Mandelkow, E., and Mandelkow, E.M. (2015). Preventive methylene blue treatment preserves cognition in mice expressing full-length pro-aggregant human Tau. Acta Neuropathol Commun 3, 25.

Hofmann, K., Bucher, P., and Tschopp, J. (1997). The CARD domain: a new apoptotic signalling motif. Trends Biochem Sci 22, 155-156.

Hosokawa, M., Arai, T., Masuda-Suzukake, M., Nonaka, T., Yamashita, M., Akiyama, H., and Hasegawa, M. (2012). Methylene blue reduced abnormal tau accumulation in P301L tau transgenic mice. PLoS One 7, e52389.

Howard, A.D., Kostura, M.J., Thornberry, N., Ding, G.J., Limjuco, G., Weidner, J., Salley, J.P., Hogquist, K.A., Chaplin, D.D., Mumford, R.A., and et al. (1991). IL-1-converting enzyme requires aspartic acid residues for processing of the IL-1 beta precursor at two distinct sites and does not cleave 31-kDa IL-1 alpha. J Immunol 147, 2964-2969.

Hsu, H., Xiong, J., and Goeddel, D.V. (1995). The TNF receptor 1-associated protein TRADD signals cell death and NF-kappa B activation. Cell 81, 495-504.

Hu, S., Snipas, S.J., Vincenz, C., Salvesen, G., and Dixit, V.M. (1998). Caspase-14 is a novel developmentally regulated protease. J Biol Chem 273, 29648-29653.

Huang, D.W., McKerracher, L., Braun, P.E., and David, S. (1999). A therapeutic vaccine approach to stimulate axon regeneration in the adult mammalian spinal cord. Neuron 24, 639-647.

Huang, K., and El-Husseini, A. (2005). Modulation of neuronal protein trafficking and function by palmitoylation. Curr Opin Neurobiol 15, 527-535.

Huang, Y.A., Zhou, B., Wernig, M., and Sudhof, T.C. (2017). ApoE2, ApoE3, and ApoE4 Differentially Stimulate APP Transcription and Abeta Secretion. Cell 168, 427-441 e421.

Huang, Y.Y., Colino, A., Selig, D.K., and Malenka, R.C. (1992). The influence of prior synaptic activity on the induction of long-term potentiation. Science 255, 730-733.

Huang, Z., Pinto, J.T., Deng, H., and Richie, J.P., Jr. (2008). Inhibition of caspase-3 activity and activation by protein glutathionylation. Biochem Pharmacol 75, 2234-2244.

Humke, E.W., Ni, J., and Dixit, V.M. (1998). ERICE, a novel FLICE-activatable caspase. J Biol Chem 273, 15702-15707.

Hyman, B.T., Van Hoesen, G.W., Damasio, A.R., and Barnes, C.L. (1984). Alzheimer's disease: cell-specific pathology isolates the hippocampal formation. Science 225, 1168-1170.

Imtiaz, B., Tolppanen, A.M., Kivipelto, M., and Soininen, H. (2014). Future directions in Alzheimer's disease from risk factors to prevention. Biochem Pharmacol 88, 661-670.

Inoue, S., Browne, G., Melino, G., and Cohen, G.M. (2009). Ordering of caspases in cells undergoing apoptosis by the intrinsic pathway. Cell Death Differ 16, 1053-1061.

James, K.E., Asgian, J.L., Li, Z.Z., Ekici, O.D., Rubin, J.R., Mikolajczyk, J., Salvesen, G.S., and Powers, J.C. (2004). Design, synthesis, and evaluation of aza-peptide epoxides as selective and potent inhibitors of caspases-1, -3, -6, and -8. J Med Chem 47, 1553-1574.

Jiang, Z.L., Fletcher, N.M., Diamond, M.P., Abu-Soud, H.M., and Saed, G.M. (2009). S-nitrosylation of caspase-3 is the mechanism by which adhesion fibroblasts manifest lower apoptosis. Wound Repair Regen 17, 224-229.

Julien, O., Zhuang, M., Wiita, A.P., O'Donoghue, A.J., Knudsen, G.M., Craik, C.S., and Wells, J.A. (2016). Quantitative MS-based enzymology of caspases reveals distinct protein substrate specificities, hierarchies, and cellular roles. Proc Natl Acad Sci USA 113, E2001-2010.

Juo, P., Kuo, C.J., Yuan, J., and Blenis, J. (1998). Essential requirement for caspase-8/FLICE in the initiation of the Fas-induced apoptotic cascade. Curr Biol 8, 1001-1008.

Kaiser, W.J., Upton, J.W., Long, A.B., Livingston-Rosanoff, D., Daley-Bauer, L.P., Hakem, R., Caspary, T., and Mocarski, E.S. (2011). RIP3 mediates the embryonic lethality of caspase-8-deficient mice. Nature 471, 368-372.

Kajiwara, Y., McKenzie, A., Dorr, N., Gama Sosa, M.A., Elder, G., Schmeidler, J., Dickstein, D.L., Bozdagi, O., Zhang, B., and Buxbaum, J.D. (2016). The human-specific CASP4 gene product contributes to Alzheimer-related synaptic and behavioural deficits. Hum Mol Genet 25, 4315-4327.

Kamens, J., Paskind, M., Hugunin, M., Talanian, R.V., Allen, H., Banach, D., Bump, N., Hackett, M., Johnston, C.G., Li, P., and et al. (1995). Identification and characterization of ICH-2, a novel member of the interleukin-1 beta-converting enzyme family of cysteine proteases. J Biol Chem 270, 15250-15256.

Kang, B.H., Ko, E., Kwon, O.K., and Choi, K.Y. (2002). The structure of procaspase 6 is similar to that of active mature caspase 6. Biochem J 364, 629-634.

Kang, T.B., Ben-Moshe, T., Varfolomeev, E.E., Pewzner-Jung, Y., Yogev, N., Jurewicz, A., Waisman, A., Brenner, O., Haffner, R., Gustafsson, E.*, et al.* (2004). Caspase-8 serves both apoptotic and nonapoptotic roles. J Immunol 173, 2976-2984.

Karran, E., and De Strooper, B. (2016). The amyloid cascade hypothesis: are we poised for success or failure? J Neurochem 139 Suppl 2, 237-252.

Kaushal, V., Dye, R., Pakavathkumar, P., Foveau, B., Flores, J., Hyman, B., Ghetti, B., Koller, B.H., and LeBlanc, A.C. (2015). Neuronal NLRP1 inflammasome activation of Caspase-1 coordinately regulates inflammatory interleukin-1-beta production and axonal degeneration-associated Caspase-6 activation. Cell Death Differ 22, 1676-1686.

Kayagaki, N., Stowe, I.B., Lee, B.L., O'Rourke, K., Anderson, K., Warming, S., Cuellar, T., Haley, B., Roose-Girma, M., Phung, Q.T., *et al.* (2015). Caspase-11 cleaves gasdermin D for non-canonical inflammasome signalling. Nature 526, 666-671.

Keller, M., Ruegg, A., Werner, S., and Beer, H.D. (2008). Active caspase-1 is a regulator of unconventional protein secretion. Cell 132, 818-831.

Kerr, J.F., Wyllie, A.H., and Currie, A.R. (1972). Apoptosis: a basic biological phenomenon with wide-ranging implications in tissue kinetics. Br J Cancer 26, 239-257.

Kesselheim, A.S., Hwang, T.J., and Franklin, J.M. (2015). Two decades of new drug development for central nervous system disorders. Nat Rev Drug Discov 14, 815-816.

Kim, Y., Choi, H., Lee, W., Park, H., Kam, T.I., Hong, S.H., Nah, J., Jung, S., Shin, B., Lee, H., *et al.* (2016). Caspase-cleaved tau exhibits rapid memory impairment associated with tau oligomers in a transgenic mouse model. Neurobiol Dis 87, 19-28.

Kischkel, F.C., Hellbardt, S., Behrmann, I., Germer, M., Pawlita, M., Krammer, P.H., and Peter, M.E. (1995). Cytotoxicity-dependent APO-1 (Fas/CD95)-associated proteins form a death-inducing signaling complex (DISC) with the receptor. EMBO J 14, 5579-5588.

Kisselev, A.F., Garcia-Calvo, M., Overkleeft, H.S., Peterson, E., Pennington, M.W., Ploegh, H.L., Thornberry, N.A., and Goldberg, A.L. (2003). The caspase-like sites of proteasomes, their substrate specificity, new inhibitors and substrates, and allosteric interactions with the trypsin-like sites. J Biol Chem 278, 35869-35877.

Klaiman, G., Champagne, N., and LeBlanc, A.C. (2009). Self-activation of Caspase-6 in vitro and in vivo: Caspase-6 activation does not induce cell death in HEK293T cells. Biochim Biophys Acta 1793, 592-601.

Klaiman, G., Petzke, T.L., Hammond, J., and LeBlanc, A.C. (2008). Targets of caspase-6 activity in human neurons and Alzheimer disease. Mol Cell Proteomics 7, 1541-1555.

Kobayashi, H., Nolan, A., Naveed, B., Hoshino, Y., Segal, L.N., Fujita, Y., Rom, W.N., and Weiden, M.D. (2011). Neutrophils activate alveolar macrophages by producing caspase-6-mediated cleavage of IL-1 receptor-associated kinase-M. J Immunol 186, 403-410.

Kobayashi, R., Sekino, Y., Shirao, T., Tanaka, S., Ogura, T., Inada, K., and Saji, M. (2004). Antisense knockdown of drebrin A, a dendritic spine protein, causes stronger preference, impaired pre-pulse inhibition, and an increased sensitivity to psychostimulant. Neurosci Res 49, 205-217.

Koenig, U., Eckhart, L., and Tschachler, E. (2001). Evidence that caspase-13 is not a human but a bovine gene. Biochem Biophys Res Commun 285, 1150-1154.

Kohler, J.E., Mathew, J., Tai, K., Blass, A.L., Kelly, E., and Soybel, D.I. (2009). Monochloramine impairs caspase-3 through thiol oxidation and Zn2+ release. J Surg Res 153, 121-127.

Kordasiewicz, H.B., Stanek, L.M., Wancewicz, E.V., Mazur, C., McAlonis, M.M., Pytel, K.A., Artates, J.W., Weiss, A., Cheng, S.H., Shihabuddin, L.S.*, et al.* (2012). Sustained therapeutic reversal of Huntington's disease by transient repression of huntingtin synthesis. Neuron 74, 1031-1044.

Kostura, M.J., Tocci, M.J., Limjuco, G., Chin, J., Cameron, P., Hillman, A.G., Chartrain, N.A., and Schmidt, J.A. (1989). Identification of a monocyte specific pre-interleukin 1 beta convertase activity. Proc Natl Acad Sci USA 86, 5227-5231.

Kroemer, G., Galluzzi, L., Vandenabeele, P., Abrams, J., Alnemri, E.S., Baehrecke, E.H., Blagosklonny, M.V., El-Deiry, W.S., Golstein, P., Green, D.R.*, et al.* (2009). Classification of cell death: recommendations of the Nomenclature Committee on Cell Death 2009. Cell Death Differ 16, 3-11.

Krupinski, J., Lopez, E., Marti, E., and Ferrer, I. (2000). Expression of caspases and their substrates in the rat model of focal cerebral ischemia. Neurobiol Dis 7, 332-342.

Kuida, K., Haydar, T.F., Kuan, C.Y., Gu, Y., Taya, C., Karasuyama, H., Su, M.S., Rakic, P., and Flavell, R.A. (1998). Reduced apoptosis and cytochrome c-mediated caspase activation in mice lacking caspase 9. Cell 94, 325-337.

Kuida, K., Lippke, J.A., Ku, G., Harding, M.W., Livingston, D.J., Su, M.S., and Flavell, R.A. (1995). Altered cytokine export and apoptosis in mice deficient in interleukin-1 beta converting enzyme. Science 267, 2000-2003.

Kuida, K., Zheng, T.S., Na, S., Kuan, C., Yang, D., Karasuyama, H., Rakic, P., and Flavell, R.A. (1996). Decreased apoptosis in the brain and premature lethality in CPP32-deficient mice. Nature 384, 368-372.

Kumar, S., Kinoshita, M., Noda, M., Copeland, N.G., and Jenkins, N.A. (1994). Induction of apoptosis by the mouse Nedd2 gene, which encodes a protein similar to the product of the Caenorhabditis elegans cell death gene ced-3 and the mammalian IL-1 beta-converting enzyme. Genes Dev 8, 1613-1626.

Kumar, S., Tomooka, Y., and Noda, M. (1992). Identification of a set of genes with developmentally down-regulated expression in the mouse brain. Biochem Biophys Res Commun 185, 1155-1161.

Kupfer, A., Aeschlimann, C., Wermuth, B., and Cerny, T. (1994). Prophylaxis and reversal of ifosfamide encephalopathy with methylene-blue. Lancet 343, 763-764.

Kuranaga, E., Kanuka, H., Tonoki, A., Takemoto, K., Tomioka, T., Kobayashi, M., Hayashi, S., and Miura, M. (2006). Drosophila IKK-related kinase regulates nonapoptotic function of caspases via degradation of IAPs. Cell 126, 583-596.

Kyathanahalli, C., Organ, K., Moreci, R.S., Anamthathmakula, P., Hassan, S.S., Caritis, S.N., Jeyasuria, P., and Condon, J.C. (2015). Uterine endoplasmic reticulum stress-unfolded protein response regulation of gestational length is caspase-3 and -7-dependent. Proc Natl Acad Sci USA 112, 14090-14095.

Lafuente, M.P., Villegas-Perez, M.P., Selles-Navarro, I., Mayor-Torroglosa, S., Miralles de Imperial, J., and Vidal-Sanz, M. (2002). Retinal ganglion cell death after acute retinal ischemia is an ongoing process whose severity and duration depends on the duration of the insult. Neuroscience 109, 157-168.

Lai, Y.C., Pan, K.T., Chang, G.F., Hsu, C.H., Khoo, K.H., Hung, C.H., Jiang, Y.J., Ho, F.M., and Meng, T.C. (2011). Nitrite-mediated S-nitrosylation of caspase-3 prevents hypoxia-induced endothelial barrier dysfunction. Circ Res 109, 1375-1386.

Lamkanfi, M., Declercq, W., Kalai, M., Saelens, X., and Vandenabeele, P. (2002). Alice in caspase land. A phylogenetic analysis of caspases from worm to man. Cell Death Differ 9, 358-361.

Lamkanfi, M., Kalai, M., Saelens, X., Declercq, W., and Vandenabeele, P. (2004). Caspase-1 activates nuclear factor of the kappa-enhancer in B cells independently of its enzymatic activity. J Biol Chem 279, 24785-24793.

Lazebnik, Y.A., Kaufmann, S.H., Desnoyers, S., Poirier, G.G., and Earnshaw, W.C. (1994). Cleavage of poly(ADP-ribose) polymerase by a proteinase with properties like ICE. Nature 371, 346-347.

Le, D.A., Wu, Y., Huang, Z., Matsushita, K., Plesnila, N., Augustinack, J.C., Hyman, B.T., Yuan, J., Kuida, K., Flavell, R.A., and Moskowitz, M.A. (2002). Caspase activation and neuroprotection in caspase-3- deficient mice after in vivo cerebral ischemia and in vitro oxygen glucose deprivation. Proc Natl Acad Sci USA 99, 15188-15193.

LeBlanc, A. (1995). Increased production of 4 kDa amyloid beta peptide in serum deprived human primary neuron cultures: possible involvement of apoptosis. J Neurosci 15, 7837-7846.

LeBlanc, A., Liu, H., Goodyer, C., Bergeron, C., and Hammond, J. (1999). Caspase-6 role in apoptosis of human neurons, amyloidogenesis, and Alzheimer's disease. J Biol Chem 274, 23426-23436.

LeBlanc, A.C. (2013). Caspase-6 as a novel early target in the treatment of Alzheimer's disease. Eur J Neurosci 37, 2005-2018.

LeBlanc, A.C., Ramcharitar, J., Afonso, V., Hamel, E., Bennett, D.A., Pakavathkumar, P., and Albrecht, S. (2014). Caspase-6 activity in the CA1 region of the hippocampus induces age-dependent memory impairment. Cell Death Differ 21, 696-706.

Lee, A.W., Champagne, N., Wang, X., Su, X.D., Goodyer, C., and LeBlanc, A.C. (2010). Alternatively spliced caspase-6B isoform inhibits the activation of caspase-6A. J Biol Chem 285, 31974-31984.

Lee, J.W., Kim, M.R., Soung, Y.H., Nam, S.W., Kim, S.H., Lee, J.Y., Yoo, N.J., and Lee, S.H. (2006a). Mutational analysis of the CASP6 gene in colorectal and gastric carcinomas. APMIS 114, 646-650.

Lee, J.W., Soung, Y.H., Kim, S.Y., Park, W.S., Nam, S.W., Lee, J.Y., Yoo, N.J., and Lee, S.H. (2006b). Somatic mutation of pro-apoptosis caspase-6 gene is rare in breast and lung carcinomas. Pathology 38, 358-359.

Lefebvre, S., Burglen, L., Reboullet, S., Clermont, O., Burlet, P., Viollet, L., Benichou, B., Cruaud, C., Millasseau, P., Zeviani, M., and et al. (1995). Identification and characterization of a spinal muscular atrophy-determining gene. Cell 80, 155-165.

Lei, B., Zhou, X., Lv, D., Wan, B., Wu, H., Zhong, L., Shu, F., and Mao, X. (2017). Apoptotic and nonapoptotic function of caspase 7 in spermatogenesis. Asian J Androl 19, 47-51.

Lemmers, B., Salmena, L., Bidere, N., Su, H., Matysiak-Zablocki, E., Murakami, K., Ohashi, P.S., Jurisicova, A., Lenardo, M., Hakem, R., and Hakem, A. (2007). Essential role for caspase-8 in Toll-like receptors and NFkappaB signaling. J Biol Chem 282, 7416-7423.

Lens, S.M., Kataoka, T., Fortner, K.A., Tinel, A., Ferrero, I., MacDonald, R.H., Hahne, M., Beermann, F., Attinger, A., Orbea, H.A.*, et al.* (2002). The caspase 8 inhibitor c-FLIP(L) modulates T-cell receptor-induced proliferation but not activation-induced cell death of lymphocytes. Mol Cell Biol 22, 5419-5433.

Leong, S.M., Tan, B.X., Bte Ahmad, B., Yan, T., Chee, L.Y., Ang, S.T., Tay, K.G., Koh, L.P., Yeoh, A.E., Koay, E.S.*, et al.* (2010). Mutant nucleophosmin deregulates cell death and myeloid differentiation through excessive caspase-6 and -8 inhibition. Blood 116, 3286-3296.

Leyva, M.J., Degiacomo, F., Kaltenbach, L.S., Holcomb, J., Zhang, N., Gafni, J., Park, H., Lo, D.C., Salvesen, G.S., Ellerby, L.M., and Ellman, J.A. (2010). Identification and evaluation of small molecule pan-caspase inhibitors in Huntington's disease models. Chem Biol 17, 1189-1200.

Li, F., Ackermann, E.J., Bennett, C.F., Rothermel, A.L., Plescia, J., Tognin, S., Villa, A., Marchisio, P.C., and Altieri, D.C. (1999). Pleiotropic cell-division defects and apoptosis induced by interference with survivin function. Nat Cell Biol 1, 461-466.

Li, H., Zhu, H., Xu, C.J., and Yuan, J. (1998). Cleavage of BID by caspase 8 mediates the mitochondrial damage in the Fas pathway of apoptosis. Cell 94, 491-501.

Li, M., Ona, V.O., Guegan, C., Chen, M., Jackson-Lewis, V., Andrews, L.J., Olszewski, A.J., Stieg, P.E., Lee, J.P., Przedborski, S., and Friedlander, R.M. (2000). Functional role of caspase-1 and caspase-3 in an ALS transgenic mouse model. Science 288, 335-339.

Li, P., Allen, H., Banerjee, S., Franklin, S., Herzog, L., Johnston, C., McDowell, J., Paskind, M., Rodman, L., Salfeld, J., and et al. (1995). Mice deficient in IL-1 beta-converting enzyme are defective in production of mature IL-1 beta and resistant to endotoxic shock. Cell 80, 401-411.

Li, P., Nijhawan, D., Budihardjo, I., Srinivasula, S.M., Ahmad, M., Alnemri, E.S., and Wang, X. (1997). Cytochrome c and dATP-dependent formation of Apaf-1/caspase-9 complex initiates an apoptotic protease cascade. Cell 91, 479-489.

Li, Z., Jo, J., Jia, J.M., Lo, S.C., Whitcomb, D.J., Jiao, S., Cho, K., and Sheng, M. (2010). Caspase-3 activation via mitochondria is required for long-term depression and AMPA receptor internalization. Cell 141, 859-871.

Lin, X.Y., Choi, M.S., and Porter, A.G. (2000). Expression analysis of the human caspase-1 subfamily reveals specific regulation of the CASP5 gene by lipopolysaccharide and interferon-gamma. J Biol Chem 275, 39920-39926.

Lin, Y., Devin, A., Rodriguez, Y., and Liu, Z.G. (1999). Cleavage of the death domain kinase RIP by caspase-8 prompts TNF-induced apoptosis. Genes Dev 13, 2514-2526.

Ling, D.S., Benardo, L.S., Serrano, P.A., Blace, N., Kelly, M.T., Crary, J.F., and Sacktor, T.C. (2002). Protein kinase Mzeta is necessary and sufficient for LTP maintenance. Nat Neurosci 5, 295-296.

Linnik, M.D., Zobrist, R.H., and Hatfield, M.D. (1993). Evidence supporting a role for programmed cell death in focal cerebral ischemia in rats. Stroke 24, 2002-2008; discussion 2008-2009.

Lippens, S., Kockx, M., Knaapen, M., Mortier, L., Polakowska, R., Verheyen, A., Garmyn, M., Zwijsen, A., Formstecher, P., Huylebroeck, D.*, et al.* (2000). Epidermal differentiation does not involve the pro-apoptotic executioner caspases, but is associated with caspase-14 induction and processing. Cell Death Differ 7, 1218-1224.

Liston, P., Roy, N., Tamai, K., Lefebvre, C., Baird, S., Cherton-Horvat, G., Farahani, R., McLean, M., Ikeda, J.E., MacKenzie, A., and Korneluk, R.G. (1996). Suppression of apoptosis in mammalian cells by NAIP and a related family of IAP genes. Nature 379, 349-353.

Liu, X., Kim, C.N., Yang, J., Jemmerson, R., and Wang, X. (1996). Induction of apoptotic program in cell-free extracts: requirement for dATP and cytochrome c. Cell 86, 147-157.

Liu, X., Zhang, H., Wang, X.J., Li, L.F., and Su, X.D. (2011). Get phases from arsenic anomalous scattering: de novo SAD phasing of two protein structures crystallized in cacodylate buffer. PLoS One 6, e24227.

Liu, X., Zou, H., Slaughter, C., and Wang, X. (1997). DFF, a heterodimeric protein that functions downstream of caspase-3 to trigger DNA fragmentation during apoptosis. Cell 89, 175-184.

Lo Conte, M., and Carroll, K.S. (2013). The redox biochemistry of protein sulfenylation and sulfinylation. J Biol Chem 288, 26480-26488.

Lockshin, R.A., and Williams, C.M. (1964). Programmed Cell Death .2. Endocrine Potentiation of the Breakdown of the Intersegmental Muscles of Silkmoths. J Insect Physiol 10, 643-649.

Long, M.J., Gollapalli, D.R., and Hedstrom, L. (2012). Inhibitor mediated protein degradation. Chem Biol 19, 629-637.

Lopez-Pastrana, J., Ferrer, L.M., Li, Y.F., Xiong, X., Xi, H., Cueto, R., Nelson, J., Sha, X., Li, X., Cannella, A.L.*, et al.* (2015). Inhibition of Caspase-1 Activation in Endothelial Cells Improves Angiogenesis: A NOVEL THERAPEUTIC POTENTIAL FOR ISCHEMIA. J Biol Chem 290, 17485-17494.

Los, M., Van de Craen, M., Penning, L.C., Schenk, H., Westendorp, M., Baeuerle, P.A., Droge, W., Krammer, P.H., Fiers, W., and Schulze-Osthoff, K. (1995). Requirement of an ICE/CED-3 protease for Fas/APO-1-mediated apoptosis. Nature 375, 81-83.

Luo, X., Budihardjo, I., Zou, H., Slaughter, C., and Wang, X. (1998). Bid, a Bcl2 interacting protein, mediates cytochrome c release from mitochondria in response to activation of cell surface death receptors. Cell 94, 481-490.

Maccioni, R.B., Vera, J.C., Dominguez, J., and Avila, J. (1989). A discrete repeated sequence defines a tubulin binding domain on microtubule-associated protein tau. Arch Biochem Biophys 275, 568-579.

MacLachlan, T.K., and El-Deiry, W.S. (2002). Apoptotic threshold is lowered by p53 transactivation of caspase-6. Proc Natl Acad Sci USA 99, 9492-9497.

Mahrus, S., Trinidad, J.C., Barkan, D.T., Sali, A., Burlingame, A.L., and Wells, J.A. (2008). Global sequencing of proteolytic cleavage sites in apoptosis by specific labeling of protein N termini. Cell 134, 866-876.

Maier, J.K., Lahoua, Z., Gendron, N.H., Fetni, R., Johnston, A., Davoodi, J., Rasper, D., Roy, S., Slack, R.S., Nicholson, D.W., and MacKenzie, A.E. (2002). The neuronal apoptosis inhibitory protein is a direct inhibitor of caspases 3 and 7. J Neurosci 22, 2035-2043.

Martin, D.P., Schmidt, R.E., DiStefano, P.S., Lowry, O.H., Carter, J.G., and Johnson, E.M., Jr. (1988). Inhibitors of protein synthesis and RNA synthesis prevent neuronal death caused by nerve growth factor deprivation. J Cell Biol 106, 829-844.

Martin, R., Desponds, C., Eren, R.O., Quadroni, M., Thome, M., and Fasel, N. (2016). Caspase-mediated cleavage of raptor participates in the inactivation of mTORC1 during cell death. Cell Death Discov 2, 16024.

Martin, S.J., Finucane, D.M., Amarante-Mendes, G.P., O'Brien, G.A., and Green, D.R. (1996). Phosphatidylserine externalization during CD95-induced apoptosis of cells and cytoplasts requires ICE/CED-3 protease activity. J Biol Chem 271, 28753-28756.

Martindale, D., Hackam, A., Wieczorek, A., Ellerby, L., Wellington, C., McCutcheon, K., Singaraja, R., Kazemi-Esfarjani, P., Devon, R., Kim, S.U*., et al.* (1998). Length of huntingtin and its polyglutamine tract influences localization and frequency of intracellular aggregates. Nat Genet 18, 150-154.

Martinon, F., Burns, K., and Tschopp, J. (2002). The inflammasome: a molecular platform triggering activation of inflammatory caspases and processing of proIL-beta. Mol Cell 10, 417-426.

Martinou, J.C., Dubois-Dauphin, M., Staple, J.K., Rodriguez, I., Frankowski, H., Missotten, M., Albertini, P., Talabot, D., Catsicas, S., Pietra, C., and et al. (1994). Overexpression of BCL-2 in transgenic mice protects neurons from naturally occurring cell death and experimental ischemia. Neuron 13, 1017-1030.

Matalova, E., Vanden Berghe, T., Svandova, E., Vandenabeele, P., Healy, C., Sharpe, P.T., and Tucker, A.S. (2012). Caspase-7 in molar tooth development. Arch Oral Biol 57, 1474-1481.

Mazzotta, G., Sarchielli, P., Caso, V., Paciaroni, M., Floridi, A., Floridi, A., and Gallai, V. (2004). Different cytokine levels in thrombolysis patients as predictors for clinical outcome. Eur J Neurol 11, 377-381.

McStay, G.P., Salvesen, G.S., and Green, D.R. (2008). Overlapping cleavage motif selectivity of caspases: implications for analysis of apoptotic pathways. Cell Death Differ 15, 322-331.

Medina, D.X., Caccamo, A., and Oddo, S. (2011). Methylene blue reduces abeta levels and rescues early cognitive deficit by increasing proteasome activity. Brain Pathol 21, 140-149.

Methot, N., Huang, J., Coulombe, N., Vaillancourt, J.P., Rasper, D., Tam, J., Han, Y., Colucci, J., Zamboni, R., Xanthoudakis, S.*, et al.* (2004). Differential efficacy of caspase inhibitors on apoptosis markers during sepsis in rats and implication for fractional inhibition requirements for therapeutics. J Exp Med 199, 199-207.

Mhatre, S.D., Tsai, C.A., Rubin, A.J., James, M.L., and Andreasson, K.I. (2015). Microglial malfunction: the third rail in the development of Alzheimer's disease. Trends Neurosci 38, 621-636.

Micheau, O., and Tschopp, J. (2003). Induction of TNF receptor I-mediated apoptosis via two sequential signaling complexes. Cell 114, 181-190.

Mikolajczyk, J., Scott, F.L., Krajewski, S., Sutherlin, D.P., and Salvesen, G.S. (2004). Activation and substrate specificity of caspase-14. Biochemistry 43, 10560-10569.

Miller, D.K., Ayala, J.M., Egger, L.A., Raju, S.M., Yamin, T.T., Ding, G.J., Gaffney, E.P., Howard, A.D., Palyha, O.C., Rolando, A.M., and et al. (1993). Purification and characterization of active human interleukin-1 beta-converting enzyme from THP.1 monocytic cells. J Biol Chem 268, 18062-18069.

Miller, T.M., Pestronk, A., David, W., Rothstein, J., Simpson, E., Appel, S.H., Andres, P.L., Mahoney, K., Allred, P., Alexander, K.*, et al.* (2013). An antisense oligonucleotide against SOD1 delivered intrathecally for patients with SOD1 familial amyotrophic lateral sclerosis: a phase 1, randomised, first-in-man study. Lancet Neurol 12, 435-442.

Miossec, C., Dutilleul, V., Fassy, F., and Diu-Hercend, A. (1997). Evidence for CPP32 activation in the absence of apoptosis during T lymphocyte stimulation. J Biol Chem 272, 13459-13462.

Mitsios, N., Gaffney, J., Krupinski, J., Mathias, R., Wang, Q., Hayward, S., Rubio, F., Kumar, P., Kumar, S., and Slevin, M. (2007). Expression of signaling molecules associated with apoptosis in human ischemic stroke tissue. Cell Biochem Biophys 47, 73-86.

Mohideen, S.S., Yamasaki, Y., Omata, Y., Tsuda, L., and Yoshiike, Y. (2015). Nontoxic singlet oxygen generator as a therapeutic candidate for treating tauopathies. Sci Rep 5, 10821.

Mohr, S., Zech, B., Lapetina, E.G., and Brune, B. (1997). Inhibition of caspase-3 by S-nitrosation and oxidation caused by nitric oxide. Biochem Biophys Res Commun 238, 387-391.

Mojica, F.J., Diez-Villasenor, C., Garcia-Martinez, J., and Soria, E. (2005). Intervening sequences of regularly spaced prokaryotic repeats derive from foreign genetic elements. J Mol Evol 60, 174-182.

Monnier, P.P., D'Onofrio, P.M., Magharious, M., Hollander, A.C., Tassew, N., Szydlowska, K., Tymianski, M., and Koeberle, P.D. (2011). Involvement of caspase-6 and caspase-8 in

neuronal apoptosis and the regenerative failure of injured retinal ganglion cells. J Neurosci 31, 10494-10505.

Moore, D.J., Zhang, L., Dawson, T.M., and Dawson, V.L. (2003). A missense mutation (L166P) in DJ-1, linked to familial Parkinson's disease, confers reduced protein stability and impairs homo-oligomerization. J Neurochem 87, 1558-1567.

Moquin, D.M., McQuade, T., and Chan, F.K. (2013). CYLD deubiquitinates RIP1 in the TNFalpha-induced necrosome to facilitate kinase activation and programmed necrosis. PLoS One 8, e76841.

Morozov, V., and Wawrousek, E.F. (2006). Caspase-dependent secondary lens fiber cell disintegration in alphaA-/alphaB-crystallin double-knockout mice. Development 133, 813-821.

Moss, D.K., Betin, V.M., Malesinski, S.D., and Lane, J.D. (2006). A novel role for microtubules in apoptotic chromatin dynamics and cellular fragmentation. J Cell Sci 119, 2362-2374.

Mukerjee, N., McGinnis, K.M., Park, Y.H., Gnegy, M.E., and Wang, K.K. (2000). Caspase-mediated proteolytic activation of calcineurin in thapsigargin-mediated apoptosis in SH-SY5Y neuroblastoma cells. Arch Biochem Biophys 379, 337-343.

Muller, I., Lamers, M.B., Ritchie, A.J., Dominguez, C., Munoz-Sanjuan, I., and Kiselyov, A. (2011a). Structure of human caspase-6 in complex with Z-VAD-FMK: New peptide binding mode observed for the non-canonical caspase conformation. Bioorg Med Chem Lett 21, 5244-5247.

Muller, I., Lamers, M.B., Ritchie, A.J., Park, H., Dominguez, C., Munoz-Sanjuan, I., Maillard, M., and Kiselyov, A. (2011b). A new apo-caspase-6 crystal form reveals the active conformation of the apoenzyme. J Mol Biol 410, 307-315.

Munday, N.A., Vaillancourt, J.P., Ali, A., Casano, F.J., Miller, D.K., Molineaux, S.M., Yamin, T.T., Yu, V.L., and Nicholson, D.W. (1995). Molecular cloning and pro-apoptotic activity of ICErelII and ICErelIII, members of the ICE/CED-3 family of cysteine proteases. J Biol Chem 270, 15870-15876.

Mungarro-Menchaca, X., Ferrera, P., Moran, J., and Arias, C. (2002). beta-Amyloid peptide induces ultrastructural changes in synaptosomes and potentiates mitochondrial dysfunction in the presence of ryanodine. J Neurosci Res 68, 89-96.

Murray, J., Giannetti, A.M., Steffek, M., Gibbons, P., Hearn, B.R., Cohen, F., Tam, C., Pozniak, C., Bravo, B., Lewcock, J.*, et al.* (2014). Tailoring small molecules for an allosteric site on procaspase-6. ChemMedChem 9, 73-77, 72.

Muzio, M., Chinnaiyan, A.M., Kischkel, F.C., O'Rourke, K., Shevchenko, A., Ni, J., Scaffidi, C., Bretz, J.D., Zhang, M., Gentz, R.*, et al.* (1996). FLICE, a novel FADD-homologous

ICE/CED-3-like protease, is recruited to the CD95 (Fas/APO-1) death--inducing signaling complex. Cell 85, 817-827.

Muzio, M., Stockwell, B.R., Stennicke, H.R., Salvesen, G.S., and Dixit, V.M. (1998). An induced proximity model for caspase-8 activation. J Biol Chem 273, 2926-2930.

Nelson, C.D., Kim, M.J., Hsin, H., Chen, Y., and Sheng, M. (2013). Phosphorylation of threonine-19 of PSD-95 by GSK-3beta is required for PSD-95 mobilization and long-term depression. J Neurosci 33, 12122-12135.

Nikolaev, A., McLaughlin, T., O'Leary, D.D., and Tessier-Lavigne, M. (2009). APP binds DR6 to trigger axon pruning and neuron death via distinct caspases. Nature 457, 981-989.

Nobel, C.S., Burgess, D.H., Zhivotovsky, B., Burkitt, M.J., Orrenius, S., and Slater, A.F. (1997). Mechanism of dithiocarbamate inhibition of apoptosis: thiol oxidation by dithiocarbamate disulfides directly inhibits processing of the caspase-3 proenzyme. Chem Res Toxicol 10, 636-643.

Noorbakhsh, F., Ramachandran, R., Barsby, N., Ellestad, K.K., LeBlanc, A., Dickie, P., Baker, G., Hollenberg, M.D., Cohen, E.A., and Power, C. (2010). MicroRNA profiling reveals new aspects of HIV neurodegeneration: caspase-6 regulates astrocyte survival. FASEB J 24, 1799-1812.

Nybo, K. (2012). GFP imaging in fixed cells. Biotechniques 52, 359-360.

Nyormoi, O., Wang, Z., and Bar-Eli, M. (2003). Sequence-based discovery of a synthetic peptide inhibitor of caspase 6. Apoptosis 8, 371-376.

O'Donnell, M.A., Perez-Jimenez, E., Oberst, A., Ng, A., Massoumi, R., Xavier, R., Green, D.R., and Ting, A.T. (2011). Caspase 8 inhibits programmed necrosis by processing CYLD. Nat Cell Biol 13, 1437-1442.

O'Leary, J.C., 3rd, Li, Q., Marinec, P., Blair, L.J., Congdon, E.E., Johnson, A.G., Jinwal, U.K., Koren, J., 3rd, Jones, J.R., Kraft, C.*, et al.* (2010). Phenothiazine-mediated rescue of cognition in tau transgenic mice requires neuroprotection and reduced soluble tau burden. Mol Neurodegener 5, 45.

Oberst, A., Dillon, C.P., Weinlich, R., McCormick, L.L., Fitzgerald, P., Pop, C., Hakem, R., Salvesen, G.S., and Green, D.R. (2011). Catalytic activity of the caspase-8-FLIP(L) complex inhibits RIPK3-dependent necrosis. Nature 471, 363-367.

Oh, W.C., Parajuli, L.K., and Zito, K. (2015). Heterosynaptic structural plasticity on local dendritic segments of hippocampal CA1 neurons. Cell Rep 10, 162-169.

Olney, J.W. (1994). Excitatory transmitter neurotoxicity. Neurobiol Aging 15, 259-260.

Olson, N.E., Graves, J.D., Shu, G.L., Ryan, E.J., and Clark, E.A. (2003). Caspase activity is required for stimulated B lymphocytes to enter the cell cycle. J Immunol 170, 6065-6072.

Ona, V.O., Li, M., Vonsattel, J.P., Andrews, L.J., Khan, S.Q., Chung, W.M., Frey, A.S., Menon, A.S., Li, X.J., Stieg, P.E.*, et al.* (1999). Inhibition of caspase-1 slows disease progression in a mouse model of Huntington's disease. Nature 399, 263-267.

Orth, K., Chinnaiyan, A.M., Garg, M., Froelich, C.J., and Dixit, V.M. (1996). The CED-3/ICE-like protease Mch2 is activated during apoptosis and cleaves the death substrate lamin A. J Biol Chem 271, 16443-16446.

Oz, M., Lorke, D.E., Hasan, M., and Petroianu, G.A. (2011). Cellular and molecular actions of Methylene Blue in the nervous system. Med Res Rev 31, 93-117.

Ozcelik, S., Sprenger, F., Skachokova, Z., Fraser, G., Abramowski, D., Clavaguera, F., Probst, A., Frank, S., Muller, M., Staufenbiel, M.*, et al.* (2016). Co-expression of truncated and full-length tau induces severe neurotoxicity. Mol Psychiatry 21, 1790-1798.

Ozturk, G., Cengiz, N., Erdogan, E., Him, A., Oguz, E.K., Yenidunya, E., and Aysit, N. (2013). Two distinct types of dying back axonal degeneration in vitro. Neuropathol Appl Neurobiol 39, 362-376.

Palmer, J.T., Rasnick, D., Klaus, J.L., and Bromme, D. (1995). Vinyl sulfones as mechanism-based cysteine protease inhibitors. J Med Chem 38, 3193-3196.

Pan, S., and Berk, B.C. (2007). Glutathiolation regulates tumor necrosis factor-alpha-induced caspase-3 cleavage and apoptosis: key role for glutaredoxin in the death pathway. Circ Res 100, 213-219.

Park, K.J., Grosso, C.A., Aubert, I., Kaplan, D.R., and Miller, F.D. (2010). p75NTR-dependent, myelin-mediated axonal degeneration regulates neural connectivity in the adult brain. Nat Neurosci 13, 559-566.

Paschal, B.M., Obar, R.A., and Vallee, R.B. (1989). Interaction of brain cytoplasmic dynein and MAP2 with a common sequence at the C terminus of tubulin. Nature 342, 569-572.

Pereira, N.A., and Song, Z. (2008). Some commonly used caspase substrates and inhibitors lack the specificity required to monitor individual caspase activity. Biochem Biophys Res Commun 377, 873-877.

Petersen, S.L., Chen, T.T., Lawrence, D.A., Marsters, S.A., Gonzalvez, F., and Ashkenazi, A. (2015). TRAF2 is a biologically important necroptosis suppressor. Cell Death Differ 22, 1846-1857.

Petzer, A., Harvey, B.H., and Petzer, J.P. (2014). The interactions of azure B, a metabolite of methylene blue, with acetylcholinesterase and butyrylcholinesterase. Toxicol Appl Pharmacol 274, 488-493.

Petzer, A., Harvey, B.H., Wegener, G., and Petzer, J.P. (2012). Azure B, a metabolite of methylene blue, is a high-potency, reversible inhibitor of monoamine oxidase. Toxicol Appl Pharmacol 258, 403-409.

Pickup, D.J., Ink, B.S., Hu, W., Ray, C.A., and Joklik, W.K. (1986). Hemorrhage in lesions caused by cowpox virus is induced by a viral protein that is related to plasma protein inhibitors of serine proteases. Proc Natl Acad Sci USA 83, 7698-7702.

Pinilla, C., Appel, J.R., Blanc, P., and Houghten, R.A. (1992). Rapid identification of high affinity peptide ligands using positional scanning synthetic peptide combinatorial libraries. Biotechniques 13, 901-905.

Pop, C., Oberst, A., Drag, M., Van Raam, B.J., Riedl, S.J., Green, D.R., and Salvesen, G.S. (2011). FLIP(L) induces caspase 8 activity in the absence of interdomain caspase 8 cleavage and alters substrate specificity. Biochem J 433, 447-457.

Portera-Cailliau, C., Hedreen, J.C., Price, D.L., and Koliatsos, V.E. (1995). Evidence for apoptotic cell death in Huntington disease and excitotoxic animal models. J Neurosci 15, 3775-3787.

Poyet, J.L., Srinivasula, S.M., Tnani, M., Razmara, M., Fernandes-Alnemri, T., and Alnemri, E.S. (2001). Identification of Ipaf, a human caspase-1-activating protein related to Apaf-1. J Biol Chem 276, 28309-28313.

Qi, L.S., Larson, M.H., Gilbert, L.A., Doudna, J.A., Weissman, J.S., Arkin, A.P., and Lim, W.A. (2013). Repurposing CRISPR as an RNA-guided platform for sequence-specific control of gene expression. Cell 152, 1173-1183.

Quan, L.T., Caputo, A., Bleackley, R.C., Pickup, D.J., and Salvesen, G.S. (1995). Granzyme B is inhibited by the cowpox virus serpin cytokine response modifier A. J Biol Chem 270, 10377-10379.

Rabizadeh, S., LaCount, D.J., Friesen, P.D., and Bredesen, D.E. (1993). Expression of the baculovirus p35 gene inhibits mammalian neural cell death. J Neurochem 61, 2318-2321.

Rahmani, B., Tielsch, J.M., Katz, J., Gottsch, J., Quigley, H., Javitt, J., and Sommer, A. (1996). The cause-specific prevalence of visual impairment in an urban population. The Baltimore Eye Survey. Ophthalmology 103, 1721-1726.

Ramcharitar, J., Afonso, V.M., Albrecht, S., Bennett, D.A., and LeBlanc, A.C. (2013a). Caspase-6 activity predicts lower episodic memory ability in aged individuals. Neurobiol Aging 34, 1815-1824.

Ramcharitar, J., Albrecht, S., Afonso, V.M., Kaushal, V., Bennett, D.A., and LeBlanc, A.C. (2013b). Cerebrospinal fluid tau cleaved by caspase-6 reflects brain levels and cognition in aging and Alzheimer disease. J Neuropathol Exp Neurol 72, 824-832.

Ran, F.A., Cong, L., Yan, W.X., Scott, D.A., Gootenberg, J.S., Kriz, A.J., Zetsche, B., Shalem, O., Wu, X., Makarova, K.S.*, et al.* (2015). In vivo genome editing using Staphylococcus aureus Cas9. Nature 520, 186-191.

Rano, T.A., Timkey, T., Peterson, E.P., Rotonda, J., Nicholson, D.W., Becker, J.W., Chapman, K.T., and Thornberry, N.A. (1997). A combinatorial approach for determining protease specificities: application to interleukin-1beta converting enzyme (ICE). Chem Biol 4, 149-155.

Rautajoki, K.J., Marttila, E.M., Nyman, T.A., and Lahesmaa, R. (2007). Interleukin-4 inhibits caspase-3 by regulating several proteins in the Fas pathway during initial stages of human T helper 2 cell differentiation. Mol Cell Proteomics 6, 238-251.

Ray, C.A., Black, R.A., Kronheim, S.R., Greenstreet, T.A., Sleath, P.R., Salvesen, G.S., and Pickup, D.J. (1992). Viral inhibition of inflammation: cowpox virus encodes an inhibitor of the interleukin-1 beta converting enzyme. Cell 69, 597-604.

Read, S.H., Baliga, B.C., Ekert, P.G., Vaux, D.L., and Kumar, S. (2002). A novel Apaf-1-independent putative caspase-2 activation complex. J Cell Biol 159, 739-745.

Renatus, M., Stennicke, H.R., Scott, F.L., Liddington, R.C., and Salvesen, G.S. (2001). Dimer formation drives the activation of the cell death protease caspase 9. Proc Natl Acad Sci USA 98, 14250-14255.

Richter, B.W., Mir, S.S., Eiben, L.J., Lewis, J., Reffey, S.B., Frattini, A., Tian, L., Frank, S., Youle, R.J., Nelson, D.L.*, et al.* (2001). Molecular cloning of ILP-2, a novel member of the inhibitor of apoptosis protein family. Mol Cell Biol 21, 4292-4301.

Riechers, S.P., Butland, S., Deng, Y., Skotte, N., Ehrnhoefer, D.E., Russ, J., Laine, J., Laroche, M., Pouladi, M.A., Wanker, E.E.*, et al.* (2016). Interactome network analysis identifies multiple caspase-6 interactors involved in the pathogenesis of HD. Hum Mol Genet 25, 1600-1618.

Riedl, S.J., Renatus, M., Schwarzenbacher, R., Zhou, Q., Sun, C., Fesik, S.W., Liddington, R.C., and Salvesen, G.S. (2001). Structural basis for the inhibition of caspase-3 by XIAP. Cell 104, 791-800.

Rodrigue, K.M., and Raz, N. (2004). Shrinkage of the entorhinal cortex over five years predicts memory performance in healthy adults. J Neurosci 24, 956-963.

Rodriguez, J., and Lazebnik, Y. (1999). Caspase-9 and APAF-1 form an active holoenzyme. Genes Dev 13, 3179-3184.

Rohn, T.T., Head, E., Nesse, W.H., Cotman, C.W., and Cribbs, D.H. (2001). Activation of caspase-8 in the Alzheimer's disease brain. Neurobiol Dis 8, 1006-1016.

Rohn, T.T., Kokoulina, P., Eaton, C.R., and Poon, W.W. (2009). Caspase activation in transgenic mice with Alzheimer-like pathology: results from a pilot study utilizing the caspase inhibitor, Q-VD-OPh. Int J Clin Exp Med 2, 300-308.

Rothe, M., Pan, M.G., Henzel, W.J., Ayres, T.M., and Goeddel, D.V. (1995). The TNFR2-TRAF signaling complex contains two novel proteins related to baculoviral inhibitor of apoptosis proteins. Cell 83, 1243-1252.

Rotonda, J., Nicholson, D.W., Fazil, K.M., Gallant, M., Gareau, Y., Labelle, M., Peterson, E.P., Rasper, D.M., Ruel, R., Vaillancourt, J.P.*, et al.* (1996). The three-dimensional structure of apopain/CPP32, a key mediator of apoptosis. Nat Struct Biol 3, 619-625.

Rovelet-Lecrux, A., Hannequin, D., Raux, G., Le Meur, N., Laquerriere, A., Vital, A., Dumanchin, C., Feuillette, S., Brice, A., Vercelletto, M.*, et al.* (2006). APP locus duplication causes autosomal dominant early-onset Alzheimer disease with cerebral amyloid angiopathy. Nat Genet 38, 24-26.

Roy, N., Deveraux, Q.L., Takahashi, R., Salvesen, G.S., and Reed, J.C. (1997). The c-IAP-1 and c-IAP-2 proteins are direct inhibitors of specific caspases. EMBO J 16, 6914-6925.

Roy, S., Bayly, C.I., Gareau, Y., Houtzager, V.M., Kargman, S., Keen, S.L., Rowland, K., Seiden, I.M., Thornberry, N.A., and Nicholson, D.W. (2001). Maintenance of caspase-3 proenzyme dormancy by an intrinsic "safety catch" regulatory tripeptide. Proc Natl Acad Sci USA 98, 6132-6137.

Sackett, D.L., Bhattacharyya, B., and Wolff, J. (1985). Tubulin subunit carboxyl termini determine polymerization efficiency. J Biol Chem 260, 43-45.

Saito, T., Matsuba, Y., Mihira, N., Takano, J., Nilsson, P., Itohara, S., Iwata, N., and Saido, T.C. (2014). Single App knock-in mouse models of Alzheimer's disease. Nat Neurosci 17, 661-663.

Sakamaki, K., Inoue, T., Asano, M., Sudo, K., Kazama, H., Sakagami, J., Sakata, S., Ozaki, M., Nakamura, S., Toyokuni, S.*, et al.* (2002). Ex vivo whole-embryo culture of caspase-8-deficient embryos normalize their aberrant phenotypes in the developing neural tube and heart. Cell Death Differ 9, 1196-1206.

Sakamaki, K., and Satou, Y. (2009). Caspases: evolutionary aspects of their functions in vertebrates. J Fish Biol 74, 727-753.

Saleh, M., Mathison, J.C., Wolinski, M.K., Bensinger, S.J., Fitzgerald, P., Droin, N., Ulevitch, R.J., Green, D.R., and Nicholson, D.W. (2006). Enhanced bacterial clearance and sepsis resistance in caspase-12-deficient mice. Nature 440, 1064-1068.

Saleh, M., Vaillancourt, J.P., Graham, R.K., Huyck, M., Srinivasula, S.M., Alnemri, E.S., Steinberg, M.H., Nolan, V., Baldwin, C.T., Hotchkiss, R.S.*, et al.* (2004). Differential modulation of endotoxin responsiveness by human caspase-12 polymorphisms. Nature 429, 75-79.

Salmena, L., Lemmers, B., Hakem, A., Matysiak-Zablocki, E., Murakami, K., Au, P.Y., Berry, D.M., Tamblyn, L., Shehabeldin, A., Migon, E.*, et al.* (2003). Essential role for caspase 8 in T-cell homeostasis and T-cell-mediated immunity. Genes Dev 17, 883-895.

Salvesen, G.S., and Dixit, V.M. (1999). Caspase activation: the induced-proximity model. Proc Natl Acad Sci USA 96, 10964-10967.

Sanes, J.R., and Lichtman, J.W. (1999). Development of the vertebrate neuromuscular junction. Annu Rev Neurosci 22, 389-442.

Sanna, M.G., da Silva Correia, J., Ducrey, O., Lee, J., Nomoto, K., Schrantz, N., Deveraux, Q.L., and Ulevitch, R.J. (2002). IAP suppression of apoptosis involves distinct mechanisms: the TAK1/JNK1 signaling cascade and caspase inhibition. Mol Cell Biol 22, 1754-1766.

Santambrogio, L., Potolicchio, I., Fessler, S.P., Wong, S.H., Raposo, G., and Strominger, J.L. (2005). Involvement of caspase-cleaved and intact adaptor protein 1 complex in endosomal remodeling in maturing dendritic cells. Nat Immunol 6, 1020-1028.

Saresella, M., Piancone, F., Marventano, I., Zoppis, M., Hernis, A., Zanette, M., Trabattoni, D., Chiappedi, M., Ghezzo, A., Canevini, M.P.*, et al.* (2016). Multiple inflammasome complexes are activated in autistic spectrum disorders. Brain Behav Immun 57, 125-133.

Sarkar, A., Balakrishnan, K., Chen, J., Patel, V., Neelapu, S.S., McMurray, J.S., and Gandhi, V. (2016). Molecular evidence of Zn chelation of the procaspase activating compound B-PAC-1 in B cell lymphoma. Oncotarget 7, 3461-3476.

Satoh, A., Nakanishi, H., Obaishi, H., Wada, M., Takahashi, K., Satoh, K., Hirao, K., Nishioka, H., Hata, Y., Mizoguchi, A., and Takai, Y. (1998). Neurabin-II/spinophilin. An actin filament-binding protein with one pdz domain localized at cadherin-based cell-cell adhesion sites. J Biol Chem 273, 3470-3475.

Sattar, R., Ali, S.A., and Abbasi, A. (2003). Molecular mechanism of apoptosis: prediction of three-dimensional structure of caspase-6 and its interactions by homology modeling. Biochem Biophys Res Commun 308, 497-504.

Saudou, F., Finkbeiner, S., Devys, D., and Greenberg, M.E. (1998). Huntingtin acts in the nucleus to induce apoptosis but death does not correlate with the formation of intranuclear inclusions. Cell 95, 55-66.

Schechter, I., and Berger, A. (1967). On the size of the active site in proteases. I. Papain. Biochem Biophys Res Commun 27, 157-162.

Scheff, S.W., and Price, D.A. (2003). Synaptic pathology in Alzheimer's disease: a review of ultrastructural studies. Neurobiol Aging 24, 1029-1046.

Schierle, G.S., Hansson, O., Leist, M., Nicotera, P., Widner, H., and Brundin, P. (1999). Caspase inhibition reduces apoptosis and increases survival of nigral transplants. Nat Med 5, 97-100.

Schirmer, R.H., Adler, H., Pickhardt, M., and Mandelkow, E. (2011). "Lest we forget you--methylene blue...". Neurobiol Aging 32, 2325 e2327-2316.

Schoenmann, Z., Assa-Kunik, E., Tiomny, S., Minis, A., Haklai-Topper, L., Arama, E., and Yaron, A. (2010). Axonal degeneration is regulated by the apoptotic machinery or a NAD+-sensitive pathway in insects and mammals. J Neurosci 30, 6375-6386.

Scott, C.W., Sobotka-Briner, C., Wilkins, D.E., Jacobs, R.T., Folmer, J.J., Frazee, W.J., Bhat, R.V., Ghanekar, S.V., and Aharony, D. (2003). Novel small molecule inhibitors of caspase-3 block cellular and biochemical features of apoptosis. J Pharmacol Exp Ther 304, 433-440.

Scoville, W.B., and Milner, B. (1957). Loss of recent memory after bilateral hippocampal lesions. J Neurol Neurosurg Psychiatry 20, 11-21.

Seaman, J.E., Julien, O., Lee, P.S., Rettenmaier, T.J., Thomsen, N.D., and Wells, J.A. (2016). Cacidases: caspases can cleave after aspartate, glutamate and phosphoserine residues. Cell Death Differ 23, 1717-1726.

Sebbagh, M., Renvoize, C., Hamelin, J., Riche, N., Bertoglio, J., and Breard, J. (2001). Caspase-3-mediated cleavage of ROCK I induces MLC phosphorylation and apoptotic membrane blebbing. Nat Cell Biol 3, 346-352.

Selkoe, D.J. (1997). Alzheimer's disease: genotypes, phenotypes, and treatments. Science 275, 630-631.

Selznick, L.A., Holtzman, D.M., Han, B.H., Gokden, M., Srinivasan, A.N., Johnson, E.M., Jr., and Roth, K.A. (1999). In situ immunodetection of neuronal caspase-3 activation in Alzheimer disease. J Neuropathol Exp Neurol 58, 1020-1026.

Serrano, L., Avila, J., and Maccioni, R.B. (1984). Controlled proteolysis of tubulin by subtilisin: localization of the site for MAP2 interaction. Biochemistry 23, 4675-4681.

Sevigny, J., Chiao, P., Bussiere, T., Weinreb, P.H., Williams, L., Maier, M., Dunstan, R., Salloway, S., Chen, T., Ling, Y.*, et al.* (2016). The antibody aducanumab reduces Abeta plaques in Alzheimer's disease. Nature 537, 50-56.

Sezgin, Z., Biberoglu, K., Chupakhin, V., Makhaeva, G.F., and Tacal, O. (2013). Determination of binding points of methylene blue and cationic phenoxazine dyes on human butyrylcholinesterase. Arch Biochem Biophys 532, 32-38.

Shabanzadeh, A.P., D'Onofrio, P.M., Monnier, P.P., and Koeberle, P.D. (2015). Targeting caspase-6 and caspase-8 to promote neuronal survival following ischemic stroke. Cell Death Dis 6, e1967.

Shang, Z., Lv, H., Zhang, M., Duan, L., Wang, S., Li, J., Liu, G., Ruijie, Z., and Jiang, Y. (2015). Genome-wide haplotype association study identify TNFRSF1A, CASP7, LRP1B, CDH1 and TG genes associated with Alzheimer's disease in Caribbean Hispanic individuals. Oncotarget 6, 42504-42514.

Sharma, D., and Kanneganti, T.D. (2016). The cell biology of inflammasomes: Mechanisms of inflammasome activation and regulation. J Cell Biol 213, 617-629.

Shi, J., Zhao, Y., Wang, K., Shi, X., Wang, Y., Huang, H., Zhuang, Y., Cai, T., Wang, F., and Shao, F. (2015). Cleavage of GSDMD by inflammatory caspases determines pyroptotic cell death. Nature 526, 660-665.

Shi, M., Vivian, C.J., Lee, K.J., Ge, C., Morotomi-Yano, K., Manzl, C., Bock, F., Sato, S., Tomomori-Sato, C., Zhu, R.*, et al.* (2009). DNA-PKcs-PIDDosome: a nuclear caspase-2-activating complex with role in G2/M checkpoint maintenance. Cell 136, 508-520.

Shi, Y. (2002). Mechanisms of caspase activation and inhibition during apoptosis. Mol Cell 9, 459-470.

Shimohama, S., Tanino, H., and Fujimoto, S. (2001). Differential subcellular localization of caspase family proteins in the adult rat brain. Neurosci Lett 315, 125-128.

Shin, H., Renatus, M., Eckelman, B.P., Nunes, V.A., Sampaio, C.A., and Salvesen, G.S. (2005). The BIR domain of IAP-like protein 2 is conformationally unstable: implications for caspase inhibition. Biochem J 385, 1-10.

Shin, S., Sung, B.J., Cho, Y.S., Kim, H.J., Ha, N.C., Hwang, J.I., Chung, C.W., Jung, Y.K., and Oh, B.H. (2001). An anti-apoptotic protein human survivin is a direct inhibitor of caspase-3 and -7. Biochemistry 40, 1117-1123.

Shindler, K.S., Zurakowski, D., and Dreyer, E.B. (2000). Caspase inhibitors block zinc-chelator induced death of retinal ganglion cells. Neuroreport 11, 2299-2302.

Shively, S., Scher, A.I., Perl, D.P., and Diaz-Arrastia, R. (2012). Dementia resulting from traumatic brain injury: what is the pathology? Arch Neurol 69, 1245-1251.

Simon, D.J., Pitts, J., Hertz, N.T., Yang, J., Yamagishi, Y., Olsen, O., Tesic Mark, M., Molina, H., and Tessier-Lavigne, M. (2016). Axon Degeneration Gated by Retrograde Activation of Somatic Pro-apoptotic Signaling. Cell 164, 1031-1045.

Simon, D.J., Weimer, R.M., McLaughlin, T., Kallop, D., Stanger, K., Yang, J., O'Leary, D.D., Hannoush, R.N., and Tessier-Lavigne, M. (2012). A caspase cascade regulating developmental axon degeneration. J Neurosci 32, 17540-17553.

Singaraja, R.R., Huang, K., Sanders, S.S., Milnerwood, A.J., Hines, R., Lerch, J.P., Franciosi, S., Drisdel, R.C., Vaid, K., Young, F.B.*, et al.* (2011). Altered palmitoylation and neuropathological deficits in mice lacking HIP14. Hum Mol Genet 20, 3899-3909.

Singh, J., Petter, R.C., Baillie, T.A., and Whitty, A. (2011). The resurgence of covalent drugs. Nat Rev Drug Discov 10, 307-317.

Sivananthan, S., Lee, A., Goodyer, C.G., and LeBlanc, A.C. (2010a). Familial amyloid precursor protein mutants cause caspase-6-dependent but amyloid β-peptide-independent neuronal degeneration in primary human neuron cultures. Cell Death Dis 1.

Sivananthan, S.N., Lee, A.W., Goodyer, C.G., and LeBlanc, A.C. (2010b). Familial amyloid precursor protein mutants cause caspase-6-dependent but amyloid beta-peptide-independent neuronal degeneration in primary human neuron cultures. Cell Death Dis 1, e100.

Skotte, N.H., Sanders, S.S., Singaraja, R.R., Ehrnhoefer, D.E., Vaid, K., Qiu, X., Kannan, S., Verma, C., and Hayden, M.R. (2017). Palmitoylation of caspase-6 by HIP14 regulates its activation. Cell Death Differ 24, 433-444.

Sleath, P.R., Hendrickson, R.C., Kronheim, S.R., March, C.J., and Black, R.A. (1990). Substrate specificity of the protease that processes human interleukin-1 beta. J Biol Chem 265, 14526-14528.

Slee, E.A., Harte, M.T., Kluck, R.M., Wolf, B.B., Casiano, C.A., Newmeyer, D.D., Wang, H.G., Reed, J.C., Nicholson, D.W., Alnemri, E.S.*, et al.* (1999). Ordering the cytochrome c-initiated caspase cascade: hierarchical activation of caspases-2, -3, -6, -7, -8, and -10 in a caspase-9-dependent manner. J Cell Biol 144, 281-292.

Smith, C.E., Soti, S., Jones, T.A., Nakagawa, A., Xue, D., and Yin, H. (2017). Non-steroidal Anti-inflammatory Drugs Are Caspase Inhibitors. Cell Chem Biol 24, 281-292.

Smith, R.A., Miller, T.M., Yamanaka, K., Monia, B.P., Condon, T.P., Hung, G., Lobsiger, C.S., Ward, C.M., McAlonis-Downes, M., Wei, H*., et al.* (2006). Antisense oligonucleotide therapy for neurodegenerative disease. J Clin Invest 116, 2290-2296.

Sohn, D., Budach, W., and Janicke, R.U. (2011). Caspase-2 is required for DNA damage-induced expression of the CDK inhibitor p21(WAF1/CIP1). Cell Death Differ 18, 1664-1674.

Sokolowski, J.D., Gamage, K.K., Heffron, D.S., LeBlanc, A.C., Deppmann, C.D., and Mandell, J.W. (2014). Caspase-mediated cleavage of actin and tubulin is a common feature and sensitive marker of axonal degeneration in neural development and injury. Acta Neuropathol Commun 2, 16.

Sordet, O., Rebe, C., Plenchette, S., Zermati, Y., Hermine, O., Vainchenker, W., Garrido, C., Solary, E., and Dubrez-Daloz, L. (2002). Specific involvement of caspases in the differentiation of monocytes into macrophages. Blood 100, 4446-4453.

Spires-Jones, T.L., Friedman, T., Pitstick, R., Polydoro, M., Roe, A., Carlson, G.A., and Hyman, B.T. (2014). Methylene blue does not reverse existing neurofibrillary tangle pathology in the rTg4510 mouse model of tauopathy. Neurosci Lett 562, 63-68.

Srinivasula, S.M., Ahmad, M., Fernandes-Alnemri, T., and Alnemri, E.S. (1998). Autoactivation of procaspase-9 by Apaf-1-mediated oligomerization. Mol Cell 1, 949-957.

Srinivasula, S.M., Ahmad, M., Fernandes-Alnemri, T., Litwack, G., and Alnemri, E.S. (1996a). Molecular ordering of the Fas-apoptotic pathway: the Fas/APO-1 protease Mch5 is a CrmA-inhibitable protease that activates multiple Ced-3/ICE-like cysteine proteases. Proc Natl Acad Sci USA 93, 14486-14491.

Srinivasula, S.M., Fernandes-Alnemri, T., Zangrilli, J., Robertson, N., Armstrong, R.C., Wang, L., Trapani, J.A., Tomaselli, K.J., Litwack, G., and Alnemri, E.S. (1996b). The Ced-3/interleukin 1beta converting enzyme-like homolog Mch6 and the lamin-cleaving enzyme Mch2alpha are substrates for the apoptotic mediator CPP32. J Biol Chem 271, 27099-27106.

Srinivasula, S.M., Hegde, R., Saleh, A., Datta, P., Shiozaki, E., Chai, J., Lee, R.A., Robbins, P.D., Fernandes-Alnemri, T., Shi, Y., and Alnemri, E.S. (2001). A conserved XIAP-interaction motif in caspase-9 and Smac/DIABLO regulates caspase activity and apoptosis. Nature 410, 112-116.

Stack, C., Jainuddin, S., Elipenahli, C., Gerges, M., Starkova, N., Starkov, A.A., Jove, M., Portero-Otin, M., Launay, N., Pujol, A.*, et al.* (2014). Methylene blue upregulates Nrf2/ARE genes and prevents tau-related neurotoxicity. Hum Mol Genet 23, 3716-3732.

Stadelmann, C., Deckwerth, T.L., Srinivasan, A., Bancher, C., Bruck, W., Jellinger, K., and Lassmann, H. (1999). Activation of caspase-3 in single neurons and autophagic granules of granulovacuolar degeneration in Alzheimer's disease. Evidence for apoptotic cell death. Am J Pathol 155, 1459-1466.

Stanger, K., Steffek, M., Zhou, L., Pozniak, C.D., Quan, C., Franke, Y., Tom, J., Tam, C., Krylova, I., Elliott, J.M.*, et al.* (2012). Allosteric peptides bind a caspase zymogen and mediate caspase tetramerization. Nat Chem Biol 8, 655-660.

Stelzl, U., Worm, U., Lalowski, M., Haenig, C., Brembeck, F.H., Goehler, H., Stroedicke, M., Zenkner, M., Schoenherr, A., Koeppen, S.*, et al.* (2005). A human protein-protein interaction network: a resource for annotating the proteome. Cell 122, 957-968.

Stennicke, H.R., and Salvesen, G.S. (1997). Biochemical characteristics of caspases-3, -6, -7, and -8. J Biol Chem 272, 25719-25723.

Stennicke, H.R., and Salvesen, G.S. (1999). Catalytic properties of the caspases. Cell Death Differ 6, 1054-1059.

Sun, C., Cai, M., Gunasekera, A.H., Meadows, R.P., Wang, H., Chen, J., Zhang, H., Wu, W., Xu, N., Ng, S.C., and Fesik, S.W. (1999). NMR structure and mutagenesis of the inhibitor-of-apoptosis protein XIAP. Nature 401, 818-822.

Sun, C., Cai, M., Meadows, R.P., Xu, N., Gunasekera, A.H., Herrmann, J., Wu, J.C., and Fesik, S.W. (2000). NMR structure and mutagenesis of the third Bir domain of the inhibitor of apoptosis protein XIAP. J Biol Chem 275, 33777-33781.

Suzuki, A., Kusakai, G., Kishimoto, A., Shimojo, Y., Miyamoto, S., Ogura, T., Ochiai, A., and Esumi, H. (2004). Regulation of caspase-6 and FLIP by the AMPK family member ARK5. Oncogene 23, 7067-7075.

Suzuki, J., Denning, D.P., Imanishi, E., Horvitz, H.R., and Nagata, S. (2013). Xk-related protein 8 and CED-8 promote phosphatidylserine exposure in apoptotic cells. Science 341, 403-406.

Suzuki, Y., Imai, Y., Nakayama, H., Takahashi, K., Takio, K., and Takahashi, R. (2001). A serine protease, HtrA2, is released from the mitochondria and interacts with XIAP, inducing cell death. Mol Cell 8, 613-621.

Svandova, E., Lesot, H., Vanden Berghe, T., Tucker, A.S., Sharpe, P.T., Vandenabeele, P., and Matalova, E. (2014). Non-apoptotic functions of caspase-7 during osteogenesis. Cell Death Dis 5, e1366.

Tacal, O., Li, B., Lockridge, O., and Schopfer, L.M. (2013). Resistance of human butyrylcholinesterase to methylene blue-catalyzed photoinactivation; mass spectrometry analysis of oxidation products. Photochem Photobiol 89, 336-348.

Takahashi-Niki, K., Niki, T., Taira, T., Iguchi-Ariga, S.M., and Ariga, H. (2004). Reduced anti-oxidative stress activities of DJ-1 mutants found in Parkinson's disease patients. Biochem Biophys Res Commun 320, 389-397.

Takahashi, A., Alnemri, E.S., Lazebnik, Y.A., Fernandes-Alnemri, T., Litwack, G., Moir, R.D., Goldman, R.D., Poirier, G.G., Kaufmann, S.H., and Earnshaw, W.C. (1996). Cleavage of lamin A by Mch2 alpha but not CPP32: multiple interleukin 1 beta-converting enzyme-related proteases with distinct substrate recognition properties are active in apoptosis. Proc Natl Acad Sci USA 93, 8395-8400.

Talanian, R.V., Quinlan, C., Trautz, S., Hackett, M.C., Mankovich, J.A., Banach, D., Ghayur, T., Brady, K.D., and Wong, W.W. (1997). Substrate specificities of caspase family proteases. J Biol Chem 272, 9677-9682.

Tamayev, R., Akpan, N., Arancio, O., Troy, C.M., and D'Adamio, L. (2012). Caspase-9 mediates synaptic plasticity and memory deficits of Danish dementia knock-in mice: caspase-9 inhibition provides therapeutic protection. Mol Neurodegener 7, 60.

Tanzer, M.C., Khan, N., Rickard, J.A., Etemadi, N., Lalaoui, N., Spall, S.K., Hildebrand, J.M., Segal, D., Miasari, M., Chau, D.*, et al.* (2017). Combination of IAP antagonist and IFNgamma activates novel caspase-10- and RIPK1-dependent cell death pathways. Cell Death Differ.

Tartaglia, L.A., Ayres, T.M., Wong, G.H., and Goeddel, D.V. (1993). A novel domain within the 55 kd TNF receptor signals cell death. Cell 74, 845-853.

Taylor, R.C., Cullen, S.P., and Martin, S.J. (2008). Apoptosis: controlled demolition at the cellular level. Nat Rev Mol Cell Biol 9, 231-241.

Tebbenkamp, A.T., Green, C., Xu, G., Denovan-Wright, E.M., Rising, A.C., Fromholt, S.E., Brown, H.H., Swing, D., Mandel, R.J., Tessarollo, L., and Borchelt, D.R. (2011). Transgenic mice expressing caspase-6-derived N-terminal fragments of mutant huntingtin develop neurologic abnormalities with predominant cytoplasmic inclusion pathology composed largely of a smaller proteolytic derivative. Hum Mol Genet 20, 2770-2782.

Tesco, G., Koh, Y.H., Kang, E.L., Cameron, A.N., Das, S., Sena-Esteves, M., Hiltunen, M., Yang, S.H., Zhong, Z., Shen, Y.*, et al.* (2007). Depletion of GGA3 stabilizes BACE and enhances beta-secretase activity. Neuron 54, 721-737.

Tesco, G., Koh, Y.H., and Tanzi, R.E. (2003). Caspase activation increases beta-amyloid generation independently of caspase cleavage of the beta-amyloid precursor protein (APP). J Biol Chem 278, 46074-46080.

Thomalla, G., Glauche, V., Koch, M.A., Beaulieu, C., Weiller, C., and Rother, J. (2004). Diffusion tensor imaging detects early Wallerian degeneration of the pyramidal tract after ischemic stroke. Neuroimage 22, 1767-1774.

Thome, M., Schneider, P., Hofmann, K., Fickenscher, H., Meinl, E., Neipel, F., Mattmann, C., Burns, K., Bodmer, J.L., Schroter, M.*, et al.* (1997). Viral FLICE-inhibitory proteins (FLIPs) prevent apoptosis induced by death receptors. Nature 386, 517-521.

Thompson, R., Shah, R.B., Liu, P.H., Gupta, Y.K., Ando, K., Aggarwal, A.K., and Sidi, S. (2015). An Inhibitor of PIDDosome Formation. Mol Cell 58, 767-779.

Thornberry, N.A. (1997). The caspase family of cysteine proteases. Br Med Bull 53, 478-490.

Thornberry, N.A., Bull, H.G., Calaycay, J.R., Chapman, K.T., Howard, A.D., Kostura, M.J., Miller, D.K., Molineaux, S.M., Weidner, J.R., Aunins, J., and et al. (1992). A novel heterodimeric cysteine protease is required for interleukin-1 beta processing in monocytes. Nature 356, 768-774.

Thornberry, N.A., Rano, T.A., Peterson, E.P., Rasper, D.M., Timkey, T., Garcia-Calvo, M., Houtzager, V.M., Nordstrom, P.A., Roy, S., Vaillancourt, J.P.*, et al.* (1997). A combinatorial approach defines specificities of members of the caspase family and granzyme B. Functional relationships established for key mediators of apoptosis. J Biol Chem 272, 17907-17911.

Tinel, A., Janssens, S., Lippens, S., Cuenin, S., Logette, E., Jaccard, B., Quadroni, M., and Tschopp, J. (2007). Autoproteolysis of PIDD marks the bifurcation between pro-death caspase-2 and pro-survival NF-kappaB pathway. EMBO J 26, 197-208.

Tinel, A., and Tschopp, J. (2004). The PIDDosome, a protein complex implicated in activation of caspase-2 in response to genotoxic stress. Science 304, 843-846.

Tiwari, M., Sharma, L.K., Vanegas, D., Callaway, D.A., Bai, Y., Lechleiter, J.D., and Herman, B. (2014). A nonapoptotic role for CASP2/caspase 2: modulation of autophagy. Autophagy 10, 1054-1070.

Tong, X.K., Lecrux, C., Rosa-Neto, P., and Hamel, E. (2012). Age-dependent rescue by simvastatin of Alzheimer's disease cerebrovascular and memory deficits. J Neurosci 32, 4705-4715.

Tounekti, O., Zhang, Y., Klaiman, G., Goodyer, C.G., and LeBlanc, A. (2004). Proteasomal degradation of caspase-6 in 17beta-estradiol-treated neurons. J Neurochem 89, 561-568.

Truman, J.W. (1990). Metamorphosis of the central nervous system of Drosophila. J Neurobiol 21, 1072-1084.

Underhill, G.H., George, D., Bremer, E.G., and Kansas, G.S. (2003). Gene expression profiling reveals a highly specialized genetic program of plasma cells. Blood 101, 4013-4021.

Unsain, N., Higgins, J.M., Parker, K.N., Johnstone, A.D., and Barker, P.A. (2013). XIAP regulates caspase activity in degenerating axons. Cell Rep 4, 751-763.

Ura, S., Masuyama, N., Graves, J.D., and Gotoh, Y. (2001). Caspase cleavage of MST1 promotes nuclear translocation and chromatin condensation. Proc Natl Acad Sci USA 98, 10148-10153.

Uribe, V., Wong, B.K., Graham, R.K., Cusack, C.L., Skotte, N.H., Pouladi, M.A., Xie, Y., Feinberg, K., Ou, Y., Ouyang, Y.*, et al.* (2012). Rescue from excitotoxicity and axonal degeneration accompanied by age-dependent behavioral and neuroanatomical alterations in caspase-6-deficient mice. Hum Mol Genet 21, 1954-1967.

Vaidya, S., and Hardy, J.A. (2011). Caspase-6 latent state stability relies on helical propensity. Biochemistry 50, 3282-3287.

Vaidya, S., Velazquez-Delgado, E.M., Abbruzzese, G., and Hardy, J.A. (2011). Substrate-induced conformational changes occur in all cleaved forms of caspase-6. J Mol Biol 406, 75-91.

Van de Craen, M., Van Loo, G., Pype, S., Van Criekinge, W., Van den brande, I., Molemans, F., Fiers, W., Declercq, W., and Vandenabeele, P. (1998). Identification of a new caspase homologue: caspase-14. Cell Death Differ 5, 838-846.

Van de Craen, M., Vandenabeele, P., Declercq, W., Van den Brande, I., Van Loo, G., Molemans, F., Schotte, P., Van Criekinge, W., Beyaert, R., and Fiers, W. (1997). Characterization of seven murine caspase family members. FEBS Lett 403, 61-69.

van Raam, B.J., Ehrnhoefer, D.E., Hayden, M.R., and Salvesen, G.S. (2013). Intrinsic cleavage of receptor-interacting protein kinase-1 by caspase-6. Cell Death Differ 20, 86-96.

Varfolomeev, E.E., Schuchmann, M., Luria, V., Chiannilkulchai, N., Beckmann, J.S., Mett, I.L., Rebrikov, D., Brodianski, V.M., Kemper, O.C., Kollet, O.*, et al.* (1998). Targeted disruption of the mouse Caspase 8 gene ablates cell death induction by the TNF receptors, Fas/Apo1, and DR3 and is lethal prenatally. Immunity 9, 267-276.

Varghese, P., Mostafa, A., Abdel-Rahman, A.T., Akberali, S., Gattuso, J., Canizales, A., Wells, C.A., and Carpenter, R. (2007). Methylene blue dye versus combined dye-radioactive tracer technique for sentinel lymph node localisation in early breast cancer. Eur J Surg Oncol 33, 147-152.

Veber, D.F., Johnson, S.R., Cheng, H.Y., Smith, B.R., Ward, K.W., and Kopple, K.D. (2002). Molecular properties that influence the oral bioavailability of drug candidates. J Med Chem 45, 2615-2623.

Velazquez-Delgado, E.M., and Hardy, J.A. (2012a). Phosphorylation regulates assembly of the caspase-6 substrate-binding groove. Structure 20, 742-751.

Velazquez-Delgado, E.M., and Hardy, J.A. (2012b). Zinc-mediated allosteric inhibition of caspase-6. J Biol Chem 287, 36000-36011.

Vesela, B., Svandova, E., Vanden Berghe, T., Tucker, A.S., Vandenabeele, P., and Matalova, E. (2015). Non-apoptotic role for caspase-7 in hair follicles and the surrounding tissue. J Mol Histol 46, 443-455.

Vigano, E., Diamond, C.E., Spreafico, R., Balachander, A., Sobota, R.M., and Mortellaro, A. (2015). Human caspase-4 and caspase-5 regulate the one-step non-canonical inflammasome activation in monocytes. Nat Commun 6, 8761.

Vigneswara, V., Akpan, N., Berry, M., Logan, A., Troy, C.M., and Ahmed, Z. (2014). Combined suppression of CASP2 and CASP6 protects retinal ganglion cells from apoptosis and promotes axon regeneration through CNTF-mediated JAK/STAT signalling. Brain 137, 1656-1675.

Vohra, B.P., Sasaki, Y., Miller, B.R., Chang, J., DiAntonio, A., and Milbrandt, J. (2010). Amyloid precursor protein cleavage-dependent and -independent axonal degeneration programs share a common nicotinamide mononucleotide adenylyltransferase 1-sensitive pathway. J Neurosci 30, 13729-13738.

Vucic, D., Stennicke, H.R., Pisabarro, M.T., Salvesen, G.S., and Dixit, V.M. (2000). ML-IAP, a novel inhibitor of apoptosis that is preferentially expressed in human melanomas. Curr Biol 10, 1359-1366.

Walder, R.Y., and Walder, J.A. (1988). Role of RNase H in hybrid-arrested translation by antisense oligonucleotides. Proc Natl Acad Sci USA 85, 5011-5015.

Waldron-Roby, E., Hoerauf, J., Arbez, N., Zhu, S., Kulcsar, K., and Ross, C.A. (2015). Sox11 Reduces Caspase-6 Cleavage and Activity. PLoS One 10, e0141439.

Waldron-Roby, E., Ratovitski, T., Wang, X., Jiang, M., Watkin, E., Arbez, N., Graham, R.K., Hayden, M.R., Hou, Z., Mori, S.*, et al.* (2012). Transgenic mouse model expressing the caspase 6 fragment of mutant huntingtin. J Neurosci 32, 183-193.

Walikonis, R.S., Oguni, A., Khorosheva, E.M., Jeng, C.J., Asuncion, F.J., and Kennedy, M.B. (2001). Densin-180 forms a ternary complex with the (alpha)-subunit of Ca2+/calmodulin-dependent protein kinase II and (alpha)-actinin. J Neurosci 21, 423-433.

Walker, N.P., Talanian, R.V., Brady, K.D., Dang, L.C., Bump, N.J., Ferenz, C.R., Franklin, S., Ghayur, T., Hackett, M.C., Hammill, L.D., and et al. (1994). Crystal structure of the cysteine protease interleukin-1 beta-converting enzyme: a (p20/p10)2 homodimer. Cell 78, 343-352.

Walsh, J.G., Muruve, D.A., and Power, C. (2014). Inflammasomes in the CNS. Nat Rev Neurosci 15, 84-97.

Wang, H.G., Pathan, N., Ethell, I.M., Krajewski, S., Yamaguchi, Y., Shibasaki, F., McKeon, F., Bobo, T., Franke, T.F., and Reed, J.C. (1999). Ca2+-induced apoptosis through calcineurin dephosphorylation of BAD. Science 284, 339-343.

Wang, J.Y., Chen, F., Fu, X.Q., Ding, C.S., Zhou, L., Zhang, X.H., and Luo, Z.G. (2014). Caspase-3 cleavage of dishevelled induces elimination of postsynaptic structures. Dev Cell 28, 670-684.

Wang, L., Miura, M., Bergeron, L., Zhu, H., and Yuan, J. (1994). Ich-1, an Ice/ced-3-related gene, encodes both positive and negative regulators of programmed cell death. Cell 78, 739-750.

Wang, S., Miura, M., Jung, Y.K., Zhu, H., Li, E., and Yuan, J. (1998). Murine caspase-11, an ICE-interacting protease, is essential for the activation of ICE. Cell 92, 501-509.

Wang, X., Bjorklund, S., Wasik, A.M., Grandien, A., Andersson, P., Kimby, E., Dahlman-Wright, K., Zhao, C., Christensson, B., and Sander, B. (2010a). Gene expression profiling and chromatin immunoprecipitation identify DBN1, SETMAR and HIG2 as direct targets of SOX11 in mantle cell lymphoma. PLoS One 5, e14085.

Wang, X., Pai, J.T., Wiedenfeld, E.A., Medina, J.C., Slaughter, C.A., Goldstein, J.L., and Brown, M.S. (1995). Purification of an interleukin-1 beta converting enzyme-related cysteine protease that cleaves sterol regulatory element-binding proteins between the leucine zipper and transmembrane domains. J Biol Chem 270, 18044-18050.

Wang, X.J., Cao, Q., Liu, X., Wang, K.T., Mi, W., Zhang, Y., Li, L.F., LeBlanc, A.C., and Su, X.D. (2010b). Crystal structures of human caspase 6 reveal a new mechanism for intramolecular cleavage self-activation. EMBO Rep 11, 841-847.

Watanabe, C., Shu, G.L., Zheng, T.S., Flavell, R.A., and Clark, E.A. (2008). Caspase 6 regulates B cell activation and differentiation into plasma cells. J Immunol 181, 6810-6819.

Wei, Y., Fox, T., Chambers, S.P., Sintchak, J., Coll, J.T., Golec, J.M., Swenson, L., Wilson, K.P., and Charifson, P.S. (2000). The structures of caspases-1, -3, -7 and -8 reveal the basis for substrate and inhibitor selectivity. Chem Biol 7, 423-432.

Wellington, C.L., Singaraja, R., Ellerby, L., Savill, J., Roy, S., Leavitt, B., Cattaneo, E., Hackam, A., Sharp, A., Thornberry, N.*, et al.* (2000). Inhibiting caspase cleavage of huntingtin reduces toxicity and aggregate formation in neuronal and nonneuronal cells. J Biol Chem 275, 19831-19838.

Wen, L.P., Fahrni, J.A., Troie, S., Guan, J.L., Orth, K., and Rosen, G.D. (1997). Cleavage of focal adhesion kinase by caspases during apoptosis. J Biol Chem 272, 26056-26061.

Werz, O., Tretiakova, I., Michel, A., Ulke-Lemee, A., Hornig, M., Franke, L., Schneider, G., Samuelsson, B., Radmark, O., and Steinhilber, D. (2005). Caspase-mediated degradation of human 5-lipoxygenase in B lymphocytic cells. Proc Natl Acad Sci USA 102, 13164-13169.

Whetsell, W.O., Jr., and Shapira, N.A. (1993). Neuroexcitation, excitotoxicity and human neurological disease. Lab Invest 68, 372-387.

Wilm, M., Shevchenko, A., Houthaeve, T., Breit, S., Schweigerer, L., Fotsis, T., and Mann, M. (1996). Femtomole sequencing of proteins from polyacrylamide gels by nano-electrospray mass spectrometry. Nature 379, 466-469.

Wilson, K.P., Black, J.A., Thomson, J.A., Kim, E.E., Griffith, J.P., Navia, M.A., Murcko, M.A., Chambers, S.P., Aldape, R.A., Raybuck, S.A., and et al. (1994). Structure and mechanism of interleukin-1 beta converting enzyme. Nature 370, 270-275.

Wilson, R., Goyal, L., Ditzel, M., Zachariou, A., Baker, D.A., Agapite, J., Steller, H., and Meier, P. (2002). The DIAP1 RING finger mediates ubiquitination of Dronc and is indispensable for regulating apoptosis. Nat Cell Biol 4, 445-450.

Wischik, C.M., Edwards, P.C., Lai, R.Y., Roth, M., and Harrington, C.R. (1996). Selective inhibition of Alzheimer disease-like tau aggregation by phenothiazines. Proc Natl Acad Sci USA 93, 11213-11218.

Wischik, C.M., Harrington, C.R., and Storey, J.M. (2014). Tau-aggregation inhibitor therapy for Alzheimer's disease. Biochem Pharmacol 88, 529-539.

Wischik, C.M., Staff, R.T., Wischik, D.J., Bentham, P., Murray, A.D., Storey, J.M., Kook, K.A., and Harrington, C.R. (2015). Tau aggregation inhibitor therapy: an exploratory phase 2 study in mild or moderate Alzheimer's disease. J Alzheimers Dis 44, 705-720.

Wong, B.K., Ehrnhoefer, D.E., Graham, R.K., Martin, D.D., Ladha, S., Uribe, V., Stanek, L.M., Franciosi, S., Qiu, X., Deng, Y.*, et al.* (2015). Partial rescue of some features of Huntington Disease in the genetic absence of caspase-6 in YAC128 mice. Neurobiol Dis 76, 24-36.

Woo, M., Hakem, R., Furlonger, C., Hakem, A., Duncan, G.S., Sasaki, T., Bouchard, D., Lu, L., Wu, G.E., Paige, C.J., and Mak, T.W. (2003). Caspase-3 regulates cell cycle in B cells: a consequence of substrate specificity. Nat Immunol 4, 1016-1022.

Xanthoudakis, S., Roy, S., Rasper, D., Hennessey, T., Aubin, Y., Cassady, R., Tawa, P., Ruel, R., Rosen, A., and Nicholson, D.W. (1999). Hsp60 accelerates the maturation of pro-caspase-3 by upstream activator proteases during apoptosis. EMBO J 18, 2049-2056.

Yang, B., El Nahas, A.M., Fisher, M., Wagner, B., Huang, L., Storie, I., Barnett, D., Barratt, J., Smith, A.C., and Johnson, T.S. (2004). Inhibitors directed towards caspase-1 and -3 are less effective than pan caspase inhibition in preventing renal proximal tubular cell apoptosis. Nephron Exp Nephrol 96, e39-51.

Yang, C., Kaushal, V., Haun, R.S., Seth, R., Shah, S.V., and Kaushal, G.P. (2008). Transcriptional activation of caspase-6 and -7 genes by cisplatin-induced p53 and its functional significance in cisplatin nephrotoxicity. Cell Death Differ 15, 530-544.

Yang, F., Sun, X., Beech, W., Teter, B., Wu, S., Sigel, J., Vinters, H.V., Frautschy, S.A., and Cole, G.M. (1998). Antibody to caspase-cleaved actin detects apoptosis in differentiated neuroblastoma and plaque-associated neurons and microglia in Alzheimer's disease. Am J Pathol 152, 379-389.

Yang, Y., Fang, S., Jensen, J.P., Weissman, A.M., and Ashwell, J.D. (2000). Ubiquitin protein ligase activity of IAPs and their degradation in proteasomes in response to apoptotic stimuli. Science 288, 874-877.

Yao, Y., Shi, Q., Chen, B., Wang, Q., Li, X., Li, L., Huang, Y., Ji, J., and Shen, P. (2016). Identification of Caspase-6 as a New Regulator of Alternatively Activated Macrophages. J Biol Chem 291, 17450-17466.

Yeh, W.C., de la Pompa, J.L., McCurrach, M.E., Shu, H.B., Elia, A.J., Shahinian, A., Ng, M., Wakeham, A., Khoo, W., Mitchell, K.*, et al.* (1998). FADD: essential for embryo development and signaling from some, but not all, inducers of apoptosis. Science 279, 1954-1958.

Yin, Y., Li, X., Sha, X., Xi, H., Li, Y.F., Shao, Y., Mai, J., Virtue, A., Lopez-Pastrana, J., Meng, S.*, et al.* (2015). Early hyperlipidemia promotes endothelial activation via a caspase-1-sirtuin 1 pathway. Arterioscler Thromb Vasc Biol 35, 804-816.

Yoshida, H., Kong, Y.Y., Yoshida, R., Elia, A.J., Hakem, A., Hakem, R., Penninger, J.M., and Mak, T.W. (1998). Apaf1 is required for mitochondrial pathways of apoptosis and brain development. Cell 94, 739-750.

Yuan, J., Shaham, S., Ledoux, S., Ellis, H.M., and Horvitz, H.R. (1993). The C. elegans cell death gene ced-3 encodes a protein similar to mammalian interleukin-1 beta-converting enzyme. Cell 75, 641-652.

Yuan, J.Y., and Horvitz, H.R. (1990). The Caenorhabditis elegans genes ced-3 and ced-4 act cell autonomously to cause programmed cell death. Dev Biol 138, 33-41.

Zamaraev, A.V., Kopeina, G.S., Prokhorova, E.A., Zhivotovsky, B., and Lavrik, I.N. (2017). Post-translational Modification of Caspases: The Other Side of Apoptosis Regulation. Trends Cell Biol.

Zhang, J., Cado, D., Chen, A., Kabra, N.H., and Winoto, A. (1998). Fas-mediated apoptosis and activation-induced T-cell proliferation are defective in mice lacking FADD/Mort1. Nature 392, 296-300.

Zhang, X., and Le, W. (2010). Pathological role of hypoxia in Alzheimer's disease. Exp Neurol 223, 299-303.

Zhang, Y., Goodyer, C., and LeBlanc, A. (2000). Selective and protracted apoptosis in human primary neurons microinjected with active caspase-3, -6, -7, and -8. J Neurosci 20, 8384-8389.

Zhang, Y., Tounekti, O., Akerman, B., Goodyer, C.G., and LeBlanc, A. (2001). 17-beta-estradiol induces an inhibitor of active caspases. J Neurosci 21, RC176.

Zhao, X., Kotilinek, L.A., Smith, B., Hlynialuk, C., Zahs, K., Ramsden, M., Cleary, J., and Ashe, K.H. (2016). Caspase-2 cleavage of tau reversibly impairs memory. Nat Med 22, 1268-1276.

Zhao, Y., Lei, M., Wang, Z., Qiao, G., Yang, T., and Zhang, J. (2014). TCR-induced, PKC-theta-mediated NF-kappaB activation is regulated by a caspase-8-caspase-9-caspase-3 cascade. Biochem Biophys Res Commun 450, 526-531.

Zheng, T.S., Hunot, S., Kuida, K., and Flavell, R.A. (1999). Caspase knockouts: matters of life and death. Cell Death Differ 6, 1043-1053.

Zheng, T.S., Hunot, S., Kuida, K., Momoi, T., Srinivasan, A., Nicholson, D.W., Lazebnik, Y., and Flavell, R.A. (2000). Deficiency in caspase-9 or caspase-3 induces compensatory caspase activation. Nat Med 6, 1241-1247.

Zhou, Q., Krebs, J.F., Snipas, S.J., Price, A., Alnemri, E.S., Tomaselli, K.J., and Salvesen, G.S. (1998). Interaction of the baculovirus anti-apoptotic protein p35 with caspases. Specificity, kinetics, and characterization of the caspase/p35 complex. Biochemistry 37, 10757-10765.

Zhou, Q., Snipas, S., Orth, K., Muzio, M., Dixit, V.M., and Salvesen, G.S. (1997). Target protease specificity of the viral serpin CrmA. Analysis of five caspases. J Biol Chem 272, 7797-7800.

Zoog, S.J., Schiller, J.J., Wetter, J.A., Chejanovsky, N., and Friesen, P.D. (2002). Baculovirus apoptotic suppressor p49 is a substrate inhibitor of initiator caspases resistant to p35 in vivo. EMBO J 21, 5130-5140.

Zou, H., Henzel, W.J., Liu, X., Lutschg, A., and Wang, X. (1997). Apaf-1, a human protein homologous to C. elegans CED-4, participates in cytochrome c-dependent activation of caspase-3. Cell 90, 405-413.

Appendix I

Title: Pharmacokinetic and toxicological evaluation of novel peptide-based drugs. (NWL-117Na)

Study plan version: 1
Principal investigator: Jan-Eric Ahlfors
Research Team: Annie Salesse DEC., Richard Frenette M.Sc. Scientist, Medicinal Chemistry

Summary: We have developed novel peptide-based drugs for treating various neurological conditions as well as for promoting neuronal repair. As part of the drug development process, it is necessary to evaluate the pharmacokinetic (PK) and toxicological parameters of these drug products in healthy animals to further validate the safety and efficacy of our drug products. In this study we evaluated the toxicity associated with a dose of 50 mg/kg, by subjecting the animals to multiple doses of the drug over a period of 28 days.
Background: A 28-day repeat dose toxicity evaluation was performed on CD1 mice at MISPRO (an AAALAC approved animal facility) for our parent drug (Compound X) using 50 mg/kg/day drug concentration. We observed no significant adverse effects or toxicity in CD1 mice when the Compound X was administered intraperitoneally. Since the drugs that we will be evaluating in this study are chemical derivatives of our parent drug (slight modification in functional groups on the parent structure to improve specificity and potency of the derivative drugs), we anticipate that there will not be any significant change in the EC50 of the derivative drugs. We also hypothesize that at higher doses, our parent drug and its derivatives shouldn't have significant toxicity. This is based on our earlier findings from CD1 mice that the Compound X was rapidly metabolized and cleared, leaving no molecular signatures or metabolites that may cause deleterious effect.
Study objectives: The objective of this study was to determine the safety, toxicity, and local tissue reaction to repeated doses of NWL-117Na at 50 mg/kg IP. To evaluate if a specific compound has any local reaction, a small pilot study of 8 animals (repeat dose, 50 mg/kg injected IP) will be performed first to determine if there are local toxic or side-effects of a compound. This pilot study will also simultaneously determine if a particular compound has high toxicity by any chance. Once no clear local side effects or systemic toxic effects are observed, the compound can then progress to the multiple-dose toxicity study.

Study design:

1. Test system:

Species:	Mice
Strain:	CD-1
Source:	Charles River Canada Inc.
Number of Female Mice Ordered:	10
Target Weight at the Initiation of Dosing:	5-6 weeks old females (20-25 g)

1.1. Justification of Test System and Number of Animals

The choice of the animal species and strain are in accordance with the standard conventions to establish a preliminary toxicity profile of our products. The CD1 mice are established experimental mouse strains used for drug screening and evaluation (Vogel HG et al., 2011). Our preliminary toxicity studies has demonstrated that the Compound X (the parent drug) did not have significant toxicity in CD1 mice.

1.2. Animal Identification:

Each animal was identified on the tail for the study number assignment, using indelible ink (permanent marker).

1.3. Environmental Acclimation

A minimum acclimation period of 5 days at the animal facility (INRS) was allowed between animal receipt and the start of treatment in order to accustom the animals to the laboratory environment.

2. Selection, Assignment, and Replacement of Animals

Animals were assigned to groups by randomization designed to achieve similar group mean body weights. Animals in poor health or at extremes of body weight range were not assigned to groups.
We used a free website for randomization: http://www.graphpad.com/quickcalcs/randomize1.cfm

The random number generator is seeded with the time of day. Each subject is first assigned to a group non-randomly. Then the assignment of each subject is swapped with the group assignment of a randomly chosen subject. The entire process is repeated twice to make sure it is really random.

Table1: Group assignment for blood collection

Assign subjects to groups *	
Subject #	Group Assigned
1	A
2	B
3	B
4	A
5	B
6	A
7	A
8	B

A= Hematology group
B= Biochemistry group

Table 2: Randomization
After the randomization we excluded the largest and the smallest animal from the study.
Before the initiation of dosing, any assigned animals considered unsuitable for use in the study were replaced by alternate animals obtained from the same shipment and maintained under the same environmental conditions. The disposition of all animals were documented in the study records.

Animal #	Body Weight (g)	Sort by BW		Sort by Arrival #		Animal Arrival #	* Study Group assigment For H/BCH	Animal Study Group #	Animal Arrival Group #	* Study Group assigment	Sort by Animal Study Group #
		Animal arrival #	BW	Arrival	BW						
1	24.56	7	21.80	1	24.56	1	24.56	A	1	24.56	A
2	22.17	8	21.90	2	22.17	2	22.17	B	4	22.57	A
3	22.02	3	22.02	3	22.02	3	22.02	B	6	24.93	A
4	22.57	2	22.17	4	22.57	4	22.57	A	8	21.90	A
5	22.34	5	22.34	5	22.34	5	22.34	B	2	22.17	B
6	24.93	4	22.57	6	24.93	6	24.93	A	3	22.02	B
7	21.80	9	23.07	8	21.90	8	21.90	A	5	22.34	B
8	21.90	1	24.56	9	23.07	9	23.07	B	9	23.07	B
9	23.07	6	24.93								
10	24.99	10	24.99								

	Spare
A=	Hematology Group
B=	Biochemistry Group

3. Food and Water supply

The animals received Teklad global 18% protein diet (cat#:2018) produced by Harlan Laboratories (Montréal, Qc. Canada) and municipal tap water treated by reverse osmosis and UV treatment in a sterile bottle, ad libitum.

4. In-life procedures, observations and measurements

Prior to the experiments, all the animals were acclimatized for 5 days as per the institutional animal care recommendations. The experiment was conducted as a set of pilot studies to screen the in vivo toxicity and pharmacokinetics of our newly developed drugs. One compound was tested to determine their dose ranges, which are tolerated by CD1 mice. A total of 8 mice were used for this study. Each animal was injected with 50 mg/Kg/day of compound every 3 days for a period of 28 days and they were euthanized at day 31.

Group 1 (compound NWL-117Na): 8 animals intraperitoneal administered with a single bolus injection of 50 mg/kg/day of drug concentration.

All animals were received an intra peritoneal injection of 50 mg/kg/day of NWL-117Na compound.

4.1. Mortality/Moribundity Checks: (by the INRS staff)

Frequency: Twice daily, once in the morning and once in the afternoon, throughout the study.

4.2. Cage side Observations:

Frequency: Following drug administration, all the animals were monitored for a period of 24 h for any adverse events (once at following time-point ranges: 0-4 h, 6-8h and 21-24 h).

4.3. Detailed clinical observation:

Frequency: Before randomization and treatment

4.4. Body Weights

Frequency: Before randomization, on treatment day 1, 4, 7, 10, 13, 16, 19, 22, 25, 28 and at the end of study on day 31.

Procedure: Animals were individually weighed.

Treatment:

Mice were randomly grouped for NWL-117Na intra peritoneal injection. The animals received 50 mg/Kg/day, dosing volume 6 mL /Kg, on day 1, 4, 7, 10, 13, 16, 19, 22, 25 and 28.

4.5. Compound:

Identification: NWL-117Na (NWL-117Na-04) for Injection, USP
Supplier: New World Laboratories
Batch (Lot) No.: 4
Expiration Date: N/A
Physical Description: Liquid
Purity: 98%
Concentration: 8.33 mg/mL
Storage Conditions: When stored at ambient temperature, the solution should be used within the next 4 hours. The mixture can be stored at +4C for a maximum of 3 days prior its use at ambient temperature. It is suggested to prepare a fresh solution every 3 days. The solution can also be stored at -29°C without deterioration (6 days). Kept in a freezer at -29°C in chemistry lab or in Freezer at -20°C in INRS.

NWL-117 bis-sodium salt (NWL-117Na): Preparation of a solution of 8.33 mg/mL of NWL-117Na in 0.9% saline (1 mL). To a sterile vial containing 8.33 mg of NWL-117Na was added at once 1 mL of 0.9% saline. The mixture was vortexed for 1 minute to give a clear solution.

4.6. Reserve Samples:

For each batch (NWL-117Na-04) of compound, a reserve sample (1 vial of 50 µL) was collected and maintained under the appropriate storage conditions.

5. Terminal procedures:

5.1. Scheduled Euthanasia

All animals were sacrificed on day 31 by exsanguination after blood collection by cardiac puncture after isoflurane anesthesia. The animals were subjected to a complete necropsy examination which included evaluation of the carcass; all external surfaces and orifices; cranial cavity and external surfaces of the brain; and thoracic, abdominal, and pelvic cavities with their associated organs and tissues.

5.2. Unscheduled Deaths

There were no unscheduled deaths.

6. Sample Collection, Processing, and Analysis:

6.1. Blood collection

Blood was collected from select animals on day 31 by cardiac puncture under isoflurane anesthesia for hematology and biochemistry analysis.

6.2. Blood analysis (H/BCH): Idexx

8 samples from treated mice and 2 samples from non-treated mice (control) were sent to IDEXX for analysis:

- 4 mice (treated) and 1 mouse (non-treated) for Hematology analysis: whole blood was analyzed fresh.
  Tube Anticoagulant: EDTA K_2 Microtainer 500 µL (#cat:cabd365974, lot#: 4064163, exp.:2015-08)
  Target Volume: 0,5 mL
  Centrifugation: N/A
  Storage: in wet ice or 4°C

Idexx test code: CCBC: WBC, RBC, Hgb, Hct, erythrocyte indices (MCV, MCH, MCHC), WBC differential, platelet count, reticulocyte count, smear evaluation by a technologist for RBC and WBC morphology and parasite screen, pathologist review of abnormal cells.

- 4 mice (treated) and 1 mouse (non-treated) for Biochemistry analysis:
  Tube: BD Microtainer serum separator tubes (SST) 250-500 µL (#cat:cabd365952, lot# 3305334, exp.:2015-01)
  Target Volume: 0,5 mL
  Centrifugation: incubate at room temperature for 20-30 min. and centrifuged at Room temperature (4 500 Rpm) for 10 min. at 4°C. Serum was transferred into the 0,5 ml Eppendorf tube.
  Storage: room temperature for 4 hours maximum or 4°C

Idexx test code: CHM02: Albumin, albumin/globulin ratio, alkaline phosphatase, ALT (SGPT), amylase, bilirubin (total), calcium, creatinine, globulin, glucose, total protein, urea.

6.3. Shipping Contact

Idexx Laboratories Inc.
Crystal Campeau
Toronto, On, M5W 5W6
T: Mobile: (514) 805-9152
T: 1-866-683-2551
E: crystal-campeau@idexx.com
Vetconnectplus.ca

The laboratory was notified the same day before shipment of the samples before 11:00 AM (to send before 1:00 PM) or before 6:00 PM (to ship before 8:00 PM). Upon receipt at the laboratory, the samples were stored under the following conditions: room temperature for 4 hours maximum or 4°C.

7. Histology:

7.1. Tissue Collection and Preservation

All major tissues and organs were collected and fixed 48 hrs in 1:10 Tissufix (CHAPTEC INC.) at room temperature.

7.2. Histology

Histopatological processing and analysis of all major tissues and organs was performed at McGill University (Goodman cancer research center histology core facility). According to their standard operating procedures, all fixed tissues were placed into cassettes and embedded into paraffin (the sternum was decalcified prior processing). Blocks were cut with a microtome and the sections were stained with Hematoxylin & Eosin (H&E), mounted and examined under a bright field microscope by Comparative Pathology Service in Mc Gill University for histopathological analysis by a certified veterinary pathologist. Each submitted tissue section was evaluated for tissue abnormalities and scored according to the intensity of the observed changes:

The tissues in paraffin block were sent back to New World Laboratories.

Table 3: Major tissue and organ inventory

Organ	Animal#							
	1	2	3	4	5	6	8	9
Skin Rigt injection site	✓	✓	✓	✓	✓	✓	✓	✓
Skin Left injection site	✓	✓	✓	✓	✓	✓	✓	✓
Liver	✓	✓	✓	✓	✓	✓	✓	✓
Spleen	✓	✓	✓	✓	✓	✓	✓	✓
Pancreas	✓	✓	✓	✓	✓	✓	✓	✓
Kidney Right	✓	✓	✓	✓	✓	✓	✓	✓
Heart	✓	✓	✓	✓	✓	✓	✓	✓
Lungs	✓	✓	✓	✓	✓	✓	✓	✓
Brain	✓	✓	✓	✓	✓	✓	✓	✓
Right Femur or sternum	✓	✓	✓	✓	✓	✓	✓	✓
Eye left (small)					✓			
Eye right (normal)					✓			

7.3. Contact

Mc Gill
Contact person
Jean-Martin Lapointe, DMV, MSc, dACVP
Comparative Pathologist
Comparative Medicine – Animal Resources Centre
McGill University
3655 Pr. Sir William Osler, rm 1440
Montreal, Qc
Canada H3G 1Y6
Phone: 514 398-4400 (00535)
email: jean-martin.lapointe@mcgill.ca

8. Results and discussion

8.1. : Mortality and clinical observation (cage side observation)

No mice were found dead, and no significant and systemic clinical signs were observed during the study, except for number 5. This animal #5, was found with a left eye smaller then the right eye (microphtalmia); this is usually a birth defect. The mouse has no signs of distress or infection. Eye was sent to the pathologist for analysis at the end of the study.

No visible tumor growth at the site of injection was observed for all groups during the entire 31 days study period.

8.2. Body Weight

Individual body weight were recorded before randomization and every three days on treatment day 1, 4, 7, 10, 13, 16, 19, 22, 25, 28 and at the end of study on day 31. There was no difference between the animals.

Table 3: Body Weight of mice treated with NWL-117Na (50mg/Kg i.p.) for 31 days.

Day	50 mg/Kg
0	22.945
1	22.945
4	23.615
7	23.63
10	24.42
13	25.08
16	25.30
19	25.97
22	26.39
25	27.34
28	27.27
31	26.66

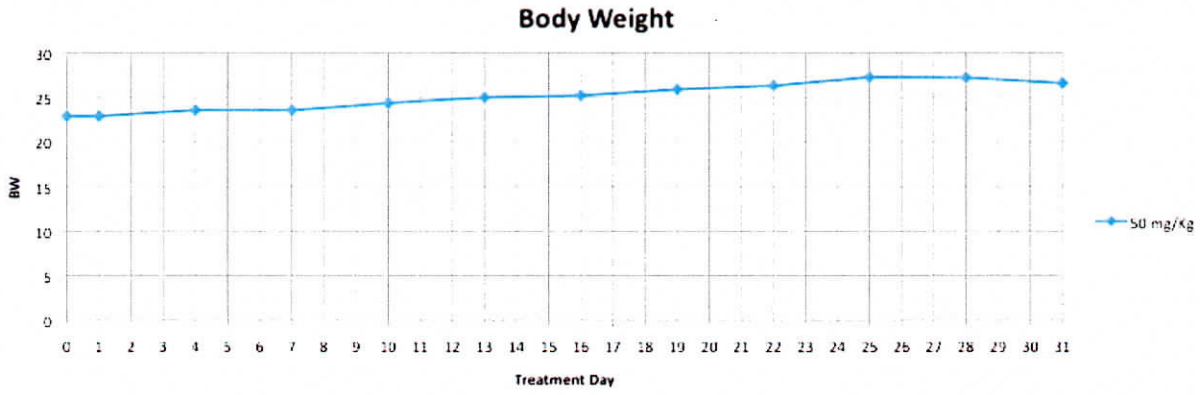

8.3. Hematology and Biochemistry analysis

Blood was collected from selected animals at the end of the study (at day 31). The hematology and Biochemistry results are comparable to the reference range from Charles River (CD-01 Mouse Hematology north American colonies Jan 2008-Dec 2011, 8-10 weeks old), Research animal resources from University of Minnesota, (http://www.ahc.umn.edu/rar/refvalues.html), "Ferrets, rabbits and rodent clinical medicine and surgery" by Katherine Quesenberry and James Carpenter. Animal #9 has a level of amylase lower than normal. It can be related to the severe hepatic dysfunction but decreased amylase is seldom clinically significant. No clinical signs were observed for that animal.

Table 4: Hematology analysis of mice treated with NWL-117Na, non-treated and reference range.

Mouse#	1	4	6	8	Average	Average 28-day tox study on CD-1 mice (NWL-53)	28-day tox study on CD-1 mice (control)	CD-1 Control mouse without injection (12 weeks)	Reference Range
RBC (x10^12/L)	9.5	10	8.6	8.7	9.2	6.01-8.51	9.4-10.3	8.9	7.9-10.1
Hematocrit (L/L)	0.45	0.47	0.4	0.41	0.4325			0.44	0.37-0.46
Hemoglobin (g/L)	148	156	131	128	140.75	105.14-129.26	129.02-153.48	144 (14.4 g/dL)	110-145
MCV (fL)	48	47	47	47	47.25	108.69-128.87	89.53-131.03	49	41-49
MCH (pg)	16	16	15	15	15.5			16	12.9-18.77
MCHC (g/L)	326	333	327	315	325.25	527.44-634.96	418.28-673.72	329	219-335
% reticulocyte	3.1	2.6	2.3	4.5	3.125			3.1	
Reticulocyte (K/uL)	294.5	260	197.8	391.5	285.95			275.9	
WBC (x10^9/L)	8.8	5.3	4.7	4.1	5.725	2.56-3.12	2.76-3.94	5.5	5.0-13.7
% Neutrophil	14.2	13.1	13.5	11.5	13.075			16	6.7-40
% Band	0	0	0	0	0			0	
% Lymphocyte	80.6	81.9	78	83.2	80.925			81.5	55-95
% Monocyte	3.4	1.9	3	1.9	2.55			0.7	0.1-3.5
% Eosinophil	1.7	2.9	5.3	3.4	3.325			1.6	0-4
%Basophil	0.1	0.2	0.2	0	0.125			0.2	0-1.5
Neutrophil (x10^9/L)	1.2	0.7	0.6	0.5	0.75	0.17-0.23	0.23-0.73	0.9	0.54-4.31
Band (x10^9/L)	0	0	0	0	0			0	
Lymphocyte (x10^9/L)	7.1	4.3	3.7	3.4	4.625	1.54-2.08	0.9-1.6	4.5	2.7-11.3
Monocyte (x10^9/L)	0.3	0.1	0.1	0.1	0.15	0.04-0.06	0.08-0.26	0	0.22-1.49
Eosinophil (x10^9/L)	0.1	0.2	0.2	0.1	0.15	0.06-0.1	0.04-0.06	0.1	0.01-0.60
Basophil (x10^9/L)	0	0	0	0	0			0	0-0.16
Platelet (x10^9/L)	1.038	1.131	1.7	1.335	1.301	358.53-489.07	321.59-452.41	1.059	100-1200 x10^3/uL
Smear Evaluation									
WBC Morphology	N	N	N	N				N	
RBC Morphology	Polychromasia -6/HPF	Polychromasia -6/HPF	Polychromasia -6/HPF	Polychromasia -6/HPF				Polychromasia -6/HPF	
PLT Morphology	Clumped platelets-marked	Clumped platelets-Mild	N	N				Clumped platelets-Mild	

Table 5: Biochemistry analysis of mice treated with NWL-117Na, non-treated and reference range.

Mouse#	2	3	5	9	Average	Average 28-day tox study on CD-1 mice (NWL-53)	28-day tox study on CD-1 mice (control)	CD-1 Control mouse without injection (12 weeks)	Reference Range
Glucose (mmol/L)	10.7	11.4	10	11.3	10.85	11.32-13.16	8.39-10.41	12.5	9.71-18
BUN (mmol/L)	8.9	7.1	7.8	6.5	7.58	5-6.5	4.43-4.57	6.8	12.14-20.59
Creatinine (umol/L)	15.03	12.38	10.61	13.26	12.82	36	36	10.61	0.2-1.1 mg/dL
Calcium (mmol/L)	2.23	2.21	2.24	2.21	2.22			2.36	4.6-9.6 mg/dL
Total Protein (g/L)	45	50	47	45	46.75	56.13-66.27	57.87-84.13	46	42-103
Albumin (g/L)	26	29	27	27	27.25			27	21-48
Globulin (g/L)	19	21	20	18	19.50			19	18-82
Alb/Glob Ratio	1.4	1.4	1.4	1.5	1.43			1.4	1.23-1.37
ALT (U/L)	27	18	21	24	22.50	41.49-49.71	34	20	17-77
ALP (U/L)	72	121	69	100	90.50	34.71-58.29	72	77	23.7-96
Bilirubin Total (umol/L)	2.39	2.57	2.22	2.22	2.35	6.42-7.58	8	1.54 (0.1 mg/dL)	0.15-0.85 mg/dL
Amylase (U/L)	937	742	674	3.779	589.19			750	
Hemolysis Index	N	N	N	N	N			N	
Icterus Index	N	N	N	N	N			N	
Lipemia Index	N	N	N	N	N			N	

8.4. Necropsy- gross pathology

The necropsy was performed at the end of study. No gross abnormality or tumor growth was observed.

8.5. Necropsy- histopathology

Changes were observed in some sections of lung, liver, pancreas and brain. In the lung of one animal, there were areas of acute hemorrhage with the alveolar lumina. This was considered most likely an agonal change, probably related to euthanasia or possibly terminal blood sampling, but most unlikely to be treatment-related. In the liver, three animals had a few small foci of mixed inflammatory cell infiltration. This is a common background observation in healthy mice, and at this minimal severity-grade it was not considered likely to be related to treatment. In the pancreas, foci of inflammatory cell infiltration (mainly histiocytes and lymphocytes) were observed in the mesentery sheets associated with the pancreas samples. The pancreatic parenchyma itself was not affected. This was considered mostly likely a consequence of inflammation secondary to the intra-peritoneal injection (since animals receiving vehicle-only injections were not submitted, it cannot be concluded whether the inflammatory reaction was secondary to the injection itself, to the vehicle, or to the administered compound). One animal had changes of vacuolation, most likely neuronal-associated, in the cerebral cortex and to a lesser extent the hippocampus. The vacuolation was bilateral, but only noted at one level of the cortex (frontal and dorsal area). This is not a commonly observed or reported background change in mice. It may have been an effect of the compound administered, or a pathologic change unrelated to the compound. The extent of the vacuolation was limited, and it was not associated with other significant changes in the brain.

Histopathology conclusion: The two changes potentially associated with treatment were inflammation in the mesentery, and neuronal vacuolation in the brain. Mesentery inflammation was likely a consequence of irritation related to the intra-peritoneal route of administration itself, but without control groups we cannot conclude whether it was a direct effect of the compound or related to the vehicle or injection. The cerebral vacuolation was observed only in one animal; it may have been a drug effect, or an unrelated problem in this animal. Additional studies would be necessary to conclude as to the possibility of a drug effect.

Pathologist: Jean-Martin Lapointe, DMV, MSc, dACVP

Table 7: Pathology results

ID	Spleen	Kidney	Heart	Skin (right side)	Skin (left side)	Sternum (bone marrow)	Lungs	Liver	Pancreas	Brain
1	wnl	wnl	wnl	wnl	wnl	wnl	Hemorrhage, alveolar, acute	Inflammatory infiltration, mixed, minimal	wnl	wnl
2	wnl	wnl	wnl	wnl	wnl	wnl	wnl	wnl	wnl	wnl
3	wnl	wnl	wnl	wnl	wnl	wnl	wnl	wnl	Inflammation, histiolymphocytic, mesentery, minimal	wnl
4	wnl	wnl	wnl	wnl	wnl	wnl	wnl	wnl	wnl	wnl
5	wnl	wnl	wnl	wnl	wnl	wnl	wnl	wnl	wnl	wnl
6	wnl	wnl	wnl	wnl	wnl	wnl	wnl	wnl	Inflammation, histiolymphocytic, mesentery, minimal	wnl
8	wnl	wnl	wnl	wnl	wnl	wnl	wnl	Inflammatory infiltration, mixed, minimal	Inflammation, histiolymphocytic, mesentery, mild	wnl
9	wnl	wnl	wnl	wnl	wnl	wnl	wnl	Inflammatory infiltration, mixed, minimal	Inflammation, histiolymphocytic, mesentery, mild	Neuronal vacuolation, cortex and hippocampus, bilateral, focal, mild

wnl: within normal limits

9. Conclusion

The primary purpose of this study was to evaluate if NWL-117Na at 50-mg/Kg intraperitoneal injection has any local reaction and toxicity. None of the injected animals formed tumors but some of them had an inflammation reaction in the mesentery. One animal has changes of vacuolation in the cerebral cortex and to a lesser extent in the hippocampus and the level of Amylase was lower than normal. This could be, or not, associated with the injection of 50 mg/Kg of NWL-117Na.

10. Appendix

10.1. Appendix #1: Pathology report (appendix in a separate document).

11. Signature

Report Approval

Report Prepared by:	**Annie Salesse**
Title	Research Associate
Signature / Date (YYYY-MM-DD)	Annie Salesse 2014-09-03
Report Reviewed and Approved by	**Jan-Eric Ahlfors**
Title	CEO-CSO
Signature / Date (YYYY-MM-DD)	2014-09-03

Comparative Medicine
Animal Resources Centre

McGill

Comparative Pathology Service
tel: (514) 398-4400 xt 00535
e-mail: jean-martin.lapointe@mcgill.ca

Pathology Report

Submitter/Investigator: Annie Salesse / New World Laboratories

Date issued: August 20th 2014

Date submitted: July 8th 2014

Objectives: Evaluate tissues in mice administered an unspecified therapeutic compound

Samples: Information from Sponsor: Mice were randomly grouped for NWL-117Na intraperitoneal injection. The animals received 50 mg/kg/day, dosing volume 6 mL/kg, on day 1, 4, 7, 10, 13, 16, 19, 22, 25 and 28. Animals were sacrificed at day 31.

Samples of liver, spleen, pancreas, skin injection sites (left and right), kidney, heart, lungs, brain, sternum and femur from 8 mice were submitted in formalin. All tissues except the femur were processed for histology. The container for animal #5 was indicated via separate email to additionally contain 2 eyes, but these were not noticed at trimming, and may have been lost. The sternum was decalcified prior to processing. Sections were stained with hematoxylin and eosin and examined by the pathologist.

Results / Discussion: see Excel table in separate document for details.

Changes were observed in some sections of lung, liver, pancreas and brain.

In the lung of one animal, there were areas of acute hemorrhage with the alveolar lumina. This was considered most likely an agonal change, probably related to euthanasia or possibly terminal blood sampling, but most unlikely to be treatment-related.

In the liver, three animals had a few small foci of mixed inflammatory cell infiltration. This is a common background observation in healthy mice, and at this minimal severity grade it was not considered likely to be related to treatment.

In the pancreas, foci of inflammatory cell infiltration (mainly histiocytes and lymphocytes) were observed in in the mesentery sheets associated with the pancreas samples. The pancreatic parenchyma itself was not affected. This was considered mostly likely a consequence of inflammation secondary to the intra-peritoneal injection. Since animals receiving vehicle-only injections were not submitted, it cannot be concluded whether the inflammatory reaction was secondary to the injection itself, to the vehicle, or to the administered compound.

One animal had changes of vacuolation, most likely neuronal-associated, in the cerebral cortex and to a lesser extent the hippocampus. The vacuolation was bilateral, but only noted at one level of the

Comparative Medicine
Animal Resources Centre

McGill

Comparative Pathology Service
tel: (514) 398-4400 xt 00535
e-mail: jean-martin.lapointe@mcgill.ca

Pathology Report

cortex (frontal and dorsal area). This is not a commonly observed or reported background change in mice. It may have been an effect of the compound administered, or a pathologic change unrelated to the compound. The extent of the vacuolation was limited, and it was not associated with other significant changes in the brain.

Conclusion:

The two changes potentially associated with treatment were inflammation in the mesentery, and neuronal vacuolation in the brain. Mesentery inflammation was likely a consequence of irritation related to the intra-peritoneal route of administration, but without control groups we cannot conclude whether it was a direct effect of the compound or related to the vehicle or injection.

The cerebral vacuolation was observed only in one animal; it may have been a drug effect, or an unrelated problem in this animal. Additional studies would be necessary to conclude as to the possibility of a drug effect.

It should be noted that any study evaluating possible toxicity of a compound should always include a control group, treated with the drug vehicle only, at the same volume and frequency as the test groups, and kept in the same conditions. This is absolutely necessary in order to be able to adequately interpret any pathologic finding observed.

(joined: Excel document with results).

Pathologist: Jean-Martin Lapointe, DMV, MSc, dACVP

Appendix #1

Comparative Pathology Service
tel: (514) 398-4400 xt 00535
e-mail: jean-martin.lapointe@mcgill.ca

Pathology results

McGill University

ID	Spleen	Kidney	Heart	Skin (right side)	Skin (left side)	Sternum (bone marrow)	Lungs	Liver	Pancreas	Brain
1	wnl	wnl	wnl	wnl	wnl	wnl	Hemorrhage, alveolar, acute	Inflammatory infiltration, mixed, minimal	wnl	wnl
2	wnl	wnl	wnl	wnl	wnl	wnl	wnl	wnl	wnl	wnl
3	wnl	wnl	wnl	wnl	wnl	wnl	wnl	wnl	Inflammation, histiolymphocytic, mesentery, minimal	wnl
4	wnl	wnl	wnl	wnl	wnl	wnl	wnl	wnl	wnl	wnl
5	wnl	wnl	wnl	wnl	wnl	wnl	wnl	wnl	wnl	wnl
6	wnl	wnl	wnl	wnl	wnl	wnl	wnl	wnl	Inflammation, histiolymphocytic, mesentery, minimal	wnl
8	wnl	wnl	wnl	wnl	wnl	wnl	wnl	Inflammatory infiltration, mixed, minimal	Inflammation, histiolymphocytic, mesentery, mild	wnl
9	wnl	wnl	wnl	wnl	wnl	wnl	wnl	Inflammatory infiltration, mixed, minimal	Inflammation, histiolymphocytic, mesentery, mild	Neuronal vacuolation, cortex and hippocampus, bilateral, focal, mild

wnl: within normal limits

As for
Jean-Martin Lapointe
pathologist from
McGill University
2014-09-03